Department of Geography and Geology
Faculty of Science
University of Copenhagen

Master's thesis

Stud.scient Anne Lausten Hansen

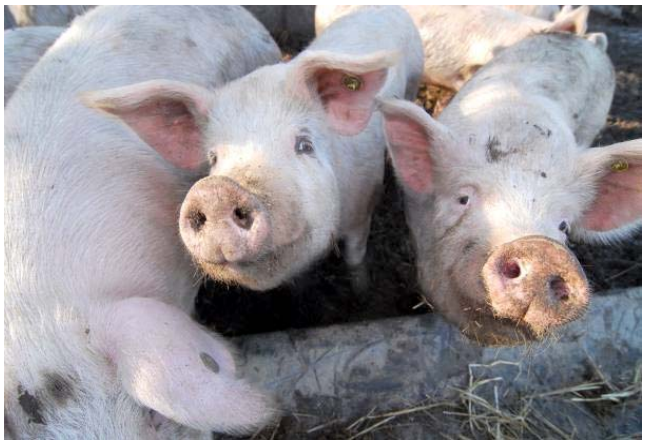

Modelling of flow and nitrate transport from root zone to stream system in Lillebæk catchment (LOOP4), Denmark

Supervisors: Karsten Høgh Jensen
Department of Geography and Geology
University of Copenhagen

Jens Christian Refsgaard & Britt Stenhøj Baun Christensen
Geological Survey of Denmark and Greenland

Submitted: 01/10/2010

Data sheet

Title of thesis:	Modelling of flow and nitrate transport from root zone to stream system in Lillebæk catchment (LOOP4), Denmark
Student:	Anne Lausten Hansen Department of Geography and Geology University of Copenhagen
Degree:	Master of Science in Geology-Geoscience with Qualification Profile in Water Resources
Submission date:	October 1st 2010
ECTS credits:	30 ECTS points
Supervisor:	Karsten Høgh Jensen Department of Geography and Geology University of Copenhagen
Co-supervisors:	Jens Christian Refsgaard Britt Stenhøj Baun Christensen Geological Survey of Denmark and Greeland
Cover images:	http://images.fyens.dk/80/496380_605_450_0_0_0_0.jpg http://c1.eatdrinkbetter.com/files/2009/06/wheat-by-bernat.jpg http://www.denstoredanske.dk/@api/deki/files/29452/=34920849.jpg http://www.bolius.dk/alt-om/have-planter-og-traeer/artikel/saadan-vedligeholder-du-havedammen/

Date stud.scient Anne Lausten Hansen

Table of contents

Preface

This thesis concludes my master degree in Geology-Geoscience with Qualification Profile in Water Resources from the Department of Geography and Geology (IGG) at University of Copenhagen. My master thesis was carried out as a part of the NICA research project at the Geological Survey of Denmark and Greenland (GEUS).

I would like to thank my supervisors Karsten Høgh Jensen (IGG), Britt Stenhøj Baun Christensen (GEUS) and Jens Christian Refsgaard (GEUS) and also everyone at the Department of Hydrology at GEUS. A special thank you is send to Lars Troldborg (GEUS), Anker Laj Højberg (GEUS) and Per Nyegaard (GEUS) for help concerning MIKE SHE and GIS related issues. Finally, I would also like to thank Anders Korsgaard for reviewing and giving professional comments and my aunt and uncle Hanne and Andrew Stearn for linguistic corrections of my thesis.

Abstract

Nitrate pollution of groundwater and surface waters is a large water resource problem in Denmark. Numerical modelling is a useful tool for describing water and nitrate processes and several Danish nitrate modelling studies have been completed using the combined Daisy/MIKE SHE modelling approach. This approach has also been applied for Lillebæk catchment and the work and results of the MIKE SHE catchment model are presented in this thesis entitled "*Modelling of flow and nitrate transport from root zone to stream system in Lillebæk catchment (LOOP4), Denmark"* by Anne Lausten Hansen. The overall water and nitrate balances are simulated acceptably on catchment scale, but the model has problems with simulating daily dynamics and on smaller scale. This is mainly due to lack of sufficient calibration data, uncertainty and lack of heterogeneity in geology and uncertainty on the location of the redox-interface. However, problems also arise due to limitations on the applied modelling approach caused by lack of full coupling between Daisy and MIKE SHE and mass depletion problems in MIKE11.

Keywords: Nitrate, reduction, physically based, modelling, catchment scale

Resumé (Danish)

Nitratforureningen af grundvand og overfladevand er et stor vandressourceproblem i Danmark. Numerisk modellering er et nyttigt værktøj til at beskrive vand og nitrat processer og flere danske nitratmodelleringsstudier er udført og disse gør brug af det kombinerede modelsystem Daisy/MIKE SHE. Dette modelsystem er også anvendt for Lillebæk opland og arbejdet samt resultaterne for MIKE SHE oplandsmodellen præsenteres i dette speciale med titlen "*Modellering af vand- og nitrattransport fra rodzonen til vandløbssytem i Lillebæk opland (LOOP4), Danmark"* af Anne Lausten Hansen. De overordnede vand- og nitratbalancer simuleres acceptabelt på oplandsskala, men modellen har problemer med at simulere den daglige dynamik samt på mindre skala. Dette skyldes primært mangel på tilstrækkelig kalibreringsdata, usikkerhed og mangel på heterogenitet i geologien samt usikkerhed på placeringen af redoxfronten. Desuden opstår problemer på grund af begrænsninger i det anvendte modelsystem i form af mangel på fuld kobling mellem Daisy og MIKE SHE samt problemer med massetab i MIKE11.

Nøgleord: Nitrat, reduktion, fysisk baseret, modellering, oplandsskala

1. Introduction and objectives

Nitrate in drinking water represents a health problem as it inhibits the oxygen uptake, especially in newborns, and is a suspect carcinogen and a drinking water standard of 50 mg nitrate-NO_3^-/l has consequently been set (National Board of Health, n.y.). However, nitrate is also an ecological problem as too high nitrate concentrations cause eutrophication of freshwater and marine environments, which in worst case can lead to oxygen depletion and declining species diversity. Increased nitrate concentrations are measured in Danish groundwater, streams, lakes and fjords and the main part of this nitrate is believed to originate from non-point pollution from agricultural areas, where the use of animal manure and fertilizer has increased (Berthelsen & Fenger, 2005).

Nitrogen is an essential plant nutrient and is added to agricultural fields as fertilizer and animal manure to promote plant growth. In the soil nitrogen is transformed to nitrate, which is easily accessible to the crop. But nitrate is also easily leached from the soil and transported with percolating water to the groundwater and further on to lakes and streams. The large input of nitrogen in Danish agriculture has caused nitrate leaching from arable land to be one of the largest challenges in water resource management in Denmark. Denmark is, according to the EU Water Framework Directive, obligated to reduce the nitrate leaching significantly and create good ecological conditions in lakes, streams and coastal waters by 2015 (Hansen, 2006).

Nitrate can be degraded naturally to free nitrogen under anaerobic conditions by the process of denitrification. The transition from aerobic and anaerobic conditions in the subsurface is called the redox-interface and for nitrate to be degraded it should be brought under this interface. The hydrogeological conditions in an area are crucial to whether or not nitrate is transported under the redox-interface with the flowing water before it reaches lakes and streams. Variations in the geological and hydrogeological conditions within a catchment lead to the existence of robust areas, from where the majority of the leached nitrate is brought under the interface and thus degraded in the groundwater before the water reaches streams and lakes, and also sensitive areas, from where nitrate is transported directly to streams and lakes without any significant reduction.

Several national action plans have been implemented since the 1980s to reduce the nitrate load from agriculture to the aquatic environment (Berthelsen & Fenger, 2005). The current approach is a general regulation and the effort is thus consistent for all areas, without any regard to the variation in natural degradation of nitrate. A differentiated approach, where efforts are focused on the sensitive areas contra the robust areas, would be more cost effective than the current approach. The transport and fate of nitrate from agricultural areas to surface waters have been analysed in several Danish studies using numerical modelling. However, with the current knowledge and available methods we cannot, at present, with sufficient security and on small enough scale designate which areas have high respective small natural degradation potential. It is therefore not currently possible to introduce a differentiated approach.

This master thesis is a part of the NICA project (nitrate reduction in geologically heterogeneous catchments), which is a research project working on the issue of identifying robust and sensitive areas of geological heterogeneity catchments, as well as indentifying the minimum scale at which models have predictive capabilities (Representative Elementary Scale (RES)). The aim of this thesis is to contribute to the NICA project with an evaluation of the current status in nitrate modelling at catchment scale and the limitations in the existing approach, using the Lillebæk catchment in Denmark as study area. The specific objectives of the thesis are:

- Creating a geological model for Lillebæk catchment based on existing borehole data
- Modelling of water flow in Lillebæk catchment and calibrating the model against measurements of hydraulic head and stream discharge
- Modelling of transport and degradation of nitrate in Lillebæk catchment and calibrating the model against measured nitrate concentrations in Lillebæk stream
- Evaluating the degree of nitrate reduction and the response time in the catchment
- Delineation of robust and sensitive areas in Lillebæk catchment using particle tracking

2. Background

2.1 Hydrological processes at catchment scale

Water is present in the atmosphere, on the land surface, in oceans, glaciers, lakes, rivers, streams and wetlands and also in the subsurface as soil water and groundwater. Water is in continuous circulation between these storages and is transferred between them by different hydrological processes such as precipitation, evaporation, transpiration, infiltration, percolation, overland flow, surface water flow and subsurface flow. This circulation of water is called the hydrologic cycle and is illustrated on figure 2.1 (Healy et al, 2007).

In hydrological studies the area of study often represents a hydrological catchment, as this is a logical unit for study of the hydrological processes. A catchment is defined as a geographical area, within which all precipitation reaching the ground surface, will flow to the same surface water body, such as a stream, lake, wetland, estuary or the sea. A catchment is delineated by the topographical watershed, which follows the highest points in the terrain (Hasholt, 2004).

In the following are the hydrological processes within a catchment described, with focus on the processes at ground surface, in the subsurface and in streams as well as the exchange of water between these. The subsurface is divided into an unsaturated and a saturated zone, for which the hydrological processes differ. The unsaturated zone is defined as the zone above the groundwater table, where the water pressure is negative and the pore space contains both water and air. The saturated zone is defined as the zone below the groundwater table, and here the water pressure is positive and the pores are fully saturated with water (Fitts, 2002).

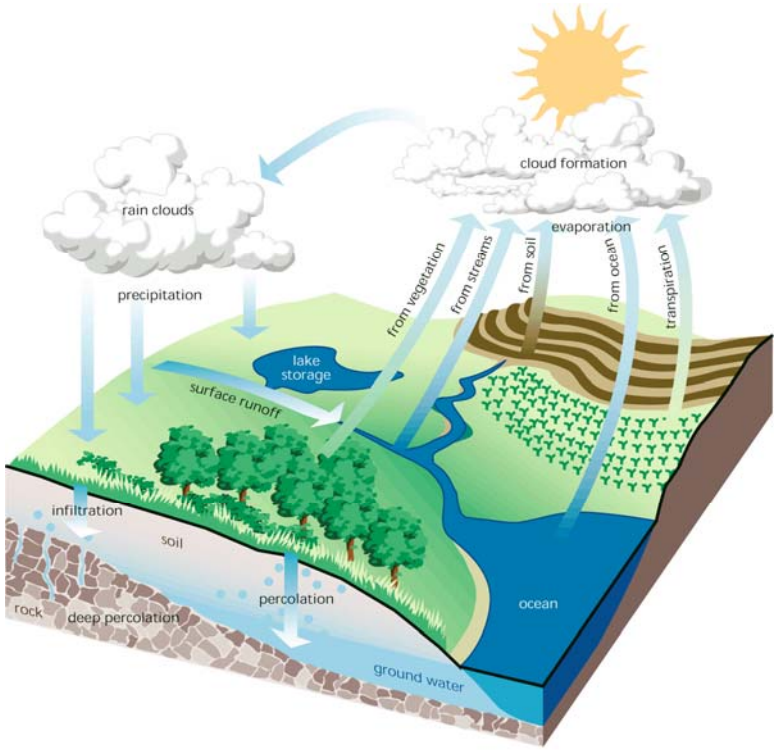

Figure 2.1 The hydrological cycle (Source: http://www.h2owell.com/images/hydrologic-cycle-big.png)

2.1.1 Ground surface

Precipitation brings water from the atmosphere to the ground surface of the catchment. At the ground surface water is either transported into the unsaturated zone by infiltration, across the surface as overland flow or back to the atmosphere by evaporation from the ground surface and interception loss from vegetation surfaces (Fitts, 2002).

Infiltration is the process where water passes through the ground surface under the influence of gravity and capillary forces (Refsgaard et al, 2003). The maximum infiltration rate is called the infiltration capacity and depends on surface permeability, water saturation of the soil and vegetation cover. If the precipitation intensity is larger than the infiltration capacity, water will puddle on the ground surface until it can infiltrate. However, if the water storage on the ground surface exceeds the storage capacity, water will run off as overland flow to surface waters or to areas where it can infiltrate (Refsgaard et al, 2003). The storage capacity of the ground surface is dependent on the topography and the vegetation cover (Hasholt, 20004).

Whether precipitation infiltrates the soil or results in overland flow is thus dependent on the precipitation intensity, permeability of the surface, vegetation cover, topography and water saturation of the soil. In areas with high permeable soils, flat topography and dry conditions most precipitation will infiltrate. However, in areas with low permeable soils, steep topography and wet conditions, a large fraction of the precipitation will become overland flow. In urban areas many surfaces are more or less impermeable, resulting in almost all water running off as overland flow (Fitts, 2002). As the precipitation intensity in Denmark most often does not exceed the infiltration capacity (Hasholt, 2004) most precipitation is infiltrated and overland flow is therefore not a large component in the hydrological cycle in Danish catchments (Refsgaard et al, 2003). However, on water saturated soils near e.g. wetlands and surface waters saturated overland flow can occur.

2.1.2 Unsaturated zone

Water enters the unsaturated zone by infiltration and capillary forces make the unsaturated zone able to withhold the water in the pores against the gravity. The pores are however only able to withhold a certain amount of water, defined as field capacity. If the water content in the unsaturated zone exceeds field capacity, the capillary forces cannot hold the water, which will drain due to gravity (Refsgaard et al, 2003).
Water in the unsaturated zone is thereby transported down into the saturated zone. Water can furthermore exit the unsaturated zone through plant uptake. As plants are able to build up a tension, they can withdraw water from the unsaturated zone against the capillary forces (Refsgaard et al, 2003).

2.1.3 Saturated zone

The saturated zone receives water from the unsaturated zone and surface waters. Outflow from the saturated zone occurs by groundwater discharge to surface waters or the sea. If the groundwater table is close to the ground surface, water can also exit the saturated zone by plant uptake and direct evaporation from the groundwater table (Healy et al, 2007). Water in the saturated zone can furthermore be removed by artificial means by groundwater abstraction for water supply or by drainage, which is done in order to lower the groundwater level if it is too close to the ground surface (Fitts, 2002).

The subsurface watershed follows the highest points in the groundwater table. The groundwater table in general follows the topography of the catchment, however, in some catchments it differs from the topography. In such catchments, where the subsurface and topographical watersheds differ, the catchment will either receive or deliver groundwater to neighbouring catchments (Hasholt, 2004).

Water in the saturated zone flows due to differences in the energy state of the water, described by the term hydraulic head. The groundwater flow is determined by the gradient in hydraulic head and the hydraulic conductivity, which is an empirical constant describing the ability of a geological media to transmit water (Fitts, 2002). Groundwater flow paths vary greatly in length and depth depending on where the groundwater recharges and the travel time within a catchment thus greatly varies as illustrated on figure 2.2. (Healy et al, 2007).

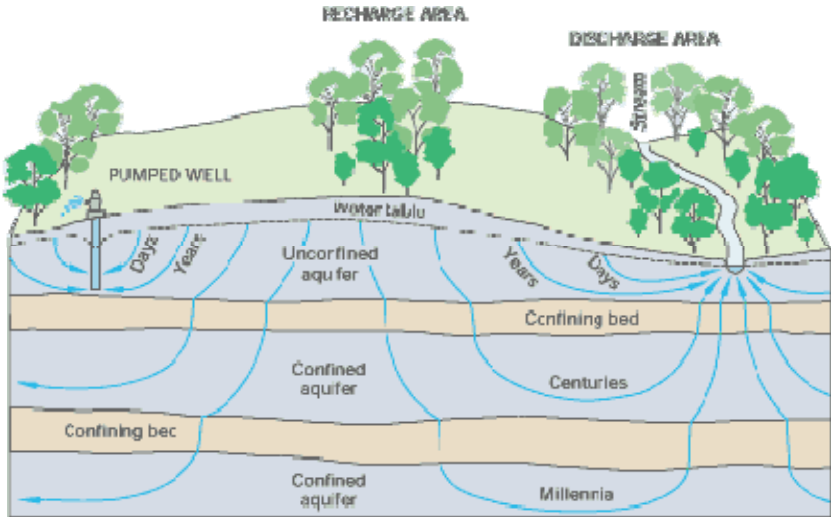

Figure 2.2 Groundwater flow patterns (Source: http://pubs.usgs.gov/circ/circ1139/images/fig03.gif)

Depending on the hydraulic conductivity of the material, the saturated zone is divided into aquifers, which are layers of high conductivity, and aquitards, which are layers of low conductivity. The main part of groundwater flow is transmitted in aquifers, whereas aquitards retard flow and most often only transmit very little water. (Fitts, 2002). Aquifers can be either unconfined or confined. An unconfined aquifer is defined as an aquifer, where the groundwater table occurs within the aquifer layer, whereas a confined aquifer is defined as an aquifer where the whole aquifer layer is saturated and a confining layer is present above. The water level in a confined aquifer thus rises above the confining layer (Fitts, 2002).

Another important parameter in relation to groundwater flow is storativity. This is a measure of the amount of water released by a unit decline in hydraulic head. In an unconfined aquifer gravity drainage is the dominant mechanism for storage change and the storativity is expressed by the specific yield (S_y), which describes the amount of water released due to a decline in groundwater table. For a confined aquifer the storativity is described by the specific storage (S_s), which is a measure of water release due to elasticity of the water and the soil matrix (Fitts, 2002). The specific storage is orders of magnitude smaller than the specific yield (Refsgaard et al, 2003).

2.1.4 Groundwater-surface water exchange

There is often hydraulic contact between groundwater and surface waters, which mean an exchange of water can happen. The most important physical parameters for describing the water exchange between groundwater and streams are the hydraulic conductivity and thickness of the sediment at the stream bottom (Refsgaard et al, 2003). The relationship between these two parameters is defined by the leakage coefficient.

A surface water body can either receive or deliver water to the groundwater depending on the hydraulic head in the surrounding groundwater (Refsgaard et al 2003). Figure 2.3 shows two situations for interaction between groundwater and a stream. If the hydraulic head in the groundwater is higher than the elevation of the water surface in the stream (A), groundwater will discharge to the stream and the stream will be a so-called gaining stream. If the hydraulic head on the other hand, is less than the elevation of the water surface, the stream will lose water to the groundwater and the stream is then a losing stream (Healy et al, 2007). In humid climates, as in Denmark, the groundwater table is generally high and streams in Denmark are thus mainly gaining streams (Fitts, 2002).

The interaction between groundwater and a stream can however shift through the year due to fluctuations in hydraulic head (Griffiths et al, 2006). A stream can also be gaining in some reaches and losing in other reaches (Healy et al, 2007). It is a common position that groundwater discharge to a stream increases with distance downstream. Studies have however shown that this is not always the case and that the topography of the catchment has a large influence on the pattern of groundwater discharge to streams (Grapes et al, 2005).

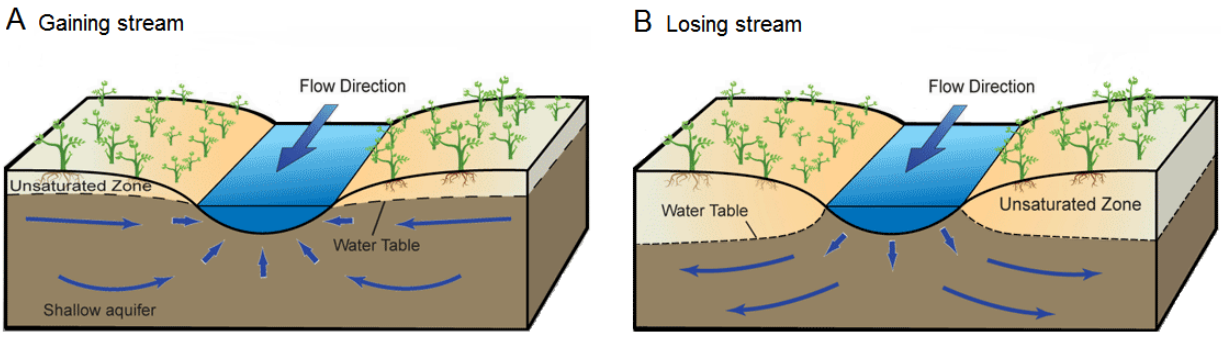

Figure 2.3 Groundwater-stream interactions. A) Gaining stream: Hydraulic head in groundwater is higher than the water surface in the stream. B) Losing stream: Hydraulic head in groundwater is lower than the water surface in the stream (Source: www.connectedwater.gov.au/processes/controlling.html)

2.1.5 Stream discharge

All water flowing in streams originate from precipitation, though the way to a stream differs greatly. Water can reach a stream as overland flow, drain flow and groundwater discharge. Overland flow and drain flow occur under and just after a precipitation event and are thus quick flow responses, which constitute the more transient component of stream discharge (see figure 2.4). These quick flow components thus result in the peaks on the stream hydrograph. Groundwater discharge responds much slower on a precipitation event and is a more constant component of stream discharge. The groundwater contribution to a stream is also called base flow. Because of the slower response, the base flow component maintains low flow during dry periods (Fitts, 2002).

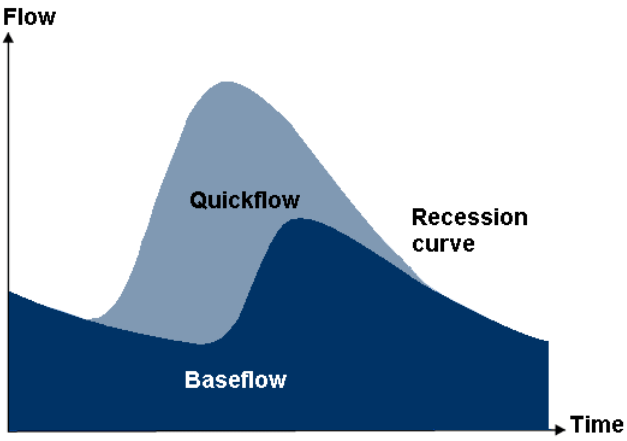

Figure 2.4 Components of a stream hydrograph

The geology of the catchment affects the discharge pattern to the stream. If the materials are very permeable, most precipitation will infiltrate, and the stream flow will mainly consist of base flow and not a lot of quick flow. This results in a rather constant stream discharge with small fluctuations. If the geology instead consists of low permeable materials, most precipitation will not infiltrate, and the stream discharge instead consists mainly of quick flow, resulting in great fluctuations in stream discharge (Fitts, 2002).

2.1.6 Water balance on catchment scale

The hydrological cycle can be described quantitatively by a water balance, which is a useful method for estimating unknown fluxes in a hydrological system. A water balance is the basic concept of conservation of mass in relation to water fluxes and can be expressed as (Fitts, 2002):

$$flux_{in} = flux_{out} + \Delta storage$$

On catchment scale the water balance is described as the flux of water in and out of the catchment as follows (Refsgaard et al, 2003):

$$P + Q_{gwin} = E_a + Q_s + Q_{gwout} + Q_a + \Delta S$$

P: precipitation
E_a: actual evapotranspitration
Q_s: stream discharge
Q_{gwout}: groundwater outflow
Q_{gwin}: groundwater inflow
Q_a: groundwater abstraction
ΔS: storage change

There is a considerable uncertainty on the water balance on catchment scale as a result of uncertainties on the estimate of the individual terms in the equation. Estimates of precipitation and evapotranspiration are particularly subject to considerable uncertainty. The measurements of these terms are most often point measurements, which are subsequently upscaled to catchment scale (Refsgaard et al, 2003).

2.2 Transport and fate of nitrate at catchment scale

Nitrogen is an important nutrient for plant growth and is used by plants for building proteins and amino acids (Mayhew, 2004). Nitrogen is added to agricultural areas as fertilizer and animal manure. The necessary amount depends on soil type, crop type and nutrient state of the soil. The use of nitrogen fertilizer greatly increased from the 1940-50s until around 1990, where after the use has been decreasing due to political actions (Berthelsen & Fenger, 2005).

2.2.1 Nitrate transport at catchment scale

The input of nitrogen in a catchment originates mainly from application of fertilizer and manure, though nitrogen is also added to the catchment by atmospheric deposition and fixation of atmospheric nitrogen (Berthelsen & Fenger, 2005). Nitrogen is present in the soil in both organic and inorganic forms. Organic nitrogen is not available for plant uptake, whereas the inorganic compounds nitrate and ammonium are plant available N-forms. Organic nitrogen is mineralized in the soil to nitrate and ammonium and is thereby made plant available (Berthelsen & Fenger, 2005).

Ammonium (NH_4^+) is a cation and can therefore participate in cation exchange and is thereby bound on the negative surfaces of soil particles. Ammonium is thus bound relatively strongly in the soil, and the ammonium that is not used by plants is therefore not leached from the soil (Berthelsen & Fenger, 2005). Nitrate (NO_3^-) however is an anion and is therefore not bound in the soil (Berthelsen & Fenger, 2005). As nitrate is not absorbed in the soil nor forms insoluble minerals that can precipitate, is nitrate that is not used by plants leached from the soil (Appelo & Postma, 2005). Nitrate is thus transported out of the root zone with the percolating water to the saturated zone, from where it is transported further on to surface waters.

2.2.2 Nitrate reduction

The most important sink in the nitrogen balance at catchment scale, besides plant uptake, is reduction of nitrate to free nitrogen (N_2) (Hansen, 2006). Nitrate reduction can take place in the soil, wetlands, stream sediments and in the saturated zone (Hansen, 2006), though the focus in this study is the reduction of nitrate in the saturated zone.

Nitrate is a strong oxidant (Berthelsen & Fenger, 2005) and will thus participate in redox-reactions, whereby nitrate is reduced to N_2. The reaction can be described by the following half-reaction (Appelo & Postma, 2005):

$$2NO_3^- + 12H^+ + 10e^- \rightarrow N_2 + 6H_2O$$

As oxygen is thermodynamically preferred compared to nitrate, reduction of nitrate will only happen under anaerobic conditions and thus in the reduced part of the saturated zone. Furthermore, for reduction of nitrate to happen, a reduced compound must be present to be the electron donor in the reaction (Appelo & Postma, 2005). Organic carbon is a very important reduced compound found in aquifer sediments (Berthelsen & Fenger, 2005). The reduction of nitrate by organic carbon is called denitrification and is describe by the reaction (Appelo & Postma, 2005):

$$5CH_2O + 4NO_3^- \rightarrow 2N_2 + 4H_2CO_3 + 2H_2O$$

Because of the relatively low temperatures in the groundwater, the reduction with organic carbon will only take place when catalyzed by microorganisms. Microorganisms catalyze redox-reactions to utilizing the energy that is released by the reaction (Berthelsen & Fenger, 2005). The rate of nitrate reduction is affected by the supply of electron donor and by temperature, due to higher biological activity at higher temperatures (Hansen, 2006).

Reduction of nitrate by organic carbon is well documented (Appelo & Postma, 2005). Though, organic carbon is not the only electron donor capable of reducing nitrate. Pyrite (FeS_2) and Fe(II) have also been found to be able to reduce nitrate. Pyrite is found in the sand and silt fraction especially on lowland soil and in anaerobic subsoils (Berthelsen & Fenger, 2005) and Fe(II) is found in clay minerals (Appelo & Postma, 2005). The nitrate reduction by pyrite can be described by the following reaction (Appelo & Postma, 2005):

$$5FeS_2 + 14NO_3^- + 4H^+ \rightarrow 7N_2 + 5Fe^{+2} + 10SO_4^{-2} + 2H_2O$$

The reaction with Fe(II) is described by the reaction (Appelo & Postma, 2005):

$$10Fe^{+2} + 2NO_3^- + 14H_2O \rightarrow N_2 + 10FeOOH + 18H^+$$

Nitrate reduction by pyrite has been reported in several studies and in Denmark by Postma et al (1991) for a sandy aquifer at Rabis Creek in Jutland (Appelo & Postma, 2005). This study also reported that if pyrite is present in the sediments, the reaction with pyrite will often be more important in the reduction of nitrate than organic carbon (Postma et al, 1991). The reduction of nitrate by Fe(II) in clay minerals was reported by Ernstsen & Mørup (1992) in a clayey aquitard at Sparresholm on Zealand in Denmark.

That nitrate is in fact removed from the saturated zone by reduction, can be verified by means of age dating of groundwater. Groundwater of less than 60-50 years of age, which must have contained considerable amounts of nitrate when recharged, now appears without nitrate in the reduced zone, and it is therefore concluded that nitrate is effectively removed by reduction in the reduced part of the saturated zone (Ernstsen & Mørup, 1992).

2.2.3 Redox-interface

The transition from oxidized to reduced conditions in the saturated zone is called the redox-interface. In Quaternary sediments nitrate is found to disappear at this interface (Hansen, 2006). This has been reported by e.g. Postma et al (1991) and Ernstsen & Mørup (1992), who found the nitrate content to decrease to below detection limit at the redox-interface.

The reduction that happens at the redox-interface is often the most important process in the total nitrate reduction on catchment scale (Alectia, 2009). Thus, the amount of nitrate reduction in the saturated zone is not only very dependent on the depth to the redox-interface, but also on the flow pattern, as the nitrate needs to be transported under the redox-interface. Figure 2.5 shows two illustrations of how the depth of the redox-interface affects the amount of nitrate reduction and amount of nitrate transported to the stream. If the depth to the redox-interface is large (A), only a small fraction of the water will flow under the redox-interface before it reaches the stream and thus most nitrate will end up in the stream. If the interface is closer to the ground surface (B), much more of the water will go under the redox-interface and a larger fraction of the nitrate will be reduced.

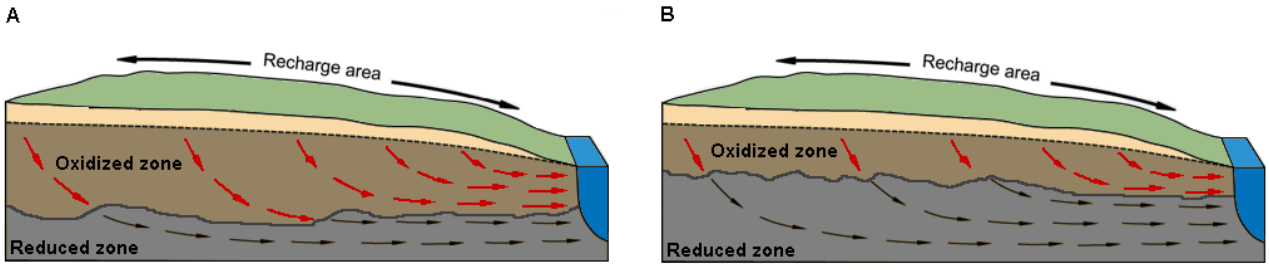

Figure 2.5 Flow patterns in relation to location of the redox-interface. The interface is located closer to ground surface in B than in A resulting in more water being transported under the interface and thus more nitrate being reduced

The depth to the redox-interface is dependent on the supply of oxidized and reduced compounds, the amount of recharge and the ability of the soil to restore the reduction capacity (Henriksen et al, n.y.). In clayey till sediments the depth to the redox-interface is, on average, 3-7 meters, whereas the redox-interface in sandy sediments is found significantly deeper at around 15-20 meters below surface (Henriksen et al, n.y.). These are, however, very general depths and the redox-interface has been found to vary significantly not only between locations, but also over short distances on the same location (Hansen et al, 2008). The large

variability makes it difficult to asses the correct location of the interface and this is therefore a large uncertainty factor in nitrate modelling at catchment scale. An additional uncertainty factor is that, in heterogeneous areas, oxidized zones can be found under the redox-interface (Henriksen et al, n.y.) as well as local anaerobic zones may be present above the redox-interface in the oxidized zone (Hansen, 2006). These zones are difficult to implement in models.

Oxidized and reduced sediments can be distinguished by colour as oxidized sediments have yellow, yellow-brown, brown and grey-brown colours and reduced sediments grey, brown-grey and black colours (Ernstsen et al, 2001). Hansen et al (2008) found that the transition zone from low to high reduction capacity in a clayey aquitard occurred within 1 meter above or below the colour change, and thus concluded the colour change of sediments as a good indication of the redox-interface. The depth to the redox-interface can thus be estimated based on colour descriptions of the sediments from borehole data, which has been done in many Danish nitrate modelling studies. Though, this only gives information on the depth to the redox-interface on point scale and the location of the interface between these points must thus be "guessed", which is most often done by means of interpolation.

2.3 Nitrate monitoring and modelling in Denmark

2.3.1 Danish aquatic environment action plans and the LOOP-programme

The growing problem of nitrate pollution of Danish groundwater and eutrophication of freshwater and marine environments led to the adoption of the first Danish action plan for the aquatic environment (the NPO-action plan) in 1985. This action plan has subsequently been followed by Aquatic Environment Plans 1, 2 and 3 in 1987, 1998 and 2004 respectively. These action plans have introduced different rules and regulations on the use of fertilize and animal manure, in addition to other actions to lower the leaching of nutrients from the agriculture (Grant et al, 2007).

In order to evaluate the effects of these action plans the Danish Agricultural Watershed Monitoring Programme LOOP (In Danish: Landovervågningsprogrammet) was established in 1989 (Grant et al, 2007). The aim of the LOOP-programme is to estimate the leaching of nutrients from cultivated areas and the transport of these to the aquatic environment by measuring water and nutrient flows in Danish catchments. This provides information to evaluate the agricultural pollution of the aquatic environment and the relationship between agricultural practice and nutrient loss (Rasmussen, 1996).

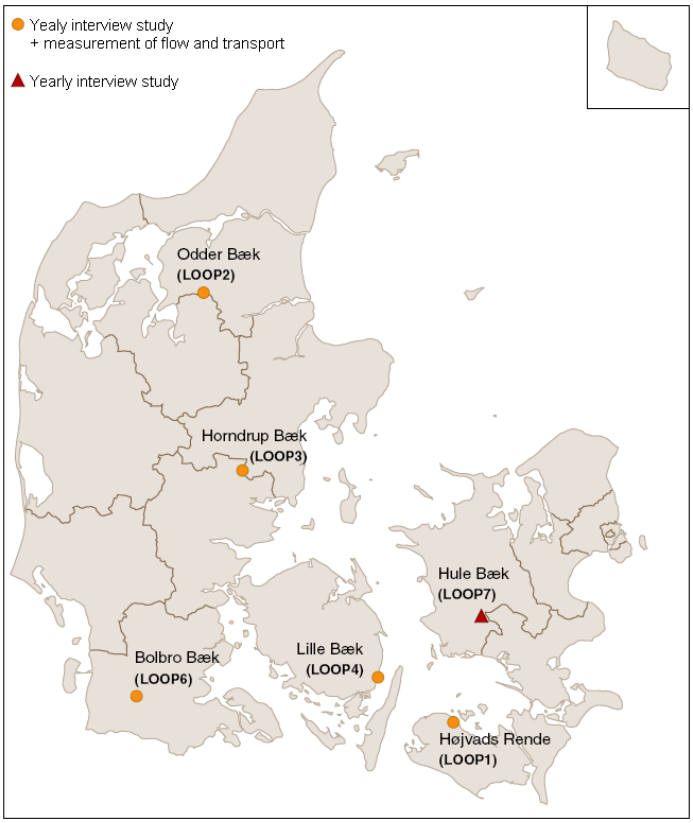

Figure 2.6 Location of the LOOP-catchments (Grant et al, 2007)

The LOOP-programme consists of 6 Danish catchments of between 5-15 km^2 (in the period 1998 - 2004 the programme consisted of 7 catchments). The location of the catchments is seen on figure 2.6. The catchments have been selected to represent the national average with respect to climate, soil type and agricultural practice. Though, as the livestock density in the LOOP catchments in 2006 increased to an average of 1.12 animal units per hectare, the livestock density in the catchments is now somewhat larger than the national average of 0.87 (2006 value) (Grant et al, 2007).

The monitoring programme consists of measurements of water flow and nutrient concentrations in all parts of the hydrological cycle in a network of measurement stations established in 5 of the 6 catchments (Grant et al, 2007). In all LOOP-catchments yearly interview studies about agricultural practice are conducted among farmers to follow the trend in farming practices and to estimate the input and output of nutrients on field level (Rasmussen, 1996).

2.3.2 Nitrate modelling at catchment scale in Denmark

Numerous model studies on the transport and fate of nitrate from agricultural areas have been reported in the literature. The models are defined based on the complexity of the process description as either pure black box models, lumped conceptual models or physically based models. Physically based models are more desirable because they are based on physical equations for the description of flow and transport, though a disadvantage is that they are very data-intensive (Hansen 2006).

The physically based models used for simulating nitrate transport can be divided into root zone models, which describe the percolation of water and leaching of nitrate from the root zone, and spatially distributed catchment models, which describe the transport and fate of nitrate from below the root zone and to the stream system. A coupling of such a root zone model with a catchment model can be used for a physically based modelling of the whole catchment system.

In nitrate modelling studies in Denmark, the combined catchment approach Daisy/MIKE SHE has been used for modelling of the entire catchment system. The Daisy/MIKE SHE modelling approach is a combination of the physically based root zone model Daisy and the distributed physically based catchment model MIKE SHE. This modelling approach enables an integrated modelling study of the movement and fate of nitrogen from its application on the field to its appearance as nitrate in the stream. It is this modelling approach that is used in this study.

In Denmark the Daisy/MIKE SHE modelling approach has been applied for the study areas of Odense catchment (Refsgaard et al, 1999; Nielsen et al, 2004; Hansen, 2006) and Karup catchment (Styczen & Storm, 1993a,b; Refsgaard et al, 1999) in addition to the LOOP areas of Odderbæk catchment (Hansen & Ramussen, 2006; Hansen et al, 2006), Højvads Rende catchment (Alectia, 2008; Alectia, 2009) and Bolbro catchment (Alectia, 2010a; Alectia, 2010b).

The general approach in the Danish studies is to include nitrate reduction in the root zone and at the redox-interface in the aquifer using an assumption of instantaneous reduction of nitrate at the redox-interface. Nitrate is assumed to be non-reactive above the redox-interface in most of the studies. Though, in Hansen et al (2009) and Hansen et al (2006) reduction in the oxidized zone has been applied in an attempt to account for local anaerobic zones above the redox-interface. Reduction in wetland areas has been included in Hansen et al (2009), Hansen et al (2006), Alectia (2008; 2009) and Alectia (2010a; 2010b) by raising the redox-interface close to ground surface in these areas. Furthermore, Hansen et al (2009) has applied reduction in the stream system. However, Hansen et al (2009) found, that the reduction in wetlands and stream sediments was limited compared to the reduction in the saturated zone.

The general findings in the Danish nitrate modelling studies are that overall water and nitrogen balances are simulated acceptable, but there are problems with simulating the daily dynamics for both water and nitrate fluxes. The models perform well on catchment scale, but the predictability of the models decrease with scale and the present models therefore do not have predictable capability on field scale.

3. Modelling framework

The modelling framework used in this study is the combined Daisy/MIKE SHE modelling approach. The Daisy model has been used for simulating percolation and nitrate leaching from the root zone and this data is used as input to MIKE SHE. The Daisy simulations have been preformed by The National Environmental Research Institute (NERI) and were thus made independently of this study. This study concerns the onwards transport of water and nitrate from the bottom of the root zone to the stream system, which is simulated with MIKE SHE. In the following sections are found a short description of Daisy and a more thorough description of MIKE SHE. Finally is the coupling of Daisy and MIKE SHE described.

3.1 Daisy

Daisy is a one-dimensional physically based root zone model. The model describes water flow as well as transport and transformation of nitrogen and carbon in the root zone of the unsaturated zone and furthermore includes a module for description of agricultural practice. Daisy is thus capable of simulating nitrate leaching from a soil column on a cultivated area (Pedersen et al, 2010). The Daisy model has been used in a large number of studies and is well validated.

Daisy simulates flow and leaching of solutes through three different pathways; matrix flow, macro pore flow and drain flow (Hansen, 2006). Matrix water flow is described as Darcy flow by Richards' equation, which is the governing differential equation for vertical water flow in an unsaturated soil (Jensen, 2004):

$$\frac{\partial \theta}{\partial t} = \frac{\partial}{\partial z}\left(K \frac{\partial \Psi}{\partial z} \right) + \frac{\partial K}{\partial z} - S \qquad (3.1)$$

θ: volumetric water content
K: unsaturated hydraulic conductivity
Ψ: pressure head
S: sink

Daisy solves Richard's equation (3.1) using a finite difference technique. The hydraulic conductivity in the unsaturated zone is variable and dependent on water content, which is a function of pressure head. These relationships can be described by parametric functions (Jensen, 2004). In the Daisy simulations preformed for the Lillebæk catchment the van Genuchten model has, in combination with Mualem's equation, been used for describing the retention and the hydraulic conductivity functions (Pedersen et al, 2010). The lower boundary in Daisy can be specified as a constant groundwater table, a gravitational gradient or a time-varying groundwater level including drains. The lower boundary condition has a large influence on the simulation results (Nielsen et al, 2004).

The nitrogen processes simulated in Daisy includes immobilization, mineralization, nitrification, denitrification, plant uptake and leaching. The distribution of solutes in the soil profile is described in Daisy by the advection-dispersion equation (Hansen, 2000).

3.2 MIKE SHE

MIKE SHE is a physically based integrated catchment model. MIKE SHE is capable of simulating flow and transport in the entire land based part of the hydrological cycle with fully dynamic exchange of water and solutes between all hydrological components (Hansen, 2006). MIKE SHE includes process models describing evapotranspiration, 1D unsaturated, 1D river, 2D overland and 3D saturated flow and transport and their interactions. MIKE SHE has a modular structure making it possible to only include the processes of relevance to a certain study and which also allows each process to be solved at its own relevant spatial and temporal scale (DHI, 2009b). The river flow is simulated using the river model MIKE11, which is a separate model. MIKE11 can be run independently of MIKE SHE and has a wide range of facilities in relation to surface water modelling beyond those used in this study. The coupling between MIKE SHE and MIKE11 is with fully dynamic feedback between the two models and is described in more detail below (DHI, 2009a). MIKE SHE has been used in a broad range of applications in many different countries by universities, research groups and consulting companies. MIKE SHE has been found to be applicable at spatial scales ranging from a single soil column to areas covering several catchments. MIKE SHE has also been used on a wide range of climatic and hydrological regimes and the model is therefore well tested (DHI, 2009b). In this study the MIKE SHE components for describing saturated, overland and river flow and transport has been used. It the following the governing equations for flow and transport for these components is described.

3.2.1 Flow description

Saturated flow

Saturated flow is mathematically described by combining the Darcy equation and the principle of conservation of mass (Fitts, 2002). The governing equation for transient three-dimensional saturated flow through an anisotropic and heterogeneous aquifer can thus be expressed as (DHI, 2009c):

$$S\frac{\partial h}{\partial t} = \frac{\partial}{\partial x}\left(K_x \frac{\partial h}{\partial x}\right) + \frac{\partial}{\partial y}\left(K_y \frac{\partial h}{\partial y}\right) + \frac{\partial}{\partial z}\left(K_z \frac{\partial h}{\partial z}\right) + Q \quad (3.2)$$

K_x, K_y, K_z: hydraulic conductivity along x, y and z axes of the model
h: hydraulic head
Q: sources/sinks
S: specific storage

This partial differential equation (3.2) is solved numerically in MIKE SHE by an iterative implicit finite difference method (DHI, 2009c). In order to solve the equation, initial and boundary conditions must be specified. In MIKE SHE boundary conditions can be specified as constant head, gradient and head-dependent flux boundaries (DHI, 2009c). The upper boundary condition for the saturated zone is, in this study, the percolation predicted by Daisy.

A special internal boundary condition that can be defined for the saturated zone is drainage by subsurface drains (DHI, 2009b). If groundwater levels exceed a specified drain level, drain flow is generated. Drain flow occurs in the layer of the model where the drain level is located and is simulated using an empirical formula. The amount of drain flow depends on the height of the groundwater table above the drain level and a specified time constant. The drain flow is routed to a recipient point using a linear reservoir routing description and the time constant describes the average retention time in the reservoir. The recipient point can be a river link, another SZ grid cell or a model boundary (DHI, 2009c).

Overland flow

The overland flow component simulates the flow of water across the ground surface. The overland flow component is required when running MIKE11 together with MIKE SHE and must therefore also be applied in study areas where overland flow is not occurring (DHI, 2009b). Fully dynamic overland flow is described by a two-dimensional version of the Saint-Venant equations. As it is numerically challenging to solve these equations, the Saint-Venant equations are simplified using a diffusive wave approximation. Using the Manning description for slope friction, the governing equations for overland flow can be expressed as (DHI, 2009c):

$$uh = M\left(-\frac{\partial z}{\partial x}\right)^{1/2} h^{5/3} \quad (3.3)$$

$$vh = M\left(-\frac{\partial z}{\partial y}\right)^{1/2} h^{5/3} \quad (3.4)$$

u: flow velocity in x-direction
v: flow velocity in y-direction
h: water depth
M: Manning number
z: ground surface level

The equations 3.3 and 3.4 are solved by an iterative implicit finite difference method. The outer boundary condition for overland flow can be defined as a specified head, which is based on the specified initial water depth in the outer cells of the model domain. Normally an initial water depth of zero is used. During the simulation the water depth at the model boundary will increase and water can discharge across the boundary. If a no-zero value is used for initial water depth, water will flow into the model until the water level in the model has increased to the specified depth. The boundary can also be specified as a no-flow boundary and MIKE SHE will then keep all overland flow inside the model domain (DHI, 2009b).

River flow

One-dimensional river flow is, as mentioned, simulated with MIKE 11. In this study MIKE 11 is applied with the fully dynamic wave description which solves the vertically integrated Saint-Venant equations. Using the Manning description of bed resistance, the basic flow equations in MIKE 11 can be expressed as (DHI, 2009a):

$$\frac{\partial Q}{\partial x} + \frac{\partial A}{\partial t} = q \tag{3.5}$$

$$\frac{\partial Q}{\partial t} + \frac{\partial \alpha\left(\frac{Q^2}{A}\right)}{\partial x} + gA\frac{\partial h}{\partial x} + \frac{gQ|Q|}{M^2 A R^{4/3}} = 0 \tag{3.6}$$

Q: discharge
A: flow area
q: lateral inflow
h: water level
g: gravity
M: Manning number
R: resistance radius
α: momentum distribution coefficient

Equation 3.5 and 3.6 are solved using implicit finite difference approximations for the computational grid defined for the river network. The computational grid consists of altering Q- and h-point, where discharge and water level respectively is calculated at each time step (DHI, 2009a).

To solve the equations 3.5 and 3.6 initial and boundary conditions must be defined. Boundary conditions must be defined at all upstream and downstream ends of river branches that are not connected to another branch. The boundary conditions can be defined as a constant flow or water level or a time-varying flow or water level boundary. At least one water level boundary condition must be defined for a river system otherwise the system will become ill-defined (DHI, 2009a).

3.2.2 Solute transport description

Saturated transport

Transport of solutes in the saturated zone is described by the three-dimensional advection-dispersion equation for a porous medium (DHI, 2009c):

$$\frac{\partial c}{\partial t} = -\frac{\partial}{\partial x_i}\left(c v_i\right) + \frac{\partial}{\partial x_i}\left(D_{ij}\frac{\partial c}{\partial x_j}\right) + R_c \qquad i, j = 1,2,3 \tag{3.7}$$

c: concentration of solute
R_c: sources/sinks
D_{ij}: dispersion coefficient tensor
v_i: velocity tensor

The advection-dispersion equation (3.7) is solved numerically using an explicit finite different scheme (DHI, 2009c). The transport mechanisms included in the equation are advective transport with the flowing groundwater and dispersive transport. Dispersion includes the spreading of solutes due to molecular diffusion and mechanical dispersion, which is spreading due to flow in a porous media. In most cases molecular diffusion is very small compared to mechanical dispersion and can therefore be neglected. Only in materials with very small conductivities and when the scale of study is small is diffusion important. When neglecting diffusion, the dispersion coefficient can be described as a function of dispersivity and flow velocity (Fitts, 2002). Mechanical dispersion occurs in all directions, though MIKE SHE offers simplifications with respect to dispersivities, and in this study the simplification of isotropy is used. Thus, the dispersivity tensor consists only of longitudinal (α_L) and transverse (α_T) dispersivity (DHI, 2009c).

The dispersion term in equation 3.7 accounts for the spreading of the solutes that is not described by the simulated advective flow due to inadequate description of the heterogeneity of the material. This means, that the more refined the description of heterogeneity is, the smaller dispersivities need to be applied in the model (DHI, 2009c).

Initial conditions and boundary conditions must be defined for solving equation 3.7. Boundary conditions can be specified as prescribed concentration and prescribed flux concentration. All no-flow boundaries in the hydrological model will be treated as no-flux boundaries in transport simulations. Catchment boundary cells with a specified head are treated as fixed concentration cells with a concentration equal to the initial concentration (DHI, 2009c). The boundary condition at the water table in the saturated zone is, in this study, the nitrate leaching predicted by Daisy.

Overland transport

In surface water the mixing and spreading of solutes is mainly due to turbulence when flow velocity reaches a certain level. This process is known as turbulence diffusion and is much more important than molecular diffusion. The spreading in surface water is thus physically different from spreading in groundwater, but the transport in surface waters is nevertheless described using the advection-dispersion equation. The transport of solutes in overland flow is described by a two-dimensional version of the advection-dispersion equation (DHI, 2009c):

$$\frac{\partial c}{\partial t} = -\frac{\partial}{\partial x_i}\left(c v_i\right) + \frac{\partial}{\partial x_i}\left(D_{ij}\frac{\partial c}{\partial x_j}\right) + R_c \qquad i, j = 1,2 \qquad (3.8)$$

c: concentration of solute
R_c: sources/sinks
D_{ij}: dispersion coefficient tensor
v_i: velocity tensor

Equation 3.8 is also solved using an explicit finite different scheme. The dispersion coefficient in overland flow depends on the uniformity of the velocity distribution and to some extent on the mean flow velocity. But as there is no general relation between dispersion and the mean flow velocity are the dispersion coefficients for overland flow assumed constant in time and are specified directly in MIKE SHE (DHI, 2009c).

River transport

The advective transport with the river flow and the dispersive transport in MIKE11 are also described using the advection-dispersion equation, but in a one-dimensional version (DHI, 2009a):

$$\frac{\partial Ac}{\partial t} + \frac{\partial Qc}{\partial x} - \frac{\partial}{\partial x}\left(AD\frac{\partial c}{\partial x}\right) = -AKc - c_s q \qquad (3.9)$$

A: cross-sectional area
c: concentration of solute
Q: discharge
D: dispersion coefficient
K: linear decay coefficient
c_s: source/sink concentration
q: lateral inflow

Equation 3.9 is solved using an implicit finite difference scheme. The boundary conditions for transport simulation in MIKE11 can be specified as a closed boundary, an open outflow boundary or an open inflow boundary with a constant or time-varying concentration (DHI, 2009a).

Reactive transport – degradation

Degradation of nitrate is included in this study in the saturated zone and is described by a first-order degradation process with an exponential decrease in concentration (DHI, 2009c):

$$\frac{\partial c}{\partial t}_{react} = \frac{-\ln 2}{\lambda} c \qquad (3.10)$$

c: concentration of solute
λ: half-life

Time step and grid size in transport simulations

As explicit methods are used for the solution of the advection-dispersion equation, time steps and grid size must not be too large as this will result in numerical errors. The maximum allowed time step (or grid size) is determined by the advective and dispersive Courant number. The advective Courant number in x-direction is defined as (DHI, 2009c):

$$\sigma_x = \frac{v_x \Delta t}{\Delta x} \qquad (3.11)$$

σ_x: advective Courant number
v_x: flow velocity
Δt: time step
Δx: grid size

The dispersive Courant number in x-direction is defined as (DHI, 2009c):

$$\Gamma_x = D_x \frac{\Delta t}{\Delta x^2} \qquad (3.12)$$

Γ_x: dispersive courant number
D: dispersion coefficient
Δt: time step
Δx: grid size

3.2.3 Particle tracking

MIKE SHE also has a forward particle tracking module, which can calculate the flow path of particles in the saturated zone based on a water flow simulation (Hansen, 2006). The particles are displaced individually in the three-dimensional saturated zone. The movement of the particles is deterministic and is based on the calculated groundwater flow. Although, a stochastic part, where the particles are also moved randomly based on a specified dispersion coefficient, can also be included in the particle movement (DHI, 2009c).

3.2.4 Coupling MIKE SHE/MIKE 11

The coupling between MIKE SHE and MIKE 11 is with fully dynamic feedback between the two models. The exchange is physically based and allows for exchange of water and solutes between the streams and the groundwater. MIKE 11 can also receive water and solutes from MIKE SHE as overland and drain flow (DHI, 2009c).

The stream reaches in MIKE 11 are coupled to MIKE SHE via river links that are located at the edge of the MIKE SHE model grids. This means that the geometry of the river is simplified in MIKE SHE and the degree of simplification depends on grid size. This assumption of the river as a line between the model grids is generally valid if the river width is small relative to the model grids, which is the case in Lillebæk (DHI, 2009c). MIKE SHE can further more only couple to river reaches that are defined as coupling reaches in MIKE11 and MIKE SHE can only couple to one coupling reach per river link, thus the reaches must not be located too closely. MIKE 11 river levels at h-points are interpolated to MIKE SHE river links, where exchange flows from overland and groundwater is calculated. These calculated exchange flows are then fed back to MIKE11 as a lateral inflow or outflow (DHI, 2009c).

The water exchange between the saturated zone and the MIKE 11 streams is defined by a conductance, which is a function of the leakage coefficient, which must be specified in MIKE 11 for each stream reach. The conductance can be calculated in three different ways in MIKE SHE/MIKE 11, as either dependent on the conductivity of the aquifer material only, the conductivity of the river bed material only or on the conductivity of both the river bed and aquifer material. In this study the conductance is specified as depending on the river bed material only.

3.3 Coupling Daisy and MIKE SHE

In the Daisy/MIKE SHE modelling approach the two model codes are coupled sequentially without any feedback from groundwater and streams to the root zone. The Daisy calculations have been performed first, and the results for water and nitrate flux for matrix flow, macro pore flow and drain flow is summed and then implemented in the MIKE SHE catchment model as an input to the top layer of the saturated zone (Hansen, 2006).

During periods of high evapotranspiration water fluxes can be upwards resulting in negative water and nitrate fluxes. MIKE SHE can withdraw water from the saturated zone in periods of negative flux, and if the top layer of the model is dry, it is possible to withdraw water from deeper layers, down to a specified maximum depth and layer. Although, if not enough water is present at this depth/layer, the rest of the negative water flux is neglected. MIKE SHE is also capable of removing nitrate from the model in the same way, though only from the top layer. If the concentration in the top layer reaches zero, the rest of the negative nitrate flux is neglect-ted (Hansen, 2006).

When combining Daisy and MIKE SHE the unsaturated zone in MIKE SHE is substituted by the Daisy calculations. This means that the unsaturated zone beneath the root zone is ignored, thus travel time in the unsaturated zone is being neglected (Hansen, 2006). As the groundwater level in the Lillebæk area in gene-rally is located relatively close to the ground surface (1 - 6 meters below surface) this is believed not to have a great effect on the following simulations.

The Daisy/MIKE SHE approach cannot simulate overland flow generated by high intensity rainfall. However, this is acceptable under Danish conditions as precipitation intensity in Denmark, as mentioned, rarely exceeds the infiltration capacity. Overland flow due to saturation from below in periods of high groundwater levels is simulated by the approach (Refsgaard et al, 1999).

4. Study area - Lillebæk catchment

The area of study is the Lillebæk catchment, which is located near Oure on the island of Funen in Denmark (figure 4.1). Lillebæk is one of the catchments in the LOOP-program (LOOP4) and has therefore been intensively monitored since 1989. Lillebæk represents a clayey catchment in the LOOP-program and has a topographical catchment area of 4.7 km^2 (Grant et al, 2007). The Lillebæk stream is a rather small stream, but is fairly steep and drops from around 50 meters above sea level to sea level over a distance of 3 kilometres. A large part of the stream is submerged in pipelines and only the lower part is a free channel (Styczen et al, 2004).

The land use is mainly intensive agriculture, covering 88% of the catchment (see figure 4.3). The rest of the area consists of 2% forest, 5% other nature and 5% roads and built-up areas (Pedersen et al, 2010). The agriculture in the Lillebæk area is characterized mainly by cereal production and is highly livestock intensive. In 2003 manure was applied to the catchment corresponding to 0.99 animal units per hectare, of which 75% originated from pigs (Pedersen et al, 2010).

Figure 4.1 The Lillebæk catchment (LOOP4) and the location on the island of Funen, Denmark

The average precipitation in the Lillebæk area for the period 1990-2004 was 839 mm/year, although the variation between the years has been rather large, as seen on figure 4.2. The years of 1996 and 2003 were the driest years in the period with less than 600 mm/year and 1994, with close to 1100 mm/year, the wettest.

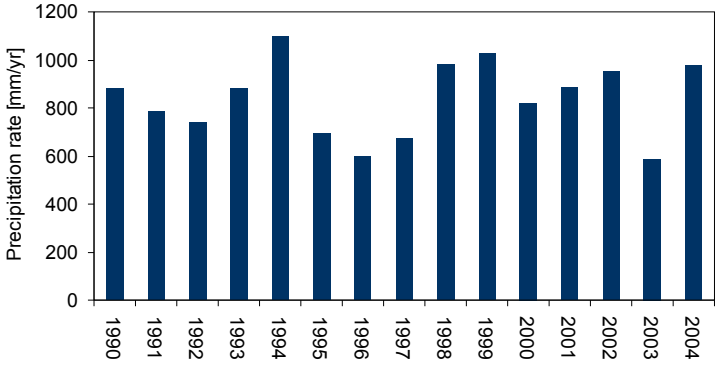

Figure 4.2 Corrected precipitation from DMI's 10x10 km grid covering the Lillebæk area

The landscape in the Lillebæk area was formed during the last ice age (the Weichsel glaciation), during which the area was covered by several ice advances as seen on figure 4.4: i.e. the Old Baltic advance, the Main (NE) advance and the Young Baltic advance (Graversen & Nyegaard, 1989). The upper soil layers in the area are dominated by glacial clayey till (figure 4.5), with some glacial melt water sand north of the LOOP4 catchment. Organic material is also found in the area around streams and in depressions (Petersen et al 1988). On figure 4.6 a digital elevation model (DEM) for the area is seen. The terrain is seen sloping toward the sea from around 50-60 meters above sea level in the western part of the LOOP4 area to a few meters at the coastline, where a low coastal cliff is present. The terrain is cut by the creek valley of Lillebæk, Isebæk and Hammesbro which has a northwest-southeast direction towards the sea (Graversen & Nyegaard, 1989).

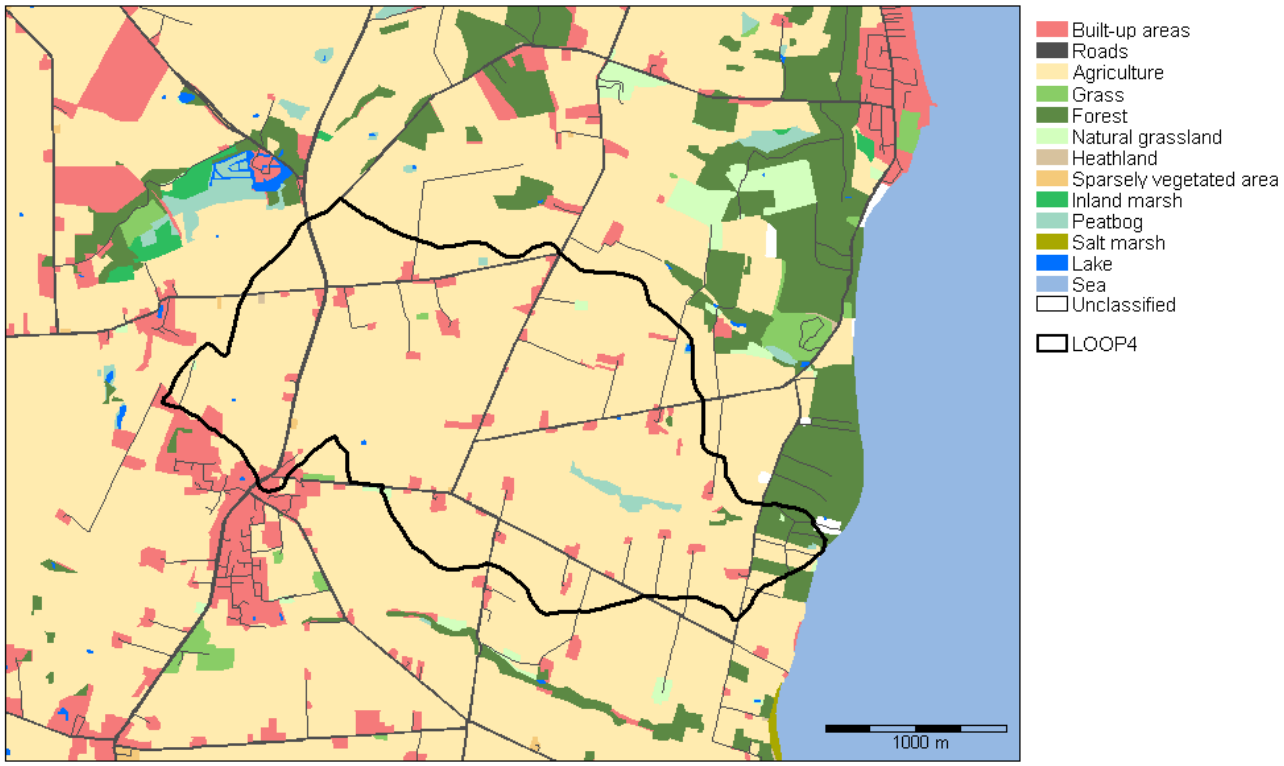

Figure 4.3 Land use in Lillebæk catchment. Land use data is from AIS (Areal Information System)

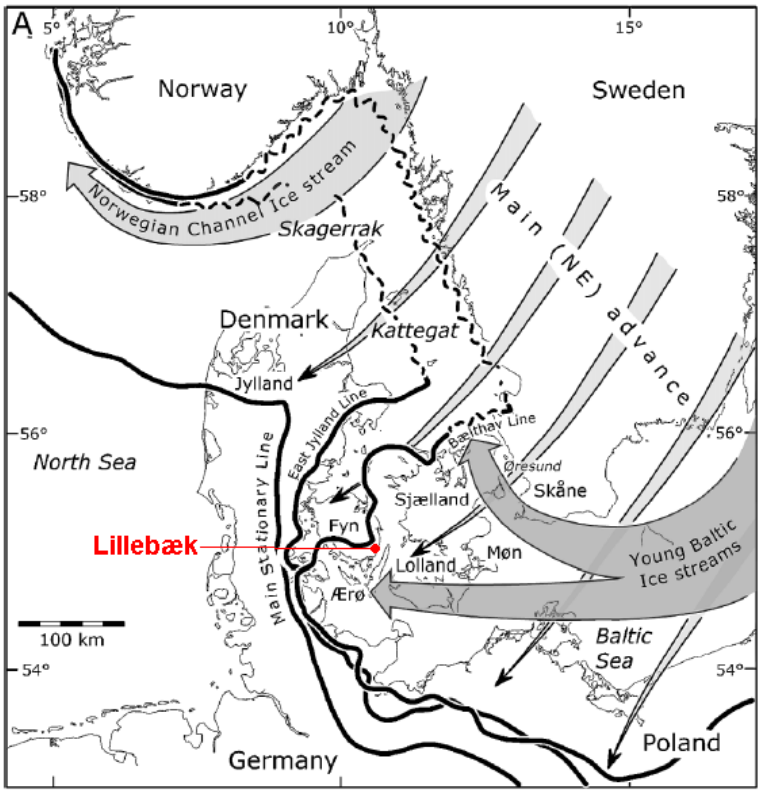

Figure 4.4 The ice movements of the Scandinavia Ice Sheet during the last part of the Weichsel glaciation. The Main Stationary Line indicates the Last Glacial Maximum (LGM) associated with the Main (NE) advance, whereas the East Jylland and Bælthav lines are associated with two Young Baltic advances (Kjær et al, 2003). The location of Lillebæk catchment is indicated on the map

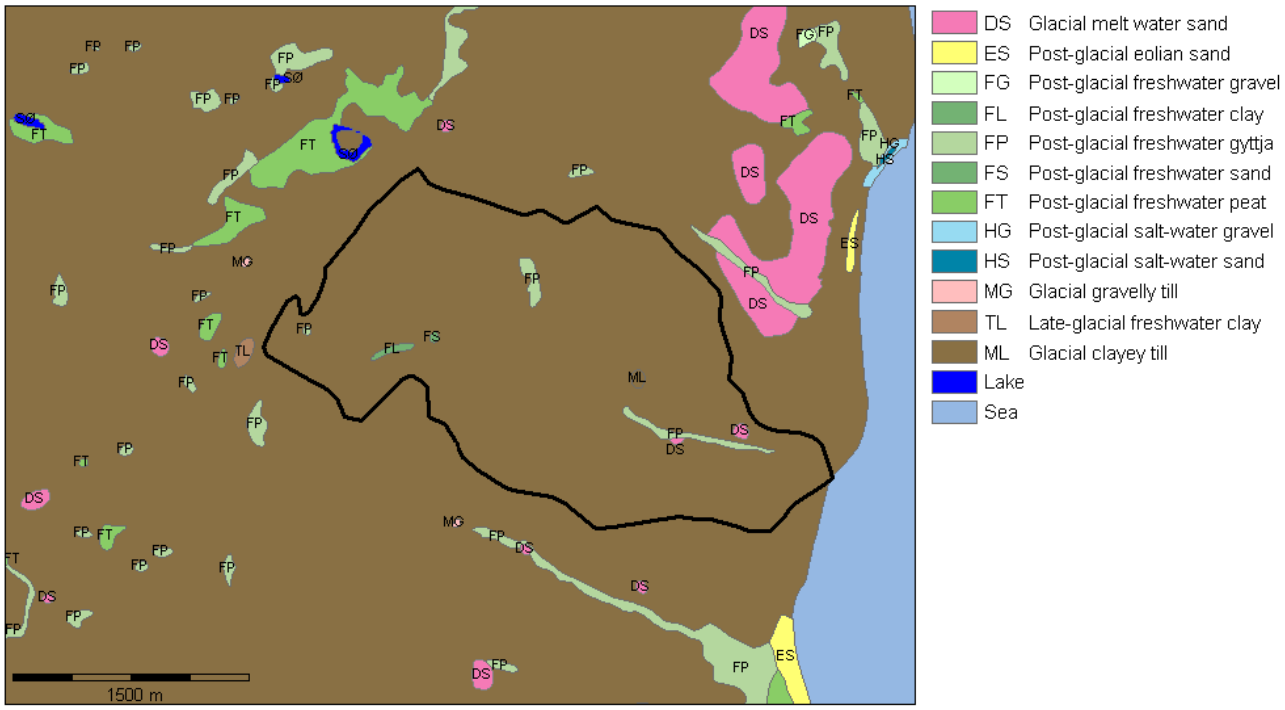

Figure 4.5 Soil map (1:25.000) for the Lillebæk area. Data is from The Danish Digital Soil map published by the Geological Survey of Denmark and Greenland

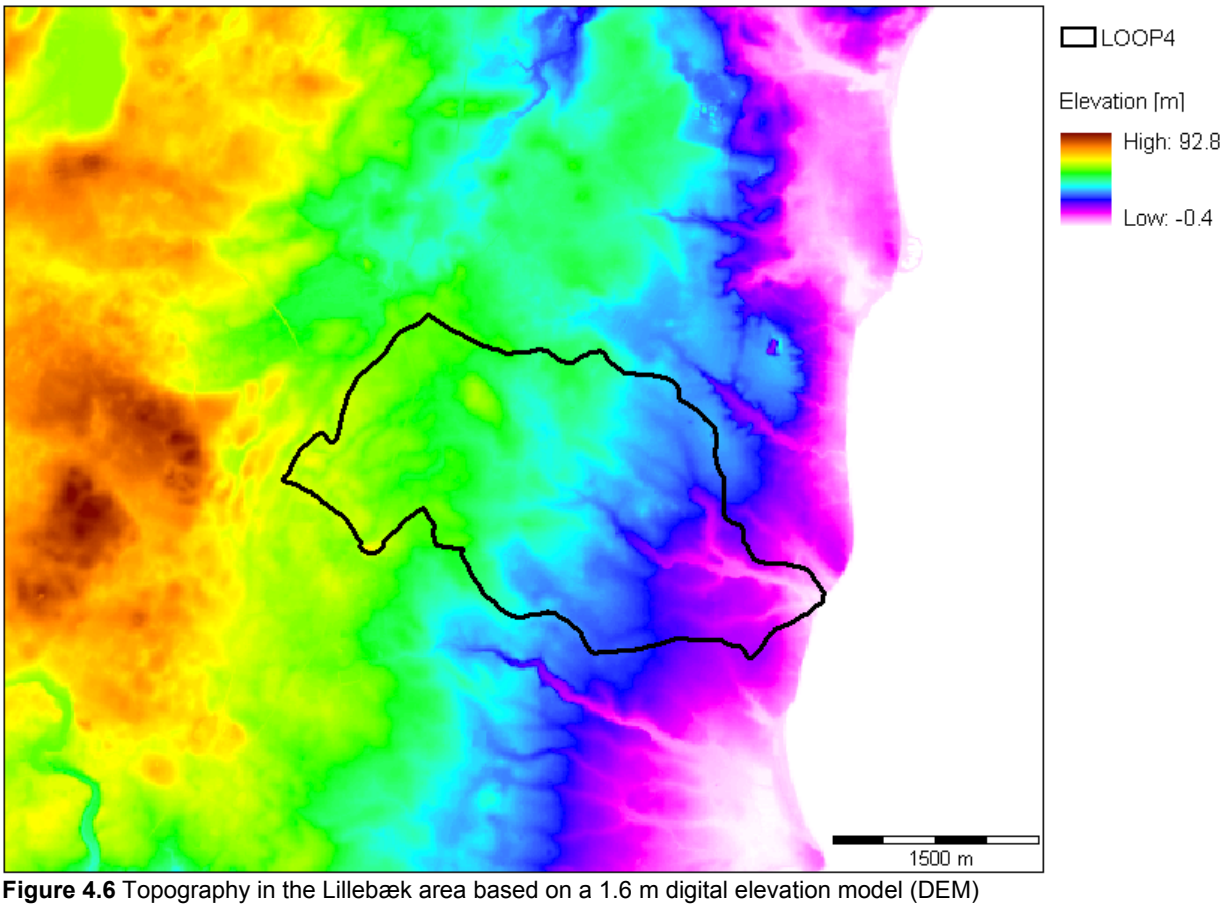

Figure 4.6 Topography in the Lillebæk area based on a 1.6 m digital elevation model (DEM)

5. Data

5.1 Geological data

Borehole data with geological information for the study area is available from the Danish Jupiter database. Borehole data for the municipality of Svendborg, which includes the Lillebæk area, is downloaded from the following website: *http://jupiter.geus.dk/servlet/DownloadPCJupiter.*

The quality of boredata can vary a lot according to the drilling method, the nature of the sediment and the carefulness when sampling and describing the sample. The geological descriptions of the sediments in Jupiter are divided into two groups: (1) Sample descriptions with interpretation of the formation environment and age made by a geologist in the lab, and (2) Sample descriptions made by the well driller in the field. The first group is defined by a double letter symbol e.g. ML (glacial clayey till) and DS (glacial melt water sand), where the first letter describes the formation environment and the second letter the lithology. The second group is described by a single letter symbol e.g. L (clay) and S (sand), which only describes the lithology (Jørgensen et al, 2008).

The quality of the boredata for the Lillebæk area has been assessed according to the depth of the borehole and the quality of the geological description of the sediments. The outcome of this assessment is seen in figure 5.1. The dark green points indicate boreholes with the best information as these boreholes are more than 15 meters deep and have good geological descriptions of the sediments. From figure 5.1 a great lack of geological data is seen in parts of the LOOP4 catchment and in a large area west of the catchment. This will greatly affect the uncertainty of the geological model. Boreholes with colour description of the sediments, which is used to assess the location of the redox-interface, is also indicated on figure 5.1. It is noted that information about sediment colour is even more scarce than lithological information.

Besides borehole data, geophysical data for the Lillebæk catchment area is also available from the Danish Gerda database. This data is, however, not included in the geological model. The reason for the exclusion of this data is partly justified by lack of time and knowledge about geophysics. However, another reason not to include geophysical data at present is the desire, later on, to compare the geological model, based exclusively on borehole data, with a geological model based on geophysical SkyTEM data, which is going to be produced in connection with the NICA project. This will give the opportunity to investigate the difference between two geological models based on different data, and the effects on the hydrological model.

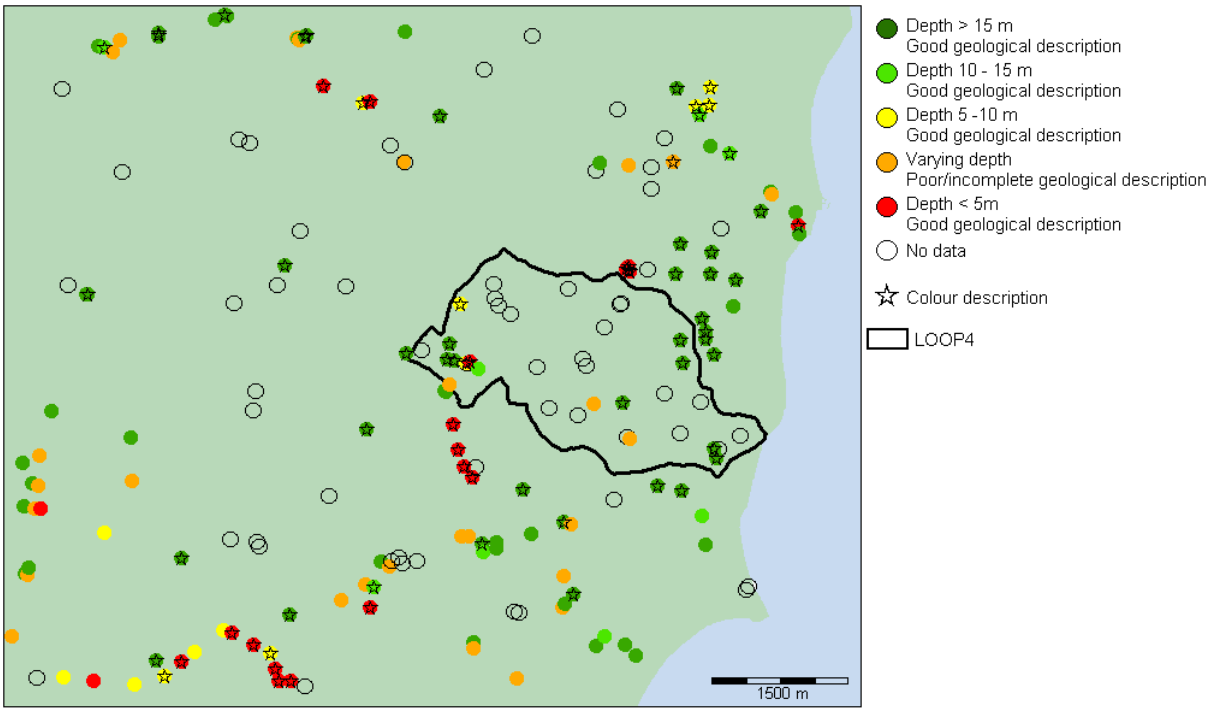

Figure 5.1 Assessment of the quality of geological information available in the Lillebæk area

5.2 Observation data

Observation data from the LOOP-program is used for calibration and validation of the hydrological model as well as the nitrate model. Observation data is obtained at 15 observation stations and 2 stream stations within the LOOP4 catchment. The location of the stations is seen on figure 5.2. At all 15 observation stations hydraulic head and N-concentrations in the saturated zone are measured. Furthermore at station 1-6 soil moisture in the unsaturated zone and drain flow and transport is measured. At the two stream stations stream discharge and N-transport in the Lillebæk are measured.

5.2.1 Hydraulic head

Hydraulic head has been measured in 17 observation wells, for which data is seen in table 5.1. All observation wells are screened between 2 and 7.4 meters below surface and are therefore not very deep. In table 5.1 the number of head observations for the period 1990-2004 is also seen, although for 4 of the wells, observations do not exist for the entire period. The observed hydraulic heads at all wells are seen in appendix 1.

5.2.2 Groundwater concentrations

Concentrations of NH_4^+, NO_2^{-2}, NO_3^- and total N have been measured at different depths at the observation stations. At most stations the wells are screened at 1.2, 3 and 5 meters below surface (m.b.s.). Groundwater concentrations are furthermore measured in 3 additional wells which are screened at greater depth. In appendix 2 data on the concentration measurements is seen, including the number of NO_3^- measurements at each well and an indication of whether nitrate is present in the well or not.

5.2.3 Discharge and nitrate transport

Stream discharge and N-transport in Lillebæk are measured at two stream stations; an upstream station (470032), covering a part of the catchment, and a downstream station (470033), covering most of the catchment. The transport in the stream is measured as total-N, nitrate-N and ammonium-N, although in the following only the nitrate-N transport is used. It should be noted that nitrate mass and concentration in the following is specified as nitrate-N. To convert from nitrate-N to nitrate-NO_3^- values must be multiplied by 4.4.

The measured average stream discharge for the period 1990-2004 was 0.017 m^3/s and 0.034 m^3/s for the upstream and downstream stations respectively. The maximum discharge observed in this period was 0.38 m^3/s upstream and 0.76 m^3/s downstream. The observed nitrate transport in Lillebæk for the period 1990-2004 was, on average, 16.7 kg nitrate-N/day at the upstream station and 28.8 kg nitrate-N/day at the downstream station. This gives an average yearly transport of around 11 ton nitrate-N out of the catchment.

Flow and nitrate transport has also been measured at 6 drain stations. However, it has only been possible to get hold of data from 5 of the 6 stations. The location of the areas that drain to these drain stations, are seen on figure 5.2. The size of these drain areas range from 1 to 4 hectares (drain areas 1 and 4 are about 1 ha, drain area 6 is about 2 ha, drain area 5 is about 3 ha and drain area 2 about 4 ha).

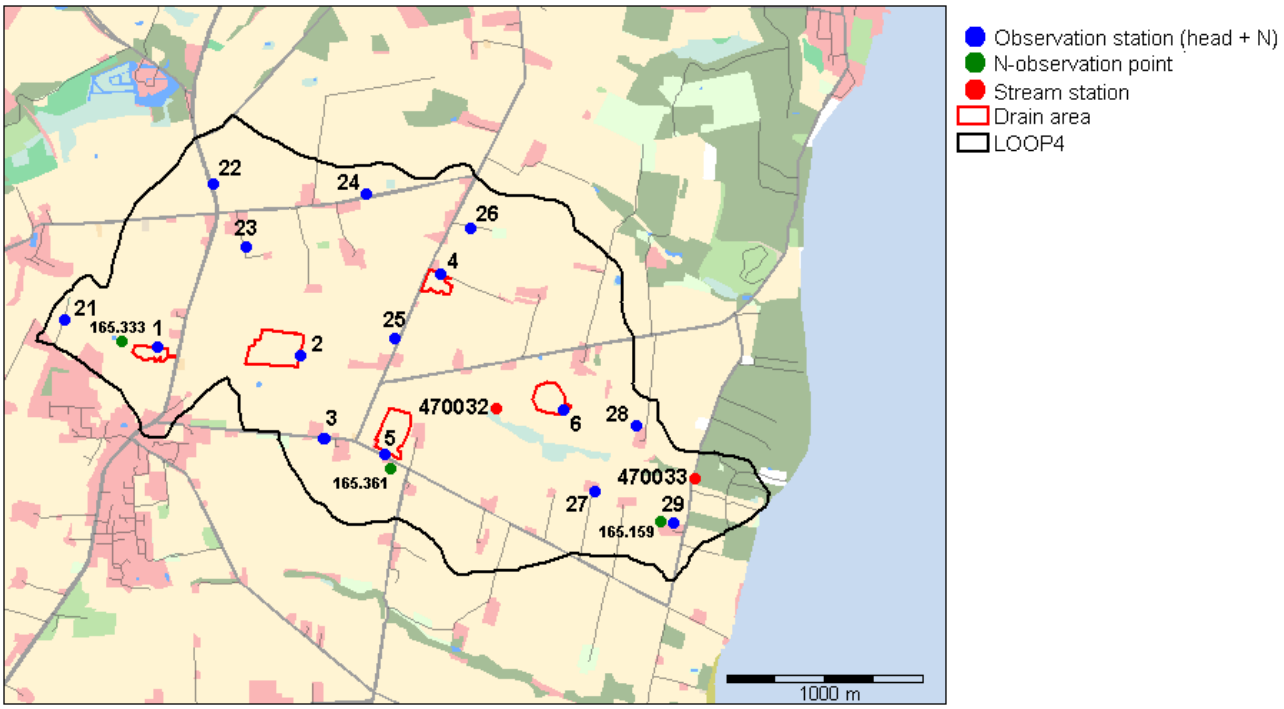

Figure 5.2 Location of observation stations, stream stations and drain areas in Lillebæk catchment

Table 5.1 Data for head observation wells for the period 1990-2004
* = observations only from 1995, ** = observation period 1990-1998, *** = observation period 1990-1995

Location	DGU no.	LOOP no.	Screen top [m.b.s.]	Screen bottom [m.b.s.]	No. head observations
1	165. 334	4.01.02.10	4.90	5.90	530
2	165. 335	4.02.02.10	4.90	5.90	525
3	165. 336	4.03.02.10	3.60	4.60	512
3	165. 369*	4.03.02.20	1.99	2.00	19
3	165. 370*	4.03.02.30	1.99	2.00	17
4	165. 337	4.04.02.10	4.70	5.70	520
5	165. 338	4.05.02.10	6.10	7.10	375
6	165. 339	4.06.02.10	4.80	5.80	524
21	165. 340	4.21.03.10	4.70	5.70	77
22	165. 341	4.22.03.10	4.70	5.70	57
23	165. 342	4.23.03.10	6.10	7.10	73
24	165. 343	4.24.03.10	5.00	6.00	78
25	165. 344**	4.25.03.10	5.80	6.80	38
26	165. 345	4.26.03.10	4.80	5.80	67
27	165. 346	4.27.03.10	4.50	5.50	76
28	165. 347	4.28.03.10	6.40	7.40	75
29	165. 348***	4.29.03.10	4.90	5.90	18

5.3 Daisy input data

Percolation and nitrate leaching from the root zone has been simulated with DAISY by the National Environmental Research Institute (NERI) and is used as input data to MIKE SHE. In the following a short description is found of how the Daisy simulations for Lillebæk have been made followed by an analysis of the Daisy results. For more information on the Daisy simulations for Lillebæk please refer to Pedersen et al (2010).

5.3.1 Daisy setup

Input data to the Daisy model consists of climate, management and soil data. Climate data is obtained from the Danish Metrological Institute's 10x10km grid for precipitation data and the 20x20km grid for data on temperature and global radiation. Precipitation data has been corrected to the ground surfaces according to Danish standards specified in Allerup et al (1998). Management data is obtained from the yearly interview study and soil data originates from soil profile investigations (Pedersen et al, 2010)

A Daisy column has been set-up for each soil water station in the catchment (observation location 1-6, see figure 5.2) and also for areas with other land uses than agriculture. The Daisy set-ups for each soil water station are calibrated against measured groundwater levels, soil water concentrations and reported crop yields. These Daisy columns are subsequently distributed to the whole LOOP4 catchment based on soil type, land use, topography and groundwater levels resulting in a Daisy column map (Pedersen et al, 2010).

Information about the agricultural practices in the catchment is available on field scale from maps for each year. These maps are stamped together, resulting in polygons with unique management history. Overlaying the resulting management map with the Daisy column map, results in the Daisy field map seen on figure 5.3. This map consists of 1249 different polygons, of which 561 are unique agricultural fields (in the following called Daisy agriculture) with a unique management and Daisy setting. The rest of the polygons are either other land uses or standard agriculture. For each of the unique agricultural fields a Daisy simulation is preformed, whereas only a single Daisy column is simulated for each of the non-agricultural land use types and the standard agriculture. Areas defined as standard agriculture are agricultural areas that did not have enough information on agricultural management to make a unique management history and therefore do not have a unique Daisy simulation (Pedersen et al, 2010). On figure 5.4 the areal distribution of the Daisy types in Lillebæk catchment is seen. The unique Daisy agriculture fields cover 70% of the area and thus represent the largest part of the area for which unique Daisy simulations have been made. The rest of the area is mainly defined as standard agriculture, which represents almost 19%.

The lower boundary condition used in the Daisy columns is defined as a time-varying shallow groundwater table (1 – 6 meter below surface). Furthermore drainage and macro pore flow is also included in the Daisy simulations (Pedersen et al, 2010). To allow the organic pools to adjust to the agricultural practice the simulation has been started in 1980 and the first 10 years has been run as a warm-up period (Pedersen et al, 2010). Therefore, in the following study, Daisy data is used from 1990 onwards.

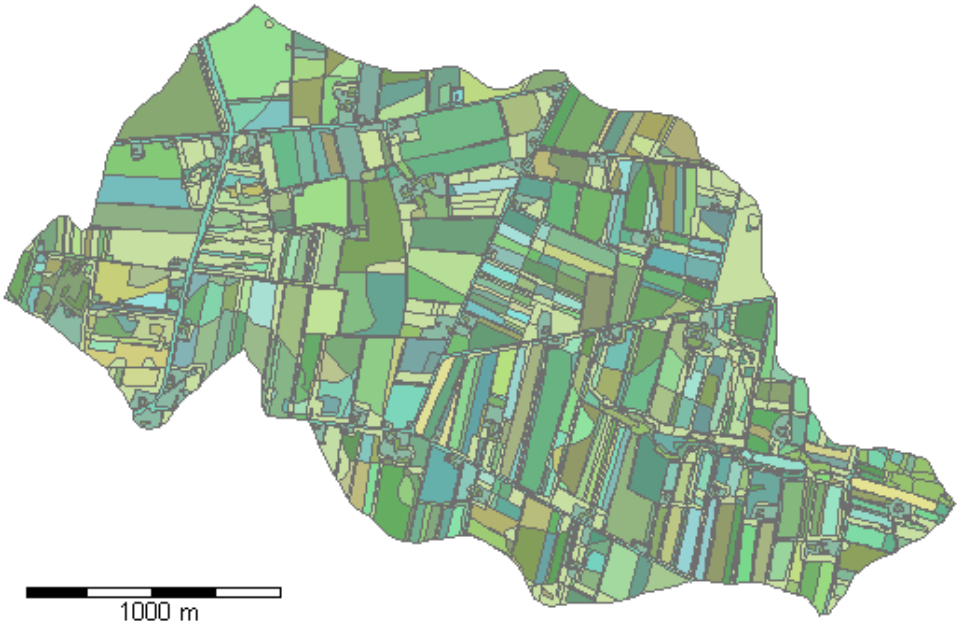

Figure 5.3 Daisy field map for Lillebæk catchment

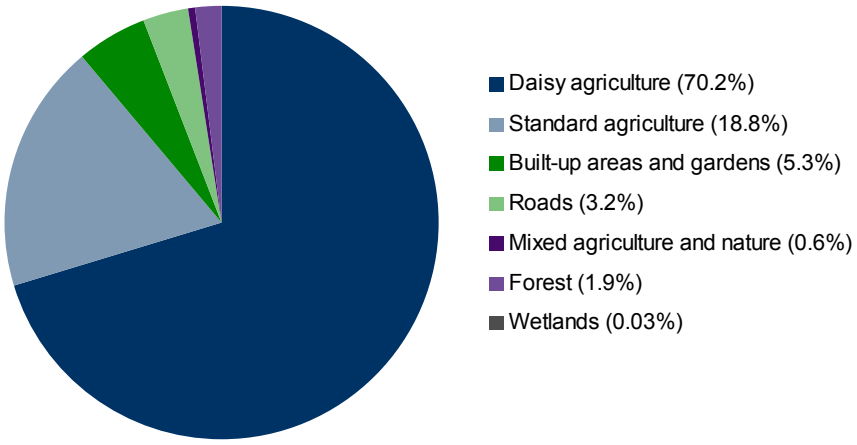

Figure 5.4 Areal distribution of Daisy types in Lillebæk catchment

5.3.2 Daisy input

The Daisy input to MIKE SHE is received from NERI as daily time series of water and N-flux for each daisy field. The Daisy input received constitutes the sum of the matrix, macro pore and drain flux. As almost all ammonium is absorbed in the soil the vast majority of the simulated N-flux from the root zone is nitrate. Nielsen et al (2004) reports that ammonium represent less than 1‰ of the mass flux from Daisy. The Daisy N-flux is therefore referred to as nitrate flux or leaching in this study.

In the following a short analysis of the Daisy input is given. The total percolation and nitrate leaching rate for the LOOP4 catchment reported in the next sections are average totals after the aggregation procedure of Daisy fields to a 10x10m grid for input to MIKE SHE (see description of the aggregation procedure in section 7.1.8). The values therefore differ slightly from the values reported in Pedersen et al (2010).

Percolation

The average yearly percolation rate in the Lillebæk catchment for the period 1990-2004 is 273 mm/year, although the percolation rate varies a lot between the years and also between the different land use types in the catchment, as seen on figure 5.5 and 5.6. These figures show great annual variation in percolation with very low percolation rates in 1996 and 2003 and high percolation rates in 1994, the same pattern as observed for precipitation (see figure 4.2).

Figure 5.5 shows the average percolation for all Daisy agriculture time series compared to the time series with the lowest and highest total percolation. The difference in percolation rate between the Daisy time series with the largest and the lowest percolation is on average 44%. On the graph the percolation for standard agriculture is furthermore shown. The standard agriculture is seen to have smaller yearly percolation rates than the average for the Daisy agriculture series in almost all years. The yearly percolation for standard agriculture is on average 6% lower than the average for Daisy agriculture series. The yearly percolation for non-agricultural areas is seen from figure 5.6 also to vary greatly, and especially the wetlands are noted to differ from the other areas.

The percolation rates also vary within the year as seen on figures 5.7 and 5.8. The percolation rates for all land use types are largest during winter and lowest during summer. During summer negative percolation is occurring due to large evapotranspiration, which results in an upwards water flux. Large negative percolation is especially seen for wetland areas, as evapotranspiration from these areas is high due to higher water availability.

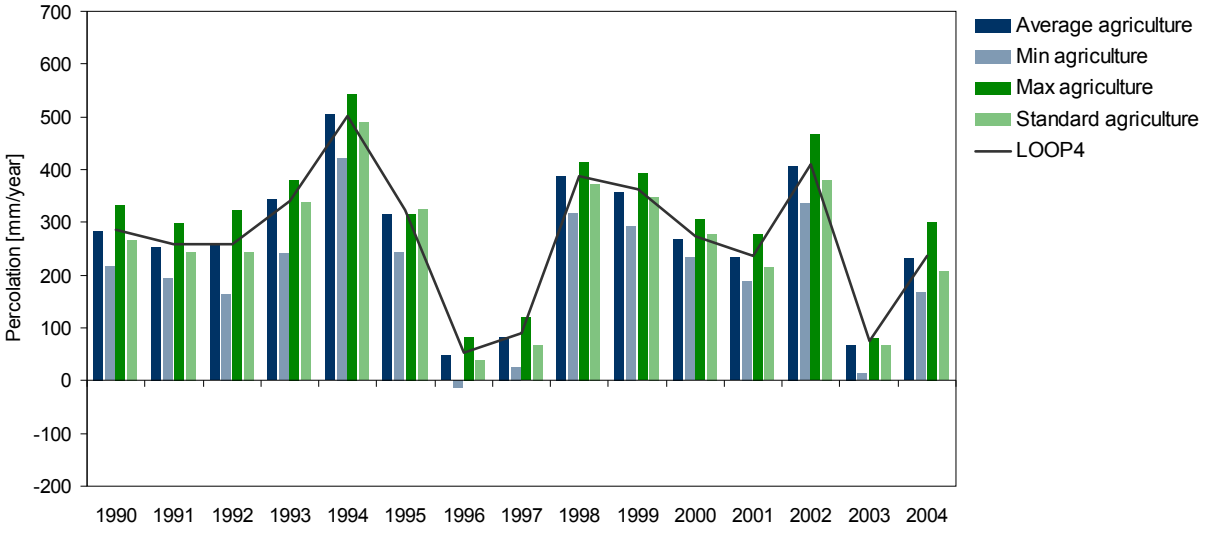

Figure 5.5 Yearly percolation [mm/year] from agricultural areas for the period 1990-2004. On the graph is seen the average percolation from Daisy agriculture, percolation from the Daisy agriculture with the highest and the lowest total percolation and also percolation from areas defined as standard agriculture. On the graph is further more seen the area-weighted average yearly percolation for the LOOP4 catchment

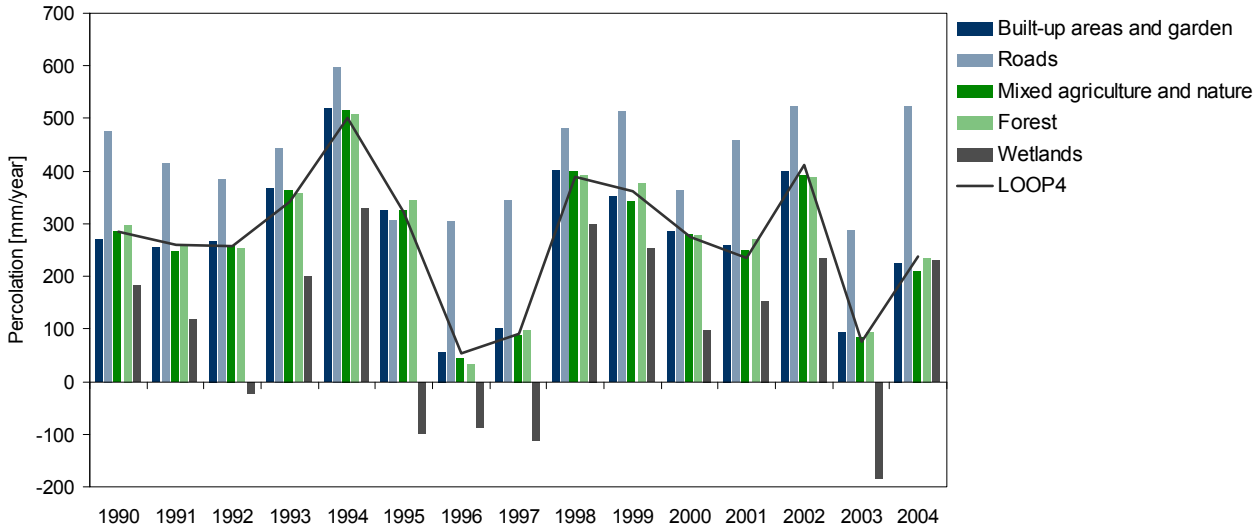

Figure 5.6 Yearly percolation [mm/year] from areas with other land uses than agriculture for the period 1990-2004. On the graph is also seen the area-weighted average yearly percolation for the LOOP4 catchment

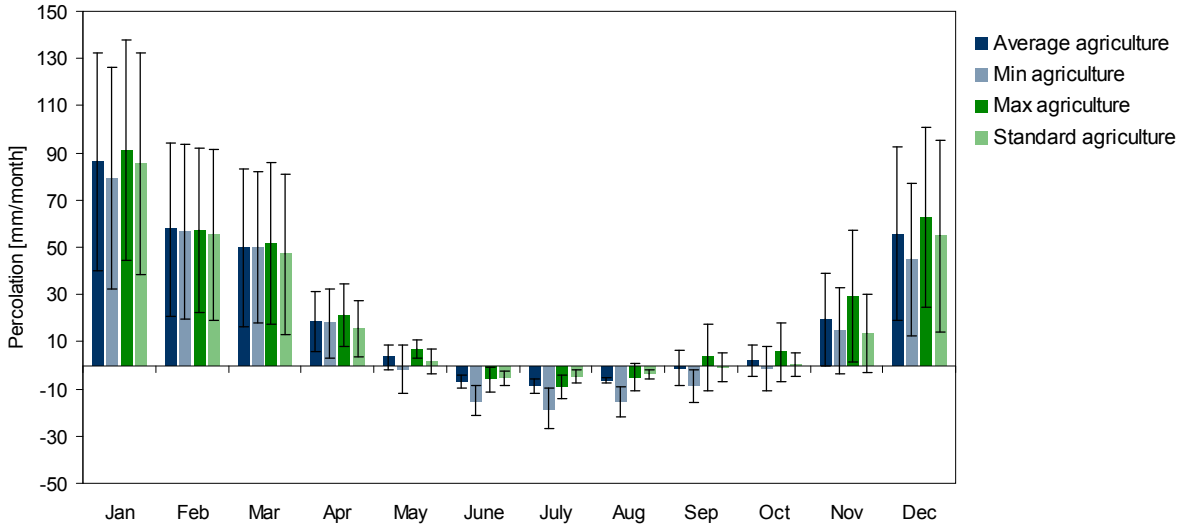

Figure 5.7 Average monthly percolation [mm/month] from agriculture for the period 1990-2004. On the graph is seen the average percolation from Daisy agriculture, percolation from the Daisy agriculture with the highest and the lowest total percolation and also percolation from areas defined as standard agriculture. The bars indicate the standard deviations

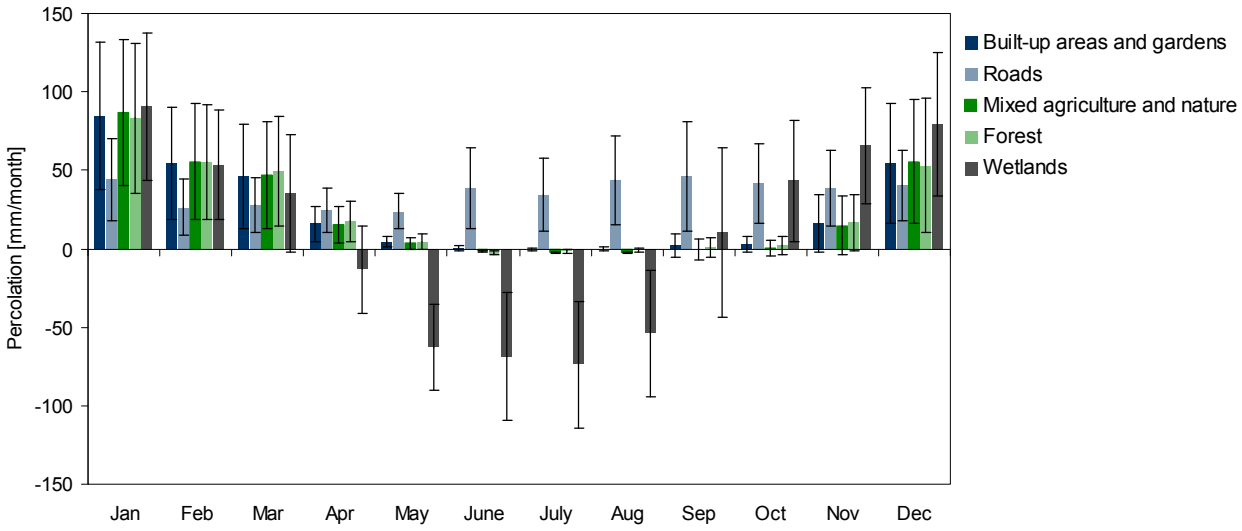

Figure 5.8 Average monthly percolation [mm/month] from areas with other land use than agriculture for the period 1990-2004. The bars indicate the standard deviations

Nitrate leaching

The average yearly nitrate leaching in the Lillebæk catchment for the period 1990-2004 is 69 kg nitrate-N/ha/year. As for percolation, the leaching also varies between years and between the different land use types in the catchment, as seen on figures 5.9 and 5.10.

Figures 5.9 and 5.10 show the variation in average yearly nitrate leaching for LOOP4 compared to the leaching from agricultural and non-agricultural areas for the period 1990-2004. It is seen that the leaching from most non-agricultural areas is much lower than for agricultural areas. Only from built-up areas and gardens a relatively large leaching is seen. The nitrate leaching from agricultural areas is seen to vary a lot and the difference between the Daisy time series with the lowest and highest total leaching is on average more than 80%. The average leaching for the Daisy agriculture series are some years larger and some years smaller than leaching from standard agriculture. On average, for the period 1990-2004, the leaching for average Daisy agriculture and standard agriculture is however quite similar (66 and 68 kg nitrate-N/ha/year respectively).

The variation in nitrate leaching within the year is seen on figures 5.11 and 5.12. As the nitrate flux is dependent on the percolation, the largest leaching rate is also seen in winter months and the smallest during summer. Negative nitrate fluxes are further more also seen in periods with upwards water flux.

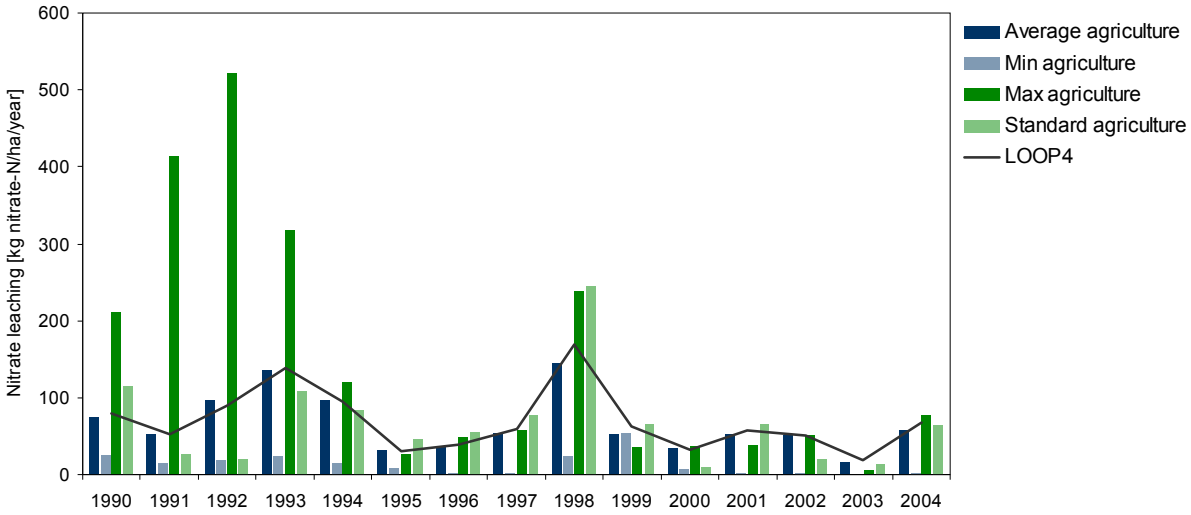

Figure 5.9 Yearly nitrate leaching [kg nitrate-N/ha/year] from agriculture for the period 1990-2004. On the graph is seen the average leaching from Daisy agriculture, leaching from the Daisy agriculture with the highest and the lowest total leaching and also leaching from areas defined as standard agriculture. On the graph is also seen the area-weighted average yearly leaching from the LOOP4 catchment

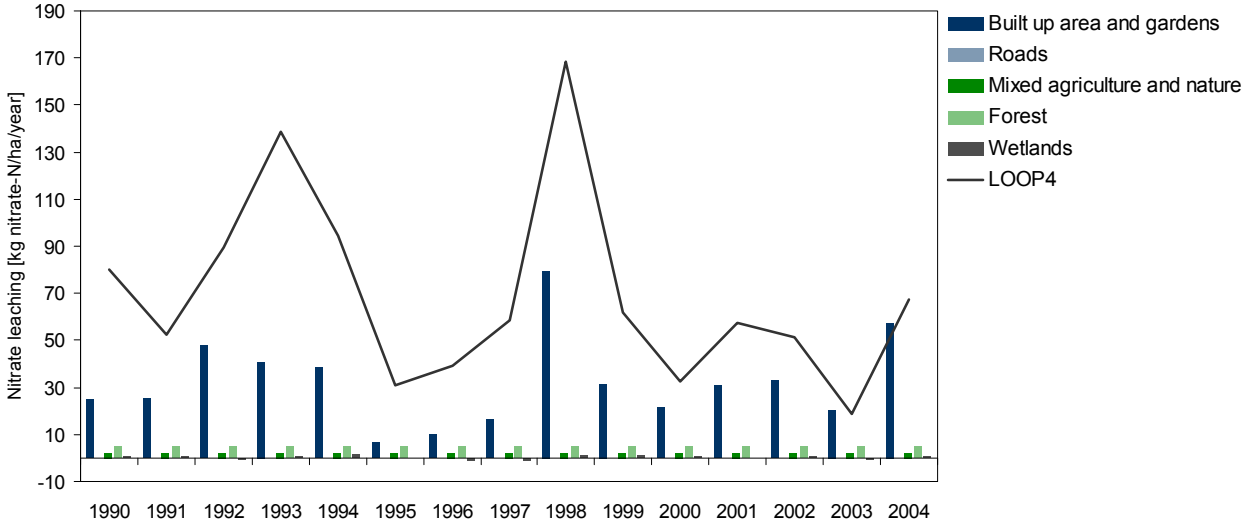

Figure 5.10 Yearly nitrate leaching [kg nitrate-N/ha/year] from areas with other land use than agriculture for the period 1990-2004. On the graph is also seen the area-weighted average yearly leaching from the LOOP4 catchment

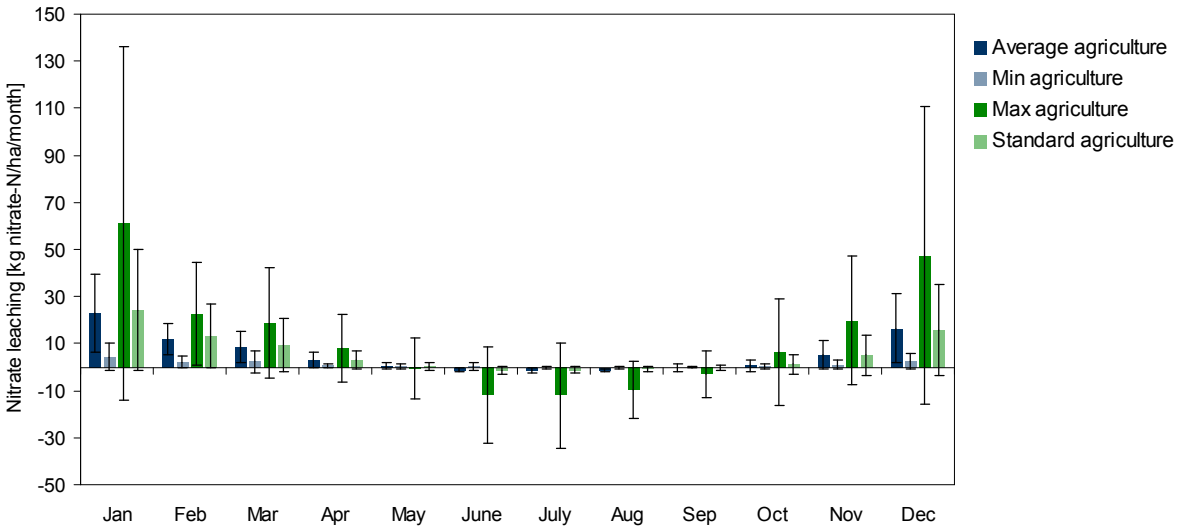

Figure 5.11 Average monthly nitrate leaching [kg nitrate-N/ha/month] from agriculture for the period 1990-2004. On the graph is seen the average leaching from Daisy agriculture, leaching from the Daisy agriculture with the highest and the lowest total leaching and also leaching from areas defined as standard agriculture. The bars indicate the standard deviations

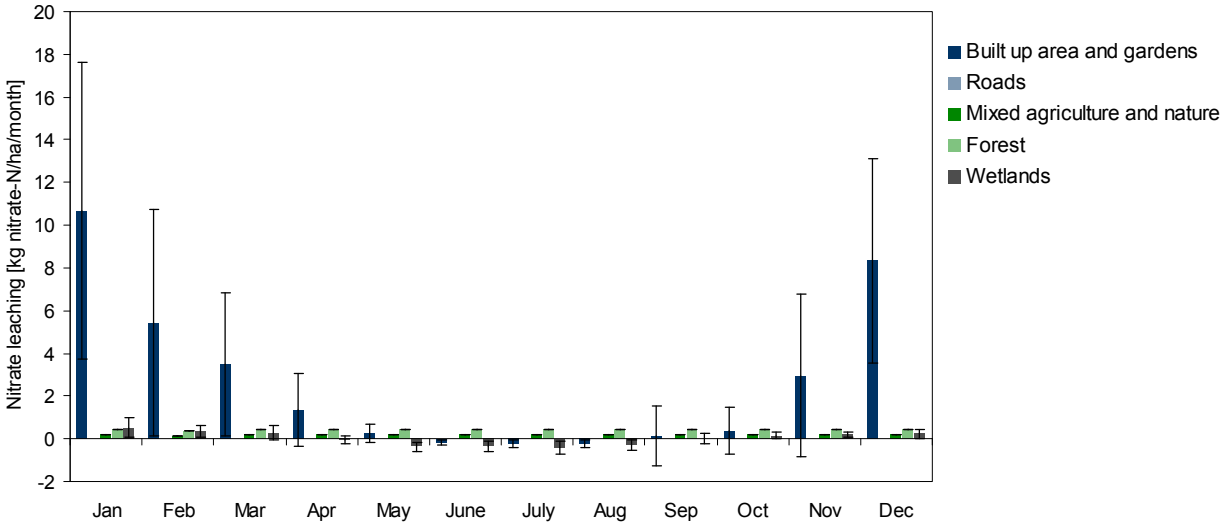

Figure 5.12 Average monthly nitrate leaching [kg nitrate-N/ha/month] from areas with other land use than agriculture for the period 1990-2004. The bars indicate the standard deviations

6. Geological model

A geological model is a description of the spatial distribution of the lithological units in an area. The geological model forms the basis for the hydrological model and therefore plays a very important role in hydrological modelling. A geological model for the Lillebæk catchment area has previously been made for a pesticide project by Styczen et al (2004) but, as this model is not covering a large enough area, a new geological model is made for this study. In the following the conceptual understanding of the geology in the Lillebæk area is first present followed by a description of the creation of the geological model. Finally profiles from the geological model are presented.

6.1 Conceptual geological understanding

The conceptual geological understanding of the area is based on the report by Graversen & Nyegaard (1989) and is presented in the following. In figure 6.1 a graphical illustration of the conceptual understanding of the geology in the Lillebæk area is seen.

The stratigraphy in the Lillebæk area consists of an upper layer of Quaternary glacial and interglacial deposits with a total thickness of 30 – 60 m. The Quaternary deposits can be divided into the following sequences. The upper Quaternary sequence is from the Weichsel glaciation and consists of glacial clayey till (ML) with a glacial melt water sand (DS) and gravel (DG) unit embedded. The middle Quaternary sequence consists of an interglacial freshwater sand (IS) deposit from the period between Eem and Weichsel. This sand deposit constitutes a coherent layer in the area and consists of a very clean quartz sand material. The lower Quaternary sequence is mainly from the Saale glaciation and consists, like the upper sequence, mainly of glacial clayey till (ML) with a glacial melt water sand (DS) and gravel (DG) unit embedded. Under the Quaternary deposits pre-Quaternary deposits are found consisting of Kerteminde marl (PL) from Selandien overlaying Bryozoan limestone (BK) from Danien. The pre-Quaternary surface in the Lillebæk area is located at elevation -16 m to -22 m and is tilting towards southwest (Graversen & Nyegaard, 1989).

The Quaternary deposits thus represent three aquifers which are separated by clayey till aquitards. The Weichsel glacial melt water sand and gravel represents the upper aquifer, the interglacial freshwater sand from Eem-Weichsel represents the middle aquifer and the Saale glacial melt water sand and gravel represent the lower aquifer. The middle aquifer has a large horizontal extent and is the main aquifer, whereas the upper and lower aquifers are of limited extent. The upper aquitard is up to 20 m thick but are, in some areas, not present as the upper and middle aquifers are locally in contact with the ground surface (Graversen & Nyegaard, 1989).

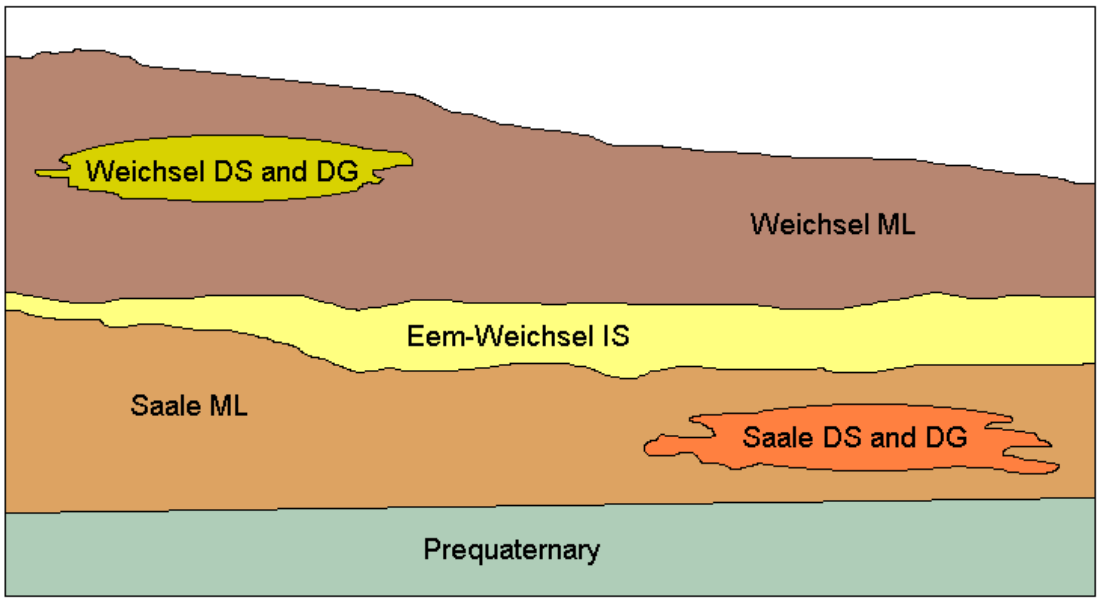

Figure 6.1 Conceptual understanding of the geology in the Lillebæk area

6.2 Model set up

The geological model is based on borehole data from the Danish Jupiter database. Borehole data gives direct information on the lithological layering, but the information is on point scale and the geology between boreholes must be assumed. The extent of the geological model is 7 x 9 km and thus somewhat larger than the Lillebæk catchment. This is done to be certain that the geological model has a large enough extent when the delineation of the hydrological model is made, as the intent is to make the hydrological model larger than the LOOP4 catchment in order to reduce boundary condition effects. The geological model is set up using the geological software GeoScene3D. The Jupiter data is downloaded to an Access database which can be imported directly to GeoScene3D and visualized three-dimensionally as seen in figure 6.2.

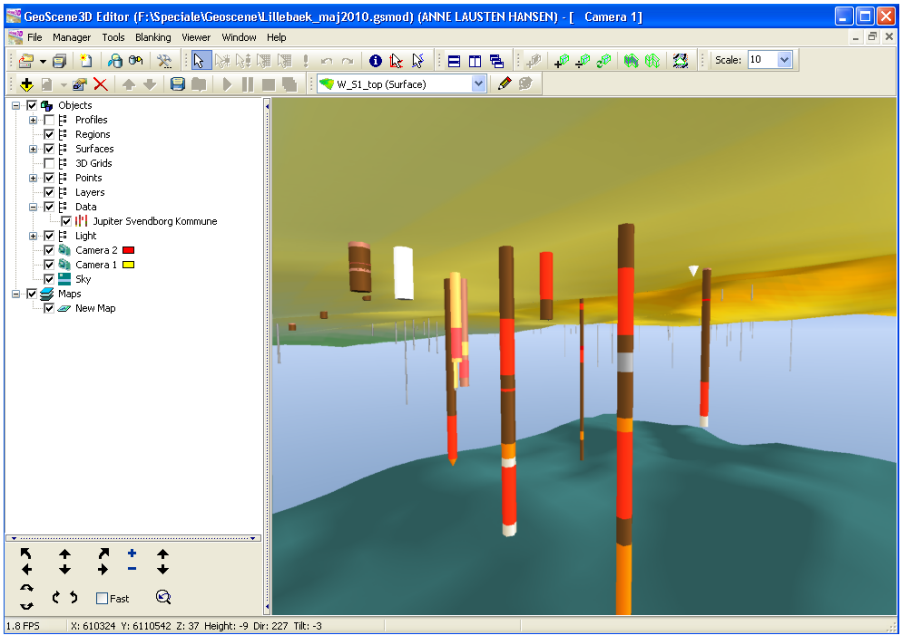

Figure 6.2 A "screen dump" from the geological software Geoscene3D

The following geological units are defined in the model based on the conceptual geological understanding of the area:

- Weichsel glacial clayey till (ML)
- Weichsel glacial melt water sand and gravel (DS, DG)
- Eem-Weichsel interglacial freshwater sand (IS)
- Saale glacial clayey till (ML)
- Saale glacial melt water sand and gravel (DS, DG)
- Pre-Quaternary surface (Selandien Kertminde clay (PL) and Danien Bryozo chalk (BK))

It is difficult to delineate the glacial sand and gravel from both Weichsel and Saale in separate units and these are therefore merged together. The clayey till units and the interglacial sand are assessed to be coherent layers in the area (Graversen & Nyegaard, 1989), and are therefore defined as separate layers in the geological model. The two units of glacial sand and gravel are believed not to be coherent and are therefore defined as lenses in the model. The horizontal extent of these lenses must therefore also be delineated. The geological layers are interpreted in the whole model area and also in areas where no data is present to prove their presence. The layers are only interpreted not to be present in an area if this can be proven by the absence of the layer in a borehole. In such areas the top and bottom of the geological layers are defined as coincident. The geological lenses are, on the contrary, only defined in areas around boreholes where the geological units are seen to be present.

The geological interpretation is performed in 2 dimensions on a number of east-west and north-south going profiles through the area. The profiles are non-linear and are placed subjectively according to the location of borehole data. Borehole data is projected onto the profiles within a buffer distance of 250 m. The interpretation of the geology is made by defining interpretation points to delineate the geological units. The geological units are defined by delineating the top and bottom of the interglacial sand layer, the two glacial sand and gravel units and the pre-Quaternary surface and assuming that the remaining is clayey till. The interpretation

points are set as both true interpretation points on boreholes, where the geology is known, and as supporting points between boreholes, where the geology is unknown, and therefore must be assumed. These supporting points are set in order to help the following interpolation of the interpretation points into 2 dimensional surfaces.

In areas with lack of geological information (see figure 5.1) the geological layers from the national DK-model for the island of Funen (the DK-model is made at GEUS) are used to support the interpretation. At model edges the geological layers are joined with the corresponding layers of the DK-model. This is done to be able to use hydraulic potentials from the DK-model to delineate the hydrological model in the following work. Information on the location of the pre-Quaternary surface is very limited and interpretation points from the DK-model are therefore included in the model for delineation of the pre-Quaternary surface.

The interpolation of the interpretation points into 2 dimensional surfaces is done using the interpolation method “topo to raster”. This interpolation method is specially designed for creating hydrologically correct surfaces and is very good at representing drainage structures, ridges and streams (ArcGIS, 2007).

6.3 Geological profiles

Profiles from the geological model are seen in figures 6.3 and 6.4 and in appendix 3 more profiles are found. In figure 6.5 the horizontal extent of the Weichsel and Saale glacial sand and gravel is seen. As the terrain slopes towards east, the upper geological layers are seen to be cut by the terrain and both the Eem-Weichsel interglacial sand and the Weichsel glacial sand and gravel lens are seen locally to reach the surface This is in accordance with the conceptual understanding and also the soil map of the area (figure 4.5), where sand is seen to be present at the surface north west of the LOOP4-catchment. The interglacial sand layer is believed to thin out towards northwest.

In appendix 4, figures showing the distribution of interpretation points used to interpolate the 2D surfaces of the geological units are found. On the figures true interpretation points, as well as supporting points, are seen. These figures thus give an idea of in which areas the uncertainty of the geological model is large. This should be kept in mind when calibrating the model as it can be expected that large residuals between observed and simulated hydraulic heads will be found in these areas will.

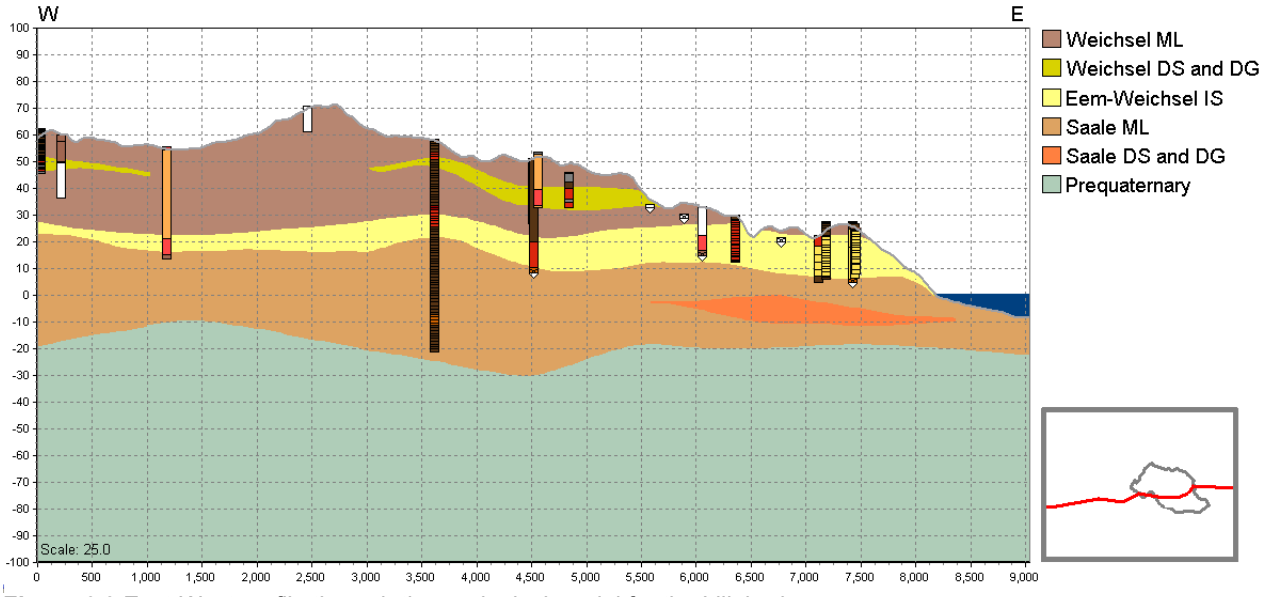

Figure 6.3 East-West profile through the geological model for the Lillebæk area

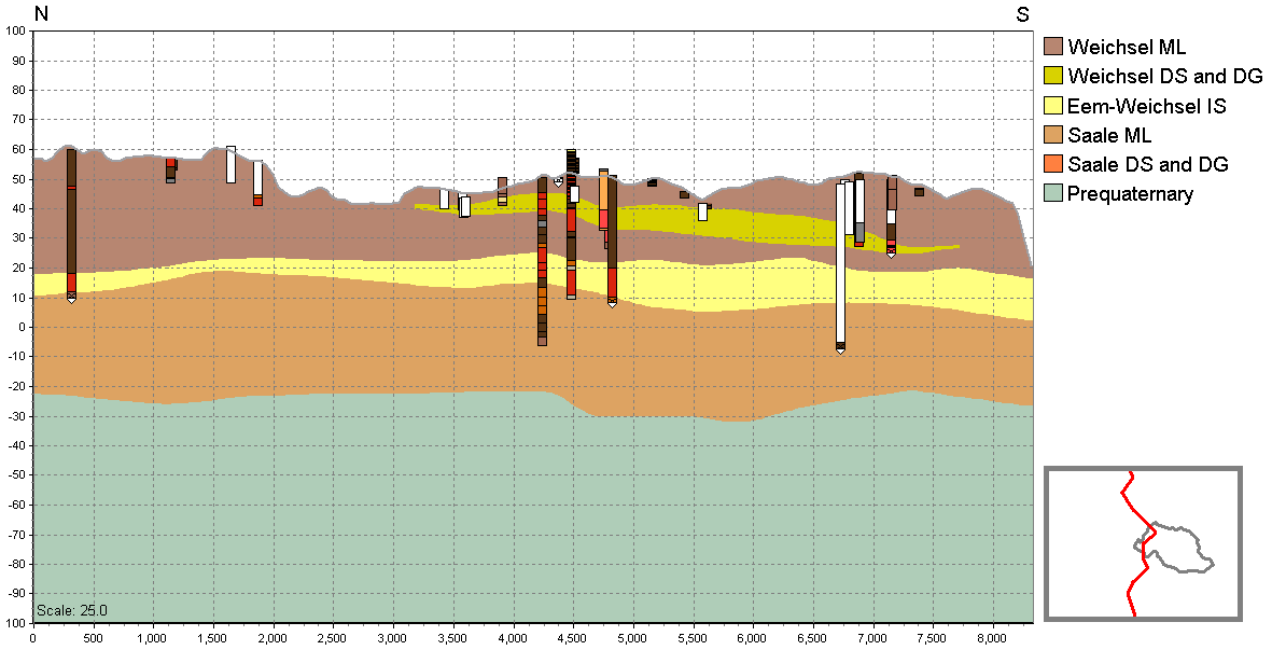

Figure 6.4 North-South profile through the geological model for the Lillebæk area

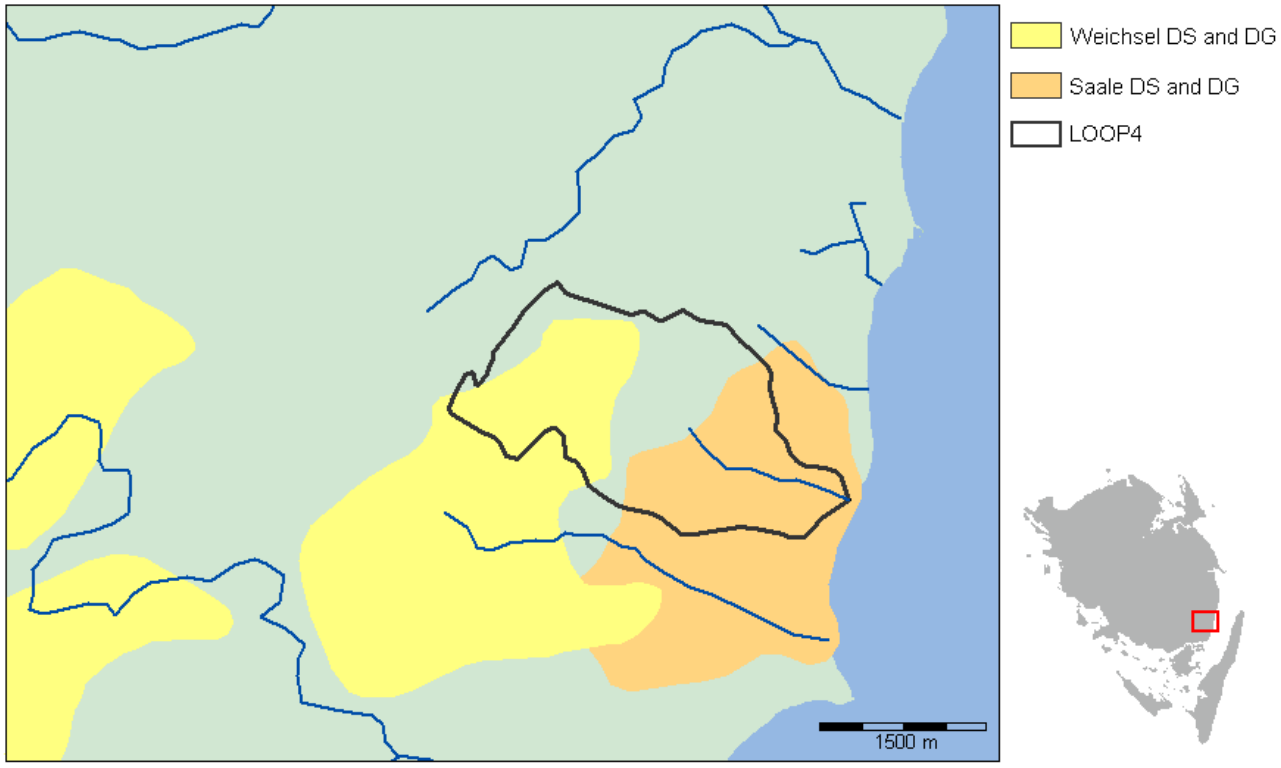

Figure 6.5 Horizontal extent of Weichsel and Saale glacial sand and gravel

7. Hydrological model

7.1 Model setup

A hydrological model has previously been made for the Lillebæk catchment in relation to the pesticide project by Styczen et al (2004) mentioned in the previously section. However, this model covers only the topographical catchment to Lillebæk. As a larger model area is delineated for this study, the only part from this previous model that is reused is a modified version of the MIKE11 setup. Furthermore, the hydrological parameters values from this model are used as initial estimates for the hydrostratigraphical units. For a thorough description of the previous model please refer to Styczen et al (2004).

7.1.1 Simulation specifications

A transient catchment model simulating 3D saturated, 2D overland and 1D river flow is set up in the modelling framework MIKE SHE. The model is run for a simulation period of 15 years from 1/1 1990 to 31/12 2004. The time step is set to 12 hours for saturated flow, 4 hours for overland flow and 1 minute for river flow.

7.1.2 Hydrostratigraphical units

The geological model presented in section 6 forms the basis for the hydrostratigraphical units defined in the hydrological model as seen on figure 7.1. The two glacial sand and gravel lenses are assumed to be hydrogeologically similar and the following 4 hydrostratigraphical units are thus defined in the hydrological model:

- Weichsel ML
- Saale ML
- Eem-Weichsel IS
- Weichsel/Saale DS and DG

The model parameters for the hydrostratigraphical units are defined as constant parameters within each unit, thus assuming each unit to be homogenous. This is, of course, not a realistic assumption in reality, but is made because of lack of knowledge about the heterogeneity of the layers.

7.1.3 Initial parameter values

The initial parameter values used in the hydrological model and the expected range of these values are seen in table 7.1. This initial guess is, as mentioned, based on the previous model by Styczen et al (2004). As this model has been calibrated and validated it is assumed that these parameter values are a good initial estimate. The relationships between vertical and horizontal conductivities as indicated in table 7.1 are kept constant throughout the calibration process. Storage coefficients are defined similar for sand and clay units.

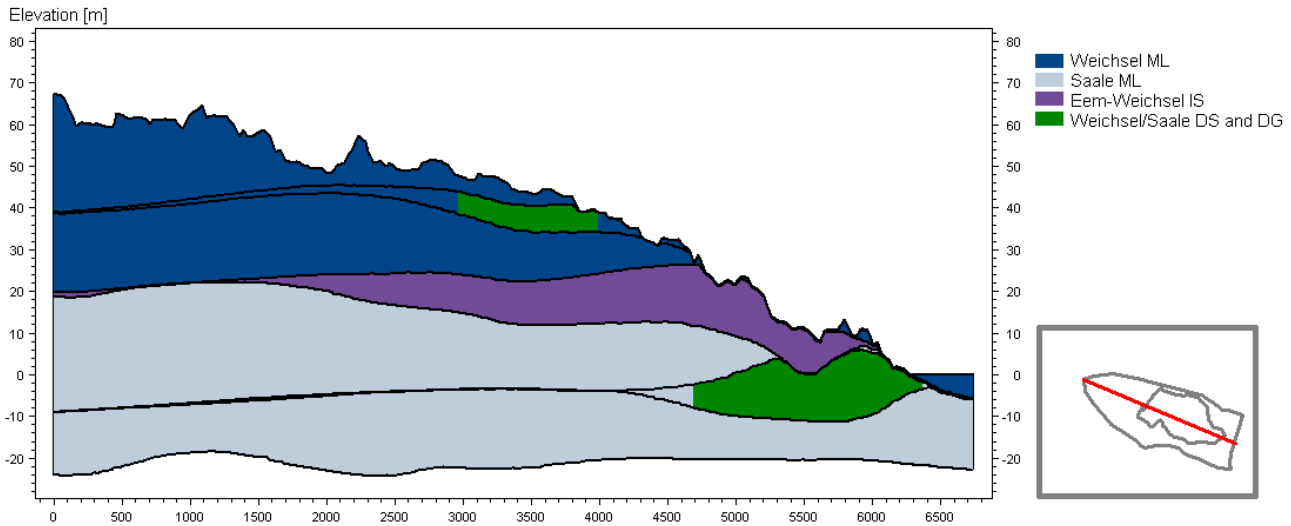

Figure 7.1 Hydrostratigraphical units and computational layers

Table 7.1 Initial parameter values and expected range

Hydrostratigraphical units

	K_h [m/s]			K_v [m/s]			S_y			S_s [1/m]		
	Initial	**Lower**	**Upper**	**Initial**	**Lower**	**Upper**	**Initial**	**Lower**	**Upper**	**Initial**	**Lower**	**Upper**
Weichsel ML	4.37E-06	1.00E-08	1.00E-04	4.37E-07	1.00E-09	1.00E-05	0.2	0.05	0.2	1.00E-03	1.00E-04	1.00E-02
Saale ML	3.74E-06	1.00E-08	1.00E-04	7.48E-08	1.00E-09	1.00E-05	0.2	0.05	0.2	1.00E-03	1.00E-04	1.00E-02
Eem-Weichsel IS	1.36E-05	1.00E-06	1.00E-02	1.36E-06	1.00E-07	1.00E-03	0.3	0.1	0.35	2.00E-03	1.00E-05	1.00E-03
Weichsel/Saale DS and DG	8.00E-05	1.00E-06	1.00E-02	4.00E-05	1.00E-07	1.00E-03	0.3	0.1	0.35	2.00E-03	1.00E-05	1.00E-03

Drainage

	Initial	**Lower**	**Upper**
Drain constant [s^{-1}]	1.00E-06	1.00E-08	1.00E-05
Max drain level [m.b.s.]	1	0.5	1

Stream flow

	Piped reaches			**Unpiped reaches**		
	Initial	**Lower**	**Upper**	**Initial**	**Lower**	**Upper**
Leakage coefficient [s^{-1}]	1.00E-10	1.00E-11	1.00E-09	1.00E-09	1.00E-10	1.00E-06
Bed resistivity (M)	10	10	100	10	10	100

Overland flow

	Initial	**Lower**	**Upper**
Manning [$m^{1/3}/s$]	10	1	100
Detention storage [mm]	0	0	5

7.1.4 Grid and computational layers

The horizontal discretization of the model is set to 50 m x 50 m. Vertically the model is divided into 7 computational layers based on the geology, so the three aquifers in the study area are contained in separate layers as seen in table 7.2. Since the Weichsel/Saale DS and DG lenses, as mentioned, have limited extent, computational layers 2 and 6 consist of both aquifer and aquitard material. A minimum thickness of 0.1 m is defined for the computational layers. As the terrain in the study area is sloping towards the coast the geological layers are cut by the terrain. This result in the computational layers thinning out towards the eastern part of the model and the layers are therefore adjusted downward to reach the minimum thickness of 0.1 m. A vertical cross section through the computational layers is seen in figure 7.1. In appendix 5 the thickness of each computational layer is seen.

Table 7.2 Computational layers in the hydrological model

Com. layer	Hydrogeology	Geology	Lower level	Avg. layer thickness [m]	Max. layer thickness [m]	Min. layer thickness [m]
1	Aquitard	Weichsel ML	Top of Weichsel DS and DG	6.2	30.6	0.1
2	Aquifer	Weichsel DS and DG Weichsel ML	Bottom of Weichsel DS and DG	1.8	10.7	0.1
3	Aquitard	Weichsel ML	Top of Eem-Weichsel IS	10.4	20.1	0.1
4	Aquifer	Eem-Weichsel IS	Bottom of Eem-Weichsel IS	7.1	17.1	0.1
5	Aquitard	Saale ML	Top of Saale DS and DG	14.5	29.2	0.1
6	Aquifer	Saale DS and DG Saale ML	Bottom of Saale DS and DG	2.7	20.4	0.1
7	Aquitard	Saale ML	Pre-quaternary surface	16.6	33.0	6.6

7.1.5 Topography

The upper delineation of the model is defined by the topography in the area. The topography is defined by a 50 m digital elevation model (DEM).

7.1.6 Model area and boundary conditions

Along a large part of the western boundary of the LOOP4 catchment the groundwater divide has found to be situated outside the catchment resulting in groundwater flow into the catchment (Styczen et al, 2004). The model area for the hydrological model is therefore made larger than the LOOP4 catchment to be able to delineate the model using a no-flow boundary and also in order to decrease boundary effects.

The delineation of the model area is based on hydraulic heads from a modified version of the DK-model for the island of Funen (the DK-model is made at GEUS). This model is set up in the MIKE SHE modelling framework and includes all hydrological process (overland flow, river flow, unsaturated flow, saturated flow and evapotranspiration). The model has a horizontal discretization of 500 m and is vertically divided into 9 computational layers. The model is, for this study, modified by implementing the geological model for Lillebæk within the area marked in figure 7.2 and the water movement is subsequently run. Hydraulic heads from the Quaternary sand layer ks2, which is comparable to the Eem-Weichsel IS layer at Lillebæk, is subtracted and imported in GIS. The hydraulic heads are subtracted as average heads for the period 2000-2003, for which the DK-model is calibrated. In GIS hydraulic head potential lines are made and the model area is then defined by drawing the model boundary perpendicular on these lines (see figure 7.2). The model area is delineated to the west, where flow arrows indicate the flow to be very small (see figure 7.3).

Two different areas have been delineated as prospective model areas, one very close to the LOOP4 area and another one which includes the streams of Hammesbro and Isebæk (see figure 7.2 and 7.3). The smaller model area is preferable in relation to CPU-time, but it is suspected that this boundary will affect the model too much. The two model areas are therefore tested to see how the boundary of the two model areas affects the groundwater flow. This is done by running a preliminary and very simplified version of the hydrological model.

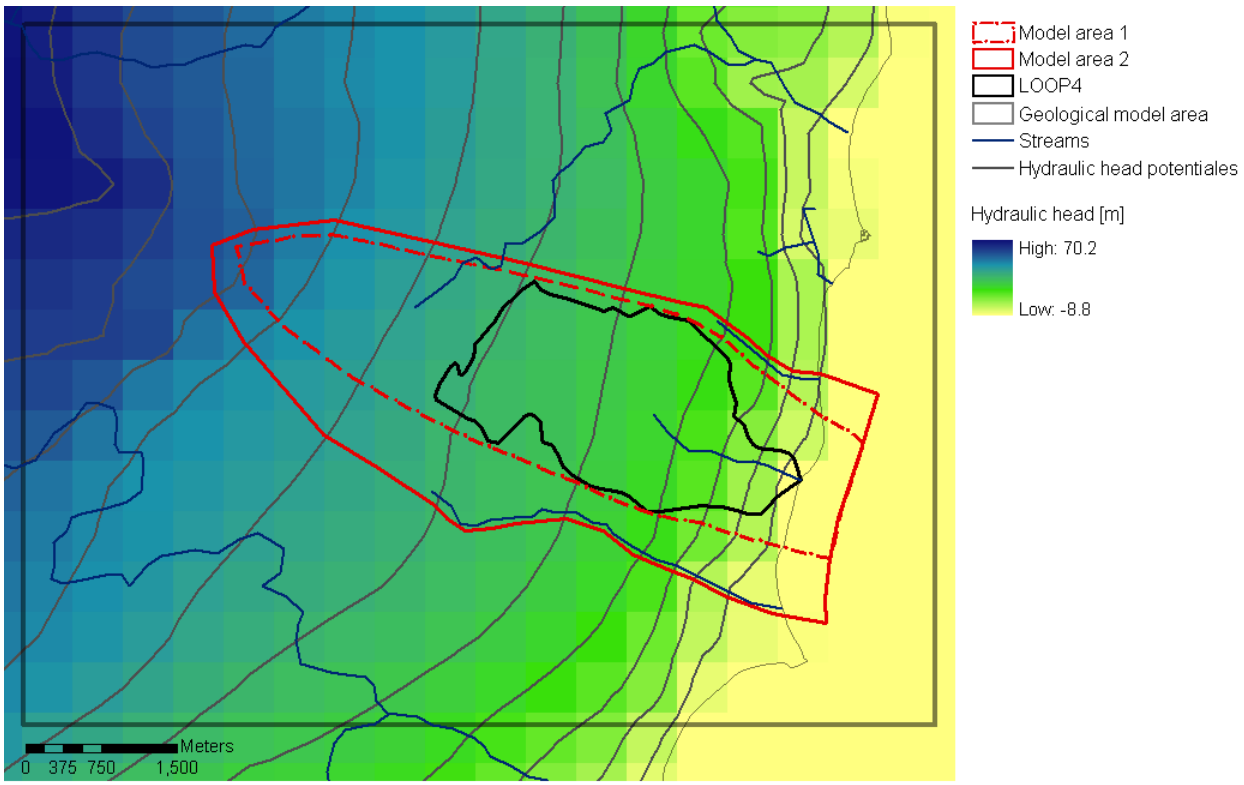

Figure 7.2 Delineation of model area based on average hydraulic heads (2000-2003) from the ks2-layer in a modified version of the DK-model of Funen (made by GEUS). The interval between the potential lines is 5 meters

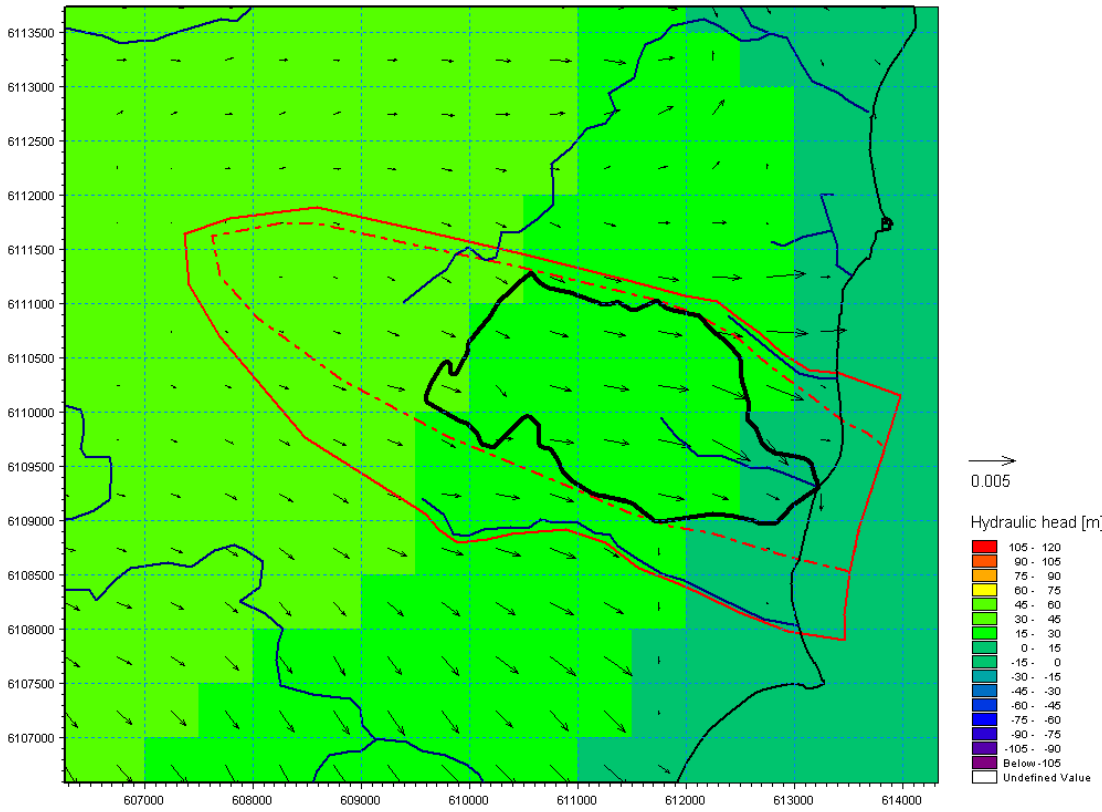

Figure 7.3 Delineation of model area based on groundwater flow arrows (31/12 2003) from the ks2-layer in a modified version of the DK-model of Funen (made by GEUS)

The results of running a simplified model version with the two model areas is seen in figures 7.4 and 7.5, which show the average hydraulic head in the Eem-Weichsel IS layer. It is seen that the two model areas result in rather different hydraulic heads, especially around the northern and southern boundary. For model area 2 the hydraulic heads indicate flow towards Isebæk and Hammesbro stream which are situated at the northern and southern boundaries. As these streams are not included in model area 1 the flow in this model is forced inwards. These results thus show that model area 1, as suspected, has rather large effects on the groundwater flow, and model area 2 is therefore chosen as the model area for the hydrological model. The model area has an area of 14.7 km^2 and the LOOP4 catchment (4.7 km^2) covers around one third of this area.

The Weichsel/Saale DS and DG lenses are not completely contained in the model area as seen on figures 7.6 and 7.7. This could be a problem if the flow in the lenses is toward the boundary of the model area. The hydraulic heads from the modified DK-model, in the layers corresponding to the lenses, indicate though that the flow in the lenses is towards east, and it seems that not including the whole of the lenses should not be a problem.

It is assumed that the delineated model area is representing a groundwater divide in the area and therefore that there is no groundwater flow into the model area along the boundaries. All vertical boundaries, except along the coastline, are thus specified as no-flow boundaries. Along the coastline a constant head of 0 meter is specified in computational layer 1, making groundwater outflow towards the sea possible. The pre-Quarternary surface, which represents the bottom of the model, is assumed to be impermeable. This is believed to be a reasonable assumption as the top of the pre-Quaternary, as mentioned, consists of Kerteminde marl which is a relativity low permeable material (Højbjerg et al, 2008). The bottom of the model is therefore also treated as a no-flow boundary.

7.1.7 Initial heads

Initial heads for the model are obtained by running the model once using initial heads of 0 m in all computational layers. The resulting heads for the 31/12 2004 from this run are then subtracted for each computational layer and used as initial heads.

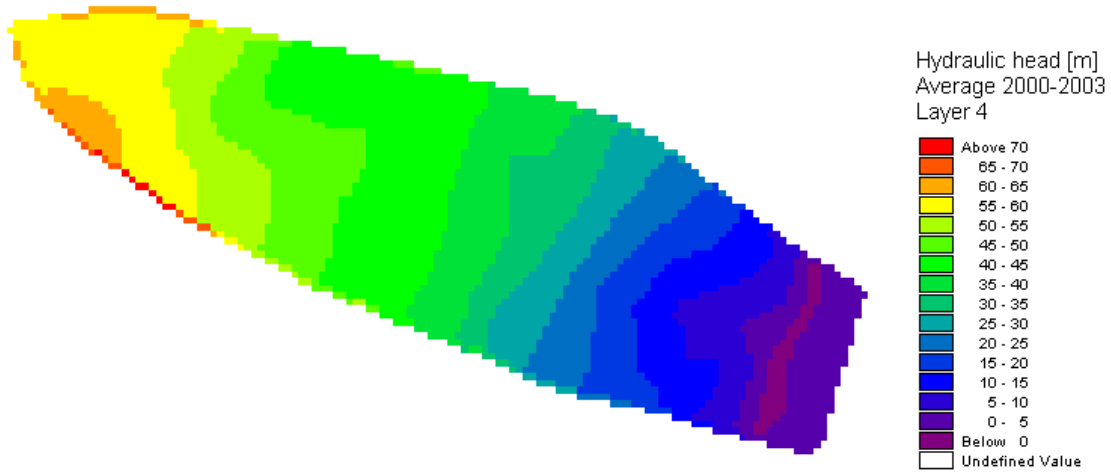

Figure 7.4 Average hydraulic head in Eem-Weichsel IS using model area 1 for a simplified version of the hydrological model

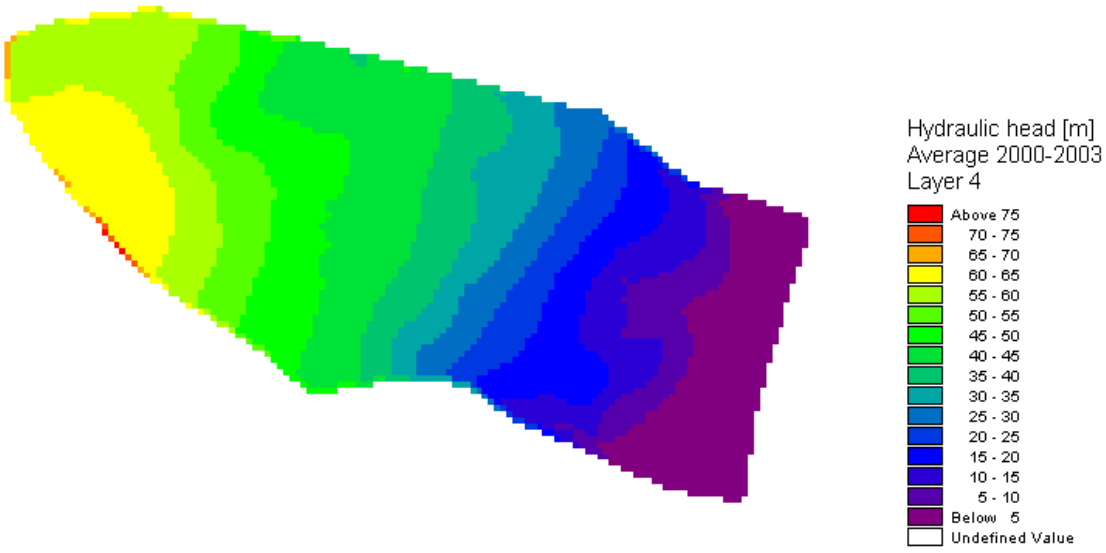

Figure 7.5 Average hydraulic head in Eem-Weichsel IS using model area 2 for a simplified version of the hydrological model

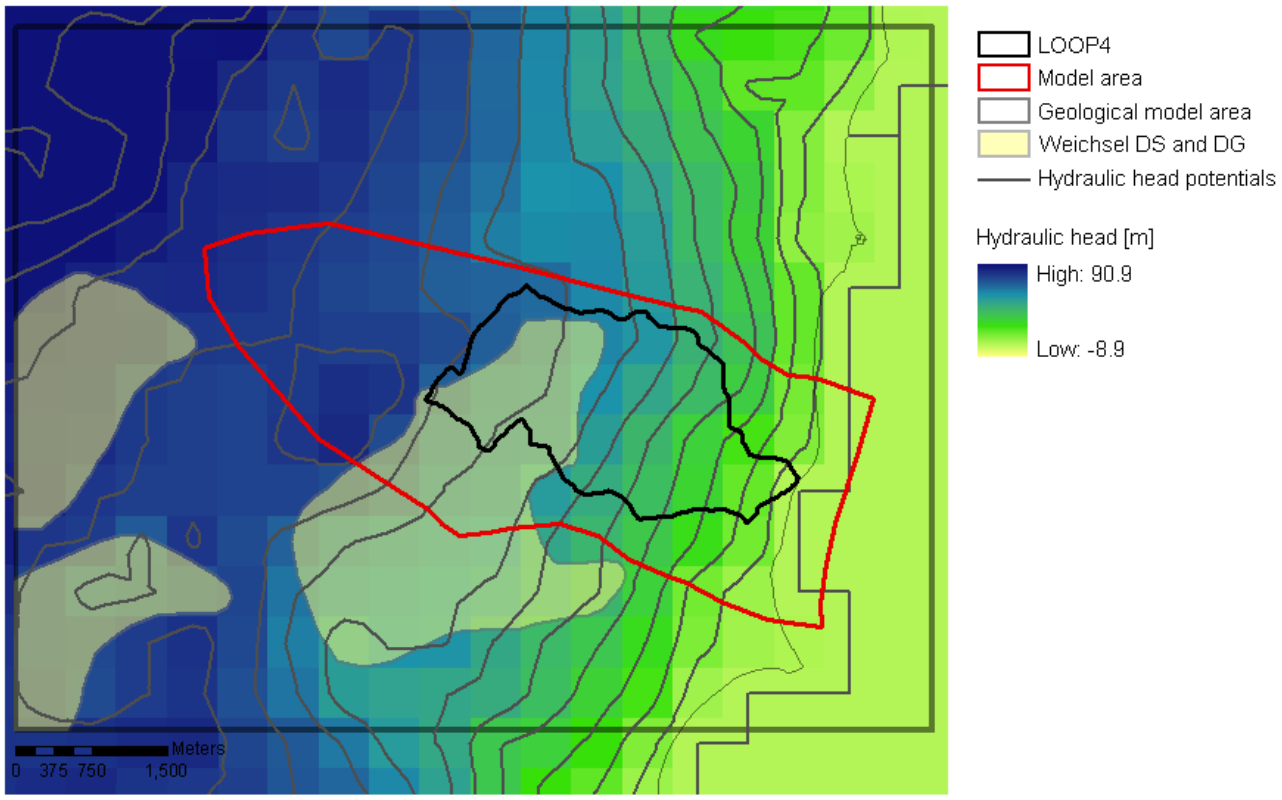

Figure 7.6 The model area compared to the extent of the Weichsel DS and DG lens. The material outside the lens consists of clayey till. The figure shows average hydraulic heads (2000-2003) from the ks1-layer in a modified version of the DK-model of Funen (made by GEUS). The interval between the potential lines is 5 m

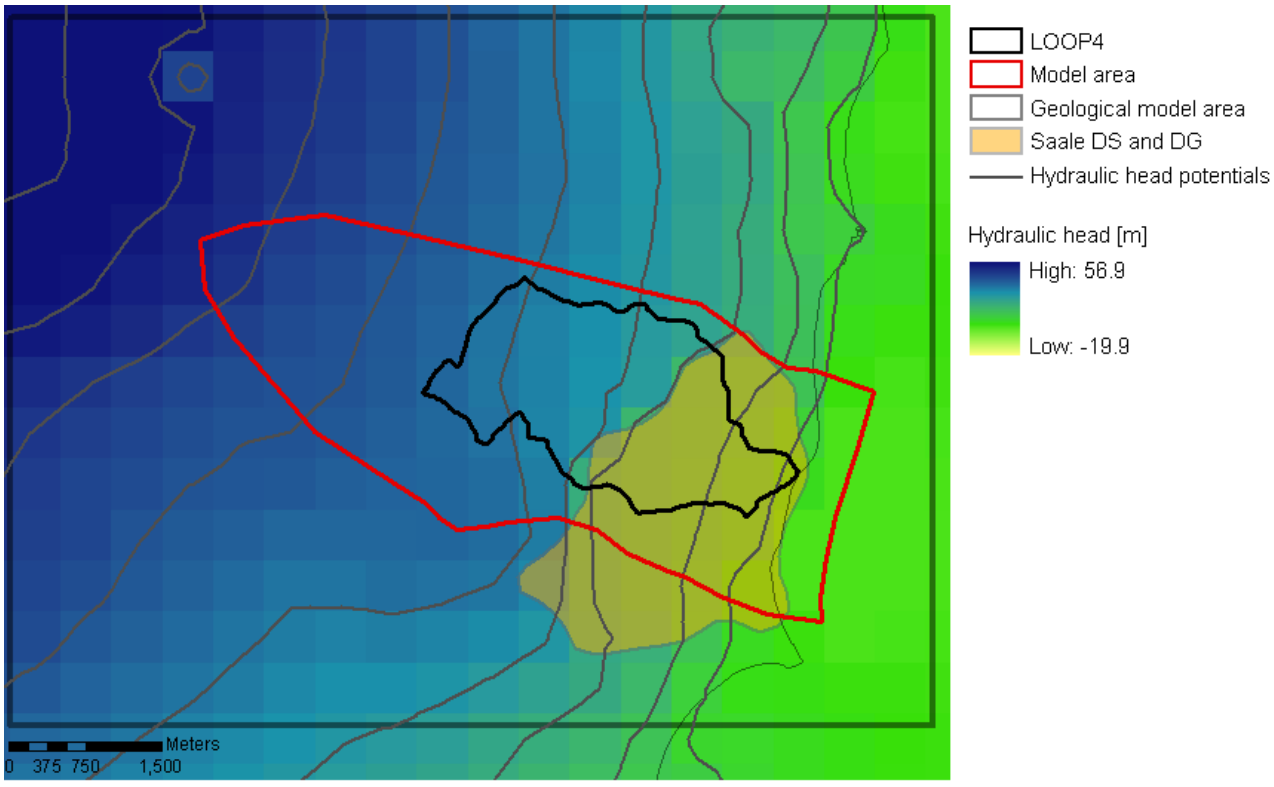

Figure 7.7 The model area compared to the extent of the Saale DS and DG lens. The material outside the lens consists of clayey till. The figure shows average hydraulic heads (2000-2003) from the ks3-layer in a modified version of the DK-model of Funen (made by GEUS). The interval between the potential lines is 5 meters

7.1.8 Daisy percolation

The Daisy percolation defines the upper boundary condition for the hydrological model. No Daisy simulations are available for the model area outside the LOOP4 catchment and the Daisy results from LOOP4 must therefore be extrapolated to cover the whole model domain. As the soil type in the area is rather uniform (see figure 4.5), the Daisy percolation time series is distributed in the area outside LOOP4 based solely on land use data from AIS (Areal Information System). A shape-file with the Daisy field polygons covering the LOOP4 area is merged with a shape-file with land use polygons covering the rest of the model area. This results in a percolation distribution map (see figure 7.8), for which a Daisy code, specifying the corresponding percolation time serie, is defined for each polygon. In the model area outside LOOP4, Daisy time series from a comparable land use type is specified for non-agricultural areas and for all agricultural areas the standard agriculture time serie is used. It is therefore only within the LOOP4 catchment the unique Daisy agriculture time series are used. The distribution of the different land use types in the LOOP4 catchment and the model area is seen in table 7.3.

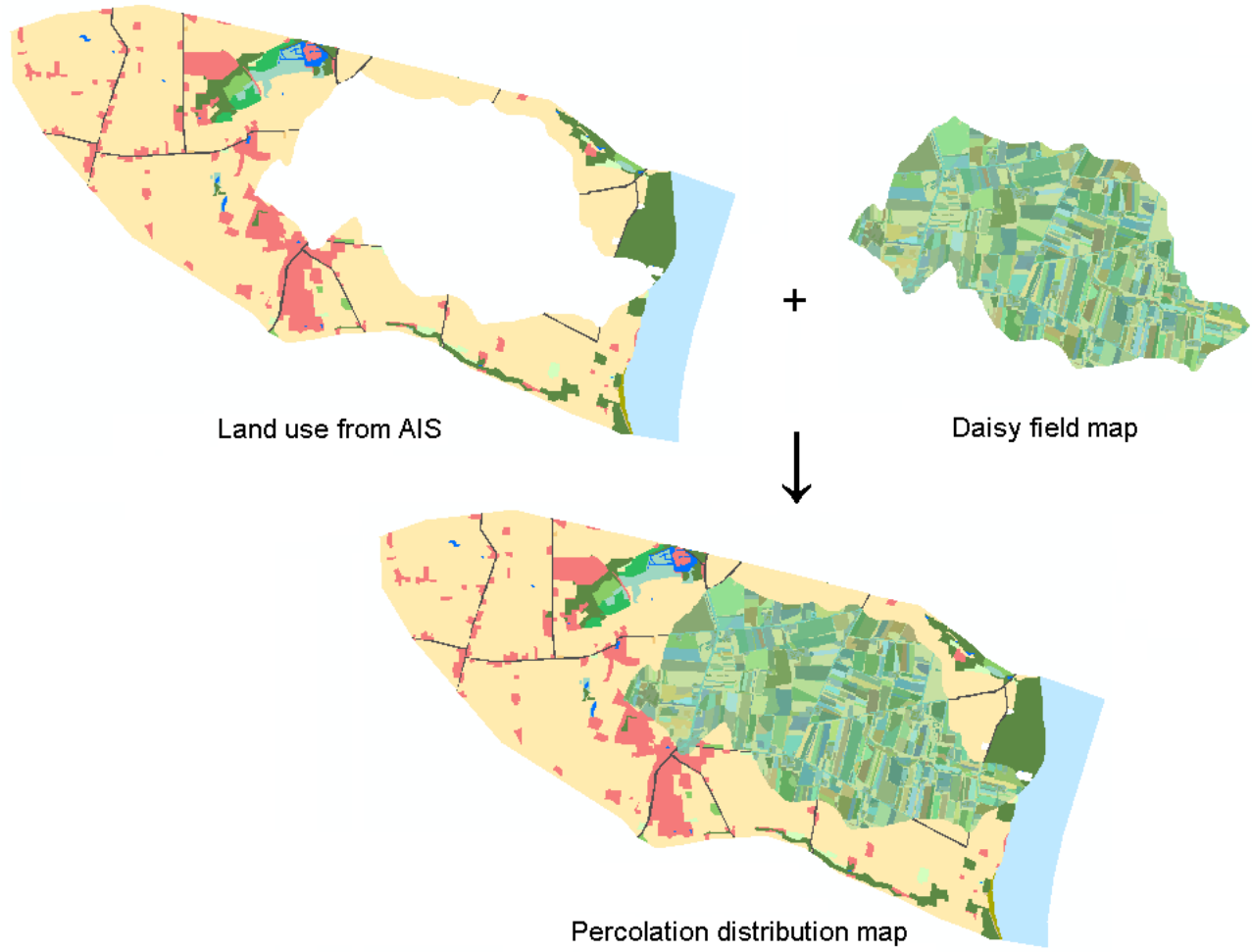

Figure 7.8 The resulting map for distributing Daisy percolation time series is a composition of the Daisy field map and land use from AIS (Areal Information System) for the model area outside LOOP4

Table 7.3 Distribution of land use types within the LOOP4 catchment and the model area

	LOOP4		Model area	
	[ha]	[%]	[ha]	[%]
Daisy agriculture	328.1	70.2	328.1	22.3
Standard agriculture	87.8	18.8	756.4	51.4
Built-up areas and gardens	24.9	5.3	118.7	8.1
Roads	14.9	3.2	32.0	2.2
Mixed agriculture and nature	2.7	0.6	14.3	1.0
Forest	8.9	1.9	81.6	5.5
Wetlands	0.2	0.0	21.8	1.5
Lakes	0.1	0.0	5.0	0.3
Sea	0.0	0.0	113.7	7.7
Total	467.6	100.0	1471.6	100.0

For implementation of the Daisy percolation in MIKE SHE, the percolation distribution map is subsequently converted to a grid using an aggregation procedure as illustrated in figure 7.9. Each grid cell is given the Daisy code from the polygon having the largest area within each grid cell. To be able to include as many of the very small polygons in the percolation distribution map a grid size of 10m x 10m is used. This grid file is then merged with a dfs0 time serie file containing all percolation time series. This results in a 10m x 10m time-varying dfs2 grid file which can be implemented in MIKE SHE. When this file is pre-processed in MIKE SHE, an average percolation time serie is calculated for each 50m x 50m grid cell in the model. In figure 7.10 the resulting average Daisy percolation for the simulation period 1990-2004 is seen, after the extrapolating and aggregation procedure.

The Daisy percolation is specified in the hydrological model as a precipitation rate with a net rainfall fraction and an infiltration fraction of 1. Negative percolation is included in the model by defining this as an *"Extra parameter"* in MIKE SHE. It is specified how far down in the model the negative percolation can be with-drawn by specifying a maximum depth and computational layer. If there is not enough water present above the maximum depth or computational layer the remainder of the negative percolation is reset to zero. It is impor-tant that the amount of negative percolation that is reset is not too large as this will affect the water balance (Hansen & Rasmussen, 2006). The maximum depth is set to 10 m and the Eem-Weichsel IS layer (computational layer 4) is specified as the maximum layer, as this layer reaches the ground surface in the eastern part of the model. These settings resulted in 0.7 - 3.75 % (2.8 - 14.9 mm over 15 years) of the total negative percolation being reset to zero in the various model runs performed during the following calibration, which seems acceptable.

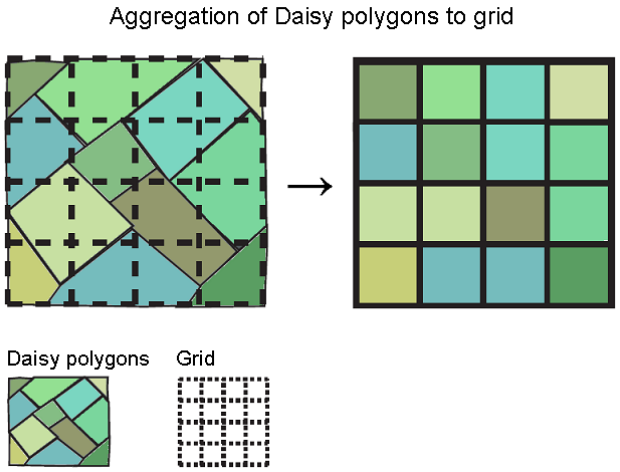

Figure 7.9 Aggregation procedure of Daisy polygons to a grid. The illustration is made after idea from Hansen (2006)

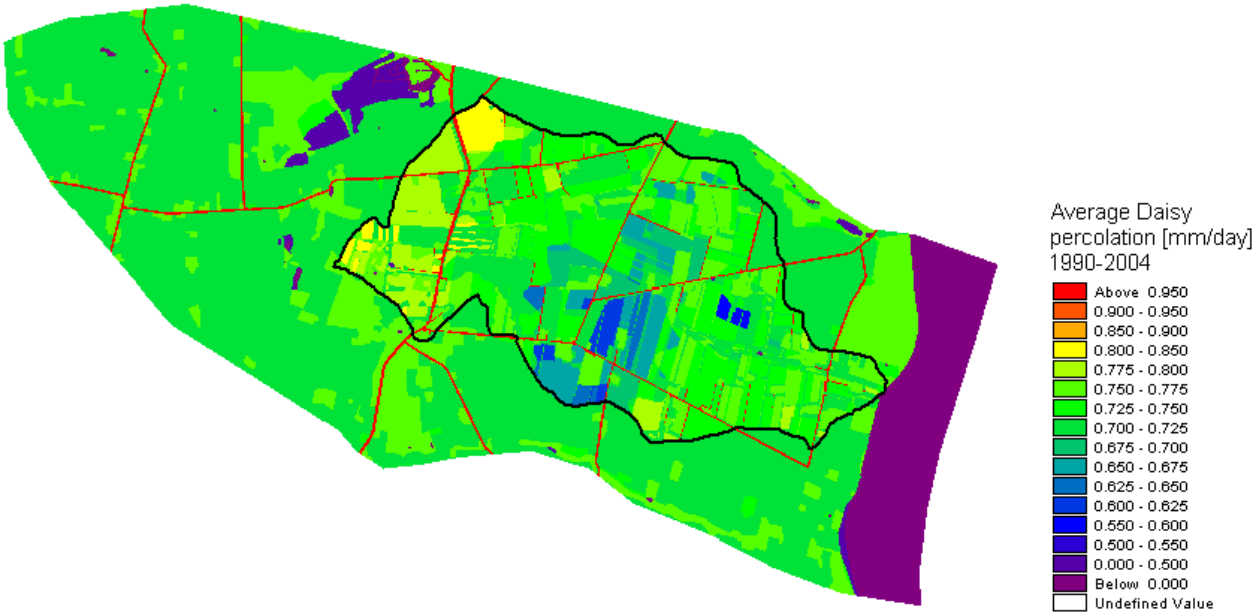

Figure 7.10 Average Daisy percolation for the model area in a 10 m x 10m grid

7.1.9 MIKE11 – stream model

The MIKE11 set up is, as mentioned above, based on the river set up from the previously model by Styczen et al (2004). This setup contains 7 river branches within the LOOP4 area (see figure 7.11). The main branch of Lillebæk is divided into a lower part, with 3 tributaries, and an upper part, with 2 tributaries. Upper Lillebæk and all tributaries are submerged in pipes and only Lower Lillebæk is a free channel (Styczen et al, 2004). The river set up from Styczen et al (2004) is modified and furthermore expanded to include the streams outside the LOOP4 area.

The position of the existing river network is adjusted in GIS, based on the 1.6 m DEM (see figure 4.6), by moving the network points to the nearest depression. The model area includes the upstream end of Tange stream and the streams of Isebæk and Hammesbro and these streams are thus included in the MIKE11 setup. The location of these streams is defined using a topographical map (1:25000) and the 1.6 m DEM.

Measurement of stream cross sections was conducted in Lower Lillebæk during the winter 1999-2000 (Styczen et al, 2004) and these cross sections are used to define the shape of Lower Lillebæk. The Lower Lillebæk has a width of 1.5 m in the upstream end and 2 m in the downstream end and the depth is around 0.5 m. For the Upper Lillebæk and the tributaries triangle shaped standard cross sections of 1 m x 0.5 m are defined. For the streams outside LOOP4 are standard cross sections of 2 m x 1 m used. The elevation of the cross sections are compared to the topography and adjusted downwards so that the highest river bank of all cross sections is below terrain level. This is done to prevent the streams from 'flying' above ground, which will influence the exchange between the streams and the saturated zone.

The entire MIKE11 river network is divided into a computational grid consisting of 86 h-points, placed at cross sections, and 71 Q-points, placed between cross sections. At the upstream end in all streams a small constant inflow (0.0001 m^3/s) is defined as boundary condition. This is done to prevent the streams from drying out, which will give instability problems. At downstream ends of Lower Lillebæk, Isebæk, Hammesbro and Tange stream constant water level boundary conditions are defined. As Lower Lillebæk, Isebæk and Hammesbro are discharging into the sea the water level elevation in these streams is set to 0 m. In Tange stream the water level elevation is set to 37.5 m, corresponding to a water depth of 0.5 m.

All MIKE11 river branches are linked to MIKE SHE for exchange with the saturated zone. The MIKE11 river network is incorporated in MIKE SHE as river links placed at model grid edges as seen on figure 7.12. This therefore results in a simplification of the MIKE11 river network due to the scale of the grid cells in MIKE SHE. All branches are defined as gaining reaches and the conductance is specified as "*river bed only*". The piped branches in Lillebæk are defined with a smaller leakage coefficient than the unpiped branches.

For use as initial condition in the stream model a hot start file is generated. This file is generated by running MIKE11 without MIKE SHE. The model is run for 5 days with a very small time step (10 sec.) to be sure the model is stable and, as initial condition is a water depth of 0.5 m in all streams defined.

7.1.10 Overland flow

The model domain does not follow the topographical catchment and therefore overland flow over the model boundary is possible. The outer boundary condition for overland flow is therefore defined as a specified head which, as mentioned in section 3.2.1, is based on the initial water depth in the outer cells of the model domain. An initial water depth of zero is used.

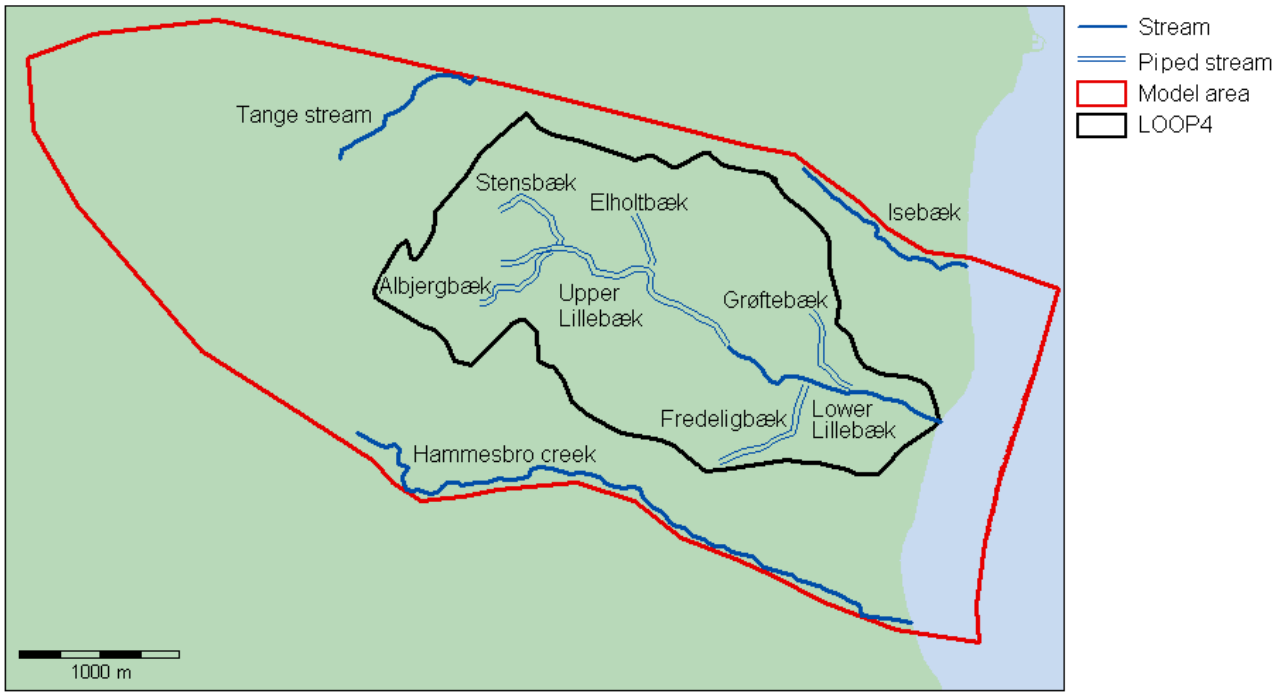

Figure 7.11 River network in MIKE11

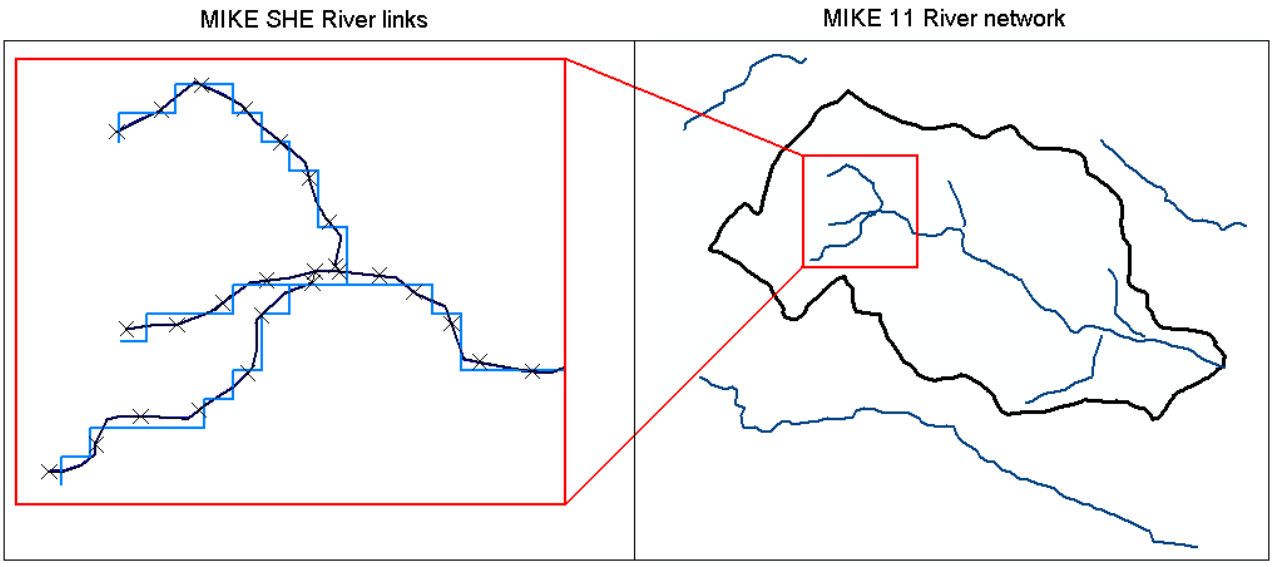

Figure 7.12 The MIKE11 river network is incorporated in MIKE SHE as river links placed at model grid edges

7.1.11 Groundwater abstraction

There are 5 abstraction plants located within the model area: Oure water supply, Elsehoved water supply, M. Voigt-Petersen, Hans Christian Rasmussen and Broholm Estate. Hans Christian Rasmussen was first established ultimo 2003 and pumped only 92 m^3 in 2004. Broholm Estate is also very new, and no data exists for this plant. These two abstractions are therefore not included in the model.

Oure water supply is the only abstraction plant with more than one well and has, in total, 6 abstraction wells. Although 3 of the wells have not been in use during the simulation period and therefore only 3 of the wells are included in the model. There is no information on the distribution of the abstraction between the 3 wells and it is therefore assumed that the total abstraction from Oure water supply is evenly distributed between the wells. The well 165.360 was first started ultimo 1993, thus until then the total abstraction is distributed between 165.148 and 165.167.

In table 7.4 data on the abstractions included in the model is seen and the location of the wells is seen on figure 7.13. The average total abstraction per year in the model area is 116876 m^3, of which almost 94% is abstracted at Oure water supply. The yearly abstraction has varied through the simulation period as seen on figure 7.14 and has increased in the last 4 years.

Table 7.4 Data on abstractions in the model area. The table shows plant name, DGU number of the active wells, geological formation in which the wells are screened, total average abstraction and the distribution of abstraction between plants

Abstraction plant	Wells (DGU no.)	Geological formation	Average abstraction [m^3/year]	Fraction of total abstraction [%]
Oure water supply	165.148 165.167 165.360	Eem-Weichsel interglacial freshwater sand	109452	93.6
Elsehoved water supply	165.128	Saale glacial melt water sand and gravel	3142	2.7
M. Voigt-Petersen	165.265	Saale glacial melt water sand and gravel	4282	3.7
		Total	116876	100

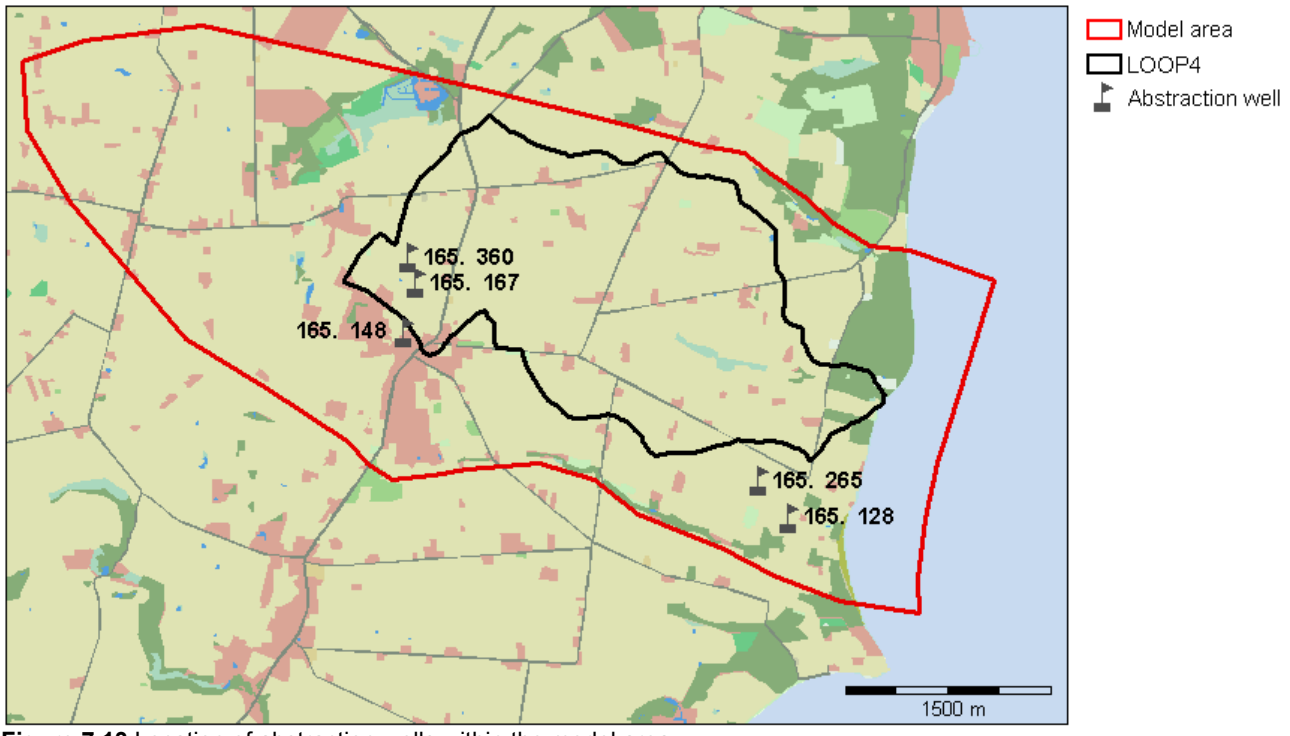

Figure 7.13 Location of abstraction wells within the model area

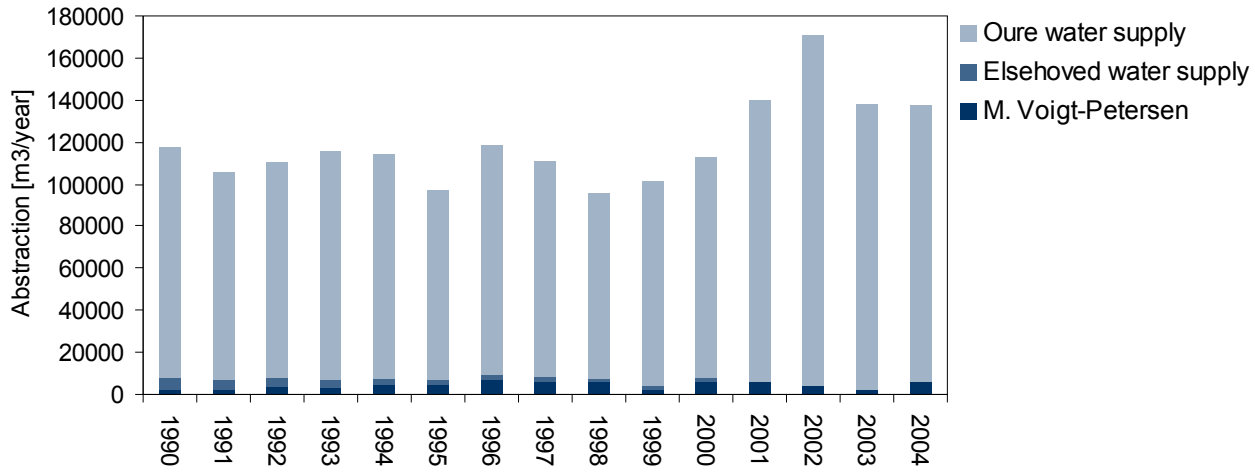

Figure 7.14 Yearly amount of groundwater abstraction in the model area and the distribution between the 3 abstraction plants

7.1.12 Drainage

Drainage is included in the entire model area using the built in drainage routing option in MIKE SHE. The drainage is based on drain codes and is very simply implemented in the model based on watersheds to the streams (see figure 7.15). Each watershed is given one drain code, which results in drainage to the nearest river link within each watershed. The model area includes a small part of a watershed belonging to a stream outside the model (light green area) and this area is given a negative drain code which, leads to drainage to the boundary in this area. In the area along the coast drainage is also lead to the boundary (dark green area). The grey area, which covers the sea, is specified with a drain code equal to 0, thus in this area drainage is not generated. The drain level is set to 1 meter below ground surface although towards the coastline the drain level is decreased so the drains reach terrain at the coast. This is done to prevent the drains from lowering the groundwater table to below sea level along the coastline and thus preventing an inwards water flow from the sea into the model area.

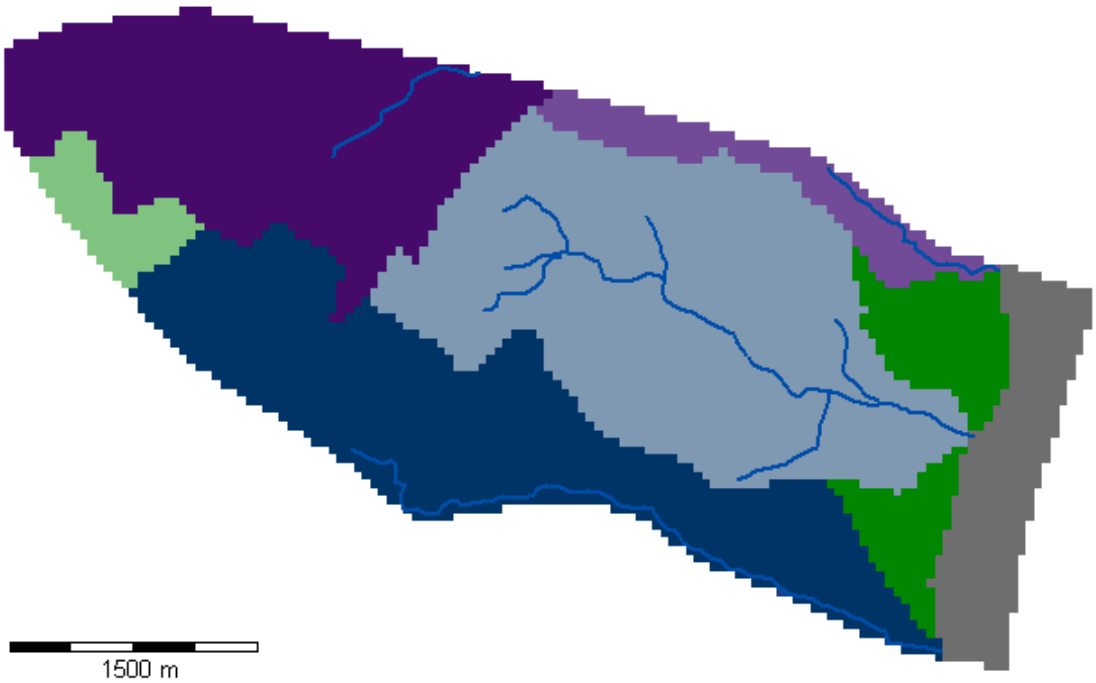

Figure 7.15 Drain code map. The drain codes are based on topographical watersheds to the streams and are defined as a constant value in each watershed. The blue and purple areas have positive drain codes and are therefore draining to the nearest river link and the green areas have negative drain codes and are draining to the boundary. The grey area covers the sea and has drain code = 0, therefore no drainage is generated here

7.2 Calibration and validation

Once the model has been set up the next step is to calibrate the model in order to optimize the model parameters in relation to observations. The calibration is performed as a manual trial-and-error calibration and is conducted as a split-sample test using the period 2000 - 2004 for calibration and 1995 – 1999 for validation. The reasoning for only making a manual calibration is that, as mentioned, it is believed that the initial parameter values are a good initial estimate as these are based on the calibrated and validated model by Styczen et al (2004).

7.2.1 Calibration targets and uncertainty estimation

The first step in the calibration process is selection of qualified observation data for use as targets in the calibration. Observation of hydraulic heads and daily stream discharge for the period 1/1 2000 -31/12 2004 is used in calibration of the hydrological model. However, for the upstream station (470032) discharge only is available for the period 1/1 1990 – 31/12 2003.

In table 7.5 the number of head observations used for calibration is seen as well as the distribution of the observations in relation to computational layers and hydrostratigraphical units. There are no head observations available for the observation wells 165.344, 165.348, 165.369 and 165.370 in the calibration period, but these wells are included in the following validation. It is seen that the vast majority of the observations are from the Weichsel ML. Only a few of the observations are from the Eem-Weichsel IS layer and the upper Weichsel/Saale DS and DG lens and none is available for the lower lens for the calibration period. It should be noted that the geology was not described when installing the observation wells, and it is in conesquence uncertain whether the wells are screened in the correct geological formation.

The uncertainty on the observation data must be estimated to assess the maximum accuracy the model can be expected to reproduce the observations with. The uncertainty on hydraulic heads consists of error on the hydraulic head measurements and of scale error in the model. The hydraulic head error is derived from measurement errors in conjunction with error on the elevation of the measurement point. The scale error occurs due to the discretization of the model into numerical grid cells of finite size. The scale error consists of interpolation error that arises when the simulated hydraulic head is interpolated between grid cells and heterogeneity error that arises because model parameters are constant within a grid cell and therefore not describing the heterogeneity within a cell (Sonnenborg & Henriksen, 2005). In table 7.6 an estimate of the different sources of uncertainties on the hydraulic heads is seen. It is assumed that the different sources of error are independent, and the square of the individual error can thus be summed. The total uncertainty on hydraulic heads can then be estimated as the square root of this sum and is, in this study, estimated to 1.16 m (Sonnenborg & Henriksen, 2005).

The uncertainty on stream discharge consists of measurement errors and if the discharge is estimated based on a Q-h relation the uncertainty also consists of errors on this transformation. Scale effects in the model also have implications in relation to stream discharge as the numerical discretization of the model, as earlier mentioned, determines how accurately the stream can be included in the model (Sonnenborg & Henriksen, 2005). The uncertainty on the stream discharge is unknown. Normally the uncertainty on discharge measurements is assumed to be not more than 10%, but, as the discharge in Lillebæk is rather small, it is suspected that the uncertainty could be higher.

Table 7.5 Hydraulic head observations used for calibration

Comp. layer	Hydrostrati-graphical unit	Obs. well (DGU no.)	Total no. of head observations	No. of head observations for calibration	Distribution of calibration targets by layer [%]
1	Weichsel ML	165.340 165.341	1055	402	29.2
2	Weichsel DS and DG	165.334 165.335	531	204	14.8
3	Weichsel ML	165.336 165.337 165.369 165.370 165.342 165.343 165.344 165.345	1721	696	50.5
4	Eem-Weichsel IS	165.338 165.339 165.346 165.347	256	77	5.6
6	Saale DS and DG	165.348	18	0	0
Total			3581	1379	100

Table 7.6 Estimate of uncertainty s_{obs} [m] on hydraulic head in Lillebæk catchment
The following values are used: Δx = 50 m, J = 0.01 m/m, C = 0.46, λ = 1.2 m, s_{lnk} = 2.3
The values for C, λ and s_{lnk} are taken from Sonnenborg & Henriksen (2005, pp. 11-7 and 11-14)

	Hydraulic head error		Scale error		Other effects[1]	Total uncertainty
	Measurement error	Elevation error	Interpolation	Heterogeneity		
General	0.005 - 0.3	0 - 2	$0.5 \cdot \Delta x \cdot J$	$C^{1/2} \cdot \lambda \cdot s_{lnk} \cdot J$	0 - 1	$\sqrt{\sum s^2}$
Lillebæk	0.05	1	0.32	0.02	0.5	1.16

1) Includes effects like vertical scale error, variation in topography and uncertainty on recharge

7.2.2 Performance criteria

The next step is to specify performance criteria which are measures of how accurate the model simulates the observed values. Both quantitative and qualitative performance criteria are used in this study and are presented below.

Quantitative criteria

The quantitative performance criteria are often based on measures of the average deviation between simulated and observed values. The performance criteria used in this study are ME, RMSE, R2 and Fbal, which evaluate the residuals in different ways and are some of the most commonly used criteria (Sonnenborg & Henriksen, 2005).

The mean error (ME) expresses the average difference between observed and simulated values. The mean error at location *i* where *n* numbers of observations exists, is expressed as (DHI, 2009c):

$$ME_i = \frac{\sum_t \left(Obs_{i,t} - Sim_{i,t}\right)}{n} \qquad \in]-\infty;\infty[$$

ME indicates if an overall error is introduced to the results and hence if the simulated values are generally too low (ME>0) or too high (ME<0). The optimal value of ME is 0.

The root mean square error (RMSE) is a measure for the deviation of the residuals. The root mean square error at location *i* where *n* number of observations exist, is calculated as (DHI, 2009c):

$$RMSE_i = \frac{1}{n}\sqrt{\sum_t \left(Obs_{i,t} - Sim_{i,t}\right)^2} \qquad \in [0;\infty[$$

When the deviation between simulated and observed values is decreasing RMSE will approach 0 and the optimal value of RMSE is thus 0.

The Nash-Suttcliffe correlation coefficient (R2) is a measure of how much of the variation in observations that is explained by the model. The Nash-Sutcliffe coefficient at location *i* where *n* number of observations exist, is expressed by (DHI, 2009c):

$$R2_i = 1 - \frac{\sum_t \left(Obs_{i,t} - Sim_{i,t}\right)^2}{\sum_t \left(Obs_{i,t} - \overline{Obs_i}\right)^2} \qquad \in]-\infty;1]$$

The Nash-Suttcliffe correlation (R2) coefficient is also called the “model efficiency” and the optimal value of R2 is 1.

The last performance criteria used in the study is Fbal, which is a measure for how well the model simulates the average stream discharge. Fbal expresses the difference in simulated and observed average discharge in percent of the observed (Sonnenborg & Henriksen, 2005):

$$Fbal = 100 \cdot \frac{\overline{Q}_{obs} - \overline{Q}_{sim}}{\overline{Q}_{obs}} \qquad \in]-\infty;100]$$

The optimal value for Fbal is 0. The average discharge is underestimated if Fbal>0 and overestimated if Fbal<0.

Factors such as hydrogeological conditions, heterogeneity, model discretization and data quality all have influence on how good a performance it is possible to obtain with the model. Therefore the acceptable level of accuracy for the model, and thus the acceptable level for the quantitative performance criteria must be specified before the calibration. This is done by defining accuracy criteria and choosing an accuracy level for the calibration. The accuracy criteria are defined as (Sonnenborg & Henriksen, 2005):

$$\beta_1 \geq \frac{ME}{\Delta h_{\max}} \qquad \beta_2 \geq \frac{RMSE}{s_{obs}} \qquad \beta_3 \geq \frac{RMSE}{\Delta h_{\max}} \qquad \beta_4 \leq R2 \qquad \beta_5 \geq \left| Fbal \right|$$

s_{obs}: Total uncertainty on hydraulic heads
Δh_{max}: Maximum head difference

In table 7.7 different levels of accuracy are seen. The aim in this study is to reach a high fidelity level for the model. With an estimated uncertainty on observed heads (s_{obs}) on 1.16 m and a total difference in hydraulic head (Δh_{max}) in the area on 44 m ME must be less than 0.44 m and RMSE less than 1.91 m to reach a level of high fidelity.

The accuracy criteria for stream discharge based on table 7.7 is Fbal < 10% and R2 > 0.75 for reaching a high fidelity level. Though, in some model studies, where the stream discharge is small, e.g. Alectia (2008) and Alectia (2010a), the accuracy criteria to stream discharge have been differentiated in relation to the size of the average discharge as seen in table 7.8. The reasoning for this is that the uncertainty on the measured discharge is larger for small flows than for large flows. The average discharge in Lillebæk is, as mentioned in section 5.2.3, 0.017 m^3/s at the upstream and 0.034 m^3/s at the downstream station. The discharge in Lillebæk is thus rather small and using the differentiated approach would be acceptable. The average flow in Lillebæk is thus so small that using the differentiated approach results in criteria to Fbal and R2 on < 100% and > 0 respectively, which are not very strict criteria. It is instead decided to specify an acceptable levels of R2 >0.50 and Fbal<20%, which is thus stricter than the differentiated approach but less strict than the level specified in table 7.7.

Table 7.7 Accuracy criteria and levels

Accuracy criteria	Low fidelity	Medium fidelity	High fidelity
β_1	0.05	0.025	0.01
β_2	2.6	2.0	1.65
β_3	0.15	0.1	0.05
β_4	0.4	0.6	0.75
β_5	30%	20%	10%

Table 7.8 Differentiated accuracy criteria for Fbal and R2 based on average stream discharge

Q [m^3/s]	Fbal [%]	R2
> 0.5	< 10	> 0.75
0.2-0.5	< 15	> 0.65
0.1-0.2	< 25	> 0.50
0.05-0.1	< 50	> 0.20
< 0.05	< 100	> 0.00

Quantitative criteria

The quantitative performance criteria for the model are defined as follows (Sonnenborg & Henriksen, 2005):

- The estimated parameter values must be realistic and within the expected range specified in table 7.1
- The residuals between simulated and observed values must be evenly distributed in time and space
- The hydrological characteristics in the area should be reproduced by the model i.e. the model should be able to simulate flow directions and the location of the groundwater watersheds correctly
- The discharge dynamics in Lillebæk stream should be simulated correctly with correct representation of discharge events

7.2.3 Sensitivity analysis

Prior to the calibration a sensitivity analysis is conducted to distinguish the most sensitive parameters on which the calibration should focus. First, a reference model is run using the initial parameters as specified in table 7.1. The initial parameter values results in an average ME on 0.74 m and an average RMSE of 1.75 m for hydraulic heads. For stream discharge the initial parameters results in a R2 on 0.47 for the upstream station and 0.20 for the downstream and thus an average R2 of 0.34.

The sensitivity analysis is carried out by increasing the model parameters with 10% one parameter at a time and subsequently evaluating the change in error compared to the reference run. The result of the sensitivity analysis with respect to change in average ME for hydraulic heads and average R2 for stream discharge is seen on figure 7.16. The analysis shows the most sensitive model parameters to be:

- Hydraulic conductivity for Weichsel ML
- Hydraulic conductivity for Saale ML
- Hydraulic conductivity for Eem-Weichsel IS
- Hydraulic conductivity for Weichsel/Saale DS and DG
- Drain time constant
- Specific yield for clay

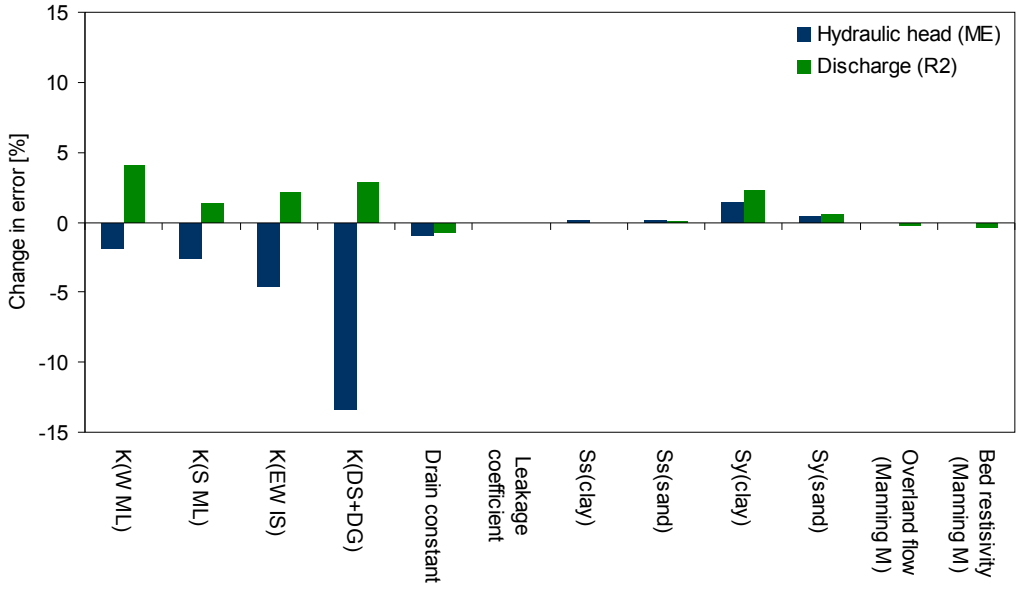

Figure 7.16 Sensitivity analysis of model parameters. The sensitivity is indicated as change in ME and R2 compared to a reference run

7.2.4 Calibration

The 6 model parameters found as the most sensitive are then targets for calibration. The first step in the calibration is performing a single-variable optimization for each of the 6 model parameters. This is done in order to find the value for each of the parameters resulting in the smallest deviation between simulated and observed and thus the optimal value. The single-variable optimization is performed by running the model with different parameter values for each of the parameters, changing one parameter at a time.

I figure 7.17 the resulting objective functions for the 6 parameters for ME and RMSE for hydraulic heads and R2 for discharge are seen. The graphs show the change in ME, RMSE and R2 as a function of chance in parameter value. The change in parameter value is indicated as a percent of the initial value. For ME and RMSE the optimal value is the value resulting in a ME/RMSE closest to 0, whereas for R2 the optimal value is the one resulting in a R2 closest to 1. It is noted that the three performance criteria do not give a clear indication of the optimal value for some of the parameters e.g. when considering the hydraulic conductivity for Weichsel ML, it is noted that the objective functions for ME and RMSE for hydraulic heads are sloping in opposite directions. For specific yield for clay the performance criteria for hydraulic heads (ME/RMSE) conflicts with the criteria for discharge (R2).

The next step is then to make a multi-variable optimization to optimize all 6 model parameters based on the results from figure 7.17. Adding more objectives to an optimization problem adds complexity as the objective function then gets multiple-dimensional. The parameters influence each other and it is therefore not certain that the value that was most optimal for a parameter under the single-variable optimization is the most optimal in the multiple-variable optimization. Because the three performance criteria do not result in the same optimal values for all parameters three different combinations of parameter values are tested; Calibration A, focusing on RMSE for hydraulic heads, Calibration B focusing on R2 for discharge and Calibration C, which is an overall assessment. In table 7.10 the combinations of parameter values are seen and in table 7.9 the resulting performance criteria.

Trying to improve the performance of the model, the specific yield and the drain constant are subsequently changed in relation to the first estimates for Calibration A and C. Additionally the detention storage and maximum drain level have also been changed, even though these parameters were not initially chosen as calibration parameters. The combination of parameter values in calibration B results in drying of cells and that only 45% of the specified abstraction can be withdrawn and it has therefore not been worked on further with this combination.

The general trend for all calibration runs is that hydraulic heads are simulated too high (see table 7.9). At the downstream station the simulated average discharge is underestimated whereas, at the upstream station, the average discharge is much too high. The model in general performs better at the downstream station than the upstream station. The calibration runs with the best overall performance are believed to be C3 and C5. Even though C3 is performing slightly better than C5 it is decided to go on with C5. The reason for this is that C5 has a lower amount of overland flow to the stream system than C3 (results not shown) due to specification of a detention storage for overland flow.

The calibrated parameter values for C5 are seen in table 7.11. It is noted that the calibration has resulted in hydraulic conductivities for Eem-Weichsel IS that is lower than for Weichsel ML, which seems improbable. It is suspected that too low hydraulic conductivities, especially for Eem-Weichsel IS, are the reason for simulation of too high hydraulic heads. Thus, trying to obtain more likely conductivities for Eem-Weichsel IS and to lower the hydraulic heads, 5 additional calibration runs are made; in C5.1 and C5.2 hydraulic conductivities for Eem-Weichsel IS are increased 10 and 100 times respectively, in C5.3 and C5.4 hydraulic conductivities for both Eem-Weichsel IS and the Weichsel/Saale DS and DG lenses are increased 10 and 100 times respectively and finally in C5.5 the hydraulic conductivities for all hydrostratigraphical units are increased 10 times. The results are seen in table 7.9, which shows that increasing the hydraulic conductivities, as expected, results in a decrease in hydraulic heads. Though, for C5.2-C5.5 the hydraulic head is now simulated much too low.

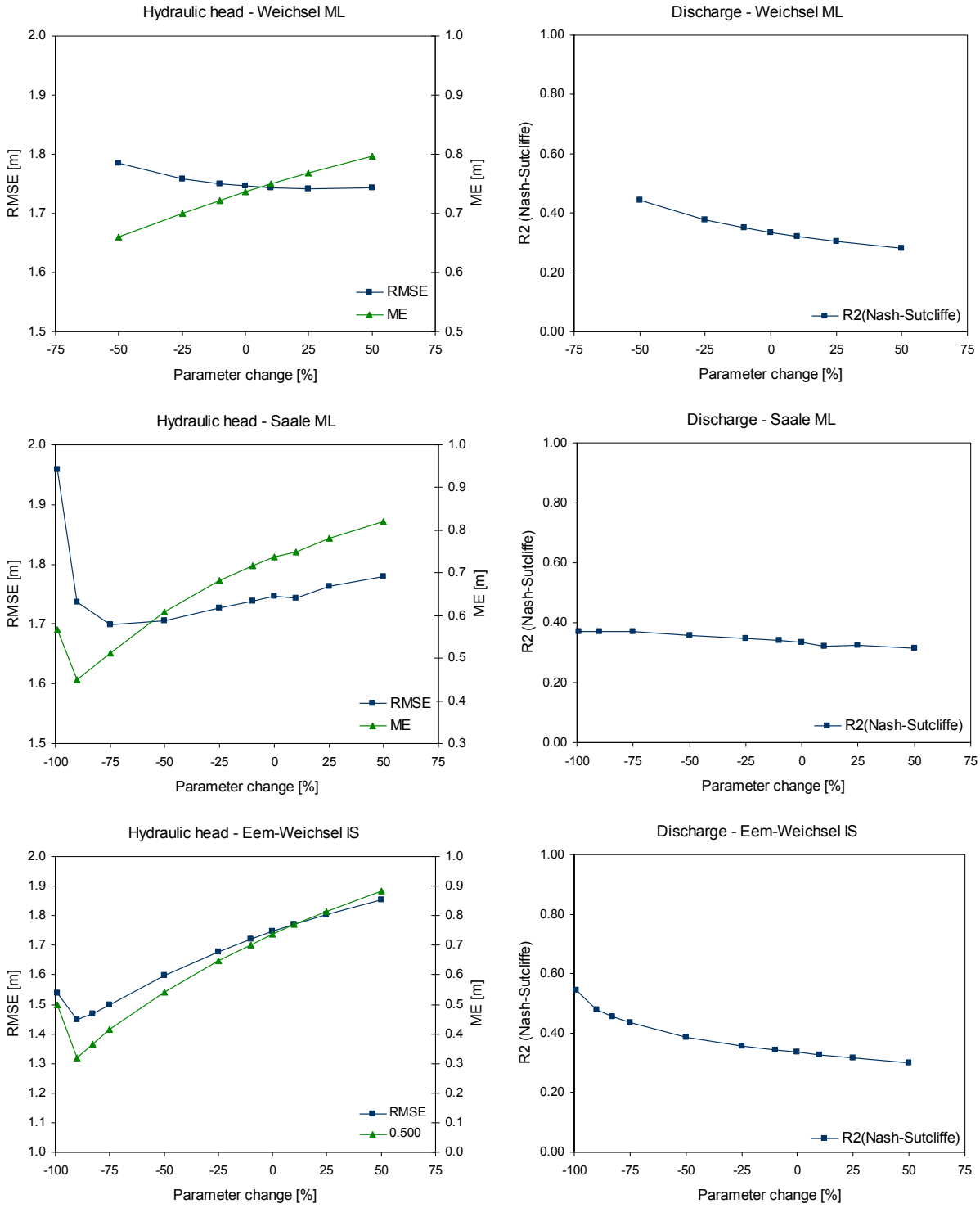

Figure 7.17 Single-variable optimization results. The graphs on the left show changes in average RMSE and ME for hydraulic head and the graphs on the right show changes in average R2 for discharge at the two stream stations

Figure 7.17 continued

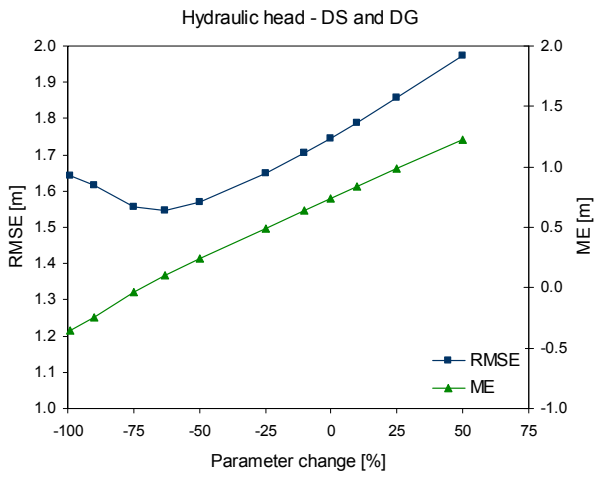

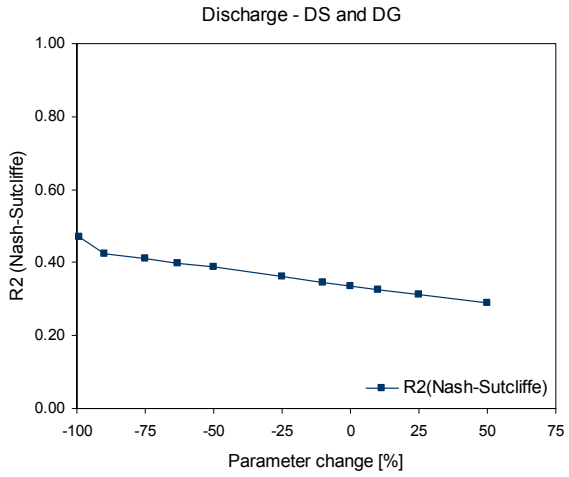

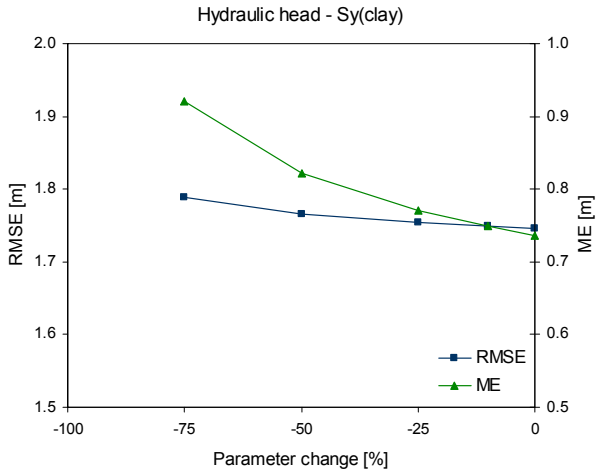

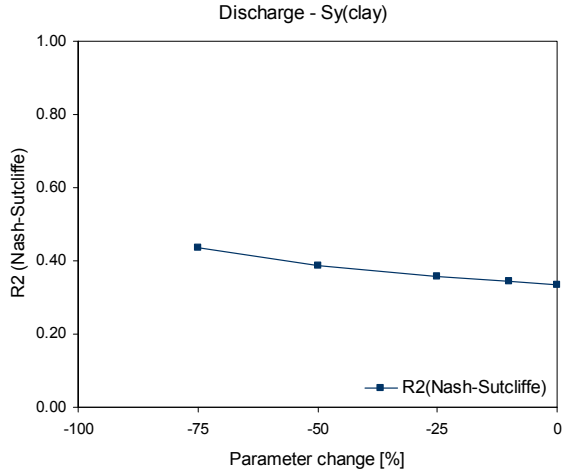

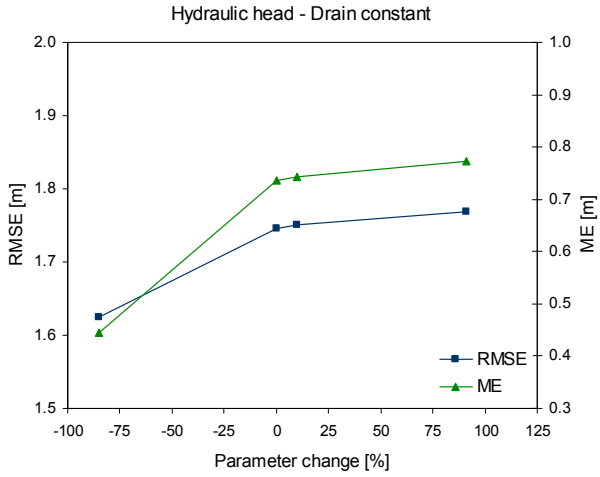

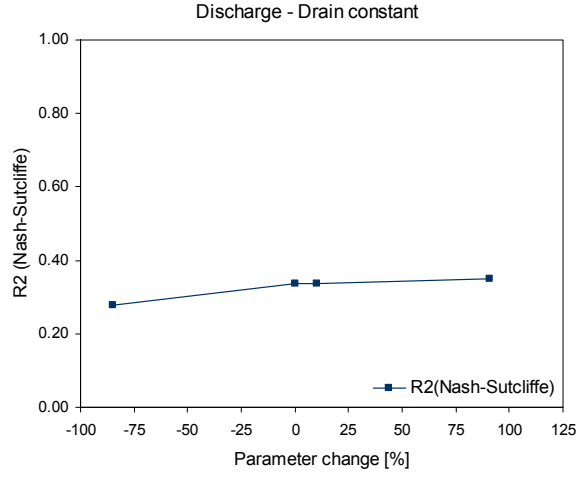

Calibration run C5.1 however, where the hydraulic conductivities for Eem-Weichsel IS are increased by an order of magnitude, is found to perform well. The Average ME error is improved compared to C5 and is only overestimating hydraulic head with 22 cm on average. C5.1 is also seen to perform better for the upstream station. The R2 has increased from 0.47 to 0.60 and the overestimation of average discharge at the up-stream station is decreased. Though, it is at the same time noted, that the performance for the downstream station has slightly decreased. The R2 has decreased from 0.55 to 0.46 and the underestimation of average discharge has slightly increased. These trends indicate that the flow pattern in the catchment has changed between C5 and C5.1 due to the increase in hydraulic conductivities in the Eem-Weichsel IS layer.

On figures 7.18 - 7.21 daily simulated discharge and yearly accumulated discharge for C5 and C5.1 for the calibration period is seen. It is seen that both C5 and C5.1 overestimate discharge during summer months and are not able to describe all peaks in the hydrographs. The largest difference between C5 and C5.1 in total yearly discharge is seen at the upstream station, where C5 simulates larger discharge in all years. It is decided to go on with C5.1 for the simulation of nitrate transport. The calibrated parameters for C5.1 are within the expected range and can be seen in table 7.11.

Table 7.9 Multiple-variable optimization results. Shown in the table are ME and RMSE for hydraulic head and R2 and Fbal for discharge at each stream station. The results for ME and RMSE are average values for all observations wells. Furthermore, the number of observations wells where ME >0.44 and RMSE>1.91 are seen in the table

	Hydraulic head				**Discharge**			
	ME		**RMSE**		**R2 (Nash-Sutcliffe)**		**Fbal**	
	Average [m]	No. of wells ME>0.44	Average [m]	No. of wells RMSE>1.91	470032	470033	470032	470033
A1	-7.48	8	1.46	2	0.41	0.38	-43.3	12.7
A2	-0.64	8	1.44	1	0.47	0.44	-42.6	13.0
A3	-0.50	10	1.42	1	0.49	0.49	-41.6	13.4
A4	-0.42	9	1.40	1	0.55	0.52	-40.6	12.4
A5	-0.28	8	1.39	1	0.49	0.55	-39.9	12.8
A6	-0.36	9	1.42	1	0.48	0.54	-40.5	13.3
A7	-0.36	9	1.42	1	0.48	0.53	-41.0	13.3
A8	-0.81	9	1.53	1	0.47	0.53	-40.6	13.9
B1	-1.08	8	1.74	5	-0.02	0.46	-62.1	-2.2
C1	-0.94	7	1.44	2	0.49	0.50	-48.0	7.6
C2	-0.81	7	1.41	2	0.45	0.52	-46.2	8.3
C3	-0.79	6	1.40	2	0.47	0.56	-46.4	7.3
C4	-0.66	8	1.37	2	0.33	0.55	-45.0	7.9
C5	-0.86	7	1.43	2	0.47	0.55	-47.0	7.6
C6	-0.87	7	1.43	2	0.46	0.54	-47.8	7.5
C7	-1.31	9	1.66	3	0.45	0.55	-47.7	8.0
C5.1	-0.22	7	1.51	3	0.60	0.48	-25.6	8.7
C5.2	3.04	11	3.69	11	0.31	0.34	63.2	-9.5
C5.3	1.33	10	2.40	7	0.57	0.33	-16.0	44.1
C5.4	4.87	13	5.29	13	0.21	-0.05	78.8	87.0
C5.5	2.22	12	2.59	6	0.20	-0.06	38.6	63.1

Table 7.10 Parameter values used in the calibration runs. The parameter values are specified as a percentage of the initial value, except for detention storage and max drain level. The parameter changed between calibration runs are marked with red

Calibration A: Hydraulic head (RMSE)

	A1	A2	A3	A4	A5	A6	A7	A8
K(Weichsel ML) [%]	+25	+25	+25	+25	+25	+25	+25	+25
K(Saale ML) [%]	-75	-75	-75	-75	-75	-75	-75	-75
K(Eem-Weichsel IS) [%]	-90	-90	-90	-90	-90	-90	-90	-90
K(DS and DG) [%]	-63	-63	-63	-63	-63	-63	-63	-63
Sy(clay) [%]	0	**-50**	**-75**	**-50**	**-75**	**-75**	**-75**	**-75**
Drain constant [%]	-85	-85	-85	**+91**	**+91**	**+91**	**+91**	**+91**
Detention storage [mm]	0	0	0	0	0	**1**	**5**	**5**
Max drain level [m.b.s.]	1	1	1	1	1	1	1	**0.5**

Calibration B: Discharge (R2)

	B1
K(Weichsel ML) [%]	-50
K(Saale ML) [%]	-99
K(Eem-Weichsel IS) [%]	-99
K(DS and DG) [%]	-99
Sy(clay) [%]	-50
Drain constant [%]	+91
Detention storage [mm]	0
Max drain level [m.b.s.]	1

Calibration C: Overall assessment

	C1	C2	C3	C4	C5	C6	C7
K(Weichsel ML) [%]	-50	-50	-50	-50	-50	-50	-50
K(Saale ML) [%]	-90	-90	-90	-90	-90	-90	-90
K(Eem-Weichsel IS) [%]	-90	-90	-90	-90	-90	-90	-90
K(DS and DG) [%]	-75	-75	-75	-75	-75	-75	-75
Sy(clay) [%]	-50	**-75**	**-50**	**-75**	**-50**	**-50**	**-50**
Drain constant [%]	-85	-85	**+91**	**+91**	**+91**	**+91**	**+91**
Detention storage [mm]	0	0	0	0	**1**	**5**	**5**
Max drain level [m.b.s.]	1	1	1	1	1	1	**0.5**

Table 7.11 Initial and calibrated parameter values for C5 and C5.1. The different in parameter values between C5 and C5.1 is marked with red

Hydrostratigraphical units

	K_h [m/s]			K_v [m/s]			S_y			S_s [1/m]		
	Initial	**C5**	**C5.1**	**Initial**	**C5**	**C5.1**	**Initial**	**C5**	**C5.1**	**Initial**	**C5**	**C5.1**
Weichsel ML	4.37E-06	2.19E-06	2.19E-06	4.37E-07	2.19E-07	2.19E-07	0.2	0.1	0.1	0.001	0.001	0.001
Saale ML	3.74E-06	3.74E-07	3.74E-07	7.48E-08	7.48E-09	7.48E-09	0.2	0.1	0.1	0.001	0.001	0.001
Eem-Weichsel IS	1.36E-05	**1.36E-06**	**1.36E-05**	1.36E-06	**1.36E-07**	**1.36E-06**	0.3	0.3	0.3	0.002	0.002	0.002
Weichsel/Saale DS and DG	8.00E-05	2.00E-05	2.00E-05	4.00E-05	1.00E-05	1.00E-05	0.3	0.3	0.3	0.002	0.002	0.002

Drainage

	Initial	**C5**	**C5.1**
Drain constant [s^{-1}]	1.00E-06	1.91E-06	1.91E-06
Max drain level [m.b.s]	1	1	1

Stream flow

	Piped reaches			**Unpiped reaches**		
	Initial	**C5**	**C5.1**	**Initial**	**C5**	**C5.1**
Leakage coefficient [s^{-1}]	1.00E-10	1.00E-10	1.00E-10	1.00E-09	1.00E-09	1.00E-09
Bed resistivity (M)	10	10	10	10	10	10

Overland flow

	Initial	**C5**	**C5.1**
Manning [$m^{1/3}/s$]	10	10	10
Detention storage [mm]	0	1	1

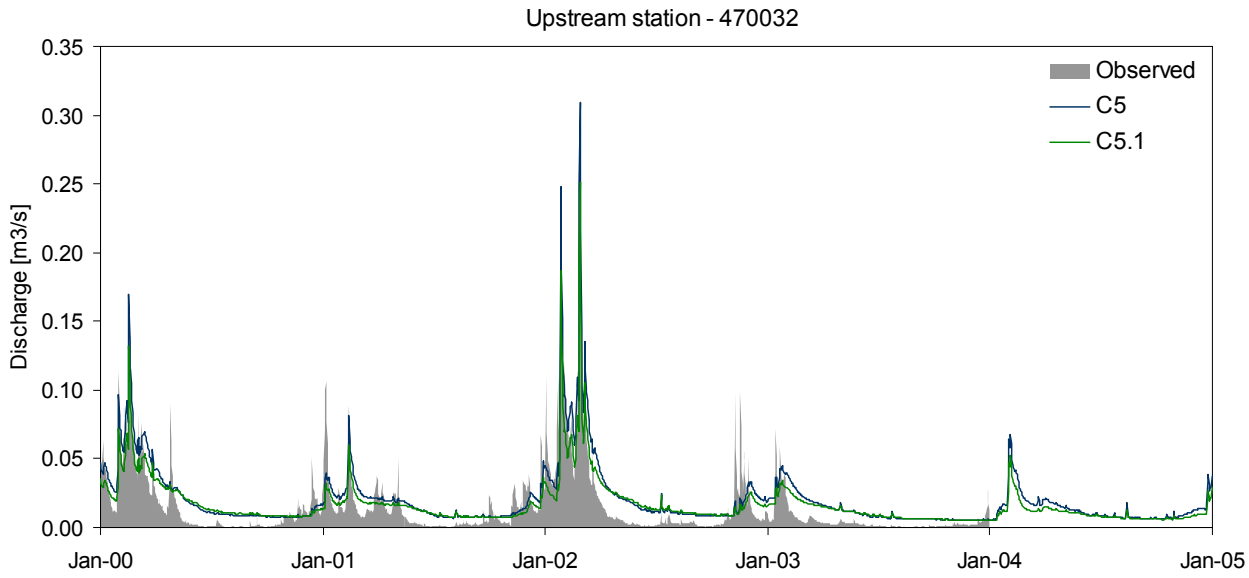

Figure 7.18 Observed and simulated daily discharge for C5 and C5.1 at upstream station (470032) for the calibration period 2000-2004

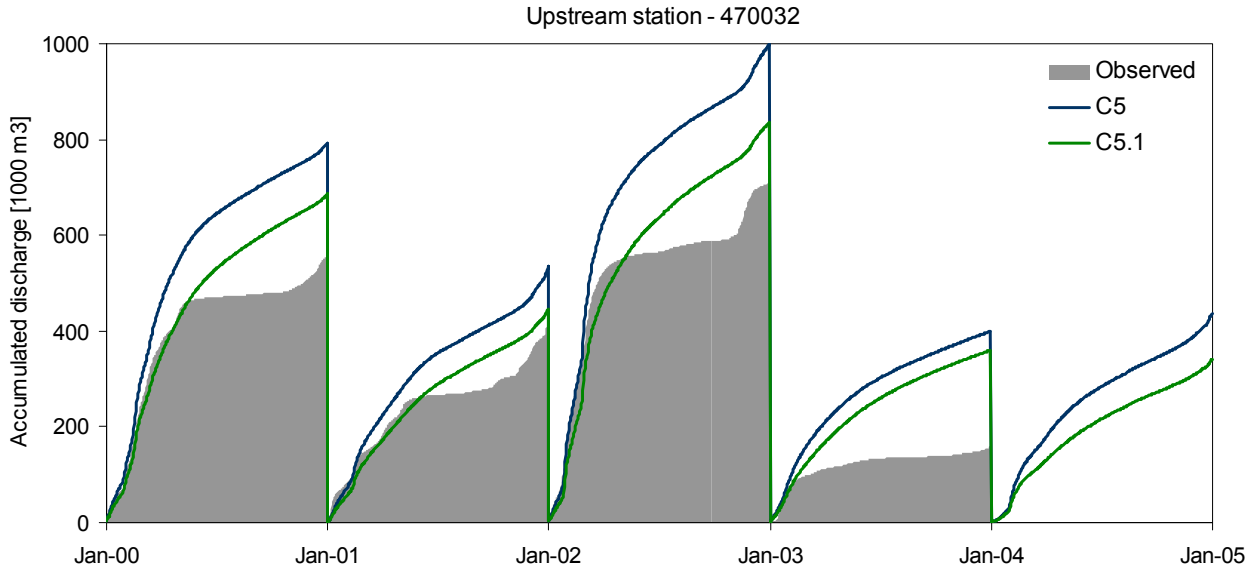

Figure 7.19 Observed and simulated yearly accumulated discharge for C5 and C5.1 at upstream station (470032) for the calibration period 2000-2004

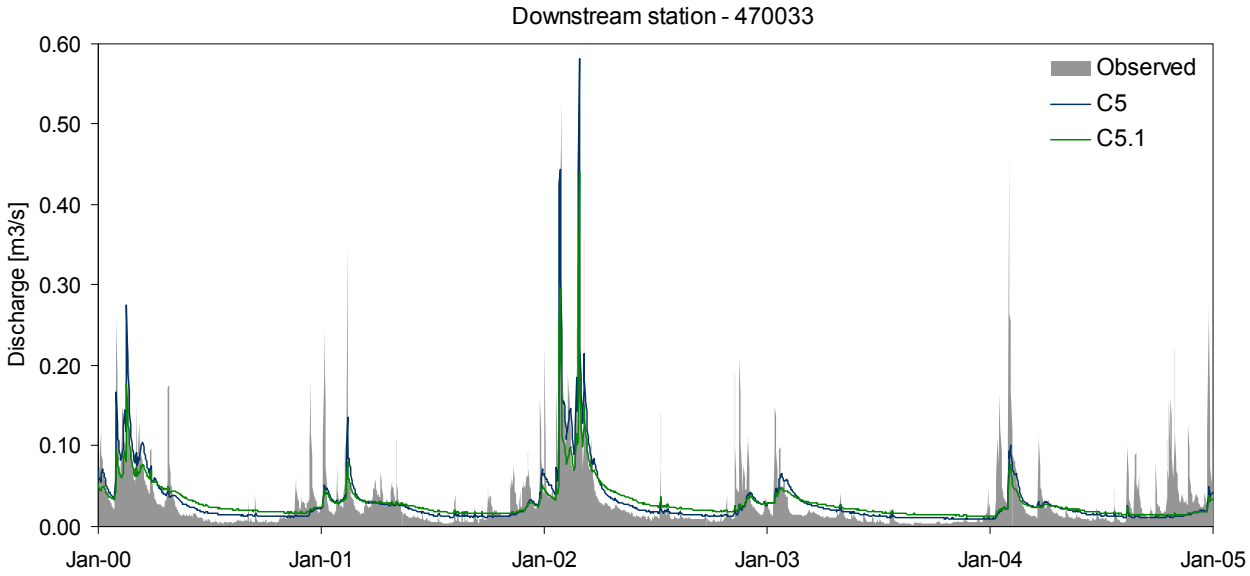

Figure 7.20 Observed and simulated daily discharge for C5 and C5.1 at downstream station (470033) for the calibration period 2000-2004

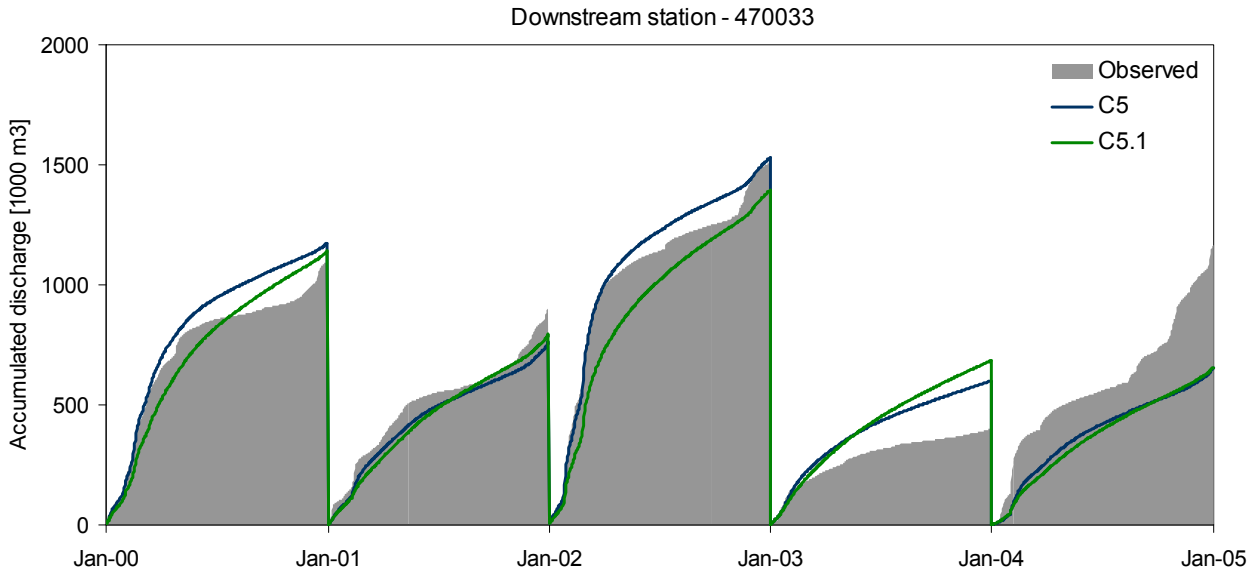

Figure 7.21 Observed and simulated yearly accumulated discharge for C5 and C5.1 at downstream station (470033) for the calibration period 2000-2004

7.2.5 Validation

The calibrated model (C5.1) is validated for the period 1/1 1995 – 31/12 1999. Before the validation the model is run a second time using hydraulic heads for the 31/12 2004 from the first run as initial heads. This is done as it is noted that the initial heads used during calibration are a little too low at some observations wells. This has a small effect on the performance criteria for the calibration period which are slightly changed compared to values reported above for the first run.

For evaluation of the model performance on smaller scale the drain areas are included in the model. This is done by specifying unique drain codes for each of the 5 drain areas as seen on figure 7.22. To be able to distinguish the discharge originating from the drain areas, the areas are specified to drain to small artificial branches that are added to the river network in the MIKE 11 set up.

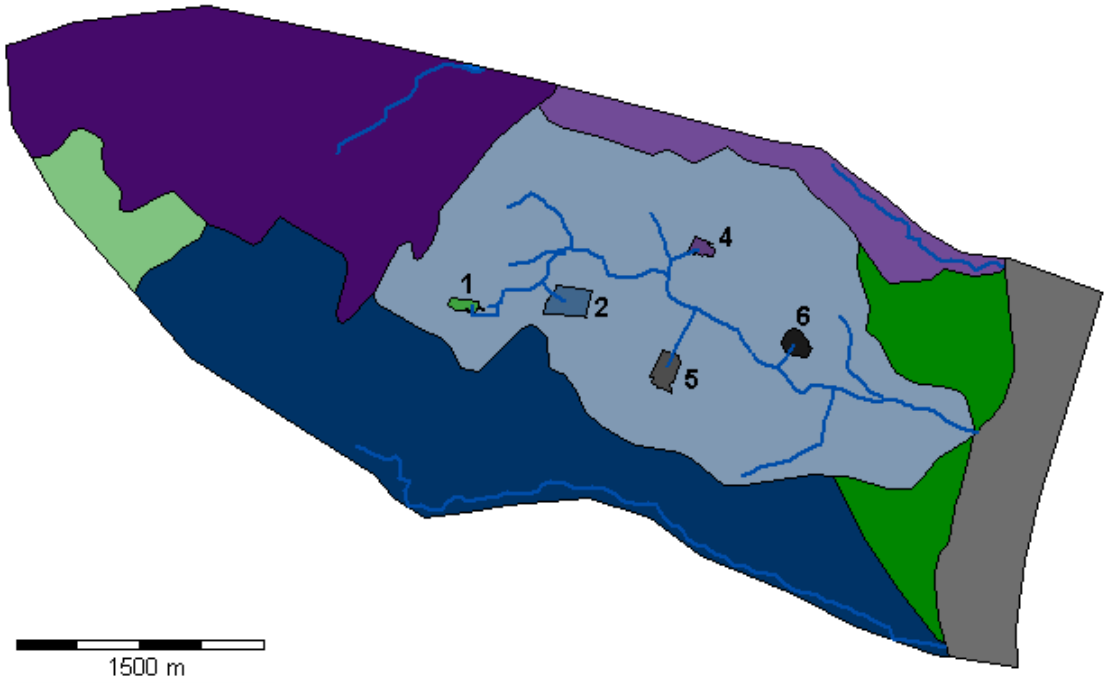

Figure 7.22 Including drain areas in the model as areas of specific drain codes

8. Nitrate model

8.1 Denitrification concept

An assumption of instantaneous reduction of nitrate at the redox-interface is applied in the study. In the reduced part of the saturated zone a half life of 1 hour is specified and above the redox-interface, where the saturated zone is oxidized, no reduction of nitrate is assumed to take place and a half life of 1000 years is therefore applied. As only a single redox depth can be specified for each model grid, the depth is thereby assumed to be constant within each 50 m grid cell. The applied denitrification concept does not include reduction in wetlands and meadows surrounding the streams or in stream sediments. Further more neither local anaerobic zones in the oxidized part of the saturated zone nor oxidized zones under the redox-interface is included. Only nitrate reduction in the saturated zone is simulated in the nitrate model for Lillebæk.

8.2 Redox-interface

The location of the redox-interface in the area is based mainly on borehole data from Jupiter. Within the model area are 32 boreholes with colour description of the sediments found, of which 14 is located within the LOOP4 catchment. The location of the boreholes with colour description is seen in figure 5.1. The methods used for drilling the boreholes are checked, as the quality of the borehole description and the location of the layer boundaries are very dependent on the drilling method. It is found that for all 32 boreholes drilling methods giving good sample quality and determination of boundaries have been used.

The location of the redox-interface is defined as the transition from oxidized to reduced colours. An oxidized layer is defined as sediments with yellow, yellow-brown, brown and grey-brown colours and a reduced layer as sediments with grey, brown-grey and black colours. In some boreholes oxidised sediments are found below layers of reduced sediments and in these cases the upper layer of reduced sediments is used to define the redox-interface. In some boreholes no reduced sediments are found, as they are not deep enough to reach the redox-interface and these boreholes can therefore not be used in the analysis. Of the 32 boreholes is it possible to locate the redox-interface in 21 of them.

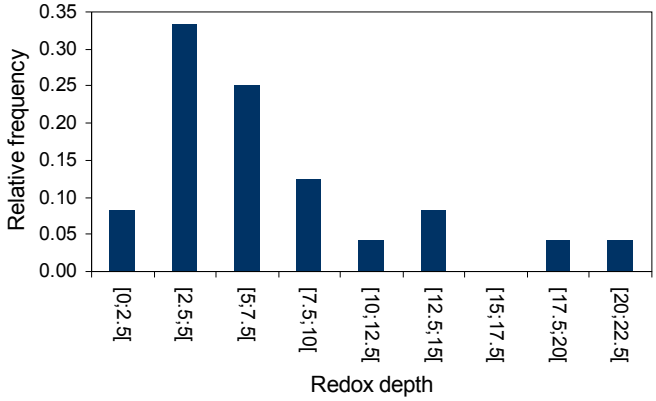

Figure 8.1 Relative frequency of redox depths within the model area

In addition to the colour analysis, the groundwater concentrations of nitrate from the LOOP4 area are also used as an indication of the location of the redox-interface. Nitrate concentrations are, as mentioned, measured in different depths and the location of the redox-interface is defined at the level where nitrate is measured in very low concentrations and thus disappears. Nitrate concentrations are measured in total in 57 wells within the LOOP4 area (see appendix 2). Though, as all except 3 wells are screened few meters below surface, only 5 of these wells can be used to determine the location of the redox-interface and, as 2 of these wells also have colour descriptions, this gives additional redox information in only 3 points.

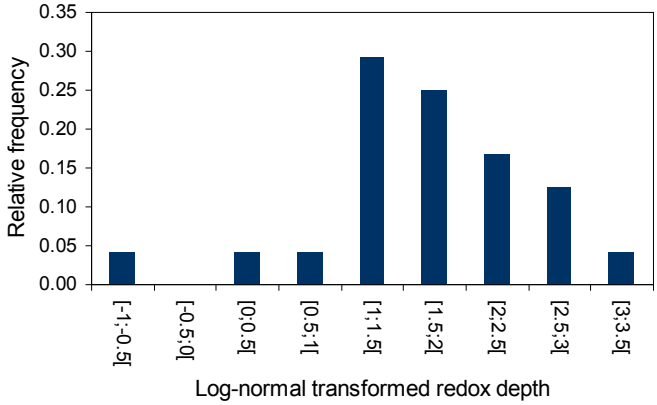

Figure 8.2 Relative frequency of log-normal transformed redox depths within the model area

In total the depth to the redox-interface is therefore known in 24 points within the model area. The frequency distribution of the interpreted redox depths and of the log-normal transformed redox depths are seen in figure 8.1 and 8.2. Neither the actual redox depths nor the log-normal transformed redox depths are seen to be normally distributed. The spatial correlation between observations can be described statistically by a semi-variogram. However, the number of redox observations in this study is believed not to be sufficient for a useful semi-variogram analysis to be made. This decision is based on the findings in Hansen & Rasmussen (2006), where a semi-variogram analysis of 20 observations of redox depths (also based on colour descriptions and nitrate concentrations) from Odderbæk catchment (LOOP2) was conducted. Hansen & Rasmussen (2006) concluded that the number and quality of data was not good enough for estimating a correlation length.

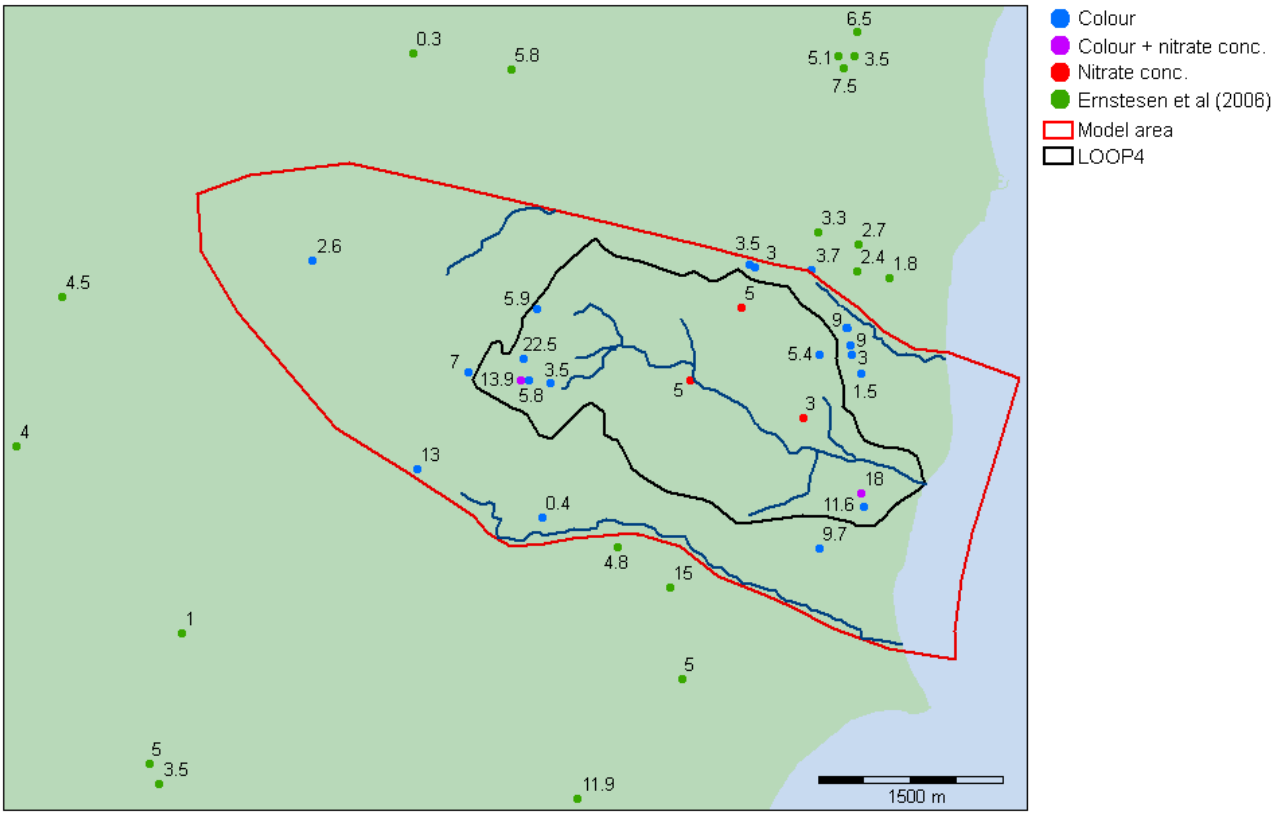

Figure 8.3 Spatial distribution of depths to the redox-interface. The data source for the interpreted redox depths are indicated by the colours of the points

The spatial distribution of the redox depths in the Lillebæk area is seen in figure 8.3. The redox depths are seen to vary a lot within short distance, especially in the western part of the LOOP4 catchment and no relation between redox depth and topography or distance to streams has been found. The location of the redox-interface between the observation points must therefore be 'assumed', which is done by means of interpolation. Hereby is the redox observation points interpolated to a two-dimensional surface for use in MIKE SHE. To support the interpolation at the edge of the model area, information on redox depths outside the model area is included. These depths are also based on colour descriptions and were analysed in a project by Ernstsen et al (2006). The redox-interface is believed to reach the surface at the coastline and therefore points of 0 m depth are added along the coastline to thereby manipulate the interpolated surface to reach the ground surface.

Different interpolation techniques have been tried for interpolation of the redox-interface. It would be preferable to use kriging to interpolate the surface, as this method takes into account the spatial behaviour of the data by quantifying the spatial variation of data by a semi-variogram. Though, using kriging for interpolation of the interpreted redox depths results in an unrealistic surface with strange looking structures (results not shown). This is an indication of, as assumed above, that the data set is not sufficient for constructing a satisfactory semi-variogram. The resulting surfaces when using a natural neighbour and an inverse distance weighted interpolation technique are seen on figure 8.4 and 8.5. It is decided to use the natural neighbour surface in the following, as the large redox depths in the western part of LOOP4 have less influence on the surroundings in this surface than in the inverse distance weighted surface.

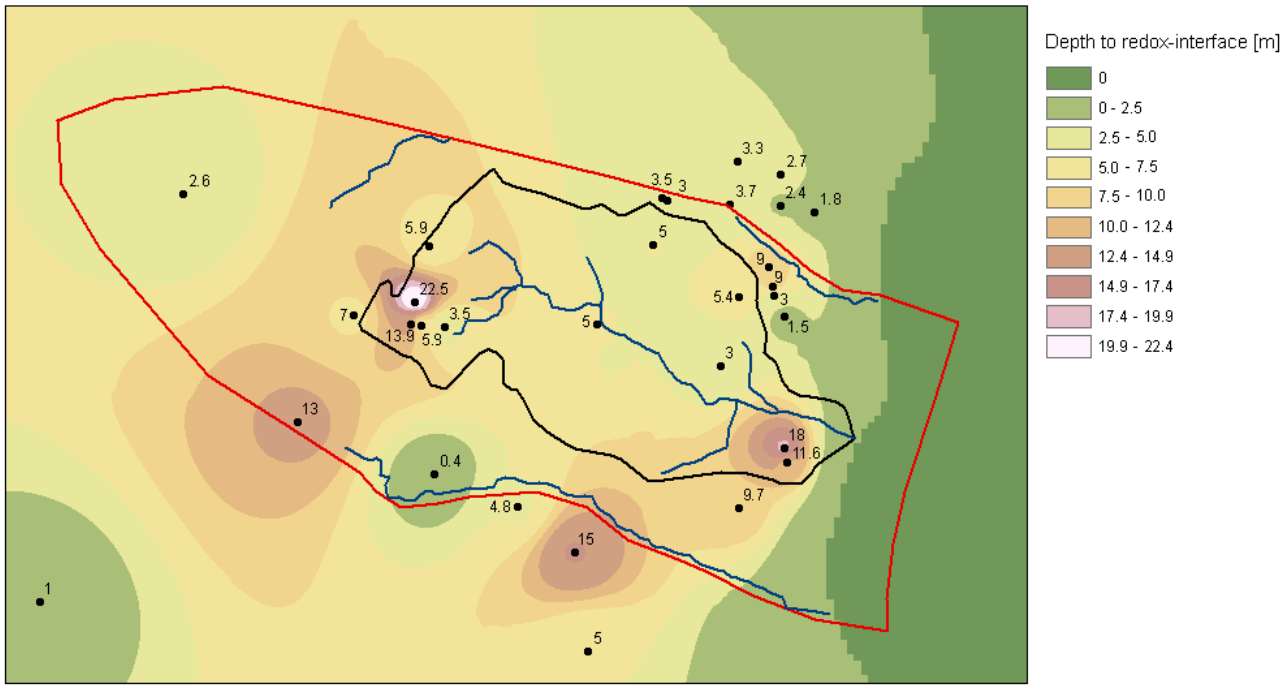

Figure 8.4 Interpolated redox-interface using inverse distance weighting (power: 3, number of search point: 12)

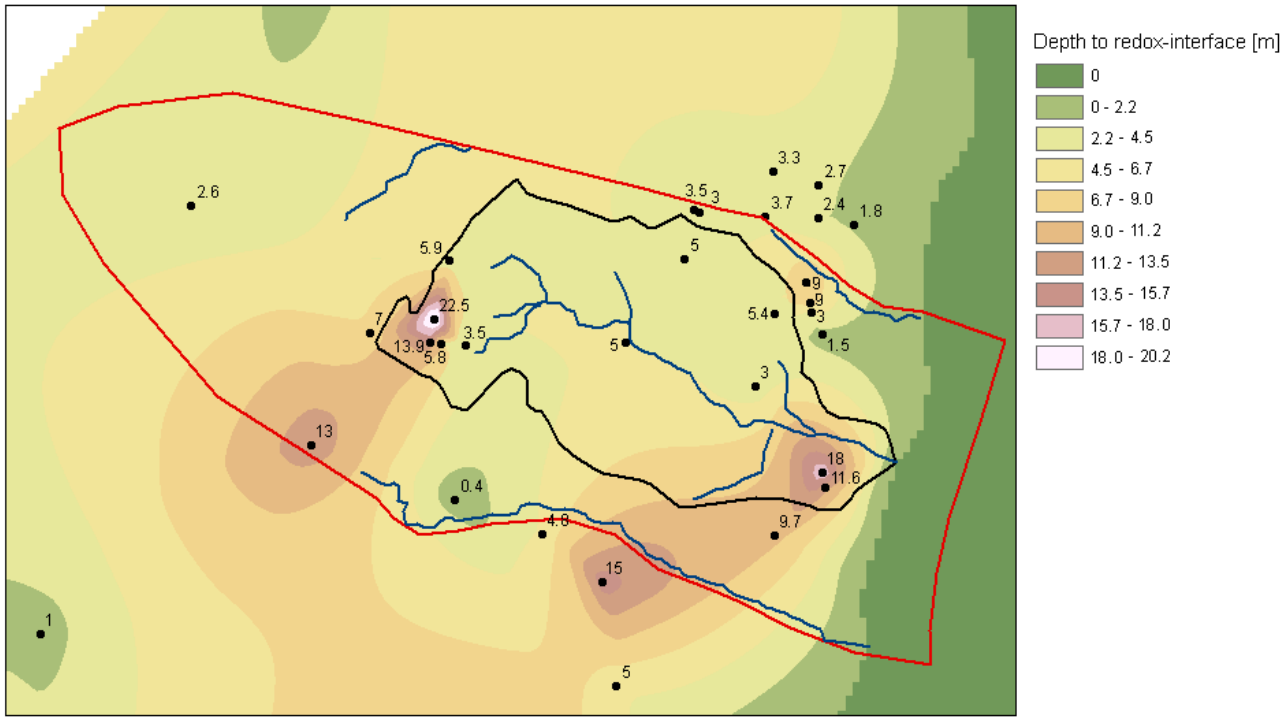

Figure 8.5 Interpolated redox-interface using natural neighbour

8.3 Model setup

8.3.1 Simulation specifications

The hydrological model, after calibration and validation, is used for modelling three-dimensional nitrate transport using the AD-module in MIKE SHE. The nitrate model is also run for the simulation period 1/1 1990 to 31/12 2004. The time step for transport in the saturated zone and in overland flow is set to 24 hours and the maximum advective and dispersive Courant numbers are set to 0.8 and 0.5 respectively. A rather small time step of 30 seconds is used for transport in the streams as the simulation becomes unstable if using a larger time step.

8.3.2 Transport parameters

When simulating transport additional parameters for the hydrostratigraphical units are required, that is porosities and dispersivities. An assumption of isotropy is applied and thus only longitudinal (α_L) and transverse (α_T) dispersivities must be specified. The transport parameters are assumed equal for the sand layer and the lenses and for the two clayey till units.

The dispersivities, and especially the vertical component, determine how much nitrate is spread under the redox-interface and thus how much nitrate is reduced. The porosity, on the other hand, determines the mean travel time of a solute along a flow line and thus has no effect on the amount of nitrate reduction. Therefore only the dispersivity values are subject to calibration, whereas, the porosity is not calibrated. A porosity of 0.2 is specified for all hydrostratigraphical units

Values for dispersivities used in the model are based on the study by Gelhar et al (1992). Gelhar et al (1992) made an analysis of data on field-scale dispersion and produced a plot of longitudinal dispersivity in relation to scale in addition to a plot of the ratio between longitudinal and transverse dispersivity in relation to scale. These two plots are used to determine dispersivity values. Two different sets of dispersivity values are defined for sand/gravel and clayey till units in the model as the scale is believed to be different between these. In the sand/gravel units the flow is mainly horizontal and the scale here is therefore equal to the length of the flow path to the streams, which on average is somewhere between 500 – 1000 meters. In the clayey till layers the flow is mainly vertical and the scale in these units is therefore equal to the thickness of the layer which is, on average, 10-20 meter. These scales result in ranges of longitudinal dispersivites and α_L/α_T ratios as seen in table 8.1. In the following calibration of the nitrate model different values of dispersivities within these ranges are tried, though keeping the α_L/α_T ratio constant.

Table 8.1 Dispersivities value ranges and α_L/α_T ratio based on Gelhar et al (1992)

	Scale [m]	α_L [m]	α_L/α_T
Sand/gravel	500 -1000	5 - 200	50
Clayey till	10 - 20	0.5 - 5	2

8.3.3 Boundary conditions

As all model boundaries, except along the coast, are specified as no-flow boundaries in the hydrological model these are treated as no-flux boundaries in the transport simulation. In the model domain covering the sea are defined as specified heads and are thus treated as fixed concentration cells with a concentration equal to the initial concentration which is set to 0 mg/l.

8.3.4 Initial concentrations

Initial concentration is set to 0 mg/l in the whole model domain during calibration of the nitrate model. As the calibration of the model is conducted for the last part of the simulation period (2000-2004), using 0 mg/l as initial concentration does not have an effect on the storage and concentrations of nitrate during the calibretion period, as these have reached an acceptable level before 2000. This was tested by running a model with concentration from the 31/12 2004 as initial concentrations and comparing the results for 2000-2004 with a simulation using initial concentration of 0 mg/l. However, using 0 mg/l as initial concentration affects the mass balance before 2000. The calibrated nitrate model is therefore subsequently run using concentrations for the 31/12 2004 from the first run as initial concentrations.

8.3.5 MIKE11

MIKE11 is set up for simulating transport by creating a MIKE11 AD setup containing boundary conditions for transport and a AD parameter file. Boundary conditions are defined at all branch ends in the river network and are specified as constant concentration boundaries of 0 mg/l. As no degradation or other processses in the stream are included in this study, only the specie in question as well as initial concentrations are needed to be specified in the AD parameter file.

8.3.6 Overland flow

For transport in overland flow an initial mass of 0 g/m^2 is specified. No dispersion and no reduction of nitrate (i.e. a half life of 1000 years is specified) is included in overland flow transport

8.3.7 Implementation of nitrate reduction and redox-interface

Nitrate reduction in the saturated zone is defined as a decay process in the model. The redox-interface is implemented in the model as a so-called water quality layer, where a half life of 1000 years is specified for the model domain above this layer and a half life of 1 hour below.

The location of the interpolated redox-interface in relation to the computational layers is seen in figure 8.6. It is noted that the interface cuts through 6 of the 7 computational layers because of the sloping terrain in the model area. Model grids below the interface are given a half life of 1 hour and model grids above a half life of 1000 years. As one model grid can only be given one value for half life, model grids that are intersected by the redox-interface are given a weighted average between the two specified half lives, depending on how large a part of the grid cell is reduced. Though, even if the redox-interface is very close to the upper grid boundary and thus almost the entire grid cell is reduced, the specified average half life will be so high that the grid cell, in reality, is oxidized and no nitrate will therefore be reduced in the cell. This is also the case even if the half life in the oxidized zone was decreased to e.g. 100 years instead of 1000 years.

In order to implement the redox-interface better in the model the computational layers must be changed. The easiest way to do this is by defining a new computational layer following the location of the interface. But, as the redox-interface in this study cuts through the computational layers this method is not possible here. Instead the top computational layer is subdivided into 4 layers. This is done by dividing the layer into two equal parts and then the upper part of these into two and then again the upper of these in two. Thereby 4 layers of 12.5%, 12.5%, 25% and 50% of the thickness of the original layer are created. Before proceeding it is checked that this refinement of the top model layer does not give rise to significant changes in model performance of the hydrological model.

As it is only the top layer that is subdivided, the implementation of the redox-interface in the computational layers below will still be inaccurate. But, as each additional computational layer increased the CPU-time for the simulations, no subdivision of the underlying layers is introduced in the model. The influence of this on the following nitrate simulations will be discussed later on.

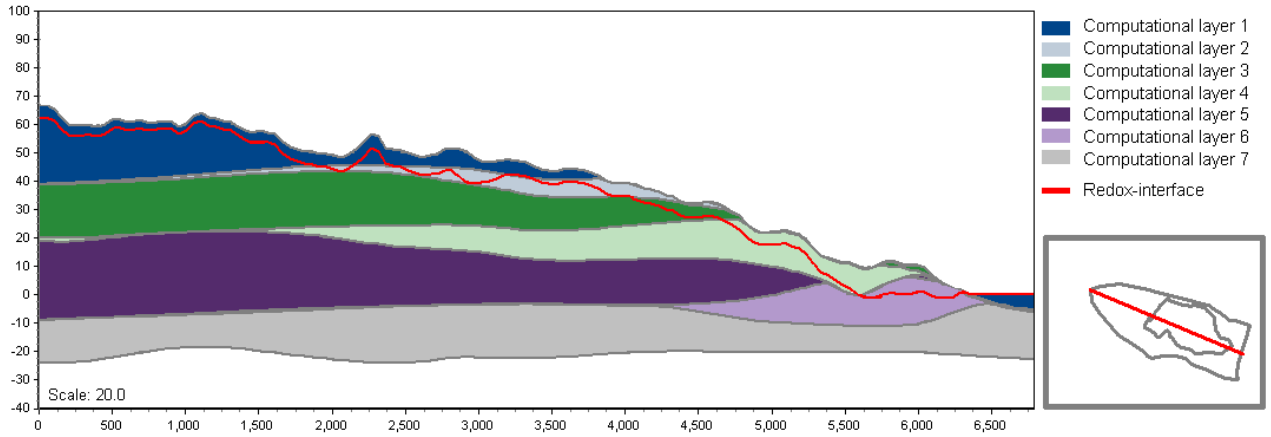

Figure 8.6 Location of the redox-interface in relation to the computational layers in MIKE SHE

8.3.8 Daisy nitrate leaching

The Daisy nitrate leaching is subject to the same extrapolation and aggregation procedure as described for percolation in section 7.1.8. The resulting average Daisy nitrate leaching for the simulation period 1990-2004, after the extrapolating and aggregation procedure, is seen in figure 8.7.

Nitrate is defined as a dissolved specie in MIKE SHE. The nitrate input from Daisy is implemented as a sub-surface source that is applied to the top computational layer over the full model domain. Unlike for water, solutes, in the situation of a negative mass flux, can only be withdrawn from the top layer of the model, which results in more nitrate than water being reset to zero. As the upper computational layer has been subdivided into 4 layers, the new top layer is rather thin and this results in a large part of the negative nitrate flux being reset to zero. For all simulation runs during the calibration around 67% of the specified negative nitrate flux is reset to zero, which seams unreasonably large. Though, as the total negative nitrate flux over the whole simulation period (1990-2004) is only 7.8% of the total nitrate input, the net input of nitrate to the model is only 5.7% to high. This is believed to be acceptable but this additional input should be kept in mind.

8.3.9 Nitrate pulse

To evaluate the response time in the groundwater and stream system due to a change in agricultural practice in the catchment a simulation of a nitrate pulse is performed. A nitrate pulse is released in the top layer of the model on the 1/1 1990 and the distribution of this pulse with time is simulated.

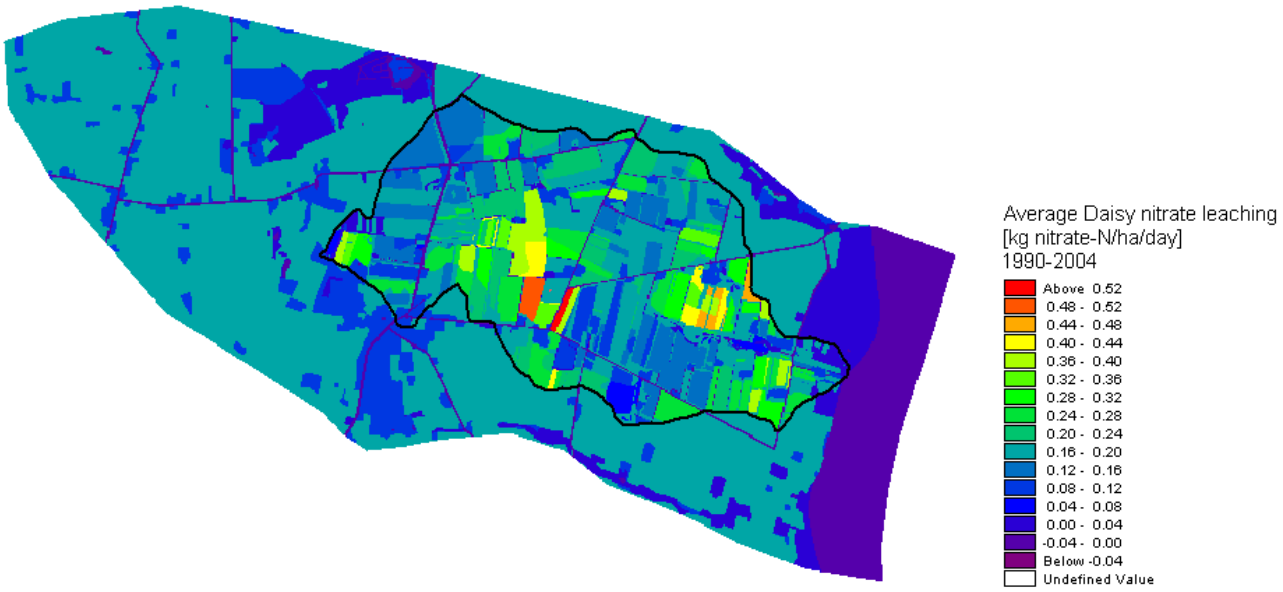

Figure 8.7 Average Daisy nitrate leaching for the model area

8.4 Calibration and validation

The calibration conducted for the nitrate model is simpler than the calibration of the hydrological model and consists only of a calibration of the dispersivities. The location of the redox-interface is not subject to any calibration as changing both dispersivities and the location of redox-interface will result in a changed nitrate reduction and thus will balance out each other. The calibration of the nitrate model is also performed as a manual trial-and-error calibration and a split-sample test using the period 2000 - 2004 for calibration period and 1995-1999 for validation.

The performance of the model is evaluated on how correctly the model simulates daily dynamics in nitrate concentration and transport as well as how accurate it simulates average nitrate concentrations and total nitrate transport in the stream at the upstream and downstream station. No quantitative performance and accuracy criteria are defined for the nitrate model as for the hydrological model.

8.4.1 Calibration

For the calibration of the nitrate model five different calibration runs are performed. The different dispersivity values used under the calibration for the sand/gravel and clay units respectively are seen in table 8.2. The maximum longitudinal dispersivity used for sand/gravel is 100 m even though the expected range goes up to 200 m (see table 8.1). The reason for not using higher dispersivities is that the larger the dispersion is the longer will the simulation time be, due to restrictions on how much mass is allowed to be moved per time step. The simulation Nitrate 1 with no dispersion takes 3.5 hours to run, whereas Nitrate 5 with a longitudinal dispersivity in the sand/gravel units of 100 m takes 220 hours.

Table 8.2 Transport parameter values used in the calibration of the nitrate model

	Sand/gravel			Clayey till		
	Longitudinal dispersivity [m]	Transverse dispersivity [m]	Porosity	Longitudinal dispersivity [m]	Transverse dispersivity [m]	Porosity
Nitrate 1	0	0	0.2	0	0	0.2
Nitrate 2	5	0.1	0.2	0.5	0.25	0.2
Nitrate 3	25	0.5	0.2	1	0.5	0.2
Nitrate 4	50	1	0.2	2	1	0.2
Nitrate 5	100	2	0.2	5	2.5	0.2

The calibration results are seen in figures 8.8-8.11 and in table 8.3 for the upstream and downstream station in Lillebæk. These results show that, when no dispersion is applied in the model, the nitrate transport and concentrations in the stream are greatly overestimated. When dispersion is applied in the model, the simulated nitrate transport and concentrations are seen to be decreased and the higher the dispersivity values, the lower the simulated nitrate transport is. However, if too large dispersivity values are applied, the nitrate transport is underestimated. These results show that, when using higher dispersivity, nitrate is spread more in the saturated zone and more nitrate is thus transported under the redox-interface and is reduced. The calibration run Nitrate 3, with dispersivity values of 25 m and 0.5 m in the sand/gravel units and 1 m and 0.5 m in the clayey till units, is chosen as the best simulation.

Table 8.3 Calibration results for the nitrate model for the period 2000-2004

	470032		470033	
	Average conc. [mg nitrate-N/l]	Total transport [ton nitrate-N]	Average conc. [mg nitrate-N/l]	Total transport [ton nitrate-N]
Observed	8.3	25.5	7.0	44.8
Difference obs - sim [%]				
Nitrate 1	-16.1	-16.5	-47.4	-11.5
Nitrate 2	-10.2	-14.7	-36.0	-6.5
Nitrate 3	4.2	1.2	-20.5	9.2
Nitrate 4	17.7	13.3	-1.7	20.1
Nitrate 5	37.8	32.3	20.8	36.8

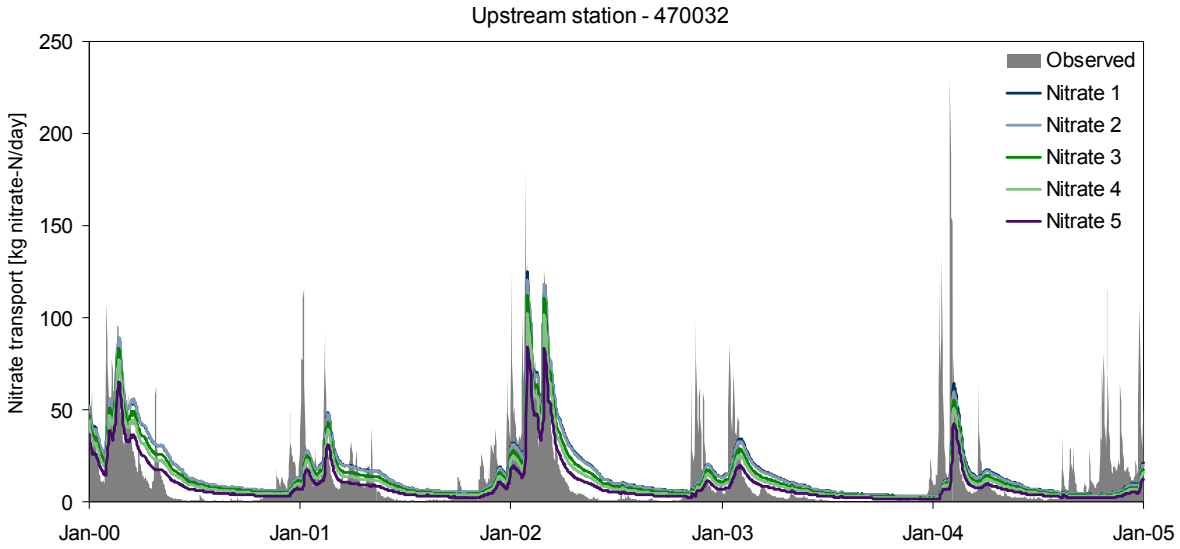

Figure 8.8 Observed and simulated nitrate-N transport [kg nitrate-N/day] at upstream station (470032). Simulated transport for the five calibration runs using different dispersivities are shown on the graph

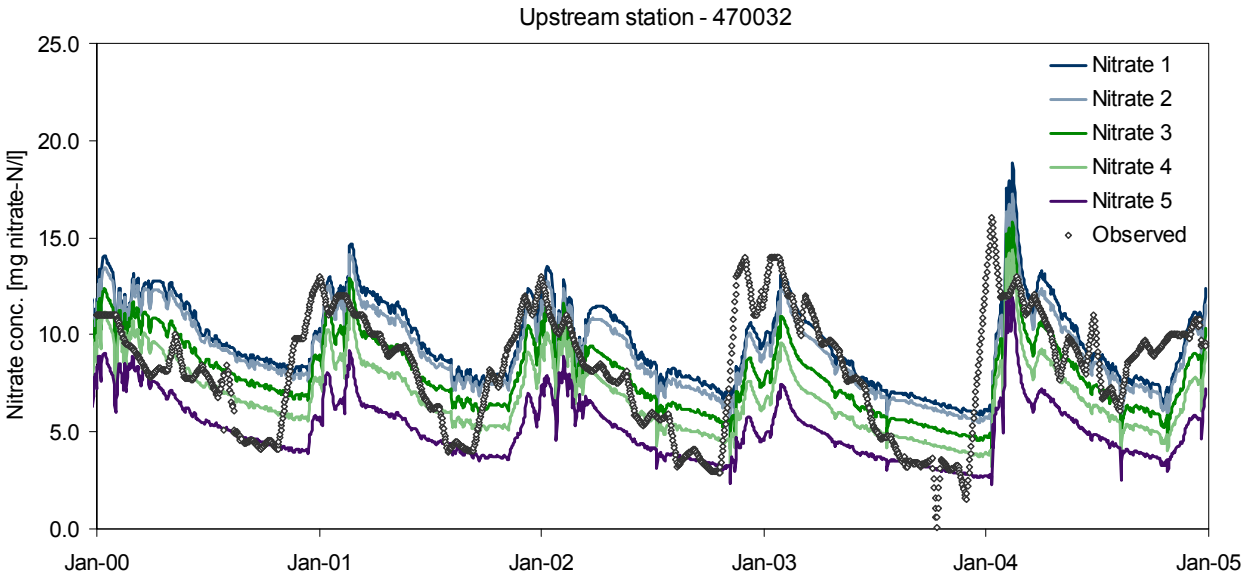

Figure 8.9 Observed and simulated nitrate-N concentration [mg nitrate-N/l] at upstream station (470032). Simulated concentrations for the five calibration runs using different dispersivities are shown on the graph

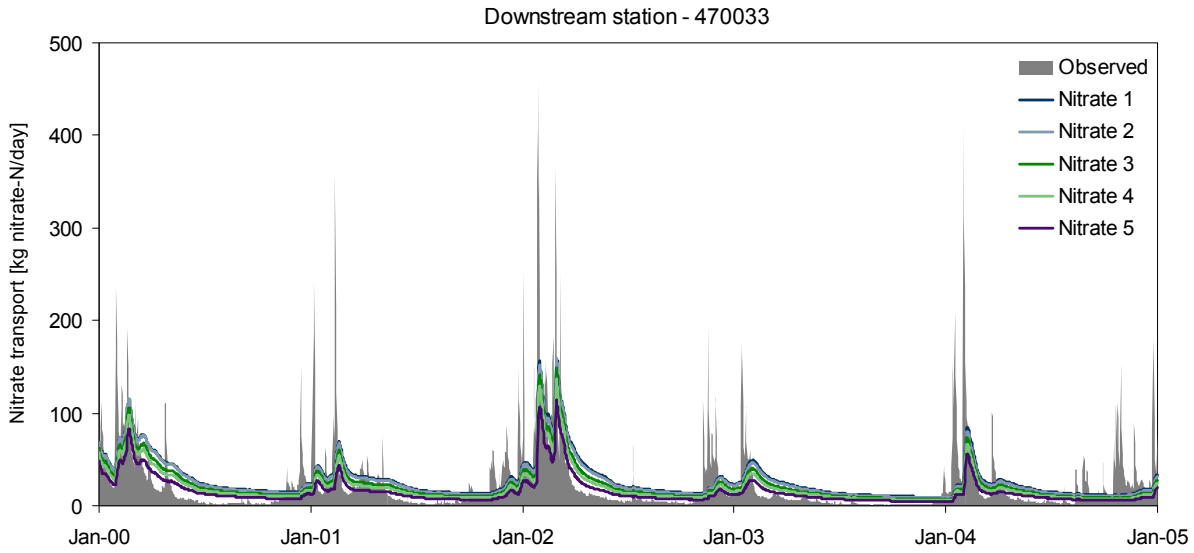

Figure 8.10 Observed and simulated nitrate-N transport [kg nitrate-N/day] at downstream station (470033). Simulated transport for the five calibration runs using different dispersivities are shown on the graph

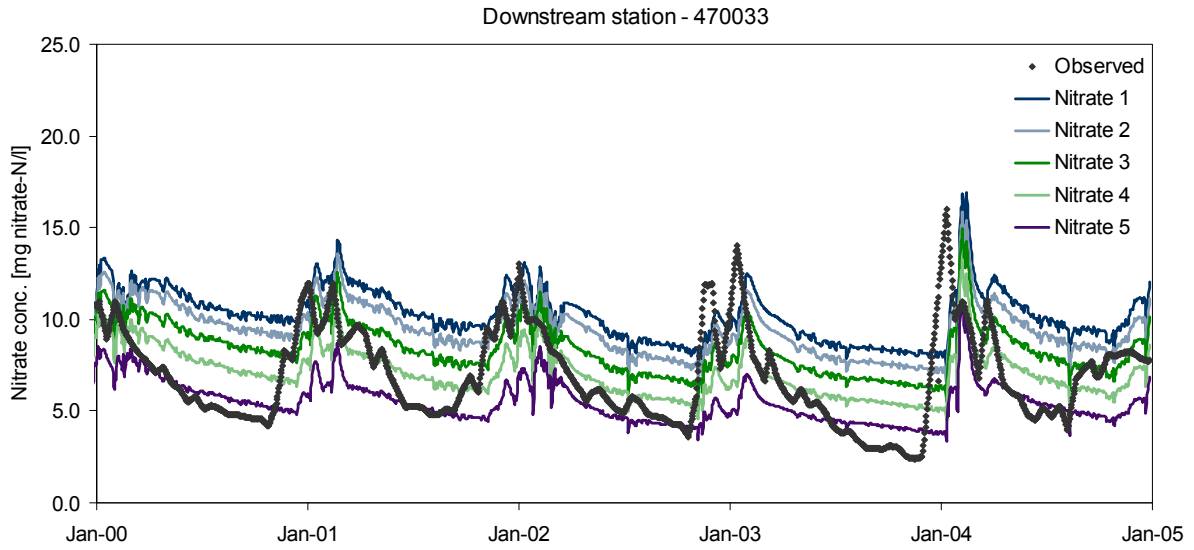

Figure 8.11 Observed and simulated nitrate-N concentration [mg nitrate-N/l] at downstream station (470033). Simulated concentrations for the five calibration runs using different dispersivities are shown on the graph

8.4.2 Validation

The nitrate model is, as the hydrological model, validated for the period 1995-2000. Before validation the calibrated nitrate model (Nitrate 3) is run using concentration from 31/12 2004 as initial concentration. For evaluation of the performance of the nitrate model on smaller scale, nitrate transport from the drain areas is also simulated.

9. Particle tracking

The particle tracking module in MIKE SHE is used to asses the flow paths in the saturated zone and thereby delineate the robust areas in the catchment, from where water crosses the redox-interface, and the sensitive areas, from where water does not cross. The delineation of these areas is suspected to be subject to great uncertainty due to uncertainty on the location of the redox-interface. Therefore, in order to evaluate the uncertainty on the delineation, particle tracking simulations with different locations of the redox-interface are performed. The location of the interpolated interface is varied by decreasing and increasing the depth to the surface by 50%, 75%, 125% and 150%.

The particle tracking simulations are performed by initially distributing 10 particles evenly in each model grid in the upper computational layer. The flow paths of these particles are then simulated by the PT module based on the three-dimensional flow field simulated with the calibrated hydrological model. No dispersion is specified in the particle tracking simulations and the movement of the particles is thus solely deterministic. The simulated flow velocities for the 10 year period 1995-2004 is used and repeated 5 times for a total simulation period of 50 years. The redox-interface is implemented as a registration zone in the model which makes it possible to record if a particle crosses the redox-interface during the simulation.

10. Results

In the following sections results from the calibration and validation of the hydrological model as well as for the nitrate model are presented. Afterwards, the resulting water balance and nitrate mass balance and finally results from the nitrate pulse and particle tracking simulations are presented. It should be noted that all results presented for the hydrological model are for the non-refined model.

10.1 Calibration and validation results

10.1.1 Hydrological model

The quantitative performance criteria for the calibrated hydrological model are seen in table 10.1 for the calibration period, the validation period and finally for the whole simulation period. In the following the results for hydraulic head are first commented on followed by the results for stream discharge.

The results in table 10.1 show that hydraulic heads are generally simulated too high. To reach a level of high fidelity for hydraulic heads, ME must be smaller than 0.44 m and RMSE smaller than 1.91 m. Values that comply to this level of accuracy are marked with green in the table 10.1, whereas values that fall below a level of medium fidelity (ME >1.10 and RMSE> 2.32) are marked with red. It is seen that the model has problems with reaching an acceptable level for ME at some observation wells, especially in the validation period. For RMSE a high fidelity level is reached for most observation wells. It is noted that the error is especially large at observation well 165.338 for both ME and RMSE.

The simulated and observed hydraulic heads for observation well 165.334 are seen in figure 10.1 and for the rest of the wells in appendix 1. These graphs show that the error on simulated hydraulic head is reasonably evenly distributed in time. It is noted from figure 10.1 that the observed head drops greatly in the dry year of 1996. The model is seen to have difficulties in simulating this drop in head and also the following increase in head.

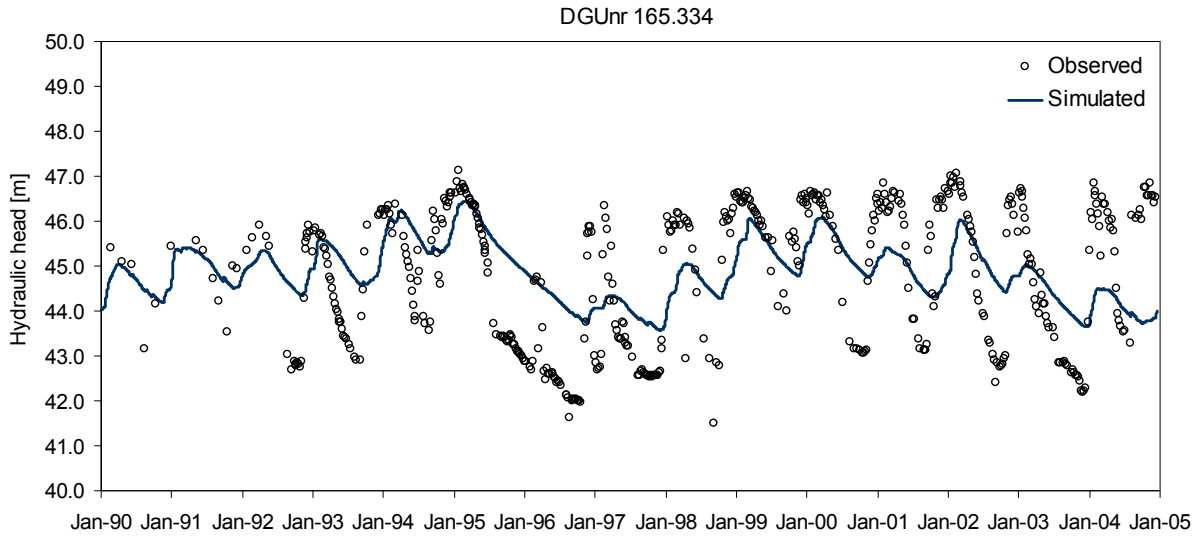

Figure 10.1 Observed and simulated hydraulic heads at observation well 165.334 for the simulation period 1990-2004

Table 10.1 Model performance for calibration, validation and whole simulation period.
NA = observation data not available

Hydraulic head: Values marked with green comply with a high fidelity level. Values marked with red falls below a medium fidelity level

Discharge: Values marked with green comply with the specified accuracy level

	Calibration period 2000-2004		**Validation period 1995-1999**		**Whole period 1990-2004**	
Hydraulic head						
DGU no.	ME [m]	RMSE [m]	ME [m]	RMSE [m]	ME [m]	RMSE [m]
165.334	**0.40**	**1.41**	**-0.36**	**1.29**	**-0.06**	**1.29**
165.335	**0.35**	**0.80**	**0.10**	**0.85**	**0.24**	**0.81**
165.336	**0.11**	**0.78**	-0.48	**1.15**	**-0.16**	**0.93**
165.369	NA	NA	**-2.80**	**2.80**	**-2.80**	**2.80**
165.370	NA	NA	-1.00	**1.02**	-1.00	**1.02**
165.337	**1.56**	**1.70**	**1.56**	**1.83**	**1.49**	**1.70**
165.338	**-4.84**	**4.86**	**-4.36**	**4.48**	**-4.69**	**4.75**
165.339	**1.42**	**1.49**	**1.12**	**1.21**	**1.31**	**1.40**
165.340	-0.95	**1.39**	**-1.21**	**1.58**	-0.93	**1.31**
165.341	**-1.92**	2.10	**-1.60**	**1.83**	**-1.59**	**1.80**
165.342	-0.83	**1.09**	**-1.33**	**1.58**	-0.97	**1.23**
165.343	**-0.17**	**0.53**	**-0.31**	**0.75**	**-0.21**	**0.60**
165.344	NA	NA	**-2.01**	2.20	**-1.82**	2.01
165.345	**2.44**	**2.61**	**2.12**	**2.36**	2.26	**2.44**
165.346	**-0.29**	**0.61**	-0.64	**0.84**	**-0.36**	**0.64**
165.347	**-0.19**	**0.27**	-0.50	**0.65**	**-0.33**	**0.44**
165.348	NA	NA	**-0.33**	**0.94**	**0.04**	**0.63**
Average	**-0.22**	**1.51**	-0.71	**1.61**	-0.56	**1.52**
Discharge						
Station no.	$R2_{(Nash-Sutcliffe)}$	Fbal [%]	$R2_{(Nash-Sutcliffe)}$	Fbal [%]	$R2_{(Nash-Sutcliffe)}$	Fbal [%]
470032	**0.60**	-25.7	**0.59**	**-14.9**	**0.56**	**-9.9**
470033	0.48	**8.5**	**0.55**	**5.0**	**0.50**	**8.1**
Average	**0.54**		**0.57**		**0.53**	

In figure 10.2 observed hydraulic heads are plotted against simulated. If there is a perfect match between simulated and observed heads all points should be on the black line. The points are seen both above the line, indicating overestimation of hydraulic head, and below the line, indicating underestimation, and this trend is general for all geological formations. The hydraulic head is seen to be highest in Weichsel ML and decreasing with depth, thus indicating a downward water flux. It is furthermore noted, that many of the points in figure 10.2 are located in clouds for each observation well and that these clouds are vertically elongated. This indicates that the simulated hydraulic heads has less variation than observed, which is also seen on the graphs in appendix 1.

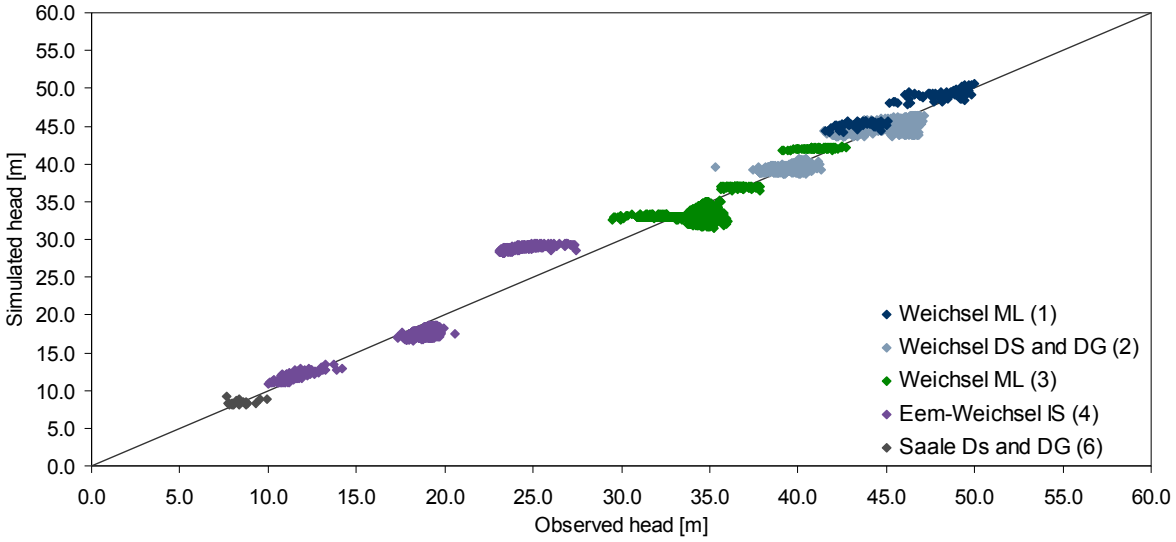

Figure 10.2 Observed versus simulated hydraulic heads for the simulation period 1990-2004. The points are colorized after which geological formation and computational layer they belong to. The line indicates a perfect match between observed and simulated head

The spatial distribution of ME for hydraulic heads is seen in figures 10.3 and 10.4 for the calibration and validation period respectively. It is noted that the spatial distribution of error is not even and the model thus does not meet the qualitative performance criteria concerning this. The large error at 165.338 is located in the southern part of the LOOP4 catchment and furthermore large errors are also seen in the northern part of the catchment. When comparing this with the quality of geological information in the area (figure 5.1) it is seen, that the areas where the model performance is not very good is coincident with areas with lack of geological information.

The simulated hydraulic head and groundwater flow directions for the main aquifer, the Eem-Weichsel IS layer, is seen in figure 10.5. For the other model layer please see appendix 6. The dominating groundwater flow is seen to be towards the sea and, as expected, groundwater flow into the LOOP4 catchment is seen to take place at the south-western boundary of the catchment. The model is believed to simulate groundwater flow directions as well as location of the LOOP4 watershed satisfactorily and hence is capable of reproducing the overall hydrological characteristics in the area.

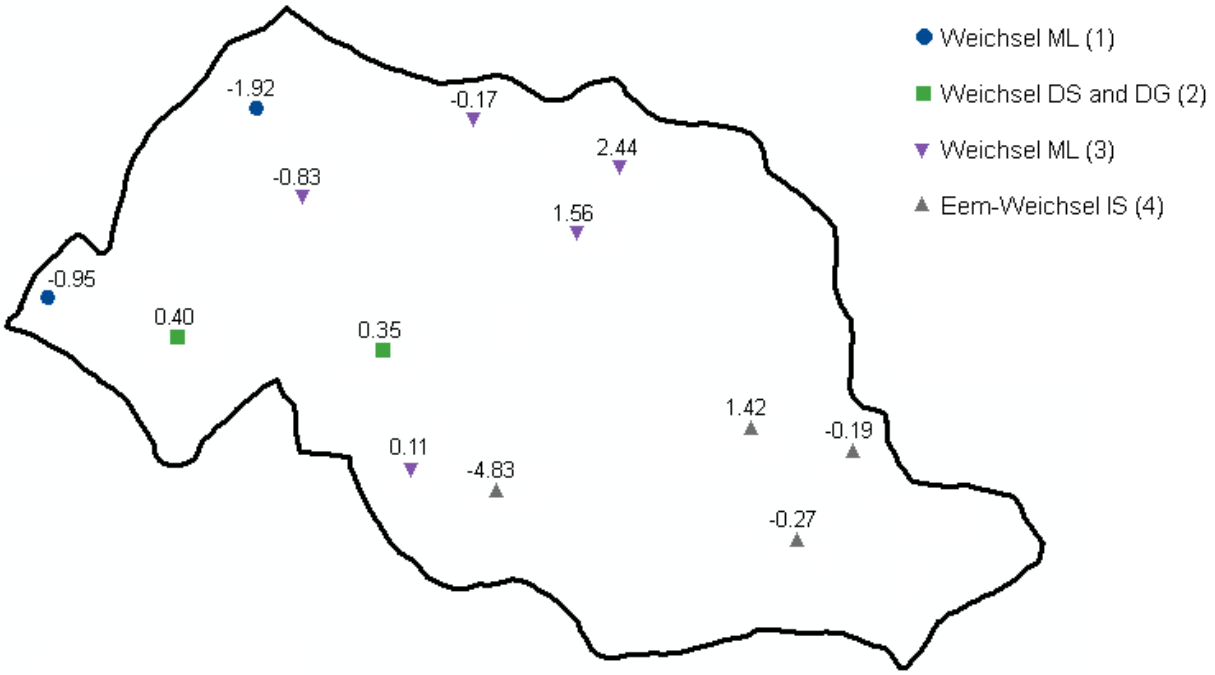

Figure 10.3 Spatial distribution of ME for hydraulic heads for C5.1 in the calibration period (2000-2004). The figure shows which geological formation and computational layer the observation wells are screened in

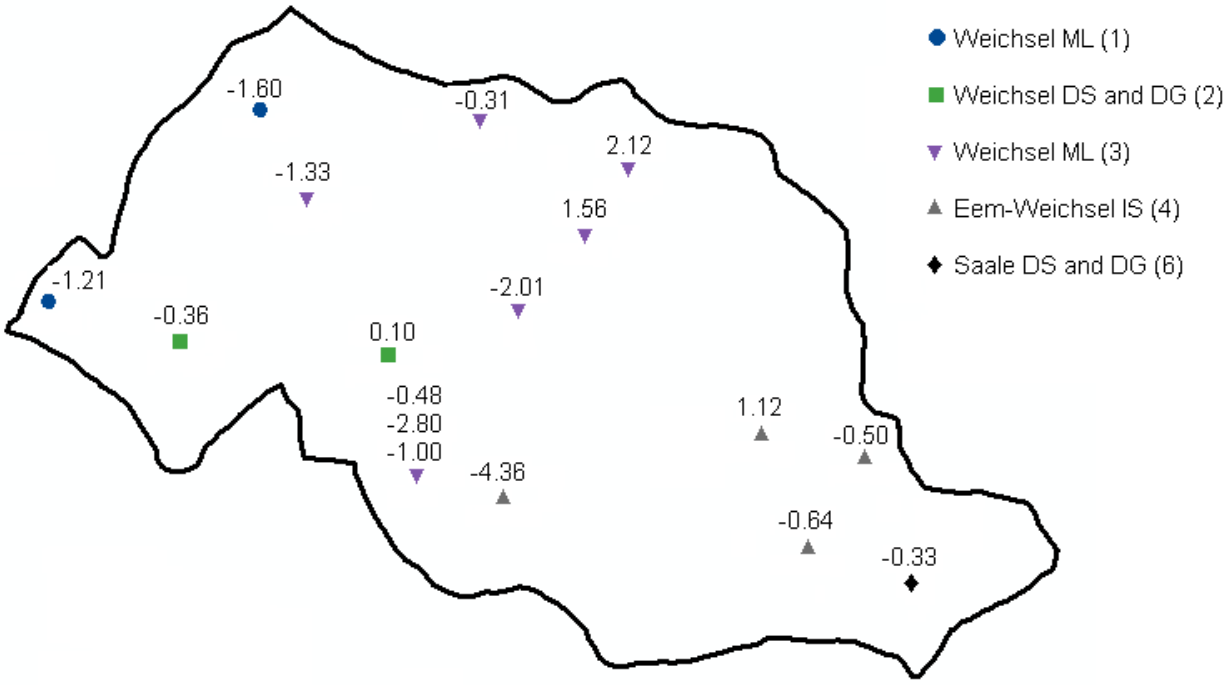

Figure 10.4 Spatial distribution of ME for hydraulic head for C5.1 in the validation period (1995-1999). The figure shows which geological formation and computational layer the observation wells are screened in. Three values of ME are seen for the same point, as three wells (165.336, 165.369 and 165.370) are located very closely here

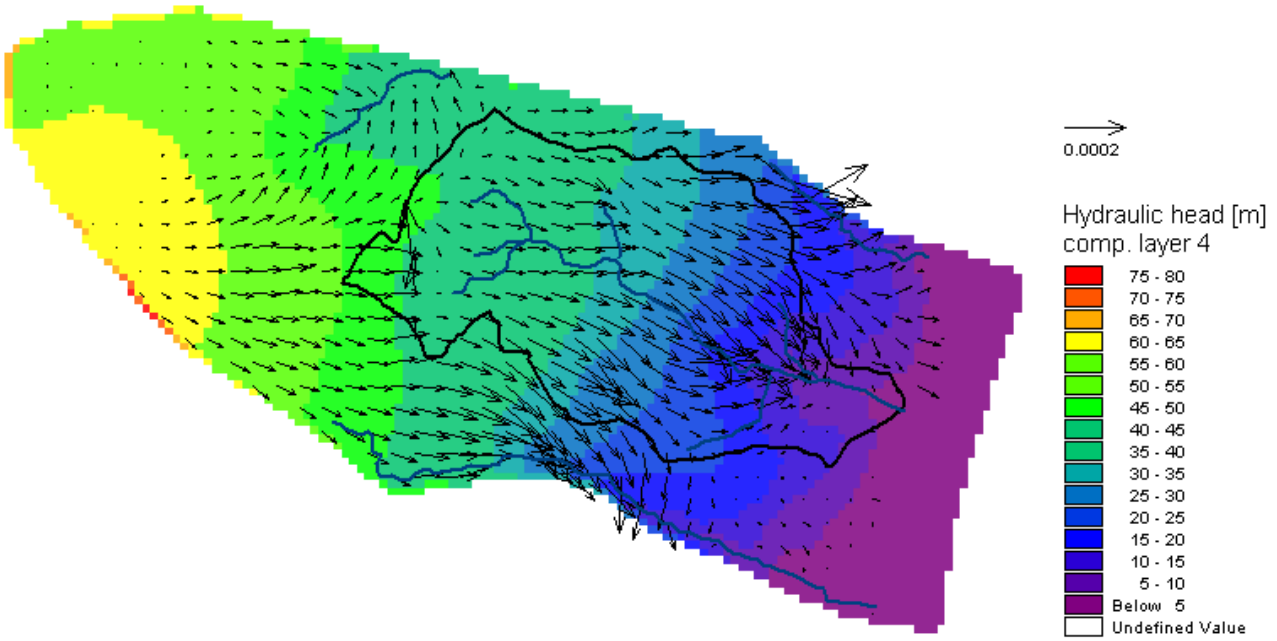

Figure 10.5 Simulated hydraulic head and groundwater flow velocity vectors for 31/12 2004 for Eem-Weichsel IS

The model performance in relation to stream discharge is, in general, reaching the specified accuracy level, except for R2 for the downstream station and Fbal for the upstream station during the calibration period (see table 10.1). In figures 10.6-10.11 simulated hydrographs, yearly accumulated discharge and cumulative frequency curves for both stream stations for the simulation period 1990-2004 are seen.

The general flow dynamic at the two stream stations is believed to be acceptably simulated. Though, some peaks in the hydrographs are not simulated by the model and during summer months, where the discharge in Lillebæk is very small, the discharge is seen to be overestimated. This overestimation of low flow is occurring at both the upstream and downstream station, though the overestimation is seen to be smaller at the downstream station. Furthermore, the recession from high flow to low flow is seen to be simulated too slowly by the model compared with observations at both stations.

The total yearly discharge is seen to be overestimated at the upstream station for most years, which is also indicated by Fbal. The total yearly discharge at the downstream station is seen to fit the observations better than at the upstream station. The total flow is, in general, underestimated at the downstream station, as also indicated by Fbal. At the downstream station overestimation of total yearly discharge is seen mainly to occur in the dry years (1997, 1996 and 2003), whereas underestimation of discharge is seen in wet years. It is believed that the model simulates the total discharge at the downstream station acceptably.

The problem with overestimation of low flows is also indicated by figures 10.8 and 10.11, which show the cumulative frequency distribution of flow events at the two stations. These curves denote that the model has problems with reproducing the distribution of flow events in Lillebæk stream. It is noted from figure 10.8, that 20% of the observed discharge rates at the upstream station is below 1 l/s, illustrating how small the flow in Lillebæk in fact is.

The simulated drain discharge from the 5 drain areas is seen on figures 10.12-10.16. The model simulates too much drainage at drain area 1, 4 and 6 and too little at drain area 2. The model is seen to be able to simulate the drainage from drain area 5 to some extent, though the Nash-Suttcliffe coefficient (R2) is only 0.08 (for whole simulation period).

The simulation results for the hydrological model are generally found to agree acceptably with observations at the downstream station and it is believed that the temporal and spatial variation of the overall water flow in the catchment is reliable. The model is, however, seen to have problems with the daily dynamics and is also found not to be able to perform well on smaller scales.

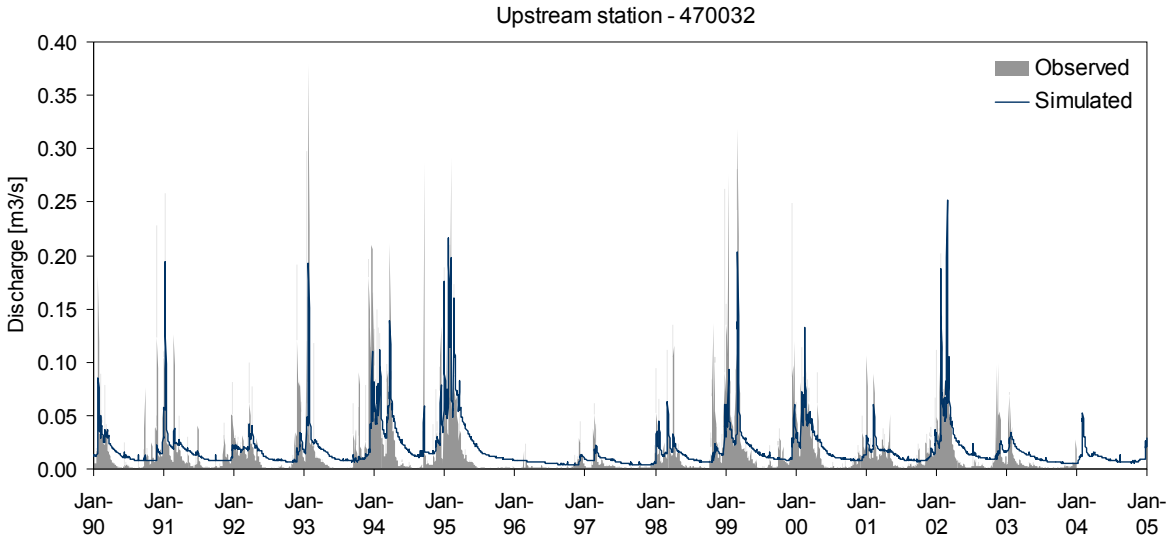

Figure 10.6 Observed and simulated daily discharge at upstream station (470032) for 1990-2004

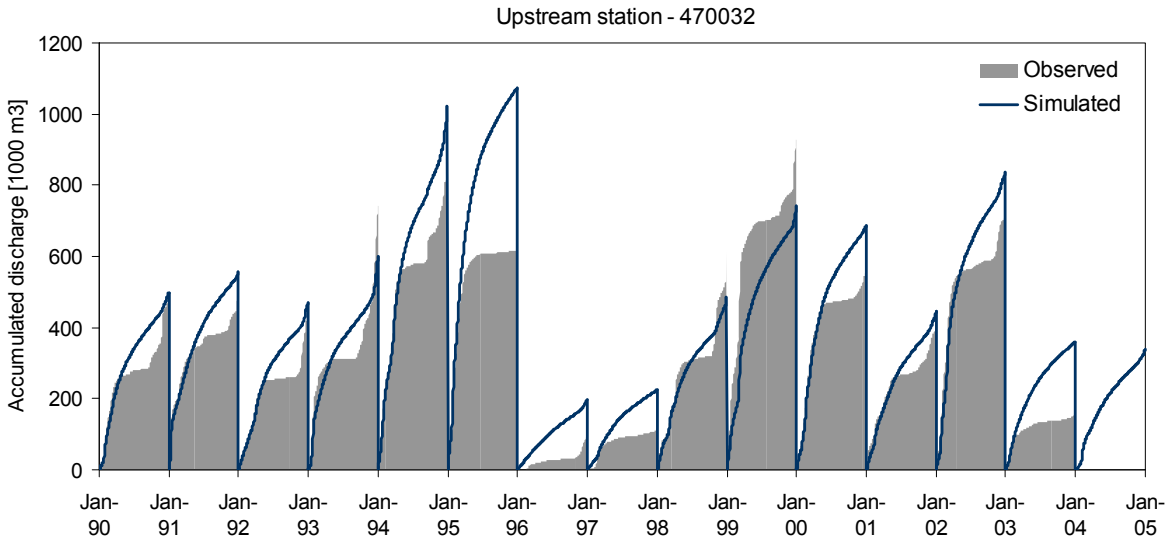

Figure 10.7 Observed and simulated yearly accumulated discharge at upstream station (470032) for 1990-2004

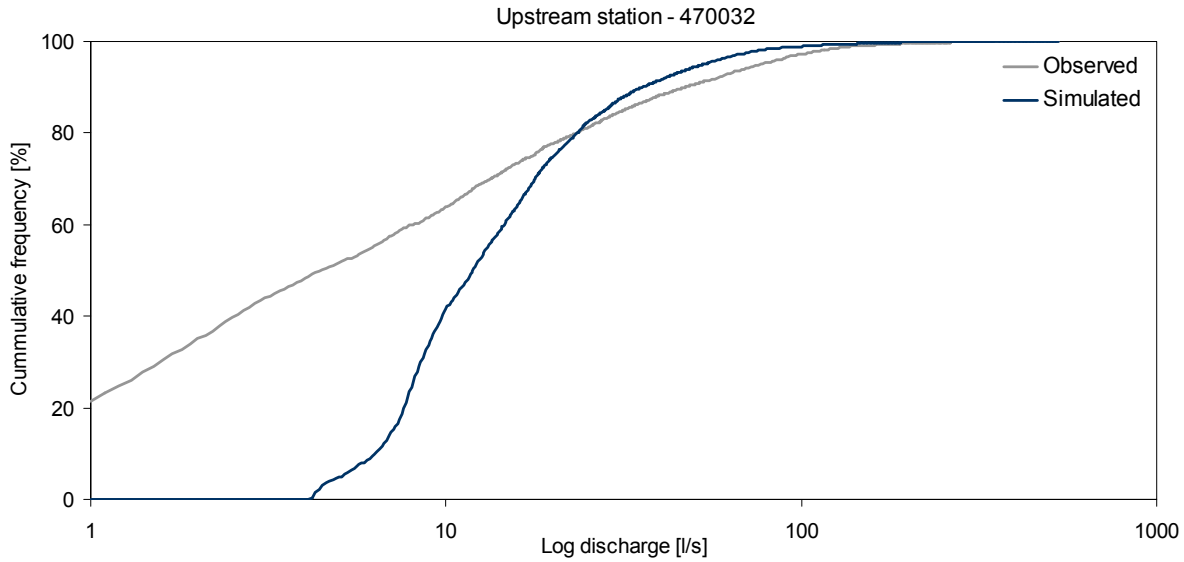

Figure 10.8 Cumulative frequency distribution of flow events at upstream station (470032). The graph shows percentage of discharge rates below a certain rate

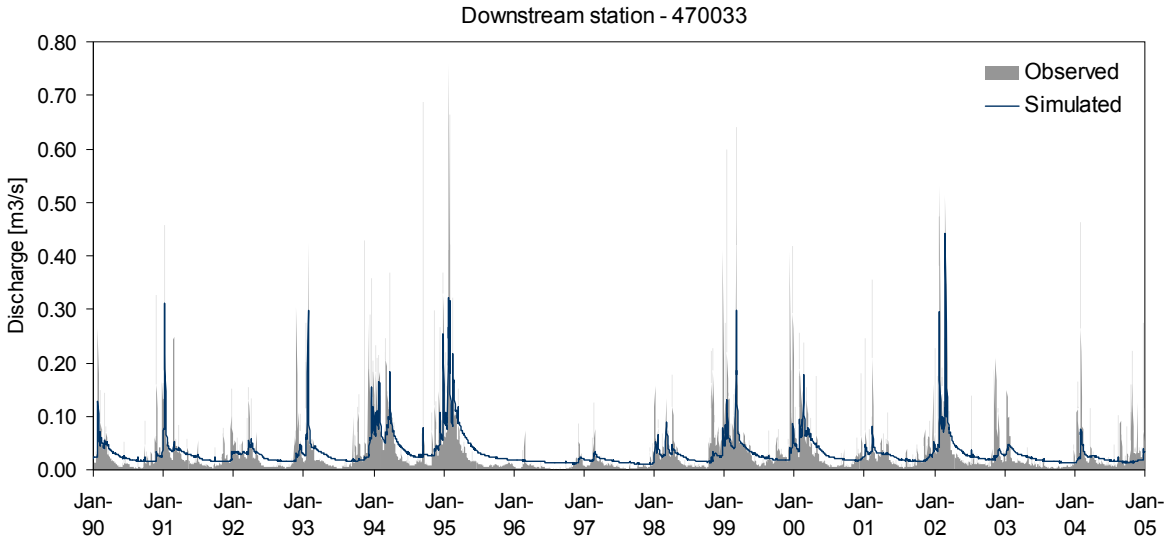

Figure 10.9 Observed and simulated daily discharge at downstream station (470033) for 1990-2004

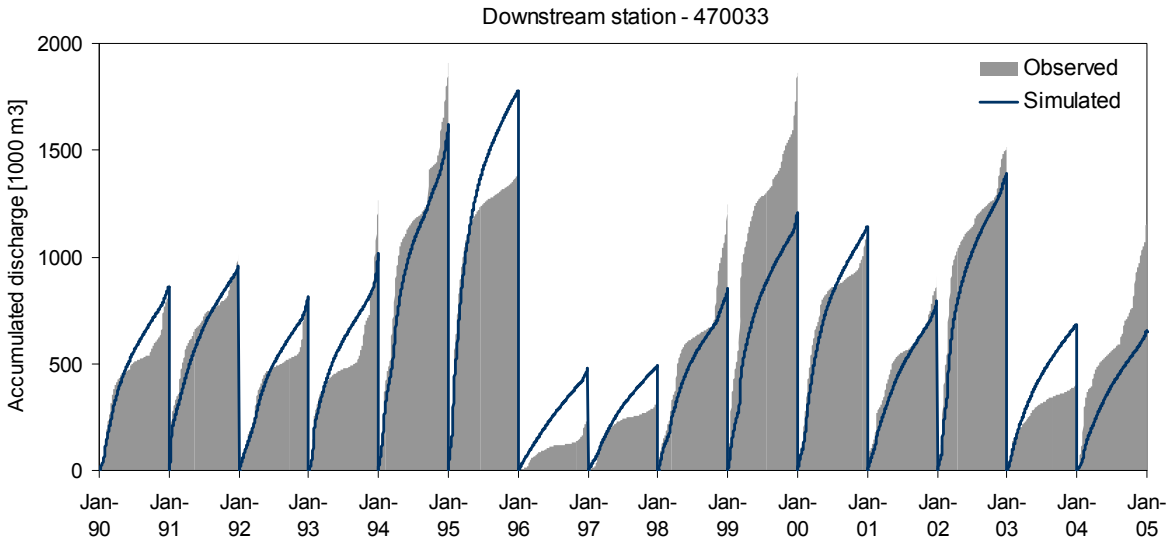

Figure 10.10 Observed and simulated yearly accumulated discharge at downstream station (470033) for 1990-2004

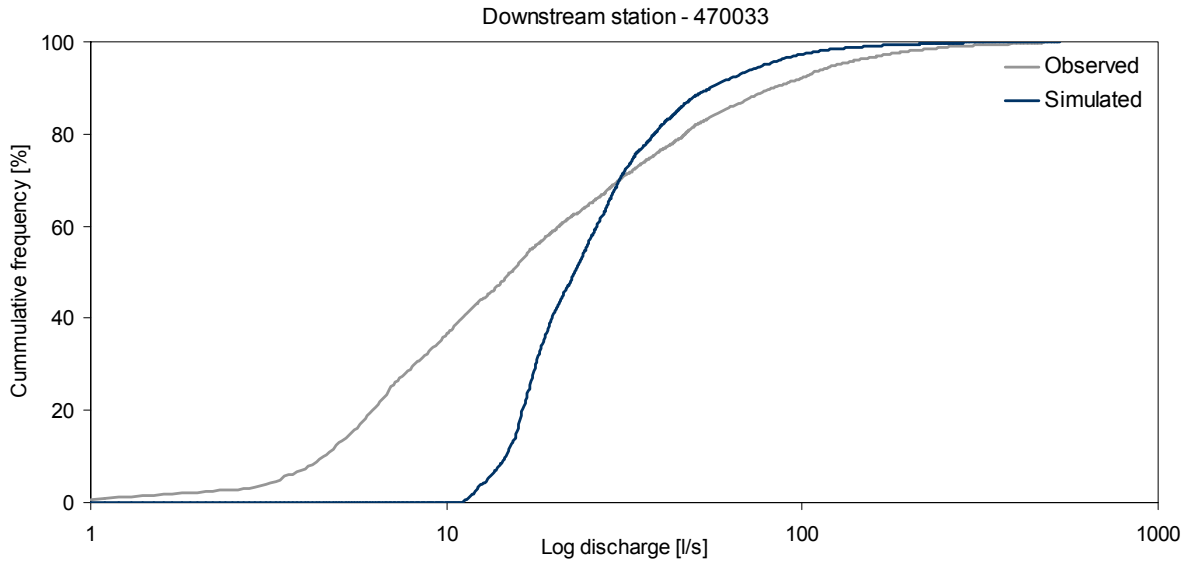

Figure 10.11 Cumulative frequency distribution of flow events at downstream station (470033). The graph shows percentage of discharge rates below a certain rate

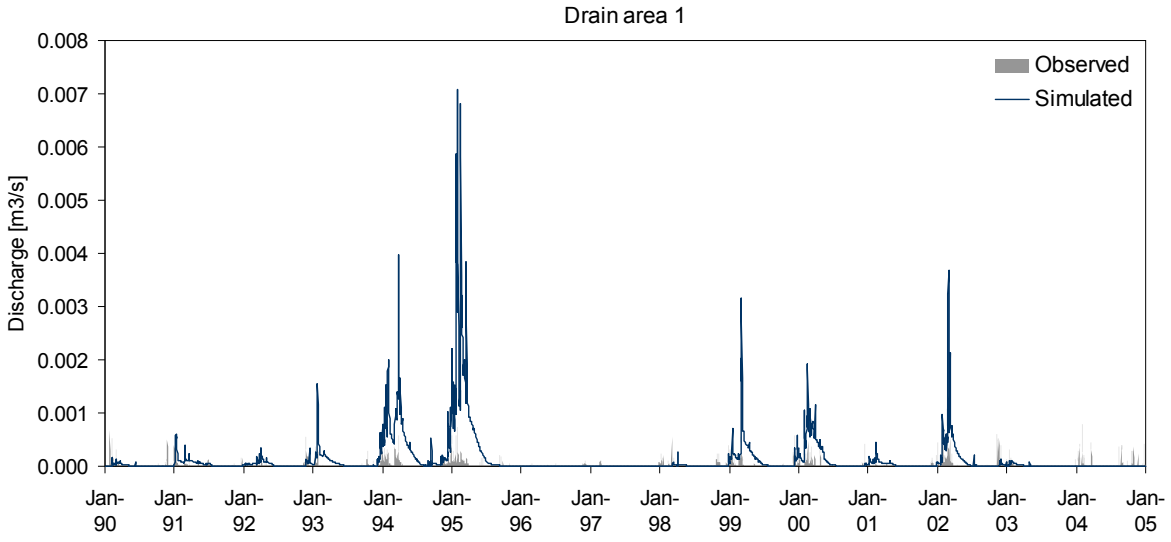

Figure 10.12 Observed and simulated drain discharge from drain area 1 for 1990-2004

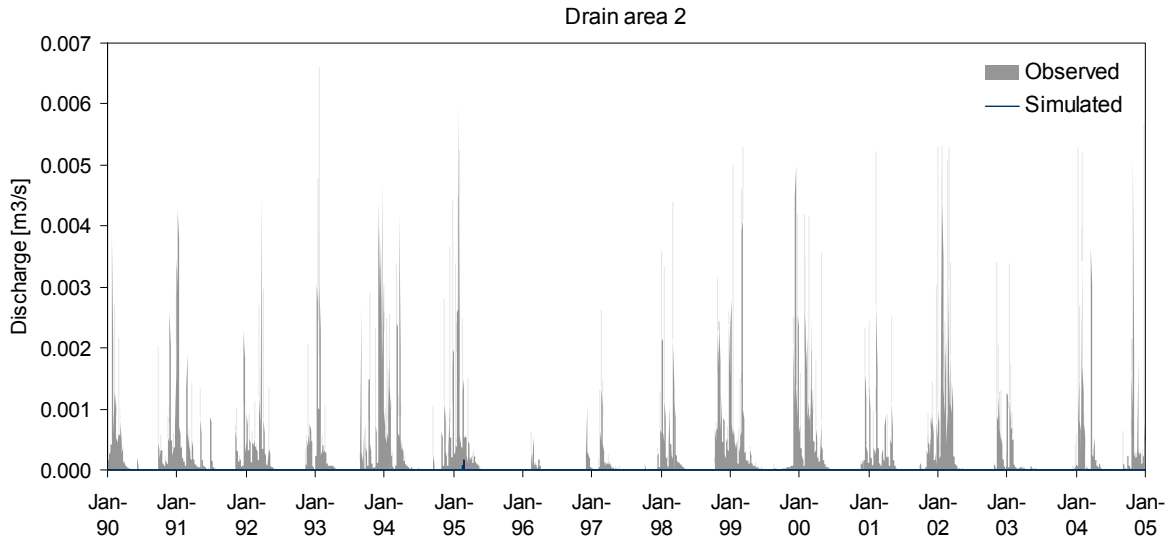

Figure 10.13 Observed and simulated drain discharge from drain area 2 for 1990-2004

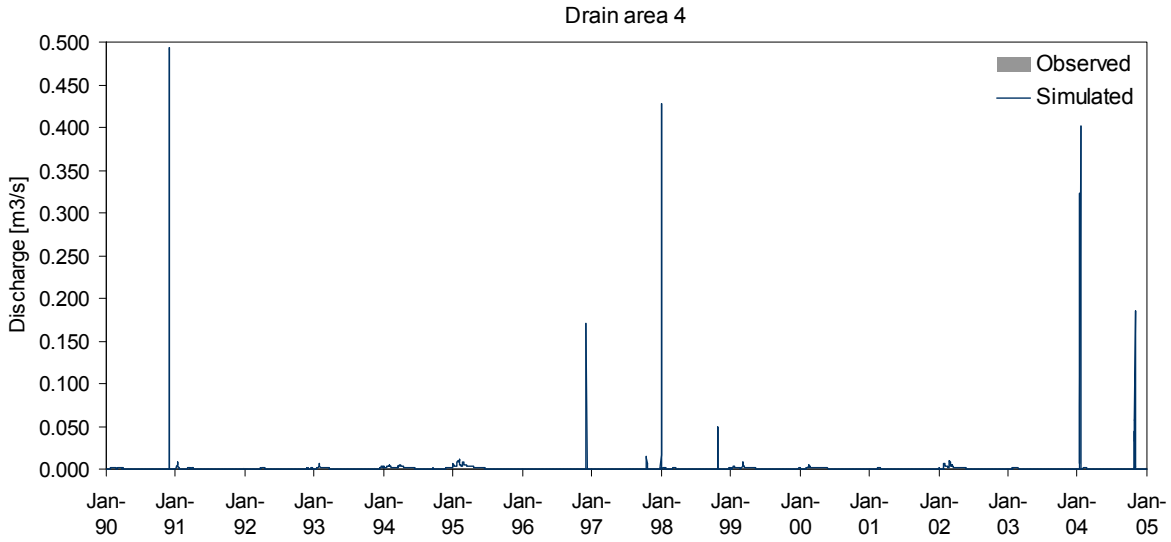

Figure 10.14 Observed and simulated drain discharge from drain area 4 for 1990-2004

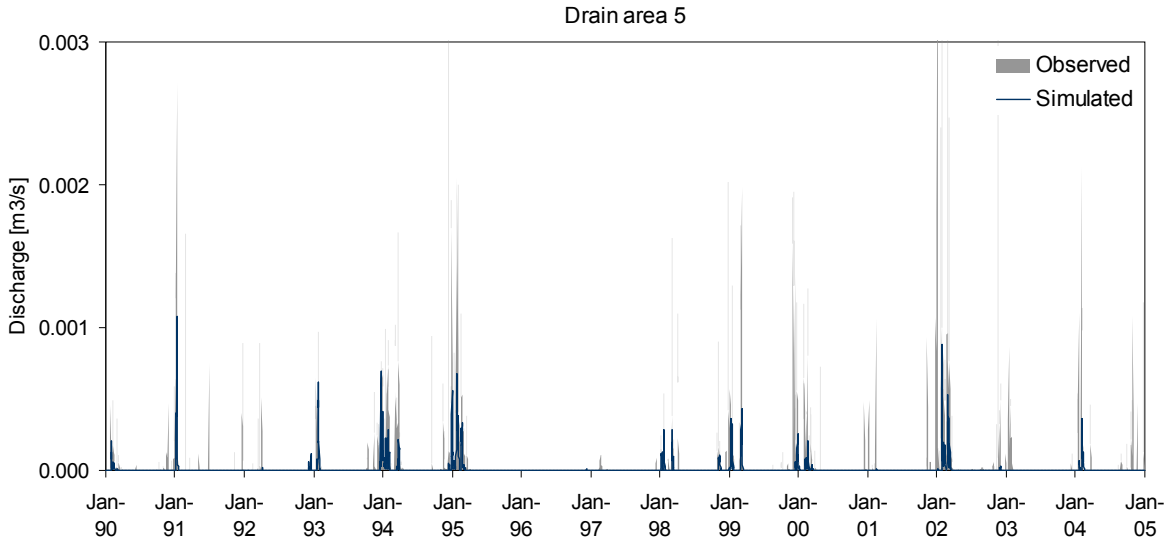

Figure 10.15 Observed and simulated drain discharge from drain area 5 for 1990-2004

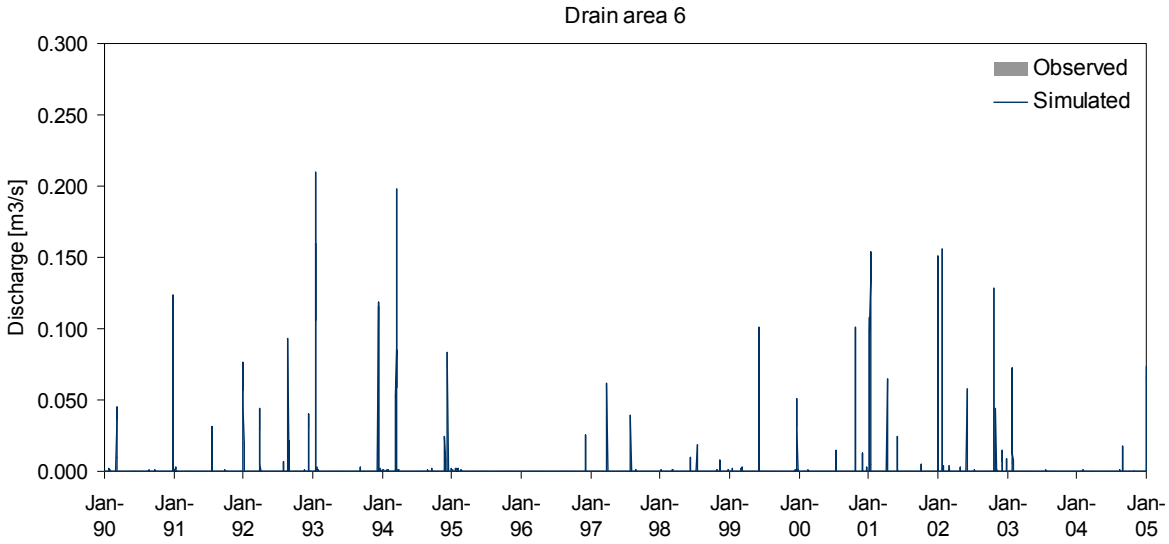

Figure 10.16 Observed and simulated drain discharge from drain area 6 for 1990-2004

10.1.2 Nitrate model

The daily nitrate-N transport and concentrations and the yearly accumulated transport at the upstream and downstream stations are seen on figures 10.17–10.22. The daily transport and concentrations are believed to follow the observed dynamics rather well. Though, some peaks in the transport are not simulated by the model and during summer the transport and concentrations are overestimated. The simulated nitrate transport thus shows the same shortcomings as discharge, which indicates that the errors from the hydrological model are carried on to the nitrate model.

The yearly accumulated nitrate-N transport for the simulation period 1990-2004 is seen to be overestimated at both stations for the years 1994, 1995, 1996, 1997,1999, 2000, 2002 and 2003. The largest percentage overestimation at the upstream station is seen in 1995 and at the downstream station in 1996. For the remaining years the total yearly transport is underestimated at both stations, but within an acceptable range from the observed transport, except for 2004 where the total transport is largely underestimated. The average total transport for the entire period 1990-2004 is overestimated at both stations, mostly, however, at the upstream station.

The observed and simulated nitrate-N transport from the 5 drain areas is seen on figures 10.23–10.27. Solute transport from the drain areas is also seen to be not very well simulated, though the trends are a bit different from the water flow. For drain areas 1 and 4 the simulated transport is too large as is also the case for discharge. Though, for drain area 6, where the discharge is too high, nitrate transport is underestimated and for drain area 5, where discharge is simulated the best, the simulated transport is too small. However, for drain area 2, where discharge is simulated too small, the model is believed to be able to reproduce the observations to some degree.

The simulated overall nitrate-N transport in the catchment is believed to agree acceptably with observations at the downstream station. Although the model is seen to have problems with simulating daily dynamics and on smaller scales, which is also the case for the hydrological model.

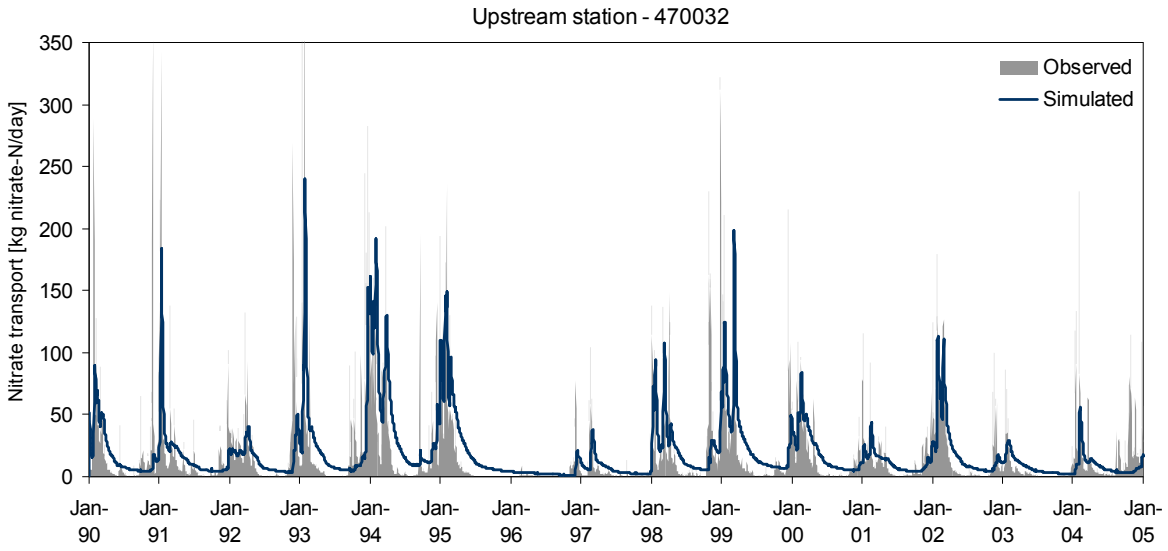

Figure 10.17 Observed and simulated daily nitrate-N transport at upstream station (470032) for 1990-2004

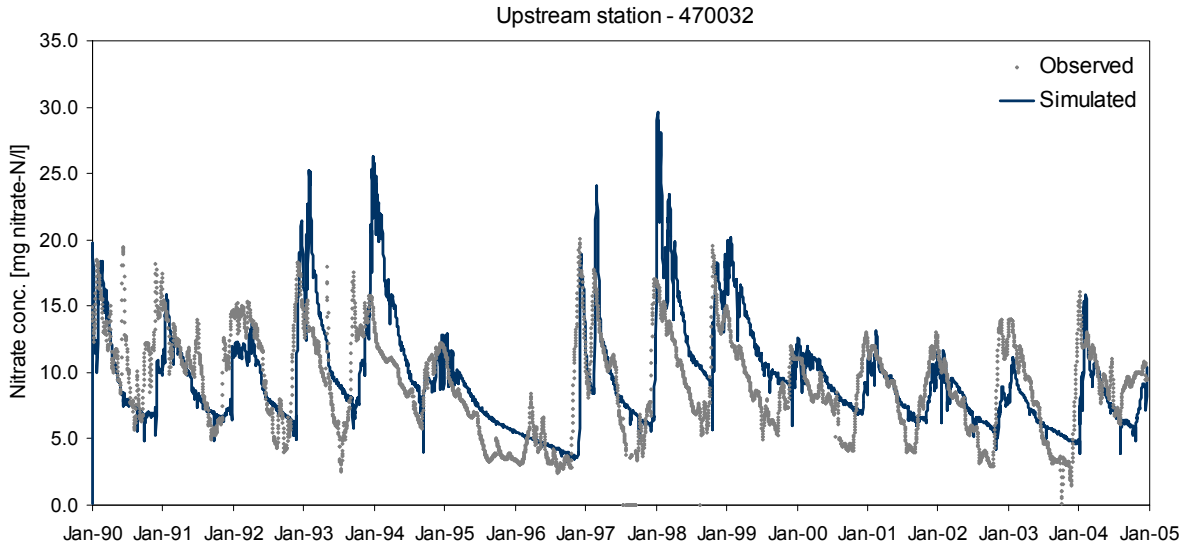

Figure 10.18 Observed and simulated daily nitrate-N concentrations at upstream station (470032) for 1990-2004

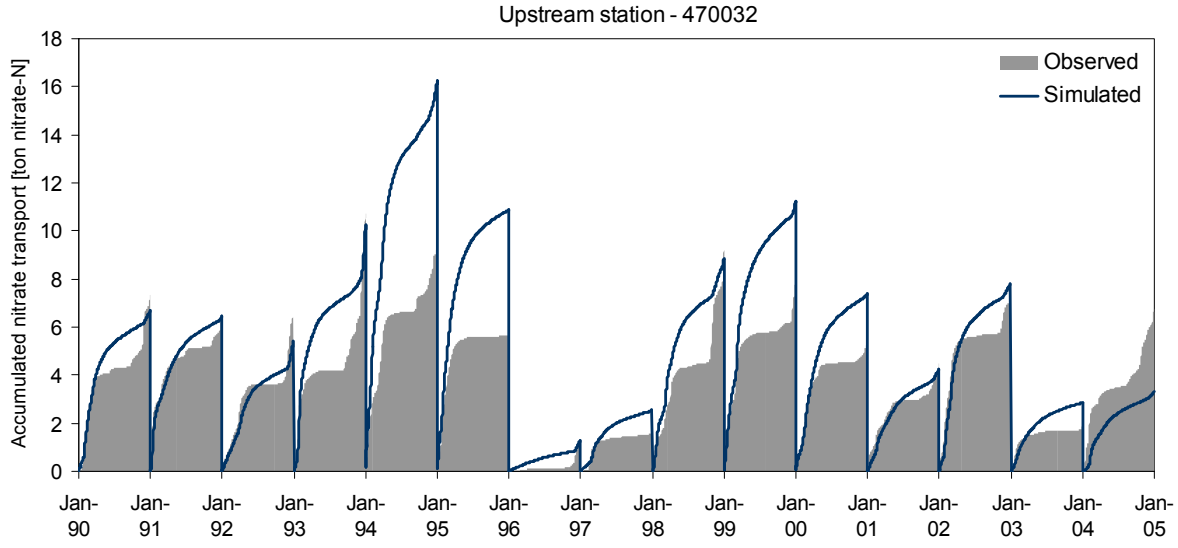

Figure 10.19 Observed and simulated yearly accumulated nitrate-N transport at upstream station (470032) for 1990-2004

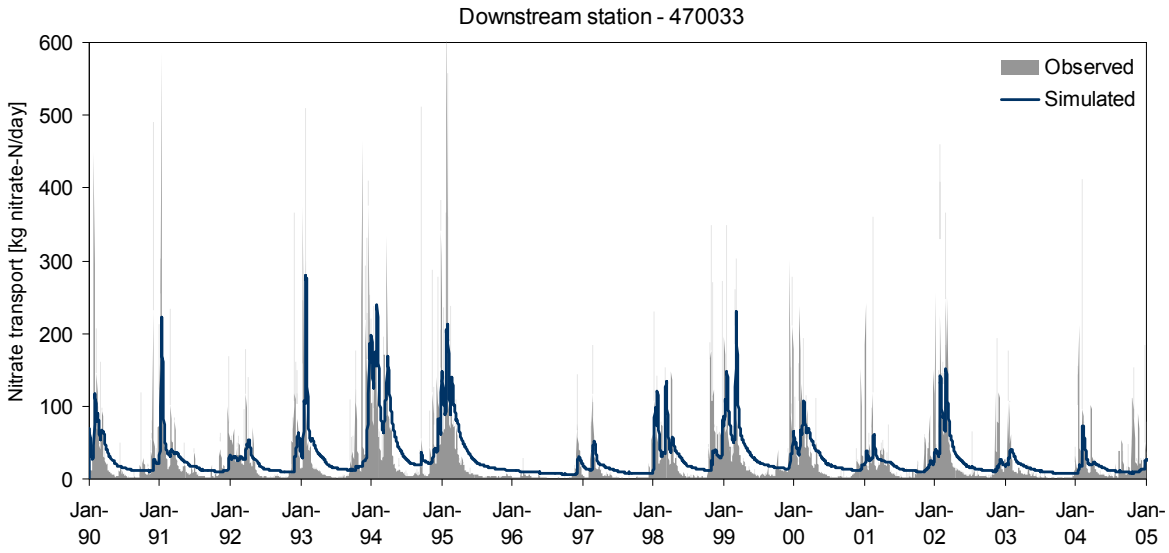

Figure 10.20 Observed and simulated daily nitrate-N transport at downstream station (470033) for 1990-2004

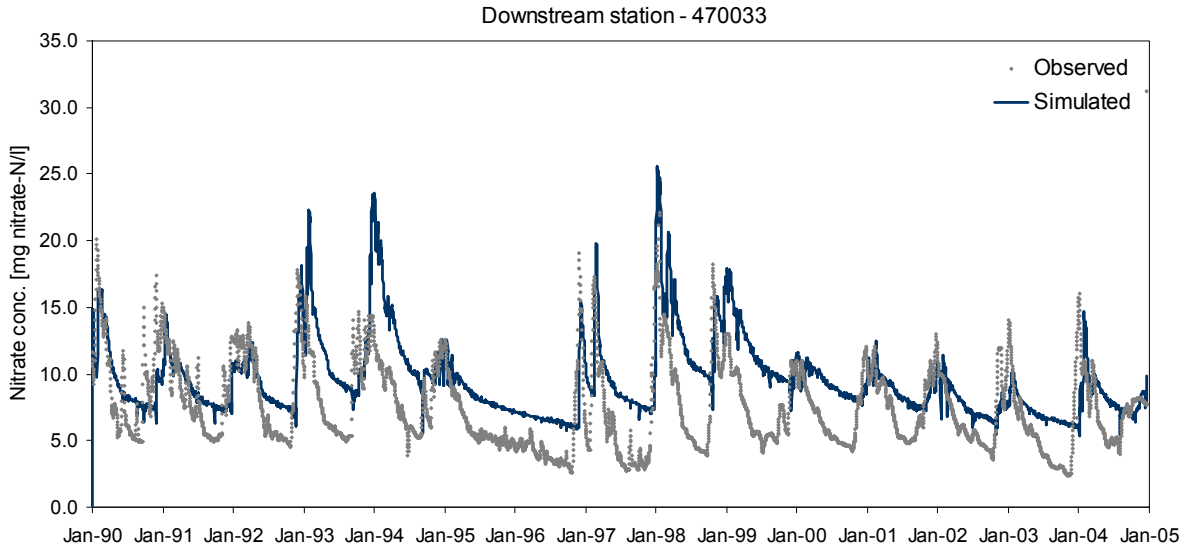

Figure 10.21 Observed and simulated daily nitrate-N concentrations at downstream station (470033) for 1990-2004

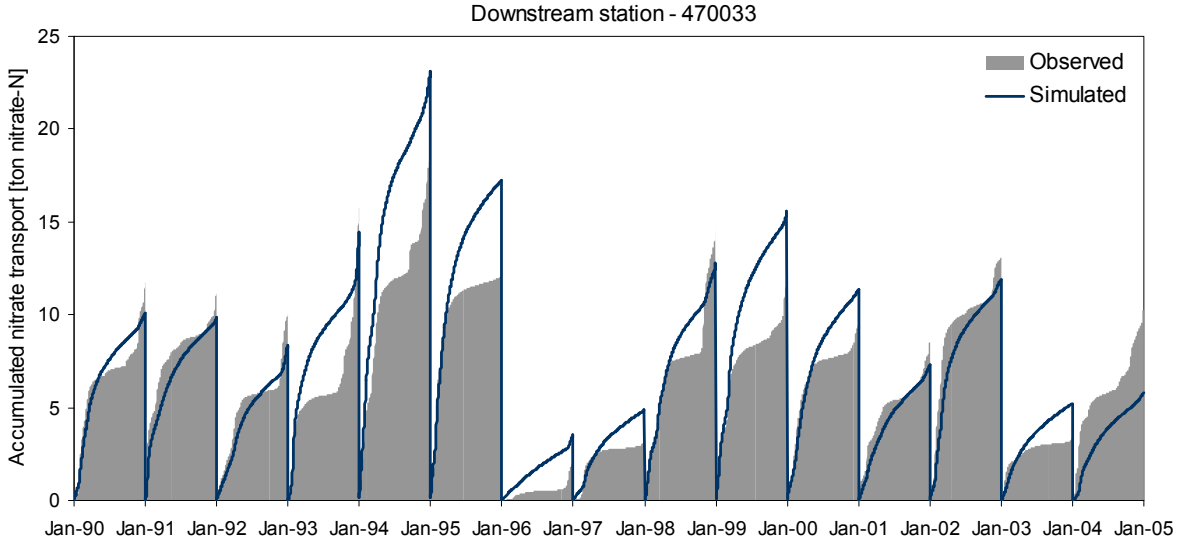

Figure 10.22 Observed and simulated yearly accumulated nitrate-N transport at downstream station (470033) for 1990-2004

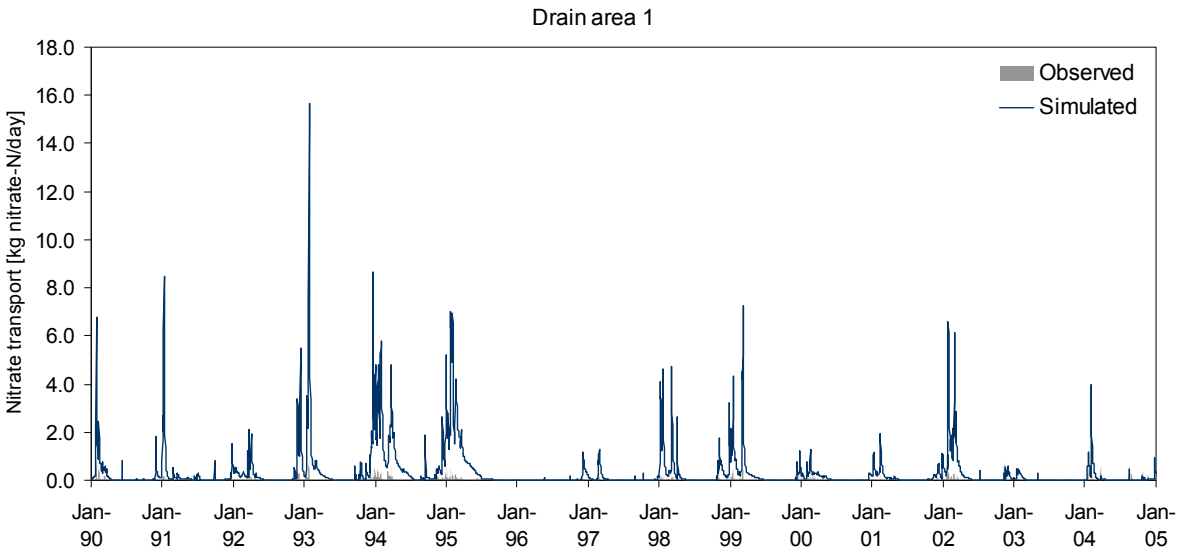

Figure 10.23 Observed and simulated daily nitrate-N transport from drain area 1 for 1990-2004

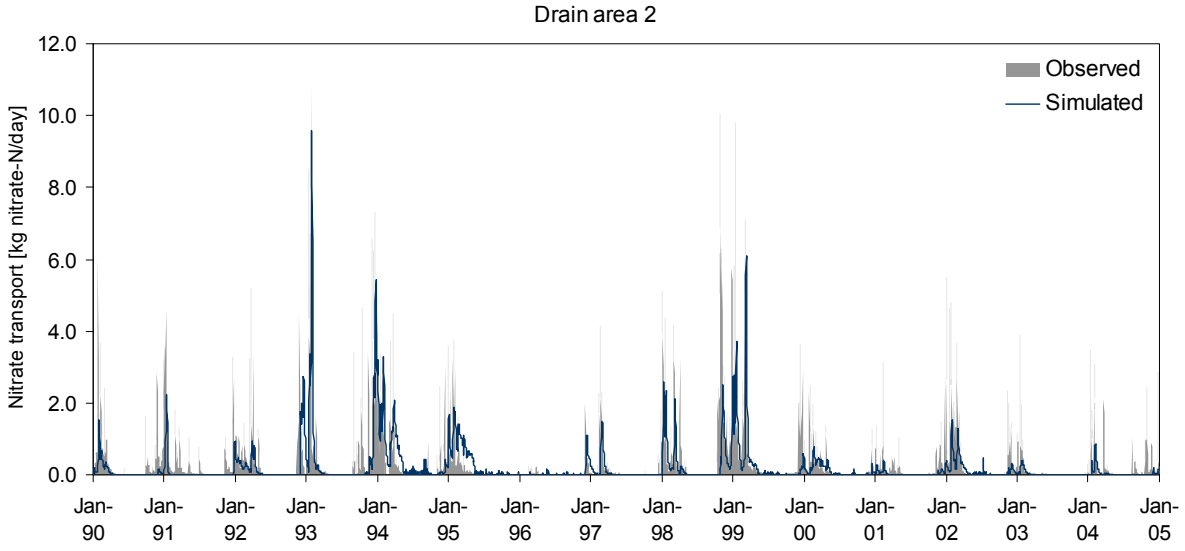

Figure 10.24 Observed and simulated daily nitrate-N transport from drain area 2 for 1990-2004

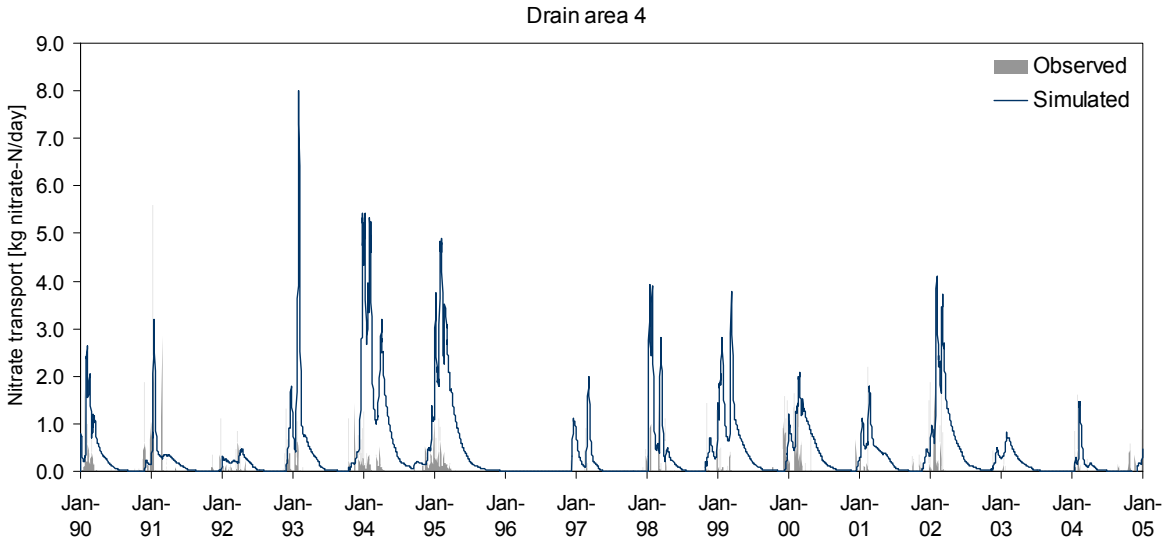

Figure 10.25 Observed and simulated daily nitrate-N transport from drain area 4 for 1990-2004

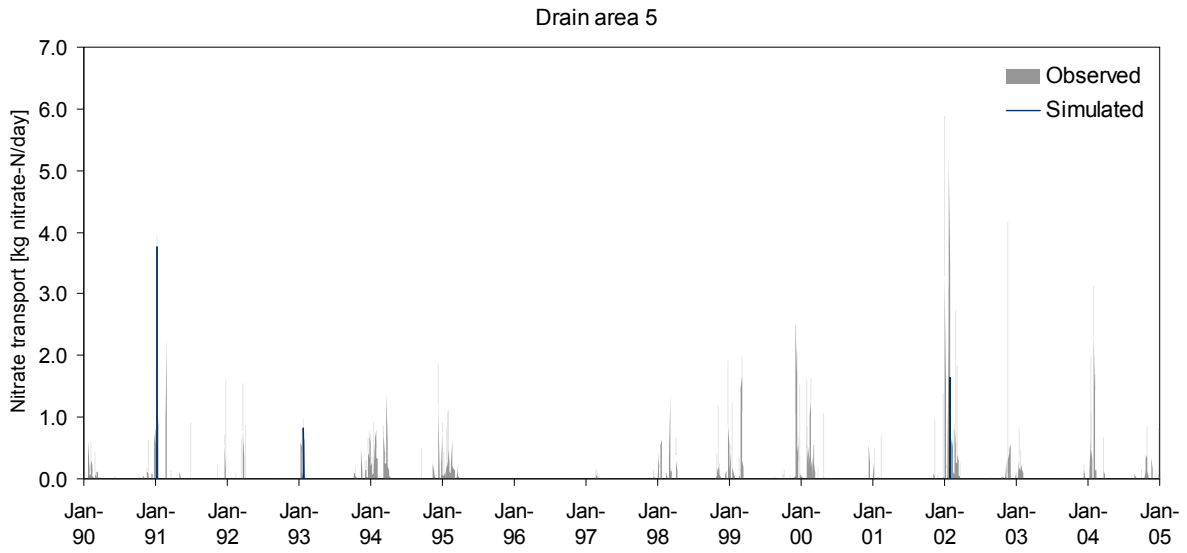

Figure 10.26 Observed and simulated daily nitrate-N transport from drain area 5 for 1990-2004

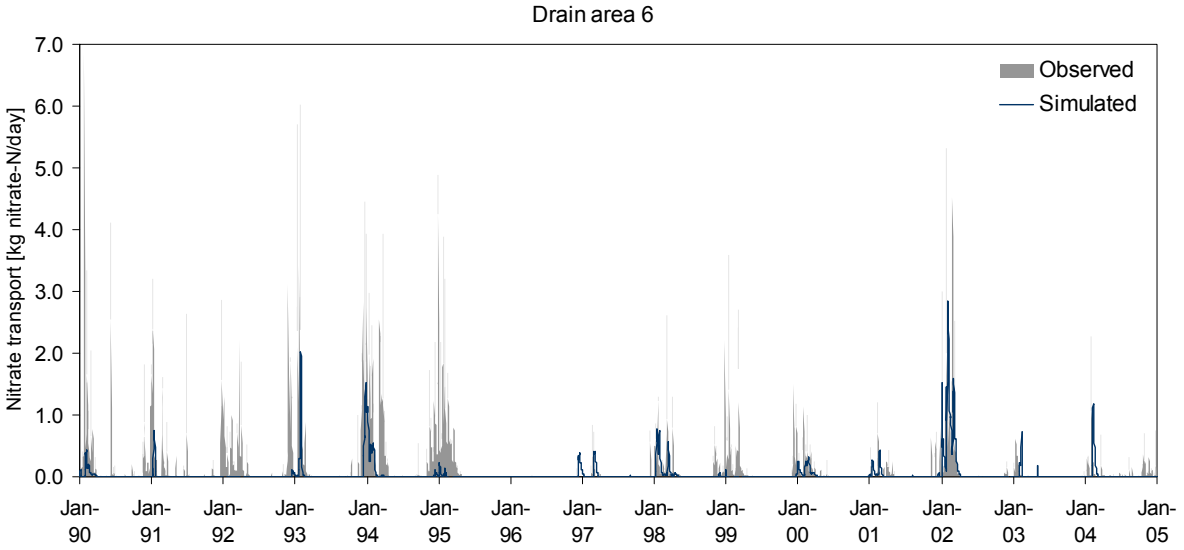

Figure 10.27 Observed and simulated daily nitrate-N transport from drain area 6 for 1990-2004

10.2 Water balance

The average yearly water balance for Lillebæk catchment is seen on figure 10.30. The figure shows all inflow and outflow fluxes to the area and also the exchange of water between the model layers. The inflow to the Lillebæk catchment consists of net percolation (i.e. the positive percolation flux minus the negative) as well as groundwater and overland inflow from the model area outside the LOOP4 catchment. The average net percolation in the LOOP4 catchment is 273 mm/year, which represents 33% of the reported average annual precipitation rate in the area. Figure 10.28 shows the percentage distribution of inflow components and the net percolation is with 80.7%, not surprisingly, seen to constitute the main part of the inflow of water to the catchment. Though, groundwater inflow is also seen to be an important inflow component accounting for 19% of total inflow. This illustrates the importance of making the model area larger than the LOOP4 catchment area. Groundwater inflow into the LOOP4 catchment was suspected to take place and is, from figure 10.30, seen mainly to occur in the Eem-Weichsel IS layer (layer 4) and the lower lens (layer 6). A small fraction of overland flow is seen to enter the catchment, which must mean that the topography, described by the 50 m DEM, is not completely coincident with the LOOP4 catchment.

The outflow from Lillebæk catchment consists of stream discharge, groundwater abstraction, groundwater outflow as well as overland and drain outflow. The percentage distribution of outflow components is seen in figure 10.29. The average yearly discharge to Lillebæk is 231 mm, which is underestimated by 7% when comparing with the observed average yearly discharge at the downstream station. The discharge to Lillebæk constitutes 68% of the total outflow and is thus the largest outflow component. The second largest outflow component is groundwater outflow representing 27%. The outflow from the saturated zone is seen to mainly occur in layers 4 and 6 (figure 10.30), i.e. the same layers as groundwater inflow is occurring. The discharge to Lillebæk originates mainly from drain flow, which accounts for 93% of the discharge and 63% of the total outflow. Drain flow is seen to be generated in the upper 5 model layers. As the computational layers thin out towards the sea, the top 5 layers are close enough to the ground surface to generate drain flow. The remaining 7% of the discharge is originating from overland flow, which represents 5% of the total outflow. Overland flow is mainly generated in areas close to the stream as the groundwater table reaches close to the surface in these areas thus making saturated overland flow possible. The base flow from the saturated zone to the stream is, on average, only 0.1 mm/year and is therefore not important in the water balance for the Lillebæk catchment. The small amount of base flow that is however generated is seen to originate from the Eem-Weichsel IS layer (layer 4).

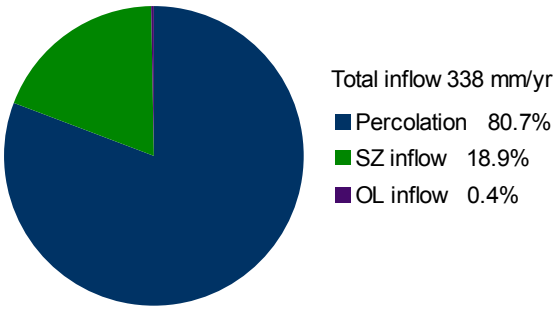

Figure 10.28 Inflow components to saturated zone

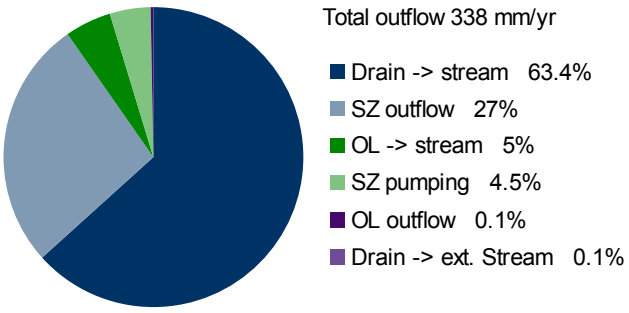

Figure 10.29 Outflow components from saturated zone

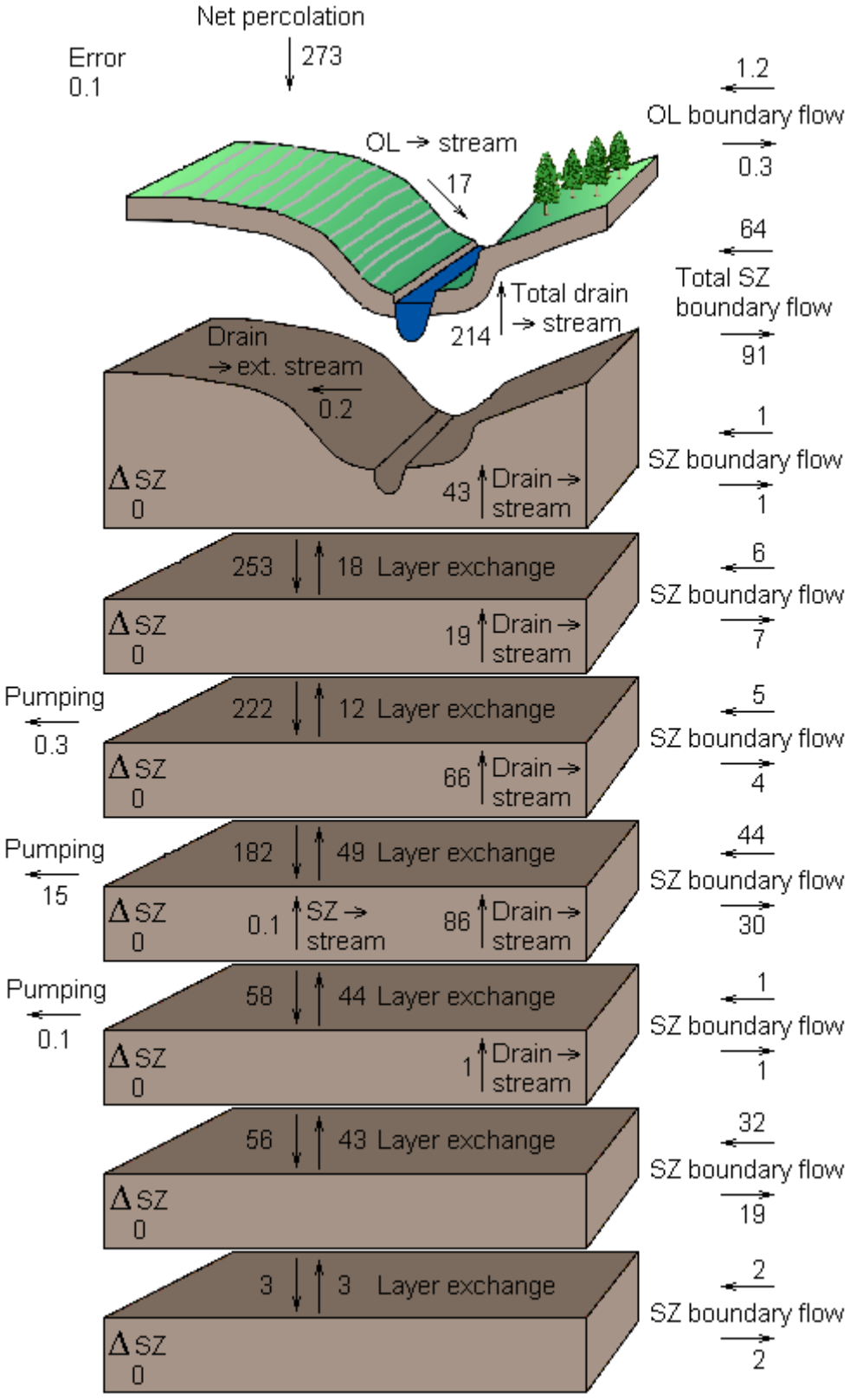

Figure 10.30 Average yearly water fluxes [mm/year] for Lillbæk catchment (LOOP4) for the simulation period 1990-2004

The annual and monthly variation in water fluxes for the simulation period 1990-2004 is seen on figures 10.31 and 10.32. The net percolation is seen to vary greatly in the period from 500 mm in 1994, the wettest year in the period, to only 53 mm in the very dry year of 1996. The fraction of precipitation that leaves the root zone as percolation also varies greatly from wet to dry years, from close to 46% in 1994 to only 9% in 1996. The amount of drain discharge to Lillebæk is seen to be related to the amount of percolation and is also seen to react quickly as a large drain flux is seen within the same month as a large percolation flux. Overland flow is seen to occur in winter months, where groundwater levels are high. The groundwater inflow and outflow is seen to be quite constant between the years as well as within the year, indicating a stable groundwater flow pattern. The storage of water in the saturated zone is from the water balance (figure 10.30) seen to be zero for the simulation period as a total, but is seen to vary between the years as well as during the year. Figure 10.32 shows how the storage is built up during winter months with large percolation and depleted again during summer months with low percolation.

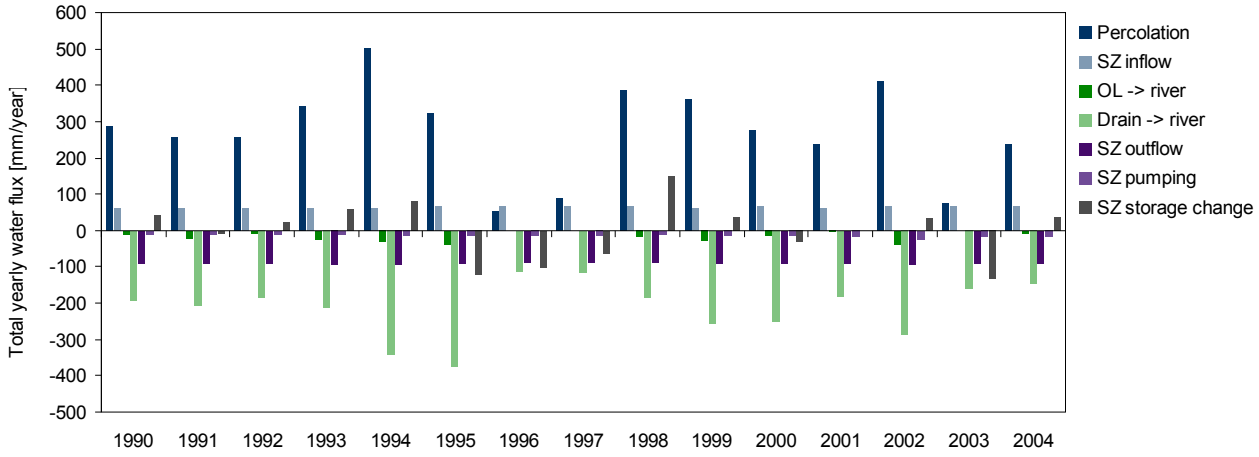

Figure 10.31 Yearly total water fluxes [mm/year] for Lillebæk catchment (LOOP4) for the simulation period 1990-2004. Inflow components are specified as positive fluxes and outflow components as negative fluxes

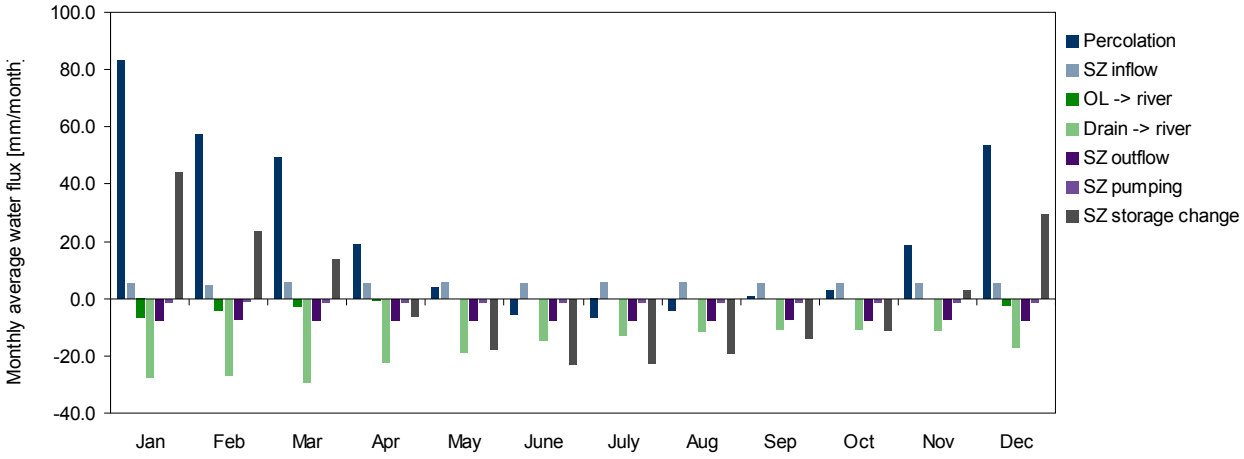

Figure 10.32 Average monthly water fluxes [mm/month] for Lillebæk catchment (LOOP4) for the simulation period 1990-2004. Inflow components are specified as positive fluxes and outflow components as negative fluxes

10.3 Nitrate mass balance

The average yearly nitrate mass balance for the model area is seen in figure 10.34. Mass balances can only be withdrawn for the whole model area and not for the LOOP4 catchment as is possible for water balances. The presented mass balance therefore also includes transport to the streams outside the LOOP4 catchment.

The input of nitrate to the model area consists entirely of the nitrate leaching predicted by Daisy which, on average, for the simulation period is 88.4 ton/year. The output components consist of mass withdrawal from the saturated zone due to negative fluxes, transport to the stream system, drain outflow and nitrate reduction in the saturated zone. The percentage distribution of output components is seen in figure 10.33. It is seen that almost 9% of the total nitrate input to the model area is withdrawn again from the saturated zone in periods of upward flux.

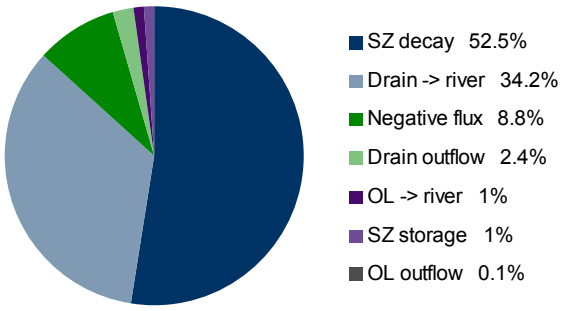

Figure 10.33 Output components from saturated zone

The single most important output component in the mass balance is seen to be the reduction of nitrate in the saturated zone. On average 47 ton/year, representing more than 50% of the nitrate leached from the root zone, is denitrified at the redox-interface.

The total mass flux to the stream system is 31.3 ton/year, representing 35% of the nitrate leaching. The main part of this is transported to the stream system by drain flow which accounts for 97% of the transport to streams and 34% of the total output from the model. A small fraction of mass is transported to the streams by overland flow. Around 50% of the total transport to the stream system in the model area is transported to Lillebæk stream and the rest to the streams outside LOOP4. Thus, the simulated average yearly transport to Lillebæk is around 15 ton/year, which is 36% higher than the observed yearly transport at the downstream station of 11 ton/year.

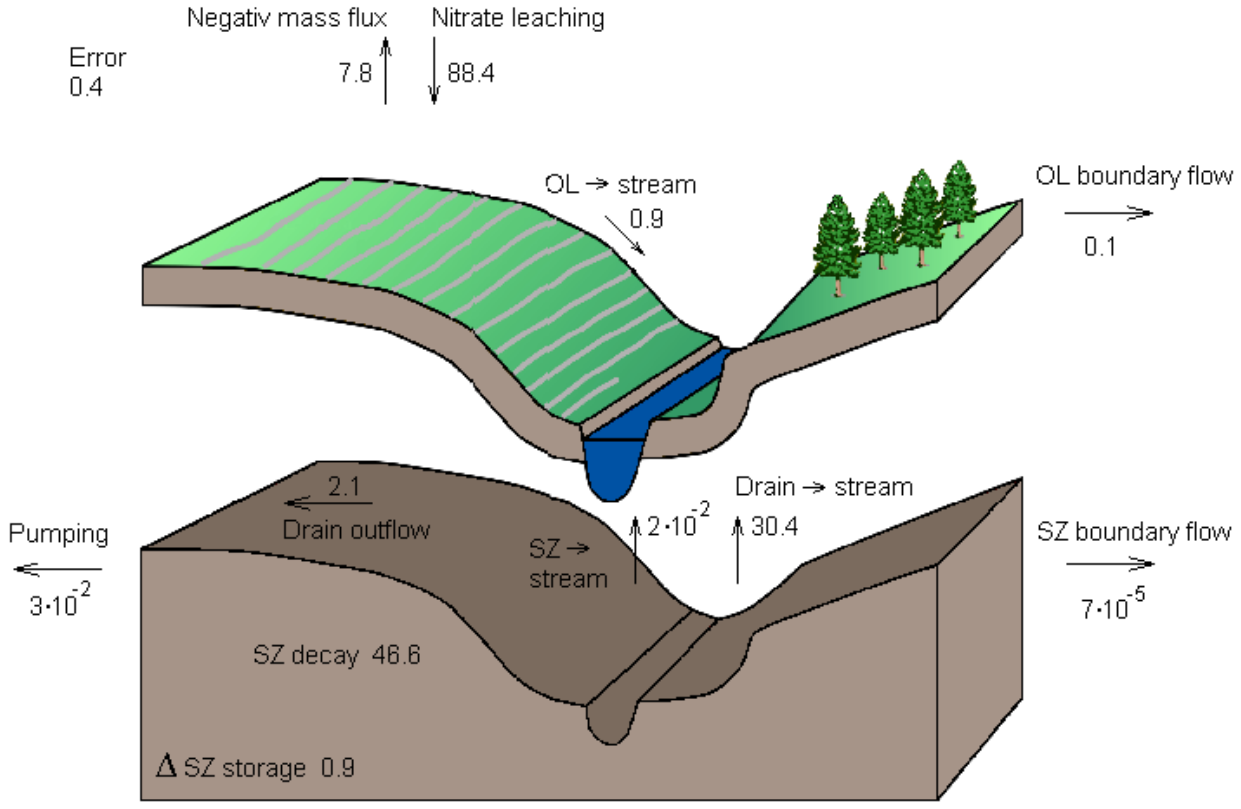

Figure 10.34 Yearly average nitrate-N fluxes [ton nitrate-N/year] for the model area for the simulation period 1990-2004

A small fraction of the mass is transported out of the model by groundwater abstraction and overland and groundwater flow. These amounts are seen to be very small though and therefore negligible in the mass balance, even though the groundwater abstraction and especially groundwater outflow represents important components in the water balance. The small mass removal by groundwater abstraction must mean that the water supply wells are screened below the redox-interface where groundwater concentrations are low. The reason for the small outflow of nitrate from the groundwater to the sea is due to the fact that the redox-interface has been raised to the ground surface at the coastline and thus almost all nitrate is reduced here.

The annual and monthly variation in nitrate fluxes for the simulation period 1990-2004 is seen on figures 10.35 and 10.36. The nitrate leaching in the model area is seen to vary greatly between the years, with the highest leaching of more than 250 ton in 1998. The reduction of nitrate is seen to be rather constant between the years, though the reduction is seen to be largest in 1998. The nitrate fluxes are seen to have a great variation with the year. Almost all of the nitrate leaching occurs in the winter months. This is due to a combination of large percolation rates and no plant growth and therefore no plant uptake of nitrate in these months. The nitrate reduction is also seen to be rather stable within the year, though a little larger in winter months. The negative mass fluxes are seen to occur during summer month where upward water fluxes take place.

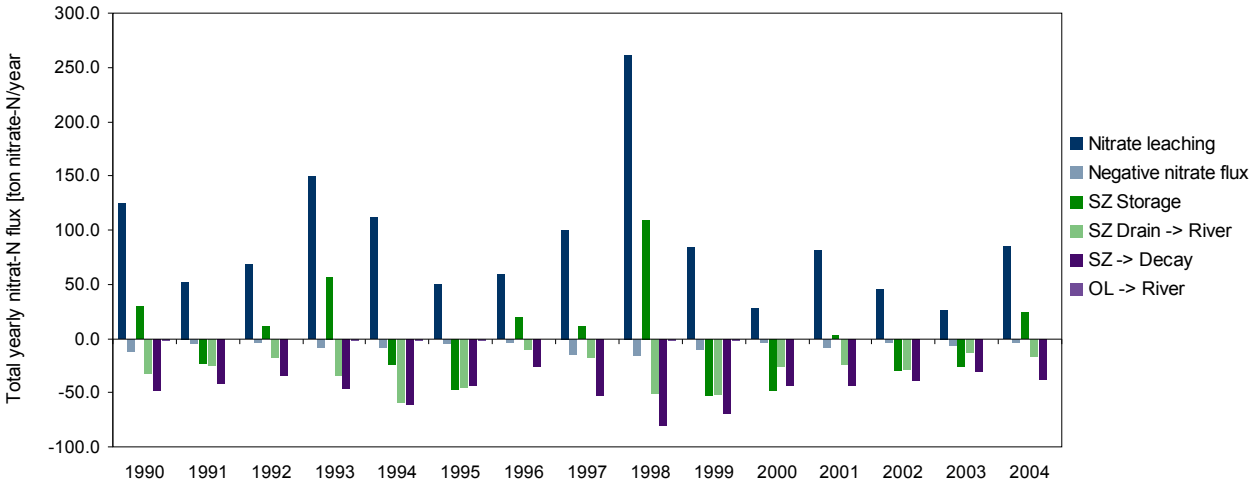

Figure 10.35 Yearly total nitrate-N fluxes [ton nitrate-N/year] for the model area for the simulation period 1990-2004. Inflow components are specified as positive fluxes and outflow components as negative fluxes

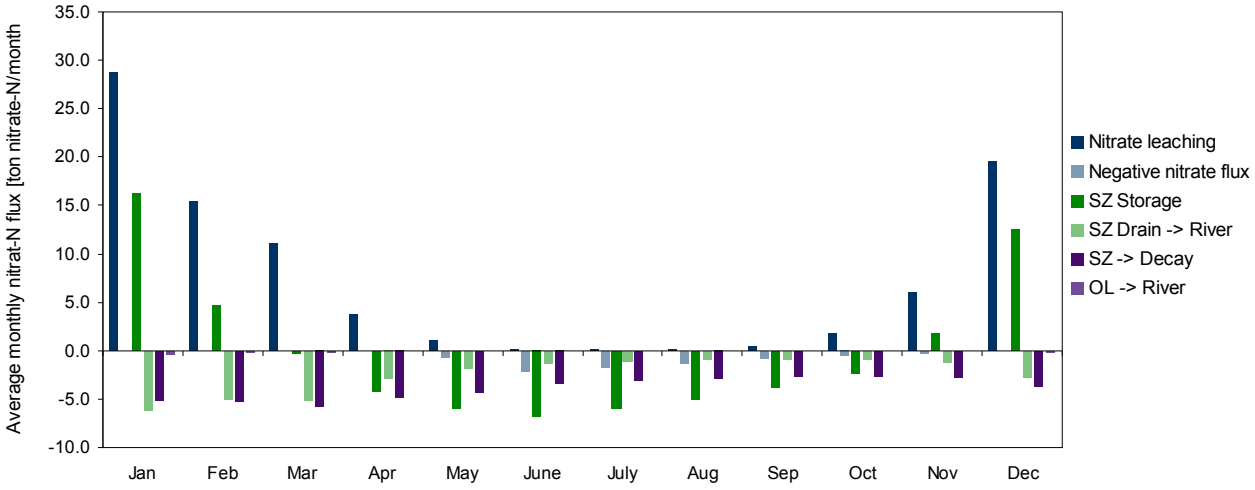

Figure 10.36 Average monthly nitrate-N fluxes [ton nitrate-N/month] for the model area for the simulation period 1990-2004. Inflow components are specified as positive fluxes and outflow components as negative fluxes

10.4 Groundwater concentrations

The average simulated nitrate-N concentrations in the saturated zone are seen in table 10.2 for each model layer. The concentrations have been converted to nitrate-NO_3^- concentrations, which are also seen in the table. The simulated groundwater concentrations are seen to be above the 50 mg nitrate-NO_3^-/l drinking water standard in the upper 5 model layers. Though in the layers below, where the groundwater abstraction in the area is taking place, the nitrate concentrations are below the drinking water standard. At the observation stations in the LOOP4 catchment an average nitrate-NO_3^- concentration of 62 mg/l has been measured in filters screened 1.2 meters below surface, 30 mg/l in filters screened at 3 meters and 26 mg/l at 5 meters for the period 1990-2004. The simulated concentrations are thus higher than the observed concentration, though within a reasonable range.

Table 10.2 Average simulated groundwater concentrations 1990-2004. Concentrations are listed as both nitrate-N and nitrate-NO_3^-

Comp. layer	Geology	Average depth to bottom of layer [m]	Nitrate-N [mg/l]	Nitrate-NO3- [mg/l]
1	Weichsel ML	0.3	14.2	62.9
2	Weichsel ML	0.6	19.1	84.6
3	Weichsel ML	1.1	19.2	85.0
4	Weichsel ML	2.2	17.8	78.8
5	Weichsel DS/DG Weichsel ML	4.1	15.7	69.5
6	Weichsel ML	12.3	8.9	39.4
7	Eem-Weichsel IS	23.0	4.5	19.9
8	Saale ML	35.7	1.5	6.6
9	Saale DS/DG Saale ML	39.7	1.0	4.4
10	Saale ML	54.7	0.0	0.0

10.5 Nitrate pulse

The response time in the catchment is analysed by simulating the transport and fate of a nitrate pulse released on the 1/1 1990. Figure 10.37 shows the distribution of the nitrate mass with time. All nitrate is at first seen to go into storage in the saturated zone. After 1 year around 20% of the nitrate has been transported to the stream system, a little more than 25% has been reduced, around 1% has been transported out of the model and 50% of the nitrate is still stored in the saturated zone. After 5 years only 16% of the nitrate is still stored in the saturated zone, around 50% has been reduced and around 30% has been transported to streams and 2% out of the model. After 7-10 years the distribution of the nitrate mass is seen to be rather stabilized which is thus representing the response time in the catchment.

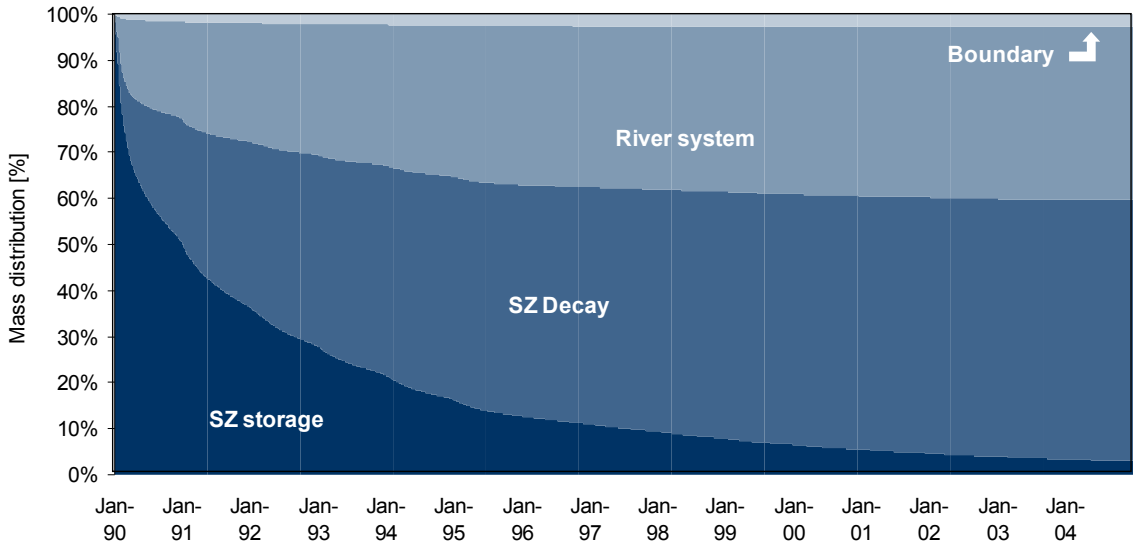

Figure 10.37 Fate of a nitrate pulse released on 1/1 1990. The graphs show how the nitrate mass is distributed in the system with time

10.6 Particle tracking

The sensitive and robust areas in the catchment with respect to nitrate pollution of the stream system have been designated using particle tracking. In figure 10.38 the fraction of particles crossing the interpolated redox-interface for each model grid is seen. The red areas indicate the most sensitive areas, where all flow lines are above the redox-interface and therefore all nitrate leached from the root zone will reach the stream without being reduced. The green areas, on the other hand, constitute the robust areas in the catchment, where the main part of the water flow is brought below the interface and thus most nitrate is reduced.

The location of the interpolated redox-interface is subject to great uncertainties, which make the delineation of the sensitive and robust areas uncertain. An uncertainty assessment of the sensitive and robust areas has been conducted by moving the redox-interface up and down and the results are seen in figure 10.39 – 10.42. It is seen that decreasing the depth to the redox-interface with 50% results in most of the LOOP4 catchment being robust areas. When increasing the depth to the redox-interface more and more of the catchment becomes sensitive areas. When the depth is increased by 150% a large part of the catchment, especially in the downstream part, is seen to be sensitive areas. The areas that are affected by changing the location of the redox-interface are marked as shaded areas on figure 10.38 and these constitute uncertain areas with respect to the delineation of sensitive and robust areas. Figure 10.38 shows that it is especially areas close to the stream and mainly in the downstream part of the LOOP4 catchment that are sensitive areas where water is flowing direct to the stream without crossing the redox-interface.

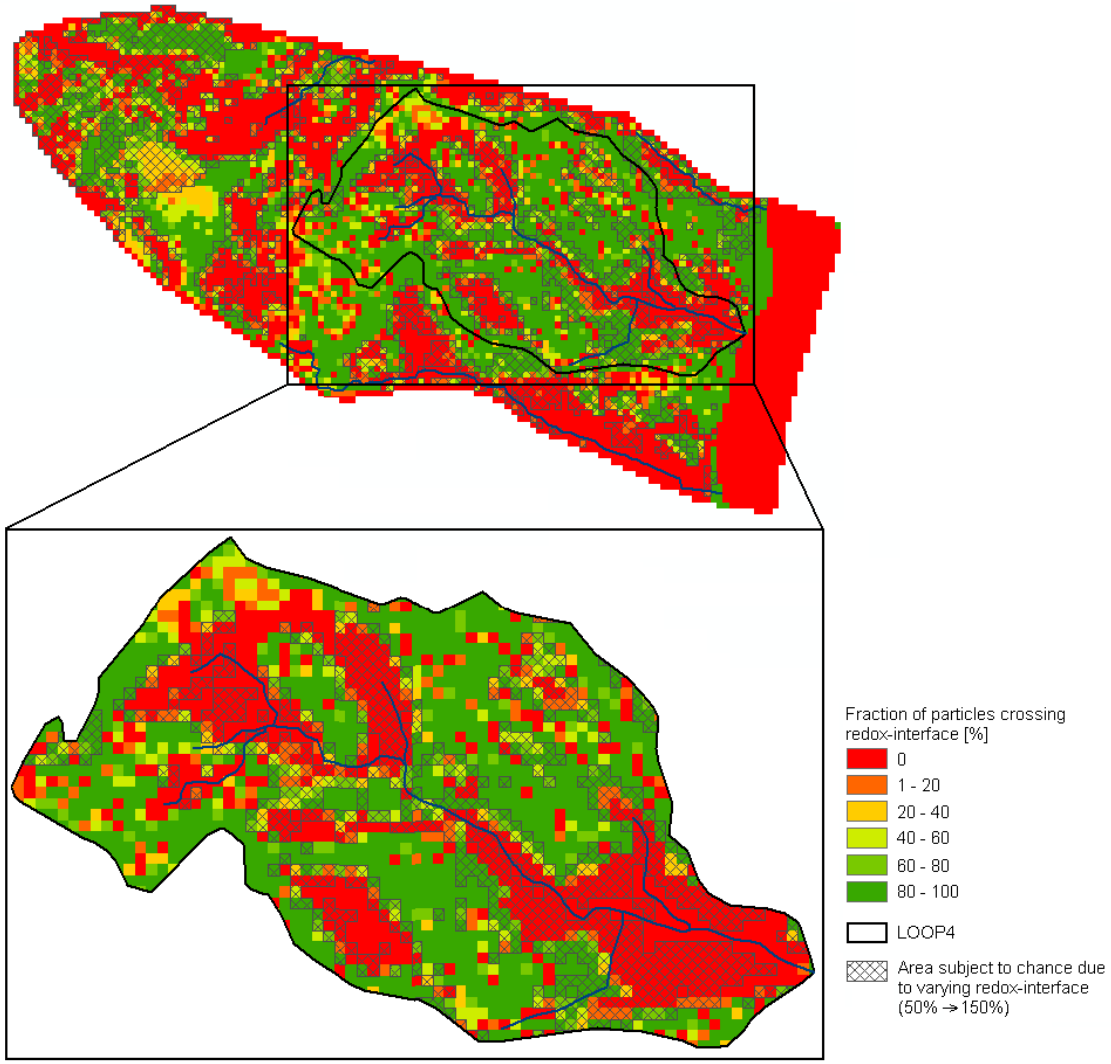

Figure 10.38 Fraction of particles crossing the redox-interface. The shaded areas constitute areas affected by uncertainties on the location of the redox-interface

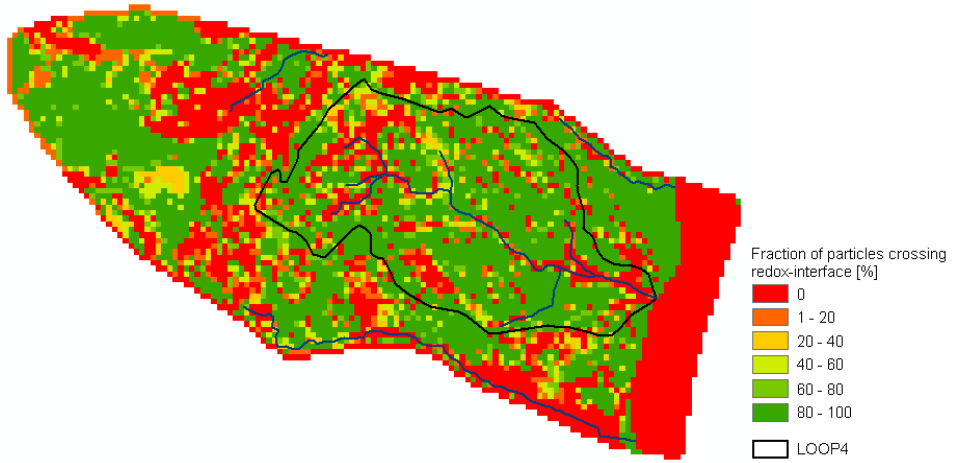

Figure 10.39 Sensitive and robust areas - Redox-interface 50 %

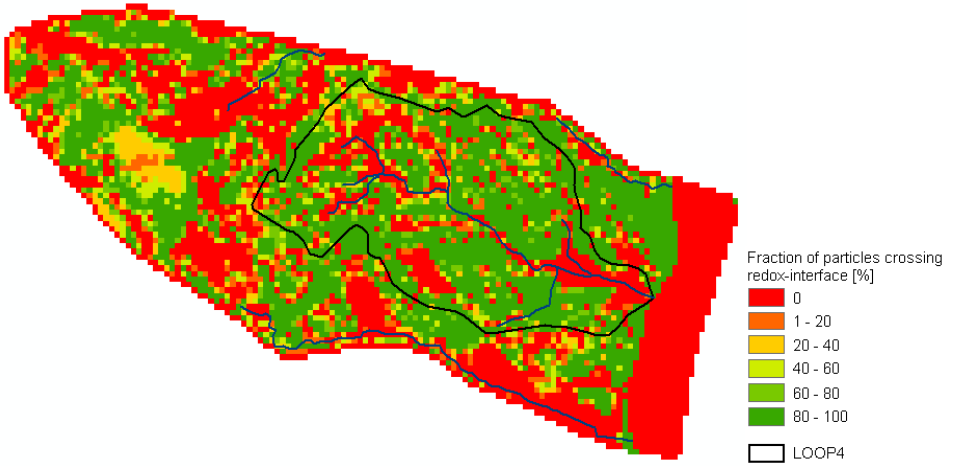

Figure 10.40 Sensitive and robust areas - Redox-interface 75 %

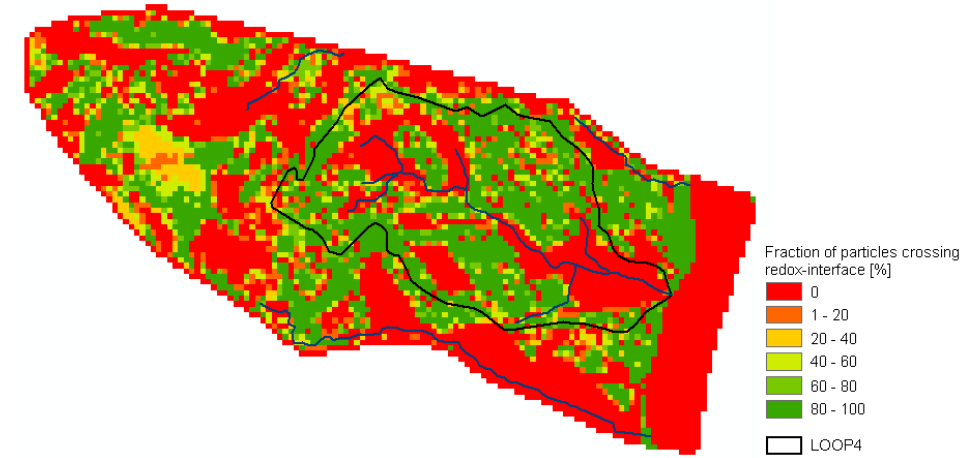

Figure 10.41 Sensitive and robust areas - Redox-interface 125 %

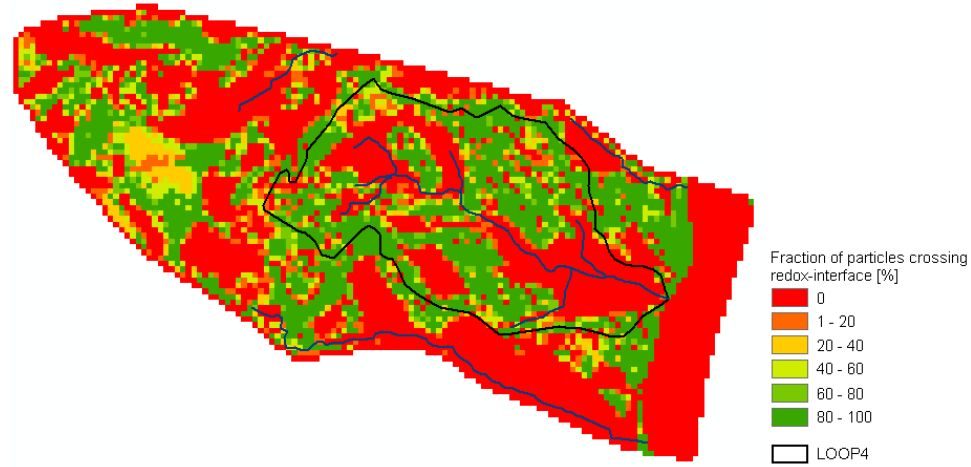

Figure 10.42 Sensitive and robust areas - Redox-interface 150 %

11. Discussion

In the following sections problems concerning the presented model results and different sources of uncertainties in the model are discussed, followed by a discussion on the choice of hydrological model and its effects on the nitrate simulations. Finally the predictive capability of the model and the current status in nitrate modelling on catchment scale is evaluated.

11.1 Model results

11.1.1 Overestimation of low flows and hydraulic heads

The runoff in the Lillebæk catchment is found to be dominated by drain flow and it is therefore important to have a good simulation of groundwater levels and dynamics in order to produce a good run-off simulation. The simulated hydraulic heads at the observation wells are, on average, overestimated, and this overestimation especially occurs during summer months (see figure 10.1 and appendix 1). This is believed to be the main reason for the overestimation of the low flow events during the summer months.

The problem concerning the simulated hydraulic heads is believed mainly to be caused by the lack of heterogeneity in hydraulic conductivities in the model layers as these are assumed constant within each layer. In order to improve the simulation of groundwater levels and thereby discharge dynamics it is required that the model gets a better description of the spatial variation in hydraulic conductivities than at present. Further more in order to simulated a larger annual variation in hydraulic heads and thereby lower heads during summer, the storativity of the geological materials should be decreased.

11.1.2 Daily dynamics in discharge and nitrate transport

The model has problems with simulating the daily dynamics in discharge and nitrate transport and is not able to reproduce all observed peaks. For the model to be able to simulate these dynamics correctly, it is required that the Daisy input describes the dynamics satisfactory, otherwise the model will never be able to reproduce it.

In figures 11.1 and 11.2 Daisy percolation is compared with the measured and simulated discharge at the down stream station (470033) for two different periods. The same comparison is made for nitrate transport in figures 11.3 and 11.4. The Daisy input is seen to be able to describe most of the observed dynamic at the downstream station for both discharge and nitrate transport although, some peaks are seen not to be described e.g. late April 2000 and during autumn 1999. Hence, in these periods, the model cannot be expected to simulate the observations and this is also seen to be the case. It is noted, however, that many peaks that are in fact described in the Daisy input are not simulated by the model. The peak in observed discharge and transport in September 1994 is particularly noted as this peak is well described by the Daisy input but very poorly reproduced by the model.

It is furthermore noted from figures 11.1–11.4, that many of the simulated peaks are delayed when compared to the observations. The reason for this is that the Daisy input is seen to peak at the same time as the observations and in some cases (e.g. January 2000) after the observed peak. Other studies using Daisy input in MIKE SHE have also reported problems with simulating daily discharge and transport dynamics e.g. Nielsen et al (2004) and Hansen et al (2009). Reasons for this are described in following sections.

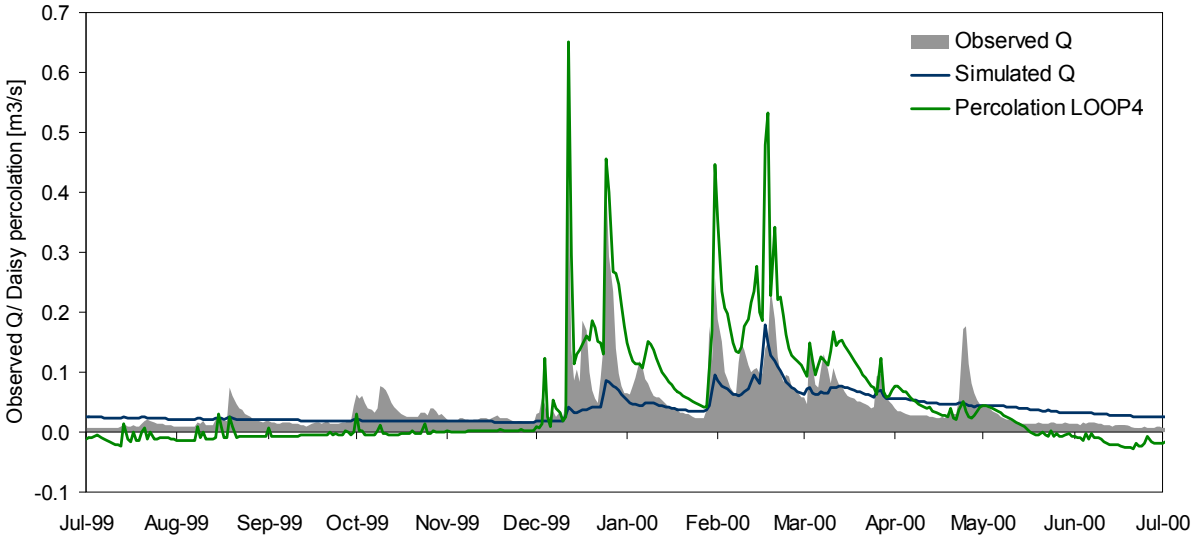

Figure 11.1 Comparison of observed and simulated discharge at downstream station (470033) and the total percolation in the LOOP4 catchment for the period July 1999- July 2000. The daisy percolation has been converted from mm/day to m^3/s to make it comparable with the observed discharge

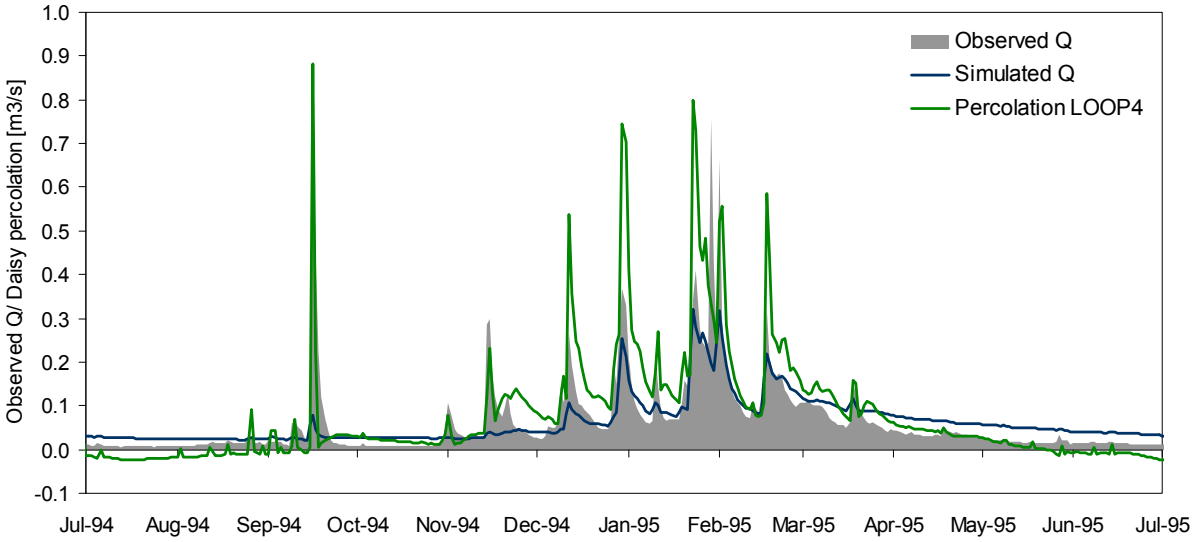

Figure 11.2 Comparison of observed and simulated discharge at downstream station (470033) and the total percolation in the LOOP4 catchment for the period July 1994- July 1995. The daisy percolation has been converted from mm/day to m^3/s to make it comparable with the observed discharge

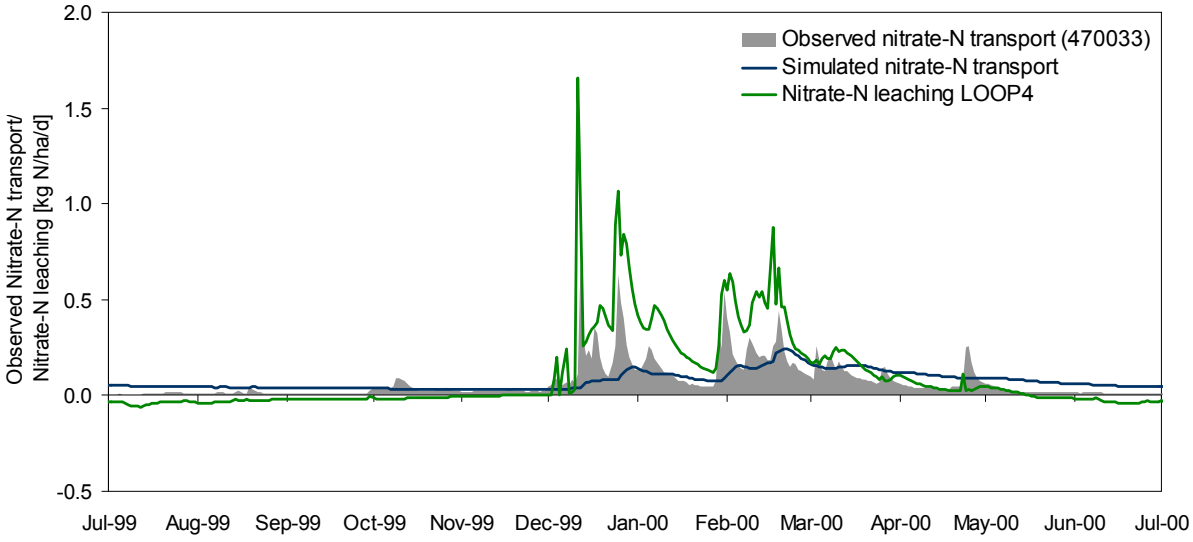

Figure 11.3 Comparison of observed and simulated nitrate transport at downstream station (470033) and the total nitrate leaching in the LOOP4 catchment for the period July 1999- July 2000. The observed transport has been converted from kg/day to kg/ha/day to make it comparable with the Daisy leaching

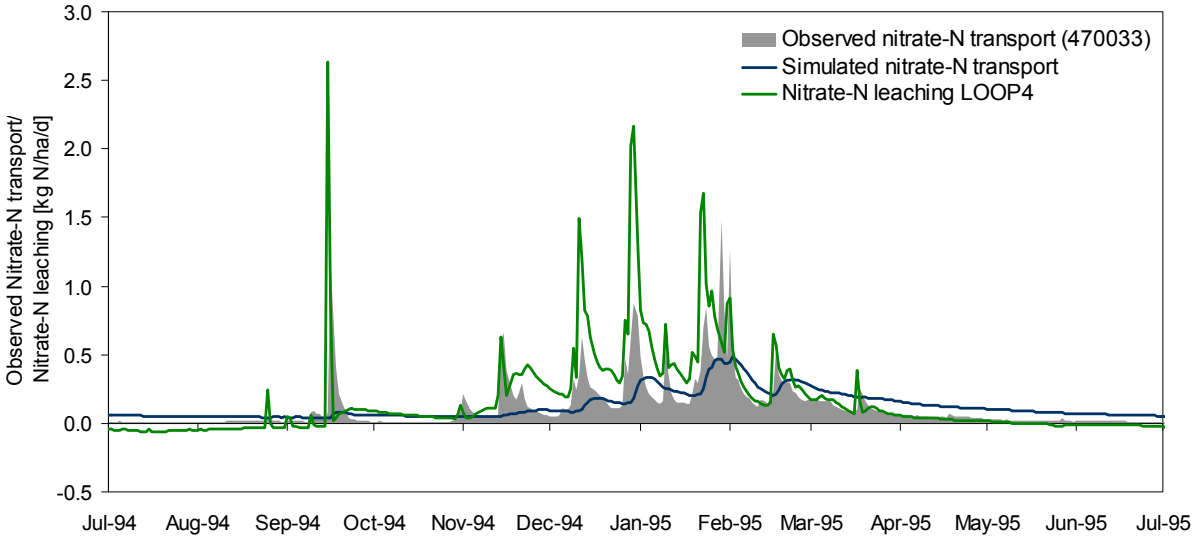

Figure 11.4 Comparison of observed and simulated nitrate transport at downstream station (470033) and the total nitrate leaching in the LOOP4 catchment for the period July 1994- July 1995. The observed transport has been converted from kg/day to kg/ha/day to make it comparable with the Daisy leaching

11.1.3 Discharge and nitrate transport from drain areas

Due to the discretization of the model into 50m x 50m grid cells it is not possible to implement the drain areas 100% correctly in the model, as seen on figure 11.5. As the drain areas are small and only cover a few model grids, this results in relatively large uncertainties on the drain areas. It is believed that this uncertainty on the drain areas is a contributing factor to the poor simulation of drain flow and transport.

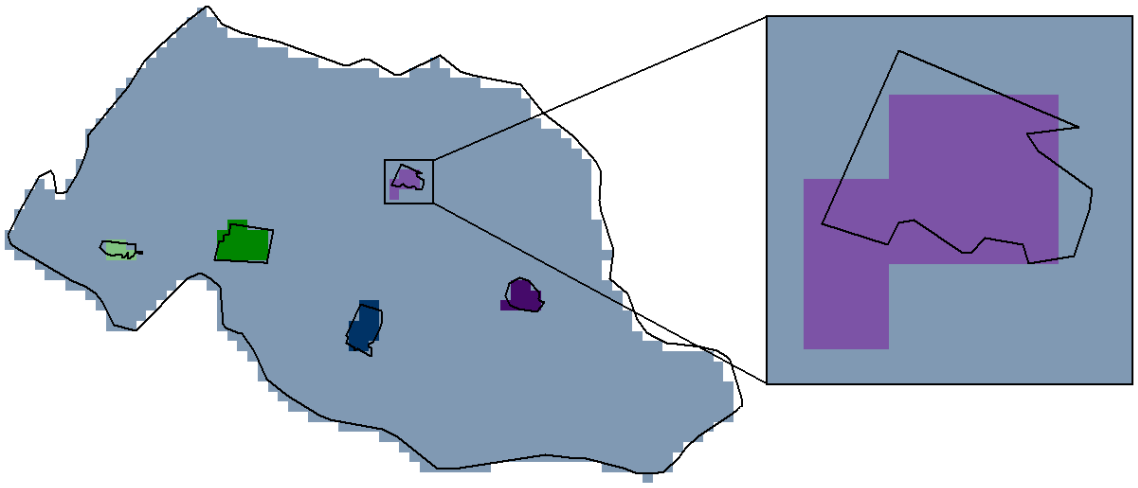

Figure 11.5 Uncertainties on drain areas due to model discretization

11.1.4 Nitrate reduction

The simulated total nitrate transport to Lillebæk of 15 ton/year is overestimated by around 36% compared to the observed transport of 11 ton/year. However, as the observed transport is subject to rather large uncertainties this overestimation is believed to be within an acceptable range. The uncertainties on observed transport are described in a subsequent section.

The overestimation of nitrate transport can be explained by overestimation of the nitrate leaching in the area and/or that not enough nitrate is reduced in the model. The actual amount of reduction in the catchment is unknown and it is therefore not possible to evaluate if the reduction is underestimated. Underestimation of nitrate reduction can be caused by too small simulated reduction in the saturated zone and/or because the denitrification concept in this study does not include reduction in anaerobic zones above the interface, wetlands and stream sediments. Although, as Hansen et al (2009), as mentioned, have found reduction in wetlands and stream sediments to be limited compared to reduction in the saturated zone, it is believed that the main reason for underestimation of nitrate reduction shall be found in the saturated zone. It is, however, still believed that the denitrification concept should be reviewed and possibly expanded in the following work on nitrate modelling in Lillebæk catchment.

The reason for underestimating the amount of reduction in the saturated zone is that not enough nitrate is brought under the redox-interface. This can be due to either a wrong flow pattern in the catchment, too small spreading of the solutes (i.e. too small dispersivities) and/or too great depth to the redox-interface. As the flow pattern in the catchment is believed to be simulated acceptably and quite large dispersivities are already used in the nitrate model, the location of the redox-interface is believed to be the main problem.

11.1.5 Response time

The simulation of a nitrate pulse showed that the distribution of the nitrate mass is stabilized after approximately 7-10 years. This indicates that a change in agricultural practice in the area will break through in the nitrate transport to the stream system within this time frame. However, whether a statistical significant change in stream concentrations will, in fact, be recognizable is uncertain as the change can be overshadowed by climatic variations. The 2006 report from the LOOP-program (Grant et al, 2007) did find a significant decrease in total N-concentration in Lillebæk from 1990 to 2004 which complies with the response time found in this study. However, as the statistical analysis did not take climatic variations into account, it is uncertain whether this observed decrease, in fact, does illustrate the effects of implementation of the aquatic environment action plans in the area.

11.1.6 Sensitive and robust areas

The results from the particle tracking show that the delineation of sensitive and robust areas is very dependent on the location of the redox-interface. As the location of the redox-interface is subject to great uncertainties, the resulting areas shown on figure 10.38 should therefore be treated with caution.

11.2 Sources of uncertainties

The uncertainties on the model outputs have not been quantitative assessed in this study, however this could have been done using a stochastic approach. In the following, possible sources, which are believed to give rise to uncertainties on the model outputs, are discussed.

11.2.1 Observation data

Uncertainties on observation data give rise to uncertainties on the model output as the model is calibrated against this data. The discharge at both stations is measured continuously (Pedersen et al, 2010). As the discharge in Lillebæk is rather small, it is suspected that the uncertainty on the discharge measurements could be high. The measurement error on hydraulic heads is believed to be small and within a range of +/- 5 cm.

The nitrate transport in Lillebæk stream is measured as pooled intensive samples (Pedersen et al, 2010). By this method samples are taken several times each day and these are pooled together to give an average daily value. The nitrate observations are therefore subject to uncertainties not only due to measurement errors but also due to uncertainty on whether the pooled samples are, in fact, representative of the transport. The nitrate concentrations are calculated based on the measured nitrate transport and discharge and are therefore subject to uncertainty on both of these factors.

Representativeness of the observation data is another important issue. The main part of the head observations used in the calibration of the hydrological model is from the Weichsel ML and only few observations from the Eem-Weichsel IS layer and the two Weichsel/Saale DS and DG lenses are available. This lack of observation data for the aquifers is a large problem as the model performance in these layers therefore can not be evaluated and this is believed to be a contributing factor to the simulation problems.

11.2.2 Daisy input data

The results from the Daisy simulation of percolation and nitrate leaching are also subject to uncertainties and this will propagate to the model output in this study. The Daisy simulated percolation and nitrate leaching follows the observed dynamics acceptably, as was also seen in figures 11.1–11.4. However, in the years 1992/93 and 1996/97 the predicted percolation is considerably higher than the observed discharge (Pedersen et al, 2010). This problem is especially seen to propagate to the simulated discharge in this study for 1996 and 1997 (see figures 10.7 and 10.10). The Daisy nitrate leaching is considerably higher than the observed transport in the years 1992/93, 1993/94, 1996/97 and 1997/98 (Pedersen et al, 2010). In these years the simulated nitrate transport is also found to be overestimated, with the largest overestimation at the downstream station in 1996 (see figures 10.19 and 10.22). A decisive factor for the nitrogen balance for the root zone is the simulated crop yield (Nielsen et al, 2004). Daisy, in general, overestimates the crop yield in the LOOP4 catchment, though for the mentioned years with high simulated nitrate leaching, the crop yield is underestimated compared to the reported yield (Pedersen et al, 2010)

The main sources of uncertainties in the Daisy results are the use of grid precipitation and the lack of heterogeneity in combination with use of many standard parameter values in the Daisy set ups (Hansen et al, 2007). The precipitation data used for the Daisy simulations originates from DMI's 10 km grid. This data uses average values for a larger area and is therefore maybe not representative for the actual precipitation in the Lillebæk area. The spatial variation in precipitation in the area is also not represented by this data though, as the LOOP4 catchment is small, this is believed to be a minor problem. An additional source of uncertainty on the precipitation is the correction applied to the data. The correction has been done according to the standard method described by Allerup et al (1998), which is using general correction parameters for the whole country based on the period 1961-90. These correction parameters are not dynamic i.e. the same correction is applied for a cold as well as for a warm winter, even though the uncertainty on measurements of solid precipitation is known to be larger than for liquid precipitation.

Daisy columns have, as mentioned, (see section 5.3.1) been set up for the 6 soil water stations in the LOOP4 catchment and for many of the parameters standard values are used. These columns are subsequently distributed to the whole catchment which results in a quite simplified description of the root zone parameters in the catchment. Hansen et al (2007) found that this lack of heterogeneity in the Daisy simulations was an important factor for problems with simulating daily dynamics, which is also seen to be a problem in this study. By introducing variability, especially of soil physical parameters and plant growth in the Daisy simulations, Hansen et al (2007) found that the simulation of dynamics was greatly improved.

11.2.3 Implementation of Daisy input in MIKE SHE

The implementation of the Daisy input in MIKE SHE gives also rise to uncertainties. As the model area in this study extends beyond the LOOP4 catchment an extrapolation of Daisy results is made. This extrapolation is solely based on land use and the percolation and nitrate leaching in the model area outside LOOP4 is, as a consequence, believed to be subject to rather large uncertainty. The subsequent aggregation procedure of Daisy polygons to model grids also gives rise to uncertainties, however, it has been attempted to reduce this uncertainty by using a small grid scale of 10 m.

11.2.4 Model parameters

It is not certain that the parameter values used in the model are the most optimal values and this is therefore also a source of uncertainty on the model output. The initial parameter values for the hydrological model are assumed to be good initial guesses as they are based on a previously calibrated model for the Lillebæk area. However, if this is not the case, it can be that a global minimum (maximum for R2) has not been reached for some of the parameters during the optimization (see section 7.2.4). Some of the objective functions plotted in figure 7.17 may only cover a local minimum and this will mean that the chosen parameter value is not the most optimal. When subsequently all parameters are changed at the same time in the multi-variable optimization, complexity is, as mentioned, added to the optimization problem.

To improve the model performance an inverse calibration of the hydrological model should be performed in the following work. Inverse calibration can be performed using the PEST parameter estimation technique. Different initial parameters should be tried to be certain that a global minimum in the objective function is reached.

11.2.5 Geological model and hydrostratigraphical units

The geological model, and thereby the description of hydrostratigraphical units, is subject to rather large uncertainty as the geological information in the area is sparse (see figure 5.1) and based solely on borehole data, which only gives point scale information. The uncertainty on the geological model propagates to the hydrological model and further on to the nitrate model. Especially the horizontal delineation of the sand and gravel lenses is uncertain. Further more, the lack of heterogeneity within the hydrostratigraphical units is a problem and this, as mentioned, is believed to a main cause for simulation problems. The model is found to have great difficulties in reproducing the observed hydraulic in the middle part of the LOOP4 catchment and this is believed to be caused by uncertainty on the geological model and/or by the lack of heterogeneity. Geophysical data for the Lillebæk area are, in the near future, going to be produced using SkyTEM. This should improve the geological understanding of the area and thus give rise to a better description of the heterogeneity of the layers in the area.

11.2.6 Boundary conditions of hydrological model

All model boundaries in the hydrological model, except along the coastline, are defined as no-flow boundaries and are delineated based on simulated hydraulic heads in the interglacial sand layer from the DK-model. However, whether the delineated model area in fact represents the actual watershed is subject to uncertainties, partly caused by the much larger model discretization of the DK-model (500m) than for the model in this study (50m). The influence of the model boundary on the simulation results has however not been tested.

11.2.7 Redox-interface

The location of the redox-interface is subject to great uncertainty as the depth to the interface can vary greatly within short distances and information of the location of the interface is very sparse in the Lillebæk area. However, if a short distance variation of the interface was potentially described in the area, it cannot be fully included in the model due to the discretization of the model. As only a single redox depth can be specified for each model grid, is the depth assumed to be constant within each 50 m grid cell

Another problem concerning the redox-interface is the implementation of the interface in relation to the computational layers, as this gave rise to problems due to the sloping of the layers. This results in that model cells are crossed by the interface (see figure 8.6) and these cells are given a weighted average between the reduced and oxidized half life. As mentioned in section 8.3.7, this average half life is so high, even if most of the cell is below the interface, that these cells will represent oxidized cells. In order to improve the implementation of the interface the upper layer was subdivided in to 4 layers, though the problem still exists in the lower model layers. Figure 11.6 shows the half lives in computational layer 6 based on the interpolated redox-interface. The purple areas are totally reduced and the red are fully oxidized. The blue, green and yellow colours indicate areas where the redox-interface crosses the model cells and thus where average half lives are specified.

In order to test the influence of this weighting of half lives on the simulated nitrate transport and reduction, a simulation is made, where the half lives are manually altered. This is done by specifying all model grids where more than half the cell is below the redox-interface (i.e. grid cells where the specified weighted average half life is < 500 years (1.6E+10 seconds)), as being totally reduced with a half life of 1 hour. The resulting half lives for computational layer 6 after this manipulation are seen in figure 11.7. It is noted that the change from oxidized to reduced conditions are much more sharp in figure 11.7.

The nitrate model is run with the changed half lives and the resulting nitrate transport and concentrations at the downstream station are seen in figures 11.8 and 11.9. It should be noted the model is run using dispersivities of 5 m/0.1 m for sand/gravel and 0.5/0.1 for clay and not the calibrated dispersivities, as this makes the simulation time much faster. The results are compared with results from a model run using the interpolated redox-interface and equal dispersivities.

Figures 11.8 and 11.9 show that changing the half-lives results in lower nitrate transport and concentrations, though maybe too low. When analysing the mass balance (results not shown) the nitrate reduction in the saturated zone is found to be much larger for the simulation with changed half lives. Hence, these results clearly indicate that the problem with implementation of the redox-interface due influence the nitrate simulations and should be worked on.

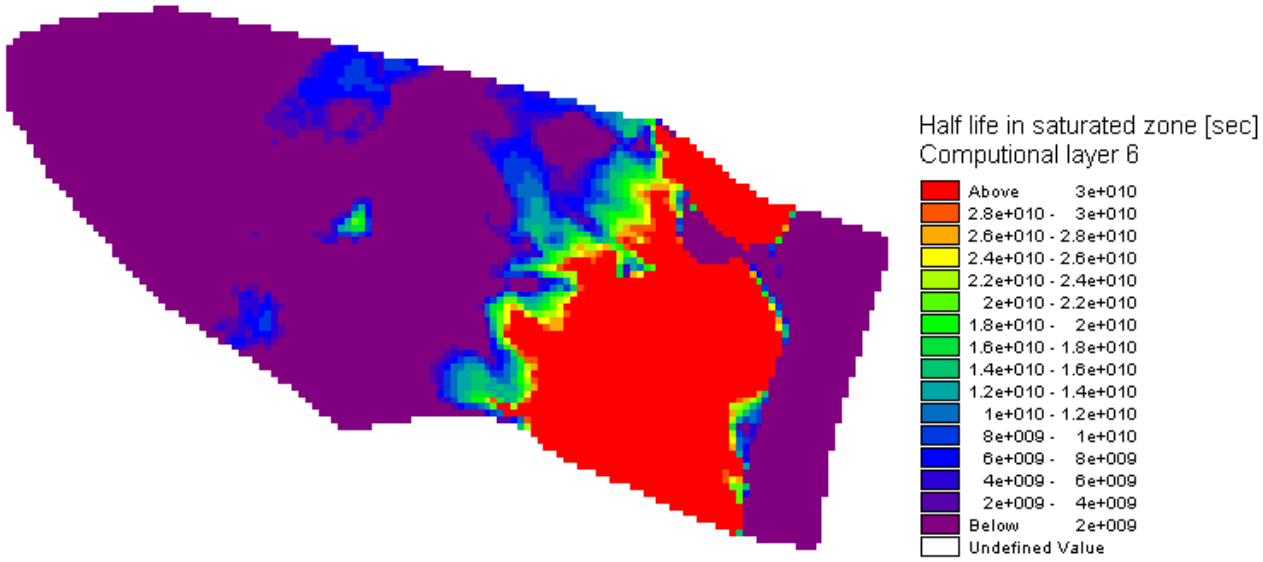

Figure 11.6 Half lives in computational layer 6 based on the interpolated redox-interface

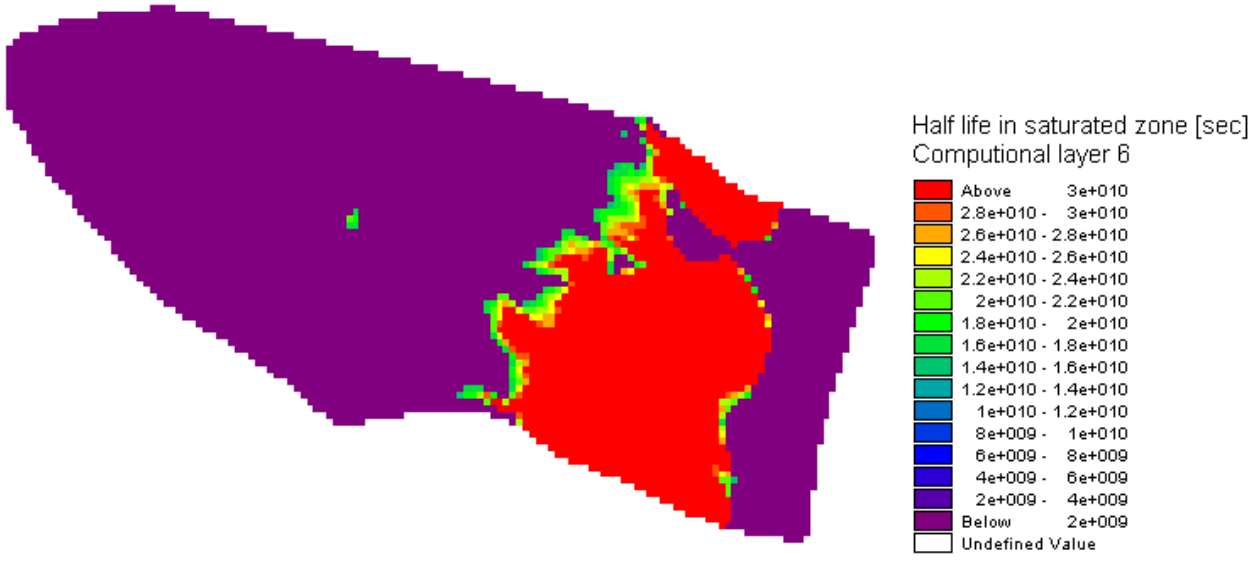

Figure 11.7 Changed half lives in computational layer 6. All model grids where more than half the cell is reduced are specified as being totally reduced with a half life of 1 hour

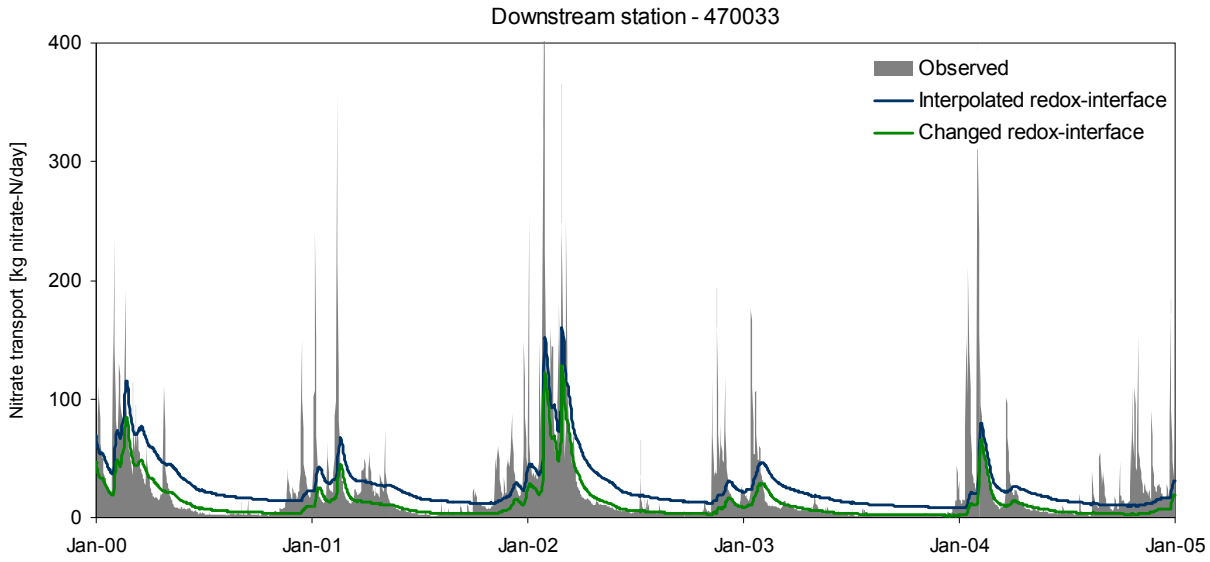

Figure 11.8 Comparison of daily nitrate transport at downstream station using the interpolated redox-interface and the changed redox-interface. It should be noted that dispersivities of 5m/0.1m for sand/gravel and 0.5m/0.1m for clay is used and not the calibrated dispersivities

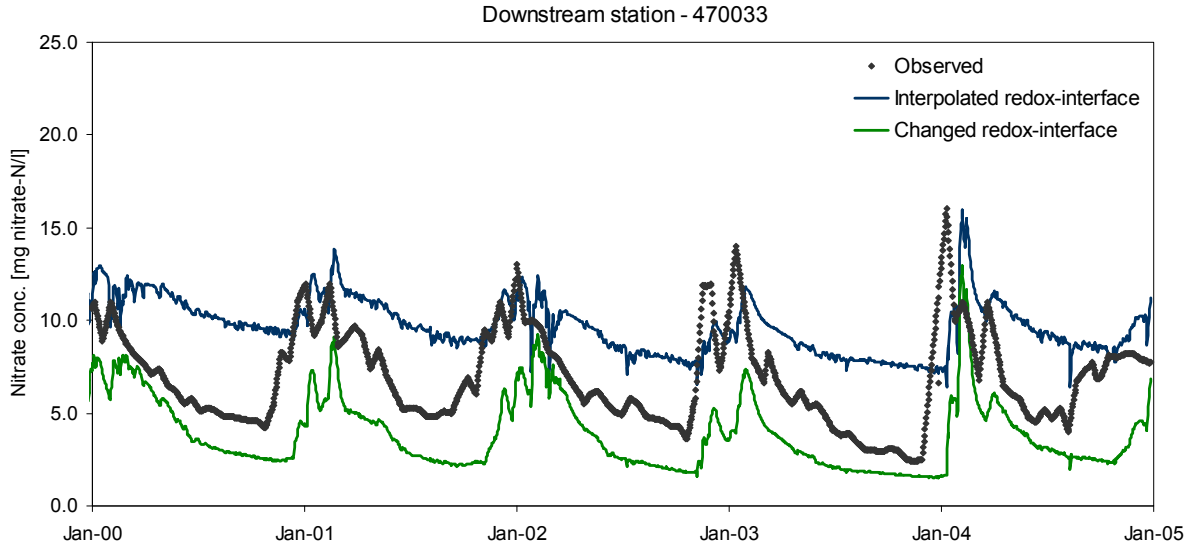

Figure 11.9 Comparison of daily nitrate concentrations at downstream station using the interpolated redox-interface and the changed redox-interface. It should be noted that dispersivities of 5m/0.1m for sand/gravel and 0.5m/0.1m for clay is used and not the calibrated dispersivities

11.2.8 Inadequate model structure

The sequential coupling between Daisy and MIKE SHE gives rise to different problems and is commented in the following. One problem is that because the Daisy simulations are performed separately from the MIKE SHE simulations of this study, the lower boundary conditions used in the Daisy simulations do not match the groundwater table simulated by MIKE SHE. This constitutes a problem as the Daisy results are much influenced by the lower boundary condition (Hansen et al, 2007; Nielsen et al, 2004).

A conceptual problem with the Daisy/MIKE SHE modelling approach is that drainage is included in both models. The drain flow generated in Daisy is not led to the stream model, but is instead added to the saturated zone in MIKE SHE together with percolation. This results in a delay of the water transport to the stream system and thus gives rise to the problems with simulation daily dynamics as seen in the study. Nielsen et al (2004) suggest compensating for this delay by using a higher drain time constant.

The sequential coupling between Daisy and MIKE SHE also gives rise to mass balance problems for both water and nitrate as MIKE SHE is not able to withdraw the entire specified negative flux and thus has to reset some of it. This results in that the net flux of water and nitrate to the saturated zone is too large compared to the actual Daisy input. In the calibrated hydrological model 0.92% of the total negative water flux is reset corresponding to 3.7 mm over the 15 year simulation period. This means that the total yearly net percolation is overestimated by 0.2 mm, which is such a small amount that it can be ignored. The neglected negative nitrate flux is though, as mentioned earlier, rather large (66%), due to the fact that nitrate, contrary to water, can only be extracted from the top layer. This results in the net nitrate input to the model to be 5.7% too large. It has, however, been discovered late in the process that this is, in fact not the case anyway.

It has been discovered, that the model makes a double accounting of negative nitrate fluxes. MIKE SHE accounts for when a negative nitrate flux is specified in the source file, and this is the mass extraction that has been mentioned until now. Though, in addition to this, nitrate is also withdrawn due to the negative water fluxes and a nitrate mass equal to water flux multiplied by the concentration in the saturated zone is removed in periods of upwards water flow. Hence this results in a double withdrawal of nitrate. The effect of this double accounting has been analyzed and it turns out, as none of the two extractions of nitrate mass account for the total negative mass flux, the problem is not too large. The negative fluxes specified in the source are only able to extract 34% of the total negative nitrate flux, as much of the negative flux, as mentioned above, is reset. The mass removed from the model due to upward water fluxes is equal to 80% of the total negative flux. In total the extraction of nitrate is thus 14% too high and the nitrate input to the model is therefore, contrary to initial belief, too low. As the negative mass flux is small compared to the net flux, the double accounting does, however, only result in the net nitrate input to be underestimated by 1.2%.

The double accounting of negative mass fluxes is, of course, conceptually wrong, though, as the error introduced is relatively small, it is believed not to have a great effect on the simulation results. The mass removal due to negative water flux can be disabled by specifying the extra parameter *"disable SZ transport to dummy UZ"* and thereby the double accounting is removed (personal communication Thomas Clausen, DHI). However, as the upwards water flux is found to be able to remove a larger fraction of the total negative mass flux than the negative fluxes specified in the source input file, it might be better to actually leave be the removal with water and, instead, reset the negative fluxes in the source input file. However, by doing this it is believed that the mass removal will never be exactly equal to the actual negative mass flux simulated by Daisy as the mass removal by this method, as mentioned, is calculated as water flux multiplied with concentration in the saturated zone.

11.2.9 Mass conserving problems in MIKE11

Hansen et al (2009) found that the solution of the advection-dispersion equation in MIKE11 is not mass conserving and that 4% of the mass input from MIKE SHE to the stream system in MIKE11 was lost due to numerical error. The depletion of mass was found to occur during high flows, whereas a small increase in mass was seen during low flows.

The extent of this problem has been evaluated for the presented study by comparing the total mass input to the stream system in the model area from MIKE SHE to MIKE11 with the total transport at the downstream ends of all river branches in MIKE11. It has been found that as much as 20% of the total mass input from MIKE SHE to MIKE11 is lost in MIKE11 during the simulation period. In figure 11.10 the daily nitrate transport from MIKE SHE to MIKE11 is compared with the daily total transport in MIKE11. It is noted that most mass in this study is lost during large transport events and therefore during large flows. On figure 11.11 the transport is accumulated per year to show the total yearly mass depletion in MIKE11. It is noted that the problem is greater in wet years than in dry years due to larger flow in these years.

The mass depletion in this study is therefore found to be much larger than in Hansen et al (2009). Though, it is known that Hansen et al (2009) started out with a much higher mass depletion and worked several weeks to reduce the problem to the reported 4% (personal communication Jens Christian Refsgaard, GEUS). An attempt has been made to reduce the problem by decreasing the time step in MIKE11 to as low as 1 second, though, this did not have any effect on the mass depletion. It is recommended in Hansen & Rasmussen (2006) to decrease the number of computational grid points in MIKE11 in order to reduce the mass depletion problem. This has not been tried, however, as it has not been possible within the time frame of this study to do more to reduce the problem.

The mass problem in MIKE11 does not have any effect on the reported nitrate mass balance and the estimated 36% overestimation of transport to Lillebæk (section 10.3) as this estimate is based on the transport from MIKE SHE to MIKE11. The problem, however, affects the calibration results for the nitrate model reported in sections 8.4.1 and 10.1.2 as these results are exported from MIKE11. The average concentrations and total transport reported in table 8.3 as well as the transport and concentrations plotted on figures 8.8–8.11 and figures 10.17–10.27 is thus, in reality, higher.

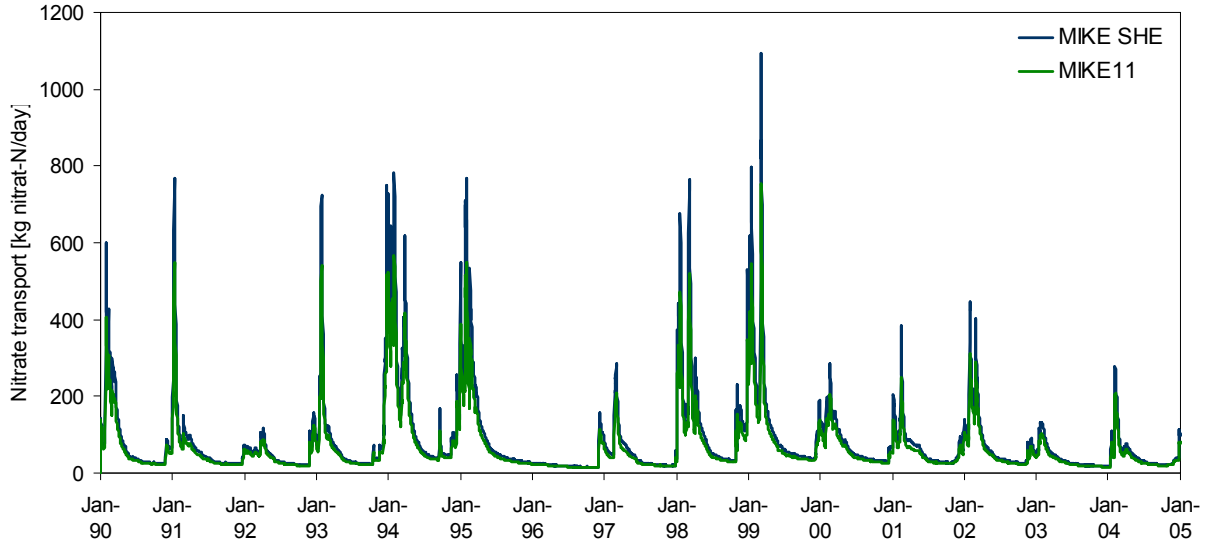

Figure 11.10 Comparison of daily nitrate transport from MIKE SHE to MIKE11 for the whole model area and the total nitrate transport in MIKE 11 at all downstream river end points

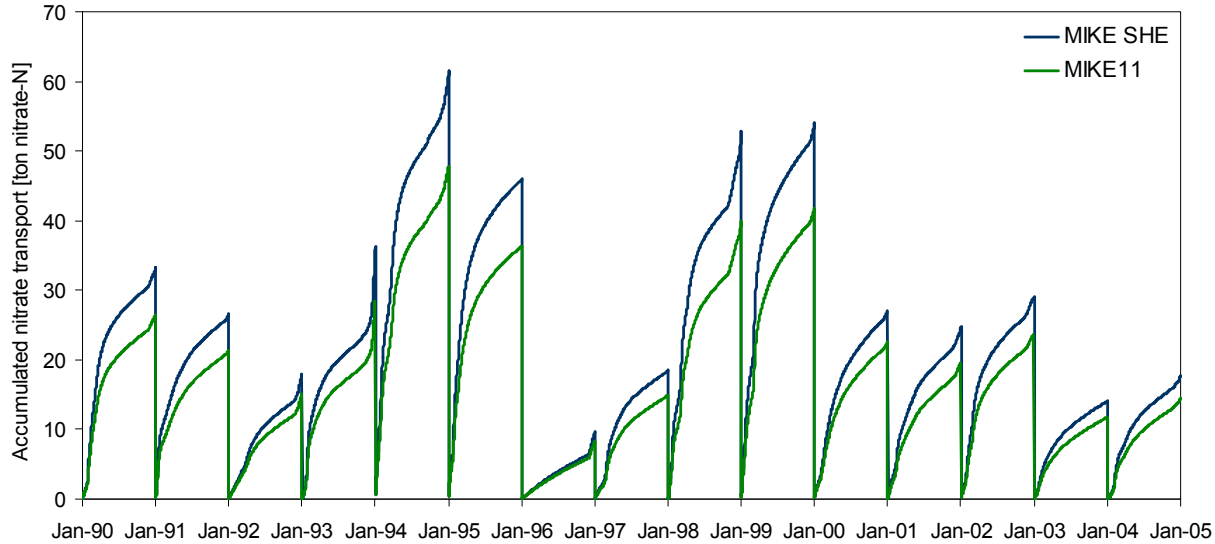

Figure 11.11 Comparison of yearly accumulated nitrate transport from MIKE SHE to MIKE11 for the whole model area and the yearly accumulated nitrate transport in MIKE 11 at all downstream river end points

11.3 Choice of hydrological model

During the calibration of the hydrological model two different models C5 and C5.1 were found to perform well, but it was chosen to proceed with C5.1 for the nitrate simulations. The only difference between C5 and C5.1 is the hydraulic conductivities in the Eem-Weichsel IS layer which are an order of magnitude higher in C5.1. Although this changes the flow pattern in the catchment, as mentioned in section 7.2.4, and the calibration results show that C5 simulates a higher average discharge at the upstream station than C5.1. A short analysis of the difference between these two hydrological models and the effects on the nitrate simulations is given below.

The flow pattern for the two hydrological models is analyzed using particle tracking by placing initially 10 particles in each cell in the top layer (NB this analysis is performed for the refined model). The particles are tracked and registered using the computational layers as registration zones, which means that particles are registered each time they cross into a computational layer. The maximum registration zone, i.e. the deepest computational layer that is reached, is seen for each grid cell in the two hydrological models on figures 11.12 and 11.13. When comparing these results for the upstream part of the LOOP4 catchment, it is seen that water in C5 mainly flows in the upper 6 layers, whereas for C5.1 particles in some areas, flow into the lower-lying Eem-Weichsel IS layer (layer 7). This indicates that increasing the conductivities of the Eem-Weichsel IS allows water to flow deeper into the model which result in less water being discharged to the upper part of Lillebæk and hence a smaller discharge at the upstream station in C5.1. When analyzing the water balances for LOO4, the main differences in water fluxes between the two models is that groundwater inflow and outflow is 40% less in C5 than in C5.1, drain flow to Lillebæk is 10% less whereas overland flow is 80% larger.

It is tested how the different flow pattern in the hydrological model C5 affects the simulated nitrate transport. The dispersivity values which are calibrated for C5.1 are used for C5 as well to make the results comparable. The results are seen in figures 11.14 and 11.15 and it is noted that the hydrological model C5 results in higher nitrate transport and concentrations in Lillebæk. When analyzing the mass balance it is seen that the reduction of nitrate in the saturated zone is more than 20% lower when using the flow model C5.

These results show the conductivities of the Eem-Weichsel IS layer is very important for the flow pattern in the catchment and that the lower conductivity in C5 results in a shallower water flow and thus in less nitrate being transported below the redox-interface. The choice of the best performing hydrological model is to some degree a subjective choice and it is seen that this choice does effect the nitrate simulations.

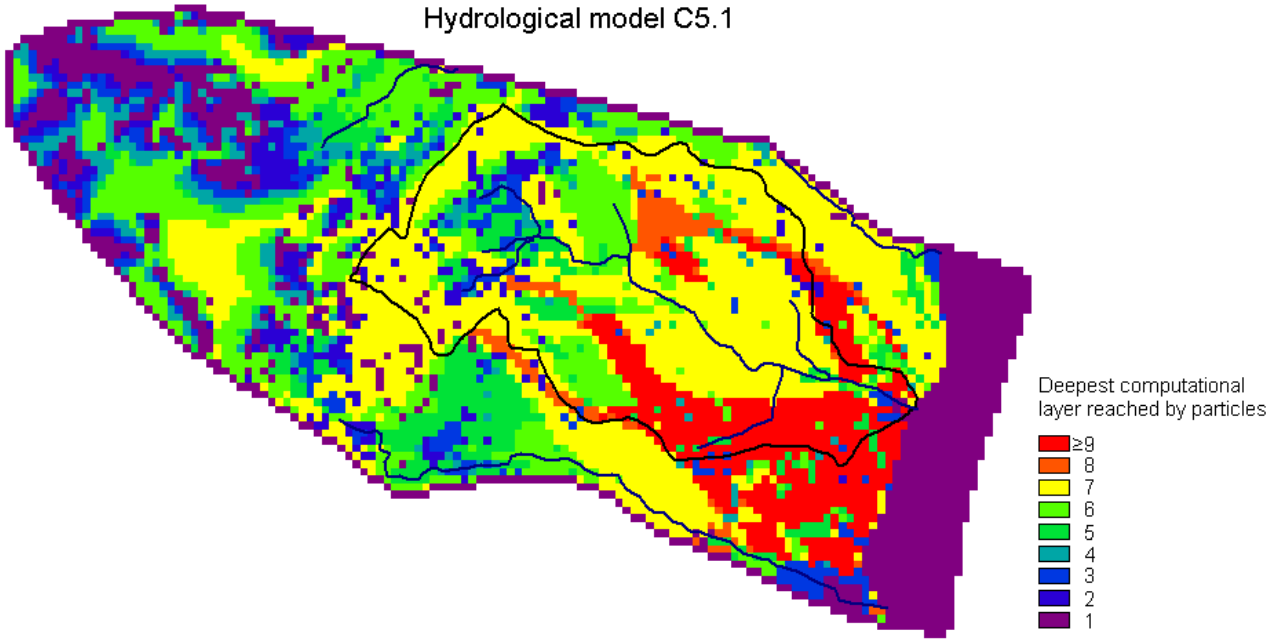

Figure 11.12 Deepest computational layer reached by particles initially placed in the top layer of the model. The result is based on particle tracking using the hydrological model C5.1 i.e. the flow model that is used in the study

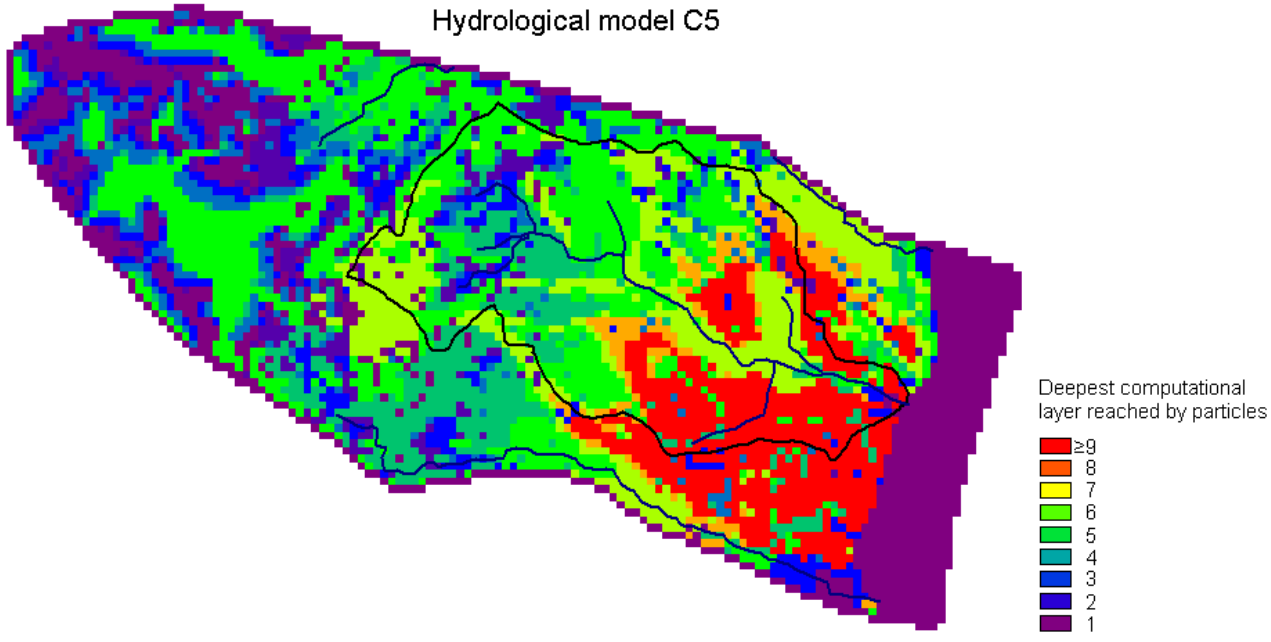

Figure 11.13 Deepest computational layer reached by particles initially placed in the top layer of the model. The result is based on particle tracking using the hydrological model C5 i.e. the flow model that is not chosen in the calibration

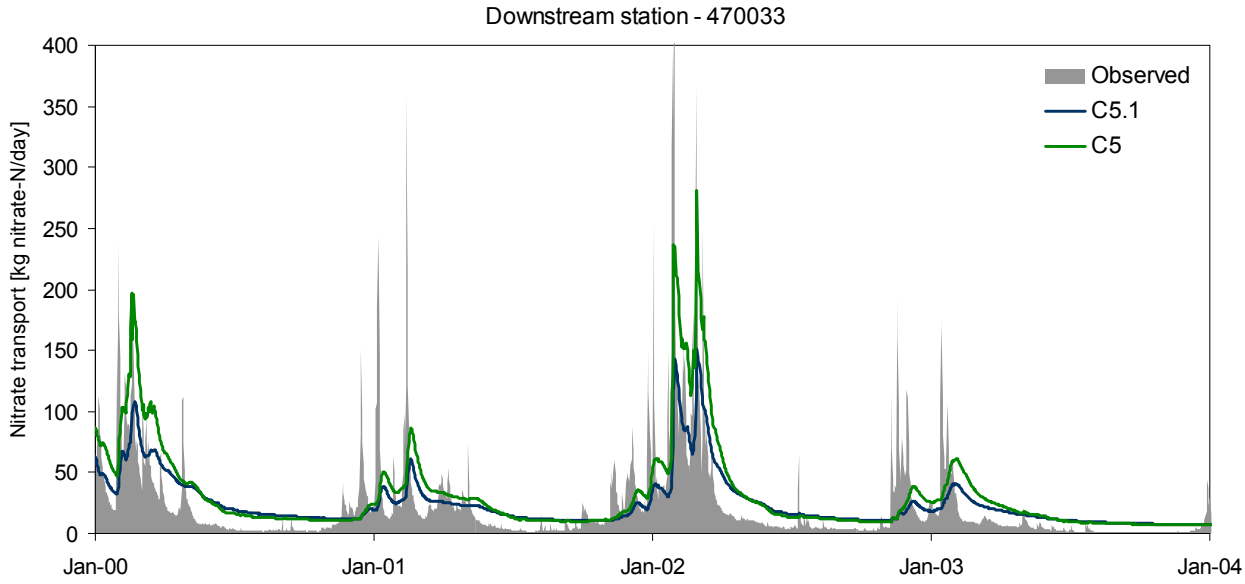

Figure 11.14 Comparison of simulated nitrate transport at downstream station using different hydrological models

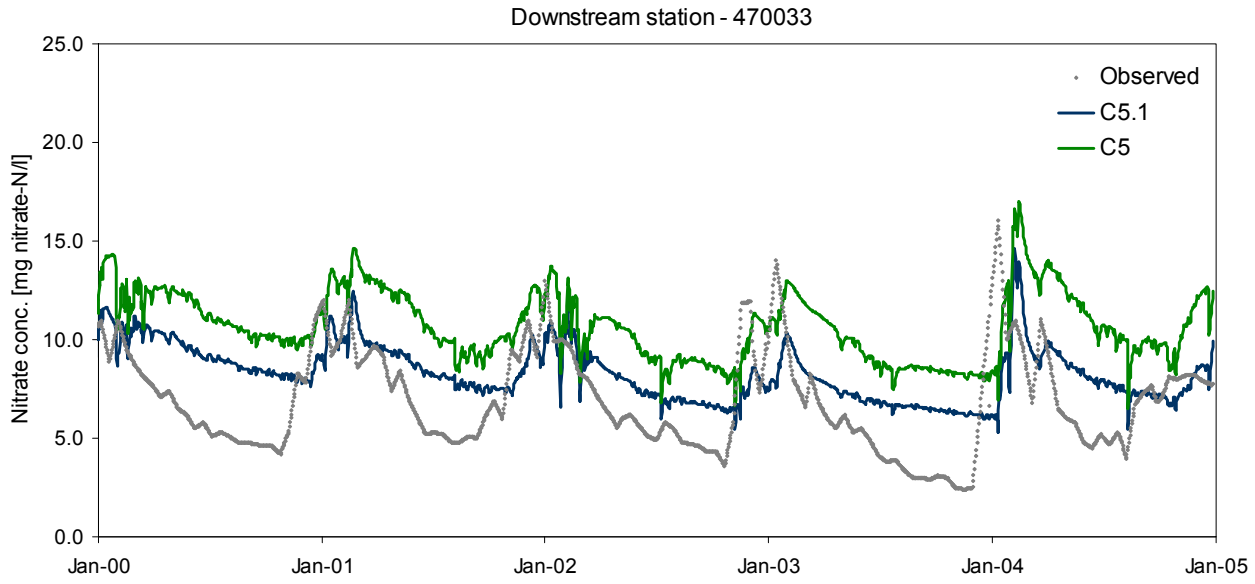

Figure 11.15 Comparison of simulated nitrate concentrations at downstream station using different hydrological models

11.4 Predictive capability of the model

The main advance with physically based models is their potentially predictive capabilities, although the big question is at what spatial and temporal scale this is?

The total yearly discharge and nitrate transport is generally found to be simulated acceptably at the down-stream station, but the model is seen to have problems with inter-annual dynamics. The model is seen to reproduce observations less well at the upstream station and not at all at scales as small as the drain areas. The evaluation of the model performance at different scale hence indicates that when scale decreases uncertainty on the model output increases. However, the minimum scale at which the model has predicttive capabilities (Representative Elementary Scale (RES)) has not been assessed in this study.

The model is believed to simulated overall water and nitrate balances acceptable at catchment scale and the predictable capability of the model is therefore believed to be limited to evaluating overall yearly balances for the Lillebæk catchment as a whole. The Daisy/MIKE SHE approach has, possibly, predictability capabilities for conditions other than the conditions it is calibrated for as both models are physically based (Hansen, 2006). This means that the model in theory should be applicable for scenario simulations. Though, this has not been performed in this study and the performance of the model should be improved before it makes sense to do so.

11.5 Evaluation of current status in nitrate modeling

Based on this study, as well as the modelling studies referred to in section 2.3.2, the current status in nitrate modelling is found to be that overall balances of water and nitrate are simulated satisfactorily on catchment scale, but uncertainties on the simulation results increases with decreasing spatial and temporal scale. The current status is accordingly that, at present, nitrate transport cannot be simulated satisfactory on a small enough scale to be able to point out sensitive versus robust areas with a large enough certainty. As a consequence a differentiated approach in relation to lowering of nitrate loss from cultivated areas cannot be implemented at present.

The problems concerning the current nitrate modelling results arises from uncertainties on and lack of heterogeneity in model parameters as well as limitations in the combined Daisy/MIKE SHE modelling approach. Lack of heterogeneity in soil physical parameters and agricultural practice is especially influencing the Daisy predicted percolation and nitrate leaching, whereas the MIKE SHE simulations are influenced by uncertainty on and lack of heterogeneity in geology as well as by the great uncertainty on the location of the redox-interface. The limitations on the current Daisy/MIKE SHE modelling approach is not only due to the lack of full coupling between Daisy and MIKE SHE, but also due to mass conserving problems in MIKE11, which causes depletion of mass in the stream system. The missing feedback from the saturated zone to the root zone results in the lower boundary in Daisy, which has great influence on the simulation results, being inconsistent with the groundwater table simulated with MIKE SHE. Furthermore drainage is included in both Daisy and MIKE SHE which conceptually is wrong and the implementation of drain flow from Daisy into MIKE SHE results in a delay of stream discharge.

12. Conclusions and future perspectives

Net percolation constitutes the main component of water inflow to the LOOP4 catchment and is, on average, 273 mm/year. Groundwater inflow along the south-western catchment boundary is, however, also found to be an important inflow component in the water balance. Discharge to Lillebæk constitutes 68% of the total outflow from the catchment and is thus the largest outflow component in the water balance. The average yearly discharge to Lillebæk is estimated to 231 mm, which is slightly underestimated when comparing with the observed average yearly discharge at the downstream station. During low flow periods, however, the model has problems with overestimation of flow, which is believed to be due the general overestimation of hydraulic heads. The discharge to Lillebæk originates mainly from drain flow, which accounts for 93% of the total discharge.

Nitrate leaching from the root zone is the only input component in the nitrate balance for the model area and is, on average, 88.4 ton/year. However, around 9% of this mass is withdrawn again from the saturated zone in periods of upward flux. The single most important output component in the nitrate mass balance is reduction of nitrate in the saturated zone. On average 47 ton/year, representing more than 50% of the nitrate leached from the root zone, is denitrified at the redox-interface. The total mass flux to the stream system is 31.3 ton/year representing 35% of the nitrate leaching. Around 50% of the total transport is transported to Lillebæk stream and the simulated average yearly transport to Lillebæk is thus 15 ton/year, which is 36% higher than the observed yearly transport at the downstream station of 11 ton/year. However, the observed transport is believed to be subject to rather larger uncertainty and the overestimation of transport is thus believed to be within an acceptable within an acceptable range. One of the reasons for overestimation of nitrate transport to Lillebæk is believed to be underestimation of reduction in the saturated zone.

Simulated groundwater concentrations in the model are higher than observed, however within a reasonable range. In the upper part of the model simulated groundwater concentrations are above the 50 mg nitrate-NO_3^-/l drinking water standard but, deeper in the model, where groundwater abstraction in the area is taking place, nitrate concentrations are below the drinking water standard.

The response time in the Lillebæk catchment is based on a nitrate pulse simulation found to be around 7-10 years. A change in agricultural practice in the area can therefore, theoretically, be expected to break through in observed nitrate transport to the stream system within this time frame, if not overshadowed by climatic variations.

Sensitive areas, where water is flowing directly to the stream without crossing the redox-interface, are mainly found close to the Lillebæk stream and in the downstream part of the LOOP4 catchment. The delineation of sensitive and robust areas is, however, subject to uncertainty due to the very sparse knowledge and therefore great uncertainty on the location of the redox-interface.

The main conclusion of this study is that overall balances of water and nitrate are simulated satisfactorily on catchment scale. However, the model has problems with simulating daily dynamics as well as predicting flow and transport on smaller scales. The model is therefore believed capable of simulating overall yearly balances on catchment scale, but the uncertainty on simulation results increases with decreasing spatial and temporal scale. The simulation problems is caused by lack of calibration data for the aquifers, uncertainty on the geological model and lack of heterogeneity in the hydrostratigraphical units, great uncertainty on the location of the redox-interface as well as limitations in the combined Daisy/MIKE SHE modelling approach. The limitations on the current Daisy/MIKE SHE modelling approach consist of lack of full coupling between Daisy and MIKE SHE and mass conservation problems in MIKE11.

The work on modelling of transport and fate of nitrate in Lillebæk catchment is going to be continued in the NICA project and the future perspectives of this work are as follows: The geological model should be updated when the geophysical SkyTEM data has been produced and the hydrological model should be recalibrated using the inverse calibration technique PEST. The location of the redox-interface is, at present, investigated in new boreholes in Lillebæk catchment and this data should be included in a new analysis of the redox-interface. The implementation of the redox-interface in the model should also be worked on. Furthermore the denitrification concept should be reviewed and expanded to included reduction in wetlands, stream sediments and anaerobic zones above the redox-interface. Finally the limitations in the modelling approach must be resolved. Work on this is already in progress as a coupling of Daisy and MIKE SHE is to be made in the NICA project, however the problem concerning mass depletion in MIKE11 must also be resolved.

13. References

Alectia (2008): *Oplandsmodel for landovervågningsopland 1 - Opstilling og kalibrering af model*. Subreport, 15th September 2008, unpuplished

Alectia (2009): *Oplandsmodel for landovervågningsopland 1 - Beregning af nitratomsætning i oplandet*. Subreport, 30th April 2009, unpuplished

Alectia (2010a): *Oplandsmodel for landovervågningsopland 6 - Fase 2: Opstilling og kalibrering af model*. Subreport, 14th July 2010, unpuplished

Alectia (2010b): *Oplandsmodel for landovervågningsopland 6 - Fase 3: Nitrattransport*. Subreport, 13th July 2010, unpuplished

Appelo, C.A.J. & Postma, D. (2005): *Geochemistry, groundwater and pollution (2.ed).* Balkema, Leiden, The Netherlands

ArcGIS (2007): *Hydrologically correct surfaces: Topo to Raster*. ArcGIS 9.2 Desktop Help >http://webhelp.esri.com/arcgisdesktop/9.2/index.cfm?TopicName=Hydrologically_correct_surfaces%3A_Topo_to_Raster< (25.07.2010)

Berthelsen, M. & Fenger, J. (Eds.) (2005): *Naturens kemi. Processer og påvirkning*. Gyldendal, Copenhagen, Denmark

DHI (2009a): *MIKE 11 – A modelling system for rivers and channels. Reference manual.* DHI, Denmark

DHI (2009b): *MIKE SHE user manual – Volume 1: User guide.* DHI, Denmark

DHI (2009c): *MIKE SHE user manual – Volume 2: Reference guide.* DHI, Denmark

Ernstsen, V., Henriksen, H.J., Platen, F.von. (2001): *Principper for beregning af nitratreduktion i jordlagene under rodzonen*. Danish Ministry of the Environment, Environmental Protection Agency, report no. 24

Ernstsen, V., Højberg, A.L., Jakobsen, P.R., von Platen, F., Tougaard, L., Hansen, J.R., Blicher-Mathiasen, G., Bøgestrand, J. & Børgesen, C.D. (2006): *Beregning af nitrat-reduktionsfaktorer for zonen mellem rodzonen of frem til vandløbet. Data og metode for 1. generationskortet*. Geological Survey of Denmark and Greenland, report 2006/93

Ernstsen, V. & Mørup, S. (1992): *Nitrate reduction in clayey till by Fe(II) in clay minerals*. In: Hyperfine Interactions, vol. 70, 1992, pp. 1001-1004

Fitts, C.R. (2002): *Groundwater Science*. Academic Press

Gelhar, L.W., Welty, C. & Rehfeldt, K.R. (1992): *A Critical Review of Data on Field-Scale Dispersion in Aquifers*. In: Water Resources Research, vol. 28, no. 7, pp. 1955-1974

Grant, R., Blicher-Mathiesen, G., Pedersen, L. E., Jensen, P. G., Madsen, I., Hansen, B., Brüsch, W. & Thorling, L. (2007): *Landovervågningsoplande 2006. NOVANA*. National Environmental Research Institute, Aarhus University, report nr. 640.

Grapes, T.R., Bradley, C. & Petts, G.E. (2005): *Dynamics of river-aquifer interactions along a chalk stream: The River Lambourn, UK.* In: Hydrological Processes, vol. 19, 2005, pp. 2035-2053

Graversen, P. & Nyegaard, P. (1989): *Hydrogeologisk kortlægning Lillebæk - Vandmiljøplanens overvågningsprogram Landovervågningsoplande LOOP4*. Geological Survey of Denmark

Griffiths, J., Binley, A., Crook, N., Nutter, J., Young,A. & Fletcher, S. (2006): *Stream flow generation in the Pang and Lambourn catchments, Berkshire, UK.* In: Journal of Hydrology, vol. 330, 2006, pp. 71-83

Hansen, J.R. (2006): *Nitrate modelling at catchment scale.* Geological Survey of Denmark and Greenland, report 2006/69, Ph.D. thesis

Hansen, J.R., Ernstsen, V., Refsgaard, J.C. & Hansen, S. (2008): *Field scale heterogeneity of redox conditions in till – Upscaling to a catchment nitrate model.* In: Hydrogeology Journal (2008) 16, pp. 1251-1266

Hansen, J.R. & Rasmussen, P. (2006): *Modellering af vand og stoftransport i mættet zone i landovervågningsoplandet Odderbæk (LOOP2). Delrapport 1 – beskrivelse af modelopsætning*. Geological Survey of Denmark and Greenland, unpuplished

Hansen, J.R., Rasmussen, P. & Christensen, B.S.B. (2006): *Modellering af vand og nitrat i mættet zone og vandløb i landovervågningsoplandet Odderbæk (LOOP2). Slutrapport*. Geological survey of Denmark and Greenland, unpuplished

Hansen, J.R., Refsgaard, J.C., Hansen, S. & Ernstsen, V. (2007): *Problems with heterogeneity in physically based agricultural catchment models.* In: Journal of Hydrology, vol. 342, issue 1-2, 2007, pp. 1-16

Hansen, J.R., Refsgaard, J.C., Ernstsen, V., Hansen, S., Styczen, M. & Poulsen, R.N. (2009) An intergrated and physically based nitrogen cycle catchment model. In: Hydrology Research, vol. 40.4, 2009, pp. 347 - 363

Hansen, S. (2000): *Daisy, a flexible Soil-Plant-Atmosphere system model – Equation section 1*. Department of Agricultural Science, The Royal Veterinary- and Agricultural University

Hasholt, B. (2004): *Kompendium i hydrologi*. Department of Geography, University of Copenhagen

Healy, R.W., Winter, T.C., LaBaugh, J.W. & Franke, O.L. (2007): *Water budgets: Foundations for effective water-resources and environmental management.* U.S. Geological Survey, Circular 1308, Reston, Virginia

Henriksen, H.J., Nyegaard, P., Ernstsen, V., Troldborg, L. & Refsgaard, J.C.(n.y.): *Betydningen af grundvandets strømningsveje, opholdstider og nitratreduktionskapacitet for kvælstofsbelastningen af vandmiljøet*. Geological Survey of Denmark and Greenland >http://www.vandmodel.dk/index.htm#notat2003< (10.06.2010)

Højbjerg, A.L., Trolborg, L., Nyegaard, P, Ondracek, M., Stisen, S., Chrostensen, B.S.B. & Nørgaard, A. (2008): *National Vandressource Model. Sjælland, Lolland, Falster og Møn – Opdatering januar 2008.* Geological survey of Denmark and Greenland, report 2008/65

Jensen, K.H. (2004): *Soil physical processes*. Department of Geology, University of Copenhagen

Jørgensen, F., Kristensen, M., Højberg, A.L., Klint, K.E.S., Hansen, C., Jordt, B.E., Richardt, N. & Sandersen, P. (2008): *Opstilling af geologiske modeller til grundvandsmodellering. Geo-vejledning 3.* Geological Survey of Denmark and Greenland

Kjær K. H., Houmark-Nielsen M. & Richardt N., (2003): *Ice-flow patterns and dispersal of erratics at the southwestern margin of the last Scandinavian Ice Sheet: signature of paleo-ice Streams*. In: Boreas, 2003 vol. 32, pp. 130-148

National Board of Health (n.y.): *Nitrat i drikkevandet* >http://www.sst.dk/Sundhed%20og%20forebyggelse/Miljoe%20og%20helbred/Vand/Drikkevand/Nitrat_i_drikkevand.aspx< (18.09.2010)

Nielsen, K., Styczen, M., Andersen, H.E., Dahl-Madsen, K.I., Refsgaard, J.C., Pedersen, S.E, Hansen, J.R, Larsen, S.E., Poulsen, R.N., Kronvang, B., Børgesen, C.D., Stjernholm, M., Vilholth, K., Krogsgaard, J., Ernstsen, V., Jørgensen, O., Windolf, J., Friis-Christensen, A., Uhrenholdt, T., Jensen, M.H., Hansen, I.S. & Wiggers, L. (2004): *Odense Fjord – Scenarier for reduction af nærigsstoffer*. National Environmental Research Institute, report nr. 485

Mayhew, S. (2004): *Oxford Dictionary of Geography (3. ed).* Oxford University Press, Oxford

Pedersen, L.E., Blicher-Mathiesen, G., Mejlhede, P. & Grant, R. (2010): *Oplandsmodellering af vand og kvælstof i umættet zone for oplandet til Lillebæk.* National Environmental Research Institute, University of Aarhus, Aarhus University, report no. 756.

Petersen, K.S., Rasmussen, L.A. & Hamberg, L. (1988): *Geologisk jordartskort Lillebæk - Vandmiljøplanens overvågningsprogram Landovervågningsopland LOOP4.* Geological Survey of Denmark

Postma, D., Boesen, C., Kristiansen, H. & Larsen, F. (1991): *Nitrate reduction in an unconfied sandy aquifer – Water chemistry, reduction processes and geochemical modeling.* In: Water Resources Research, vol. 27, pp. 2027-2045

Rasmussen, P. (1996): *Monitoring shallow groundwater quality in agricultural watersheds in Denmark.* In: Environmental Geology (1996) 27, pp. 309-319.

Refsgaard, J.C., Kern-Hansen, C., Plauborg, F., Ovesen, N.B. & Rasmussen, P. (2003): *Ferskvandets kredsløb og tidslige variationer.* In: Ferskvandets Kredsløb, NOVA 2003 report, chap. 6

Refsgard, J.C., Thorsen, M., Jensen, J.B., Kleeschulte, S. & Hansen, S. (1999): *Large scale modelling of groundwater contamination from nitrate leaching*. In: Journal of Hydrology, vol. 122, 1999, pp. 117-140

Sonnenborg, T.O. & Henriksen, H.J. (Eds.) (2005) *Håndbog i grundvandsmodellering*. Geological Survey of Denmark and Greenland, report 2005/80

Styczen, M., Petersen, S., Kristensen, M. Jessen, O.Z., Rasmussen, D., Andersen & Sørensen, P.B. (2004): *Calibration of Models Describing Pesticide Fate and Transport in Lillebæk and Odder Bæk Catchment*. Ministry of Environment, Danish Protection Agency, Pesticides Research no. 62.

Styczen, M. & Storm, B. (1993a): *Modelling of N-movements on catchment scale – a tool for analysis and decision making. 1. Model description.* In: Fertilizer Research, vol. 36, 1993, pp.1-6

Styczen, M. & Storm, B. (1993b): *Modelling of N-movements on catchment scale – a tool for analysis and decision making. 2. A case study.* In: Fertilizer Research, vol. 36, 1993, pp.7-17

Appendix 1 Observed and simulated hydraulic head in Lillebæk catchment (LOOP4)

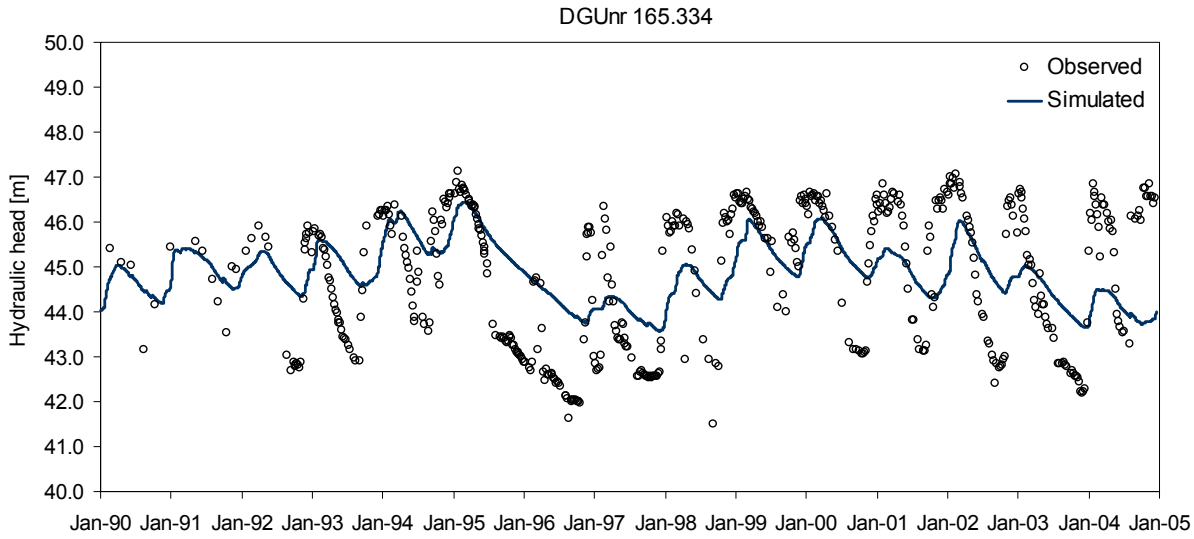

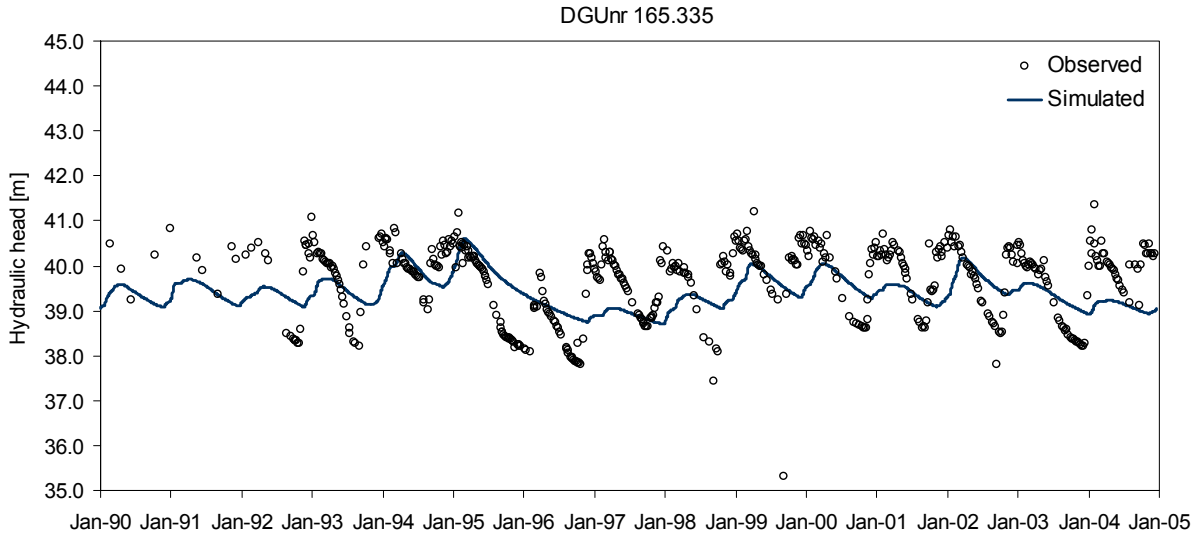

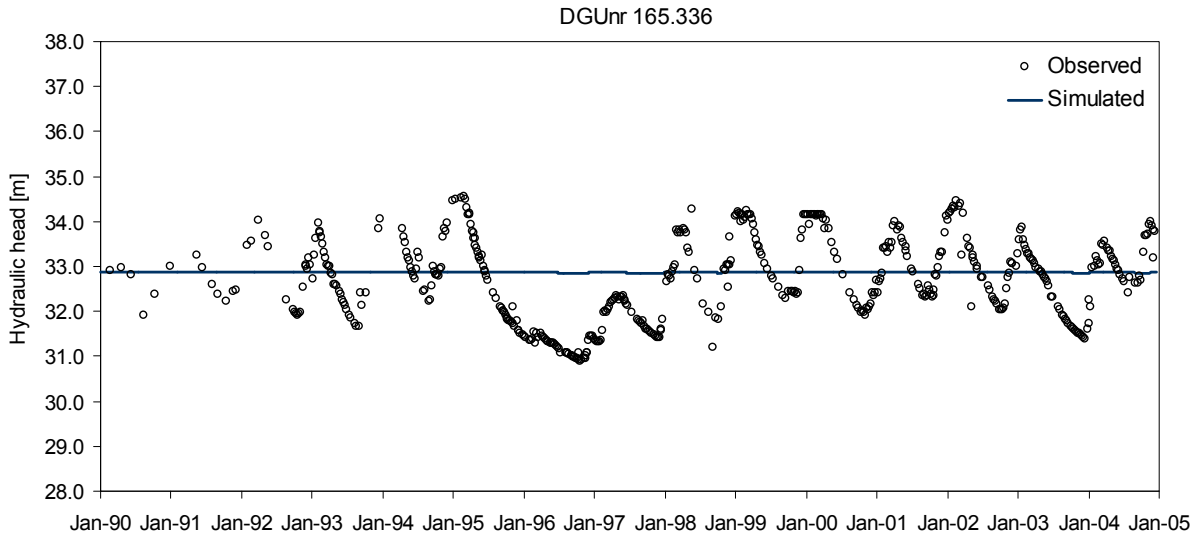

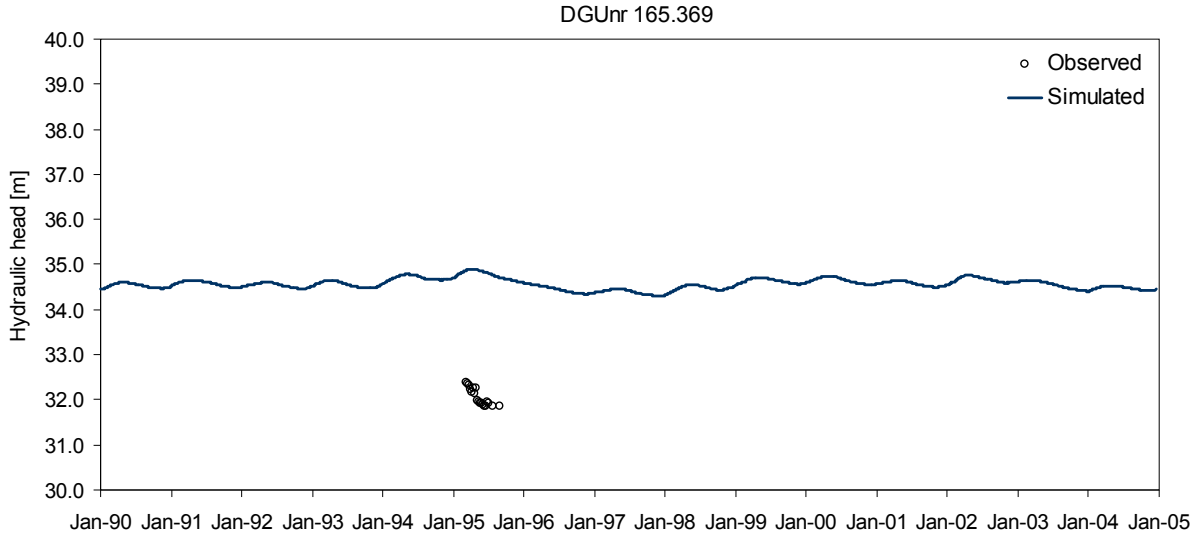
DGUnr 165.369
Observed
Simulated
Hydraulic head [m]
40.0
39.0
38.0
37.0
36.0
35.0
34.0
33.0
32.0
31.0
30.0
Jan-90 Jan-91 Jan-92 Jan-93 Jan-94 Jan-95 Jan-96 Jan-97 Jan-98 Jan-99 Jan-00 Jan-01 Jan-02 Jan-03 Jan-04 Jan-05

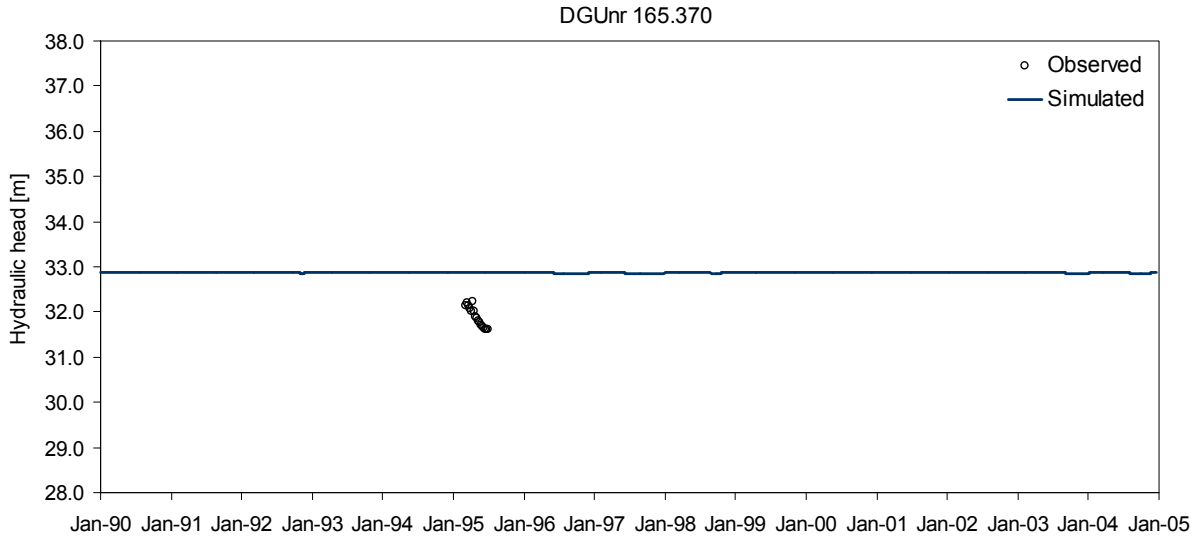
DGUnr 165.370
Observed
Simulated
Hydraulic head [m]
38.0
37.0
36.0
35.0
34.0
33.0
32.0
31.0
30.0
29.0
28.0
Jan-90 Jan-91 Jan-92 Jan-93 Jan-94 Jan-95 Jan-96 Jan-97 Jan-98 Jan-99 Jan-00 Jan-01 Jan-02 Jan-03 Jan-04 Jan-05

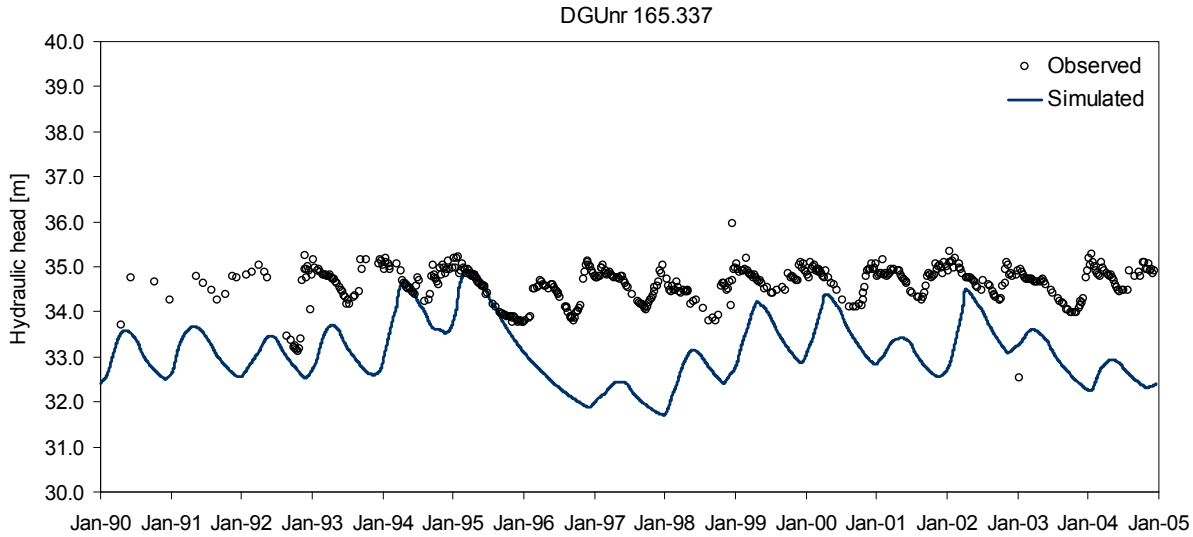
DGUnr 165.337
Observed
Simulated
Hydraulic head [m]
40.0
39.0
38.0
37.0
36.0
35.0
34.0
33.0
32.0
31.0
30.0
Jan-90 Jan-91 Jan-92 Jan-93 Jan-94 Jan-95 Jan-96 Jan-97 Jan-98 Jan-99 Jan-00 Jan-01 Jan-02 Jan-03 Jan-04 Jan-05

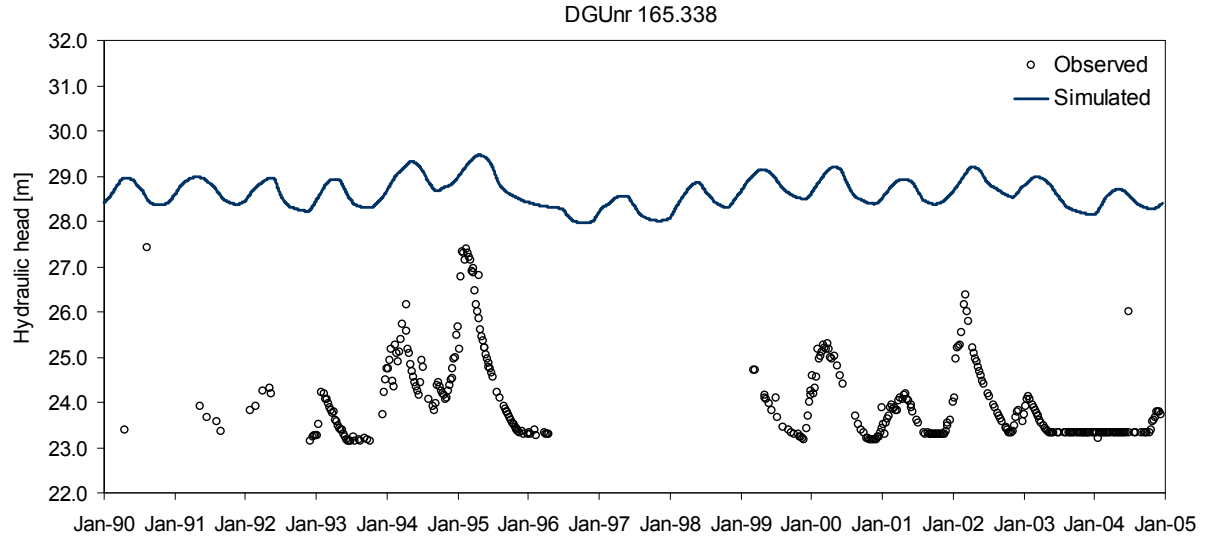
DGUnr 165.338
Observed
Simulated
Hydraulic head [m]
32.0
31.0
30.0
29.0
28.0
27.0
26.0
25.0
24.0
23.0
22.0
Jan-90 Jan-91 Jan-92 Jan-93 Jan-94 Jan-95 Jan-96 Jan-97 Jan-98 Jan-99 Jan-00 Jan-01 Jan-02 Jan-03 Jan-04 Jan-05

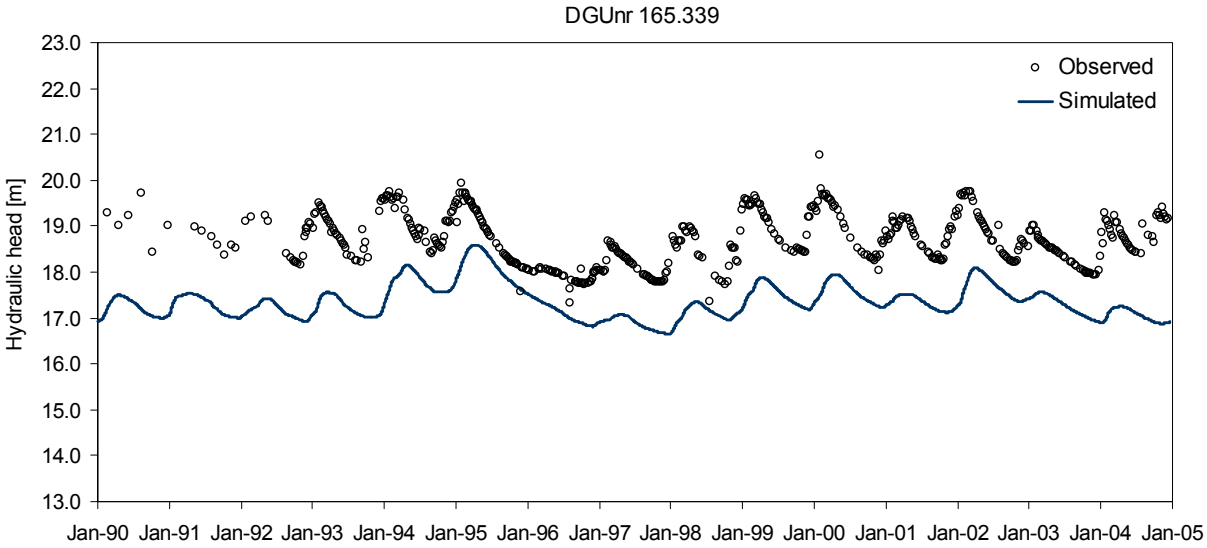
DGUnr 165.339
Observed
Simulated
Hydraulic head [m]
23.0
22.0
21.0
20.0
19.0
18.0
17.0
16.0
15.0
14.0
13.0
Jan-90 Jan-91 Jan-92 Jan-93 Jan-94 Jan-95 Jan-96 Jan-97 Jan-98 Jan-99 Jan-00 Jan-01 Jan-02 Jan-03 Jan-04 Jan-05

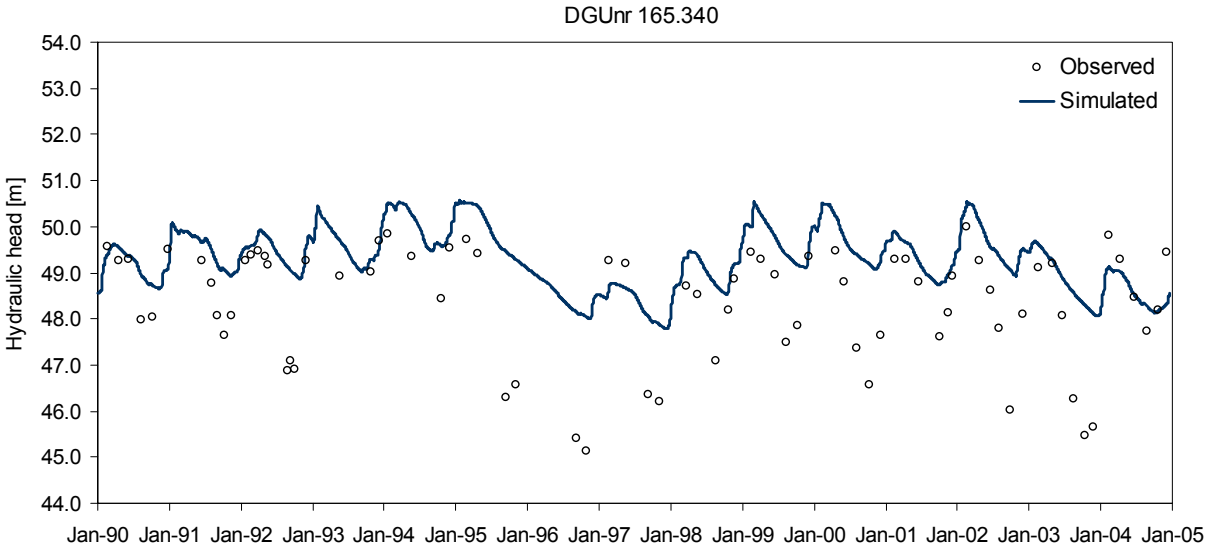
DGUnr 165.340
Observed
Simulated
Hydraulic head [m]
54.0
53.0
52.0
51.0
50.0
49.0
48.0
47.0
46.0
45.0
44.0
Jan-90 Jan-91 Jan-92 Jan-93 Jan-94 Jan-95 Jan-96 Jan-97 Jan-98 Jan-99 Jan-00 Jan-01 Jan-02 Jan-03 Jan-04 Jan-05

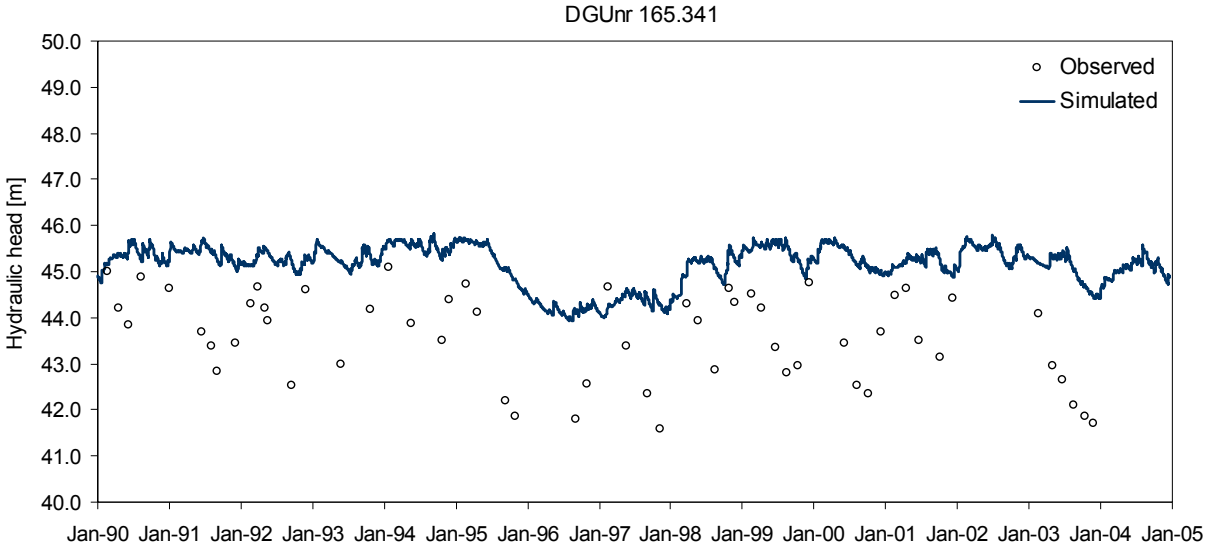
DGUnr 165.341
Observed
Simulated
Hydraulic head [m]
50.0
49.0
48.0
47.0
46.0
45.0
44.0
43.0
42.0
41.0
40.0
Jan-90 Jan-91 Jan-92 Jan-93 Jan-94 Jan-95 Jan-96 Jan-97 Jan-98 Jan-99 Jan-00 Jan-01 Jan-02 Jan-03 Jan-04 Jan-05

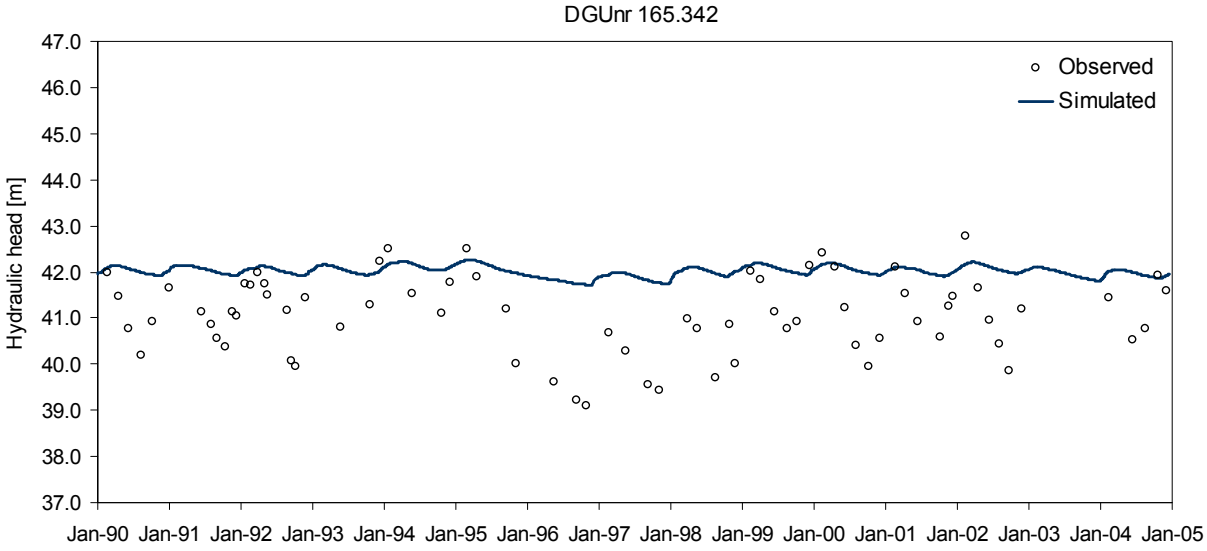
DGUnr 165.342
Observed
Simulated
Hydraulic head [m]
47.0
46.0
45.0
44.0
43.0
42.0
41.0
40.0
39.0
38.0
37.0
Jan-90 Jan-91 Jan-92 Jan-93 Jan-94 Jan-95 Jan-96 Jan-97 Jan-98 Jan-99 Jan-00 Jan-01 Jan-02 Jan-03 Jan-04 Jan-05

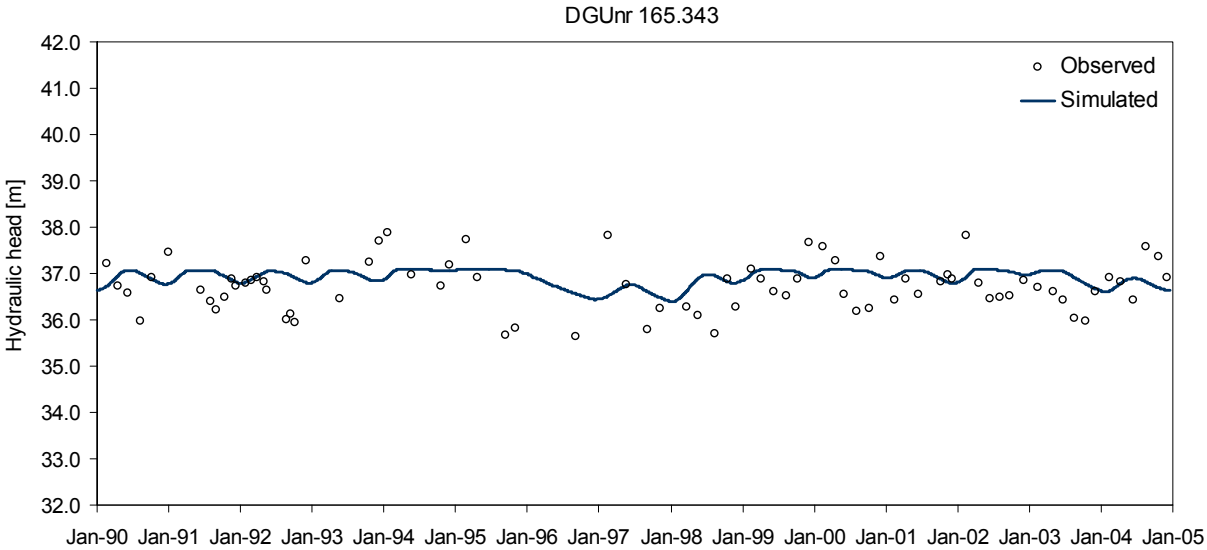
DGUnr 165.343
Observed
Simulated
Hydraulic head [m]
42.0
41.0
40.0
39.0
38.0
37.0
36.0
35.0
34.0
33.0
32.0
Jan-90 Jan-91 Jan-92 Jan-93 Jan-94 Jan-95 Jan-96 Jan-97 Jan-98 Jan-99 Jan-00 Jan-01 Jan-02 Jan-03 Jan-04 Jan-05

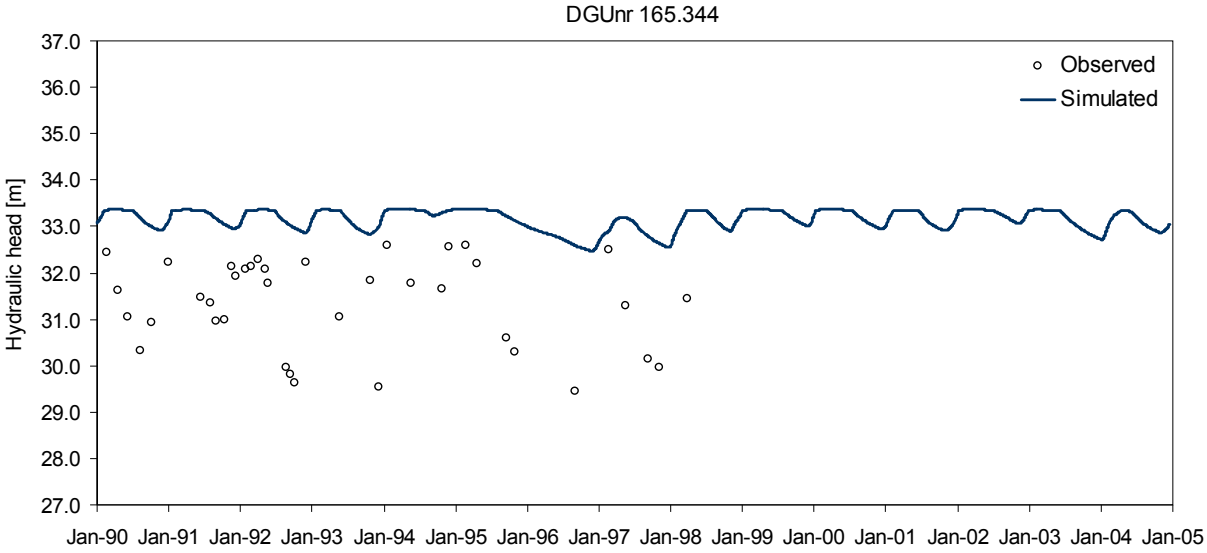
DGUnr 165.344
Observed
Simulated
Hydraulic head [m]
37.0
36.0
35.0
34.0
33.0
32.0
31.0
30.0
29.0
28.0
27.0
Jan-90 Jan-91 Jan-92 Jan-93 Jan-94 Jan-95 Jan-96 Jan-97 Jan-98 Jan-99 Jan-00 Jan-01 Jan-02 Jan-03 Jan-04 Jan-05

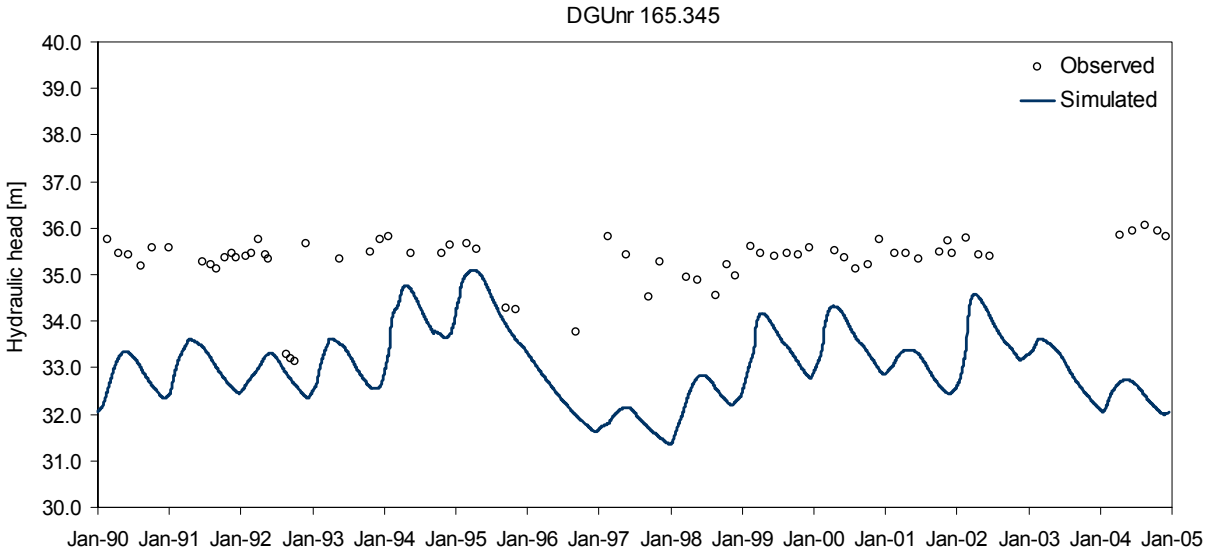
DGUnr 165.345
Observed
Simulated
Hydraulic head [m]
40.0
39.0
38.0
37.0
36.0
35.0
34.0
33.0
32.0
31.0
30.0
Jan-90 Jan-91 Jan-92 Jan-93 Jan-94 Jan-95 Jan-96 Jan-97 Jan-98 Jan-99 Jan-00 Jan-01 Jan-02 Jan-03 Jan-04 Jan-05

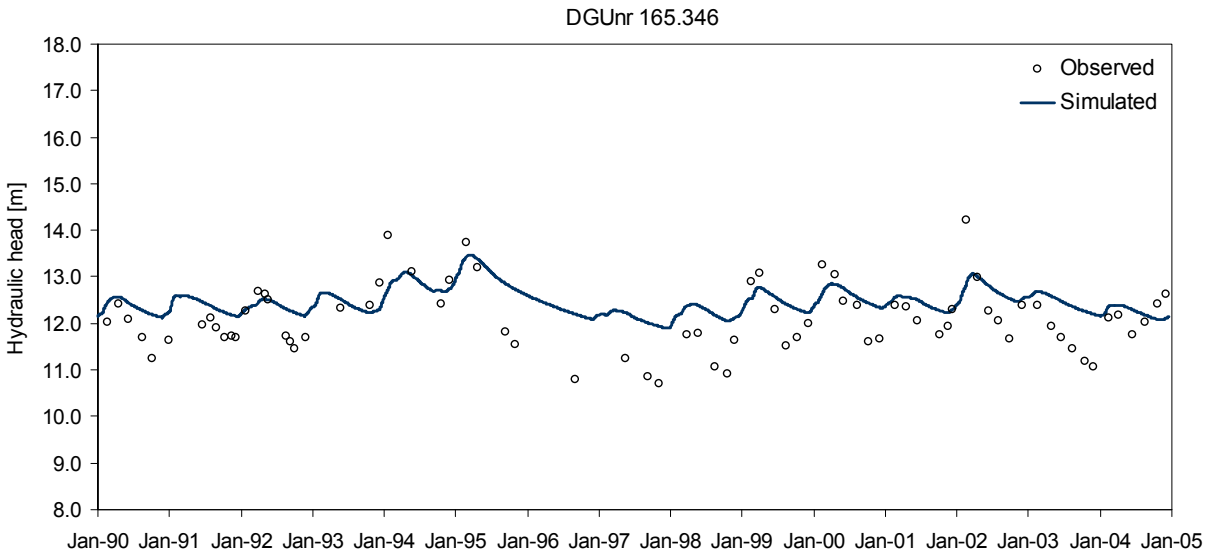
DGUnr 165.346
Observed
Simulated
Hydraulic head [m]
18.0
17.0
16.0
15.0
14.0
13.0
12.0
11.0
10.0
9.0
8.0
Jan-90 Jan-91 Jan-92 Jan-93 Jan-94 Jan-95 Jan-96 Jan-97 Jan-98 Jan-99 Jan-00 Jan-01 Jan-02 Jan-03 Jan-04 Jan-05

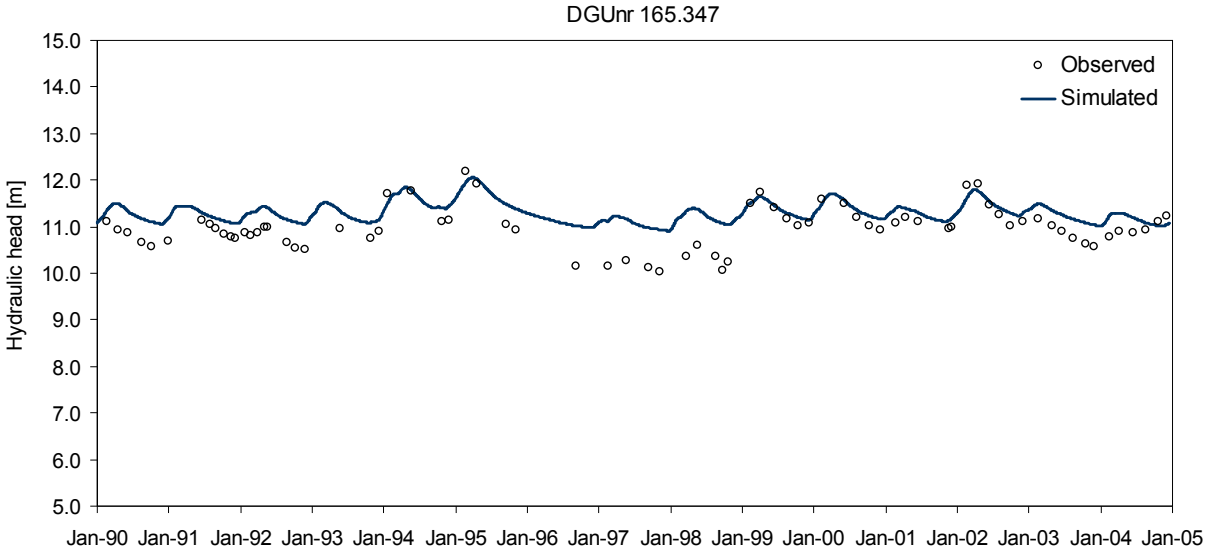
DGUnr 165.347
Observed
Simulated
Hydraulic head [m]
15.0
14.0
13.0
12.0
11.0
10.0
9.0
8.0
7.0
6.0
5.0
Jan-90 Jan-91 Jan-92 Jan-93 Jan-94 Jan-95 Jan-96 Jan-97 Jan-98 Jan-99 Jan-00 Jan-01 Jan-02 Jan-03 Jan-04 Jan-05

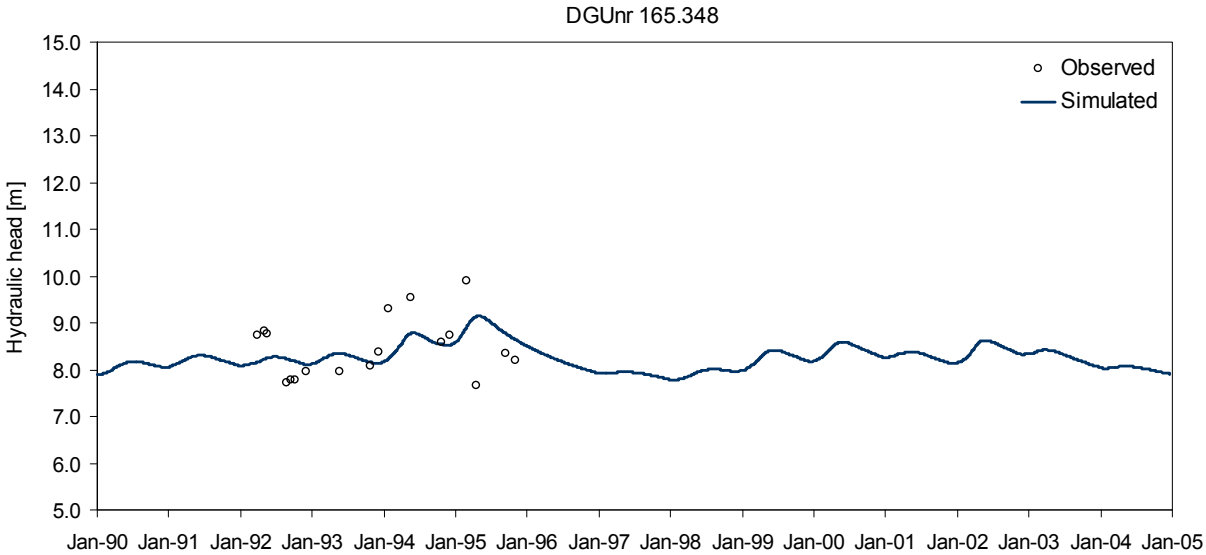
DGUnr 165.348
Observed
Simulated
Hydraulic head [m]
15.0
14.0
13.0
12.0
11.0
10.0
9.0
8.0
7.0
6.0
5.0
Jan-90 Jan-91 Jan-92 Jan-93 Jan-94 Jan-95 Jan-96 Jan-97 Jan-98 Jan-99 Jan-00 Jan-01 Jan-02 Jan-03 Jan-04 Jan-05

Appendix 2 Groundwater concentrations of nitrate in Lillebæk catchment (LOOP4)

Table A2.1 Data for groundwater observation wells and measurements of nitrate concentrations in the groundwater for the period 1989-2005

Location	DGU no.	Screen top [m.b.s.]	Screen bottom [m.b.s]	No. NO_3^- observations	Nitrate present
1	165. 295	1.2	1.5	2	+
	165. 296	3	3.3	46	+
	165. 297	5	5.3	62	+
	165. 298	1.2	1.5	4	+
	165. 299	3	3.3	35	+
	165. 300	5	5.3	78	+
2	165. 302	3	3.3	5	+
	165. 303	5	5.3	108	+
	165. 304	1.2	1.5	1	+
	165. 305	3	3.3	87	+
	165. 306	5	5.3	96	+
3	165. 307	1.2	1.5	3	+
	165. 308	3	3.3	90	+
	165. 309	5	5.3	29	+
	165. 310	1.2	1.5	1	+
	165. 311	3	3.3	8	+
	165. 312	5	5.3	116	+
4	165. 313	1.2	1.5	3	+
	165. 314	3	3.3	47	+
	165. 315	5	5.3	80	+
	165. 316	1.2	1.5	3	+
	165. 317	3	3.3	94	+
	165. 318	5	5.3	21	+
5	165. 319	1.2	1.5	1	+
	165. 320	3	3.3	8	+
	165. 321	5	5.3	71	+
	165. 322	1.2	1.5	9	+
	165. 323	3	3.3	33	+
	165. 324	5	5.3	2	+
6	165. 326	3	3.3	11	+
	165. 327	5	5.3	109	+
	165. 328	1.2	1.5	6	+
	165. 329	3	3.3	76	
	165. 330	5	5.3	99	

Table A2.1 continued

Location	DGU no.	Screen top [m.b.s.]	Screen bottom [m.b.s]	No. NO_3^- observations	Nitrate present
21	165. 268	1.2	1.5	2	+
	165. 270	5	5.3	40	+
22	165. 272	3	3.3	11	+
	165. 273	5	5.3	26	+
23	165. 274	1.2	1.5	1	+
	165. 275	3	3.3	39	+
	165. 276	5	5.3	66	+
24	165. 277	1.2	1.5	3	+
	165. 278	3	3.3	64	+
	165. 279	5	5.5	62	+
25	165. 281	3	3.3	34	+
	165. 282	5	5.3	30	
26	165. 283	1.2	1.5	6	+
	165. 284	3	3.3	11	+
	165. 285	5	5.3	86	
27	165. 286	1.2	1.5	1	+
	165. 287	5	5.3	40	+
	165. 288	7	7.3	77	+
28	165. 291	6.2	6.5	33	
29	165. 294	5	5.3	1	+
	165. 333 1	16.9	17	23	
	165. 333 2	15.9	16	24	
	165. 333 3	14.9	15	23	
	165. 333 4	13.9	14	26	
	165. 333 5	12.9	13	25	+
	165. 333 6	11.9	12	26	+
	165. 333 7	10.9	11	39	+
	165. 333 8	9.9	10	49	+
	165. 333 9	7.9	8	18	+
	165. 333 10	6.9	7	55	+
	165. 333 11	5.9	6	15	
	165. 333 12	4.9	5	18	+
	165. 333 13	3.9	4	15	+
	165. 333 14	2.9	3	17	+
	165. 333 15	1.9	2	16	+
	165. 159	18	30	8	
	165. 361	20	20	9	+

Appendix 3 Geological profiles from the geological model

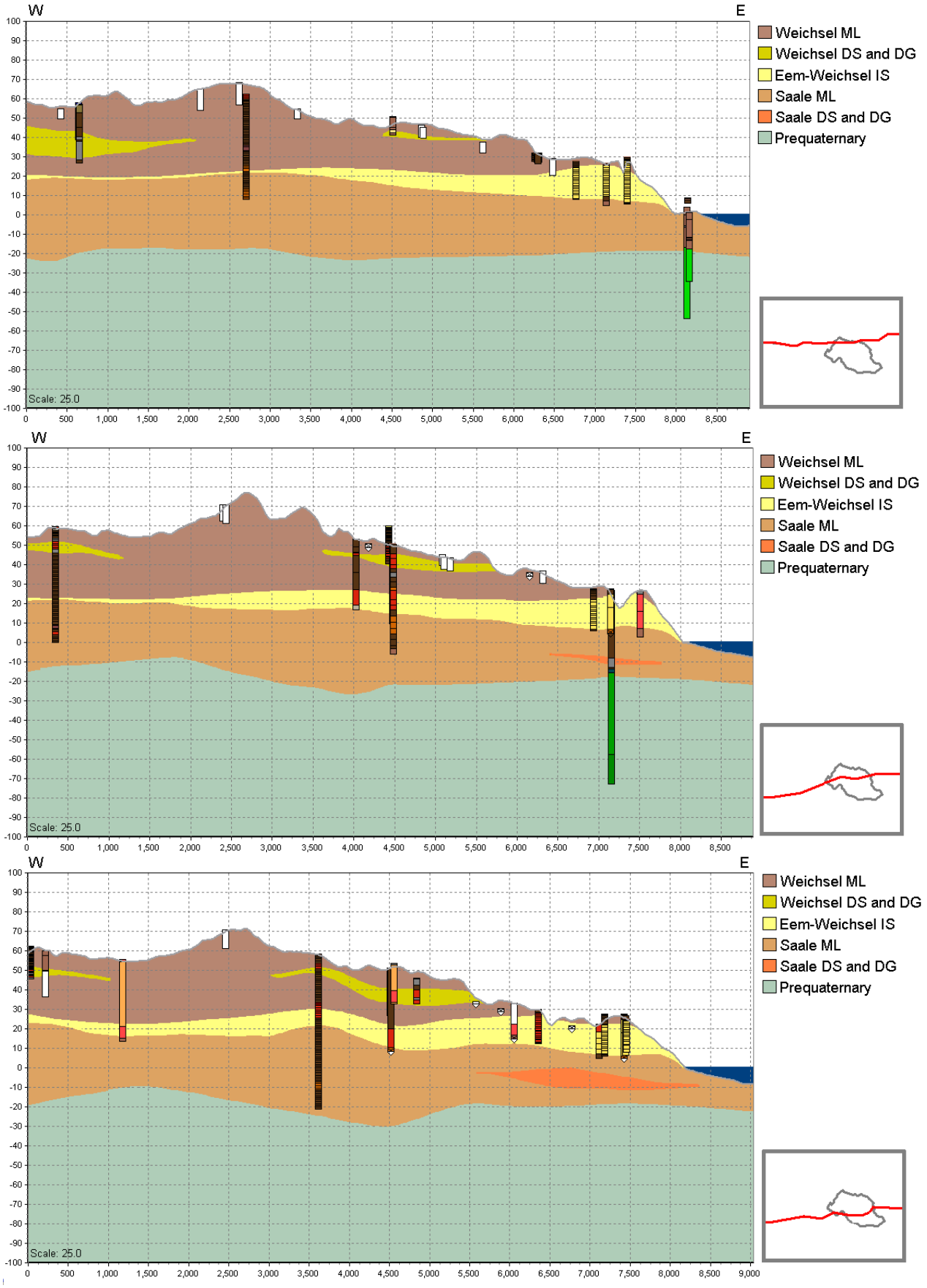

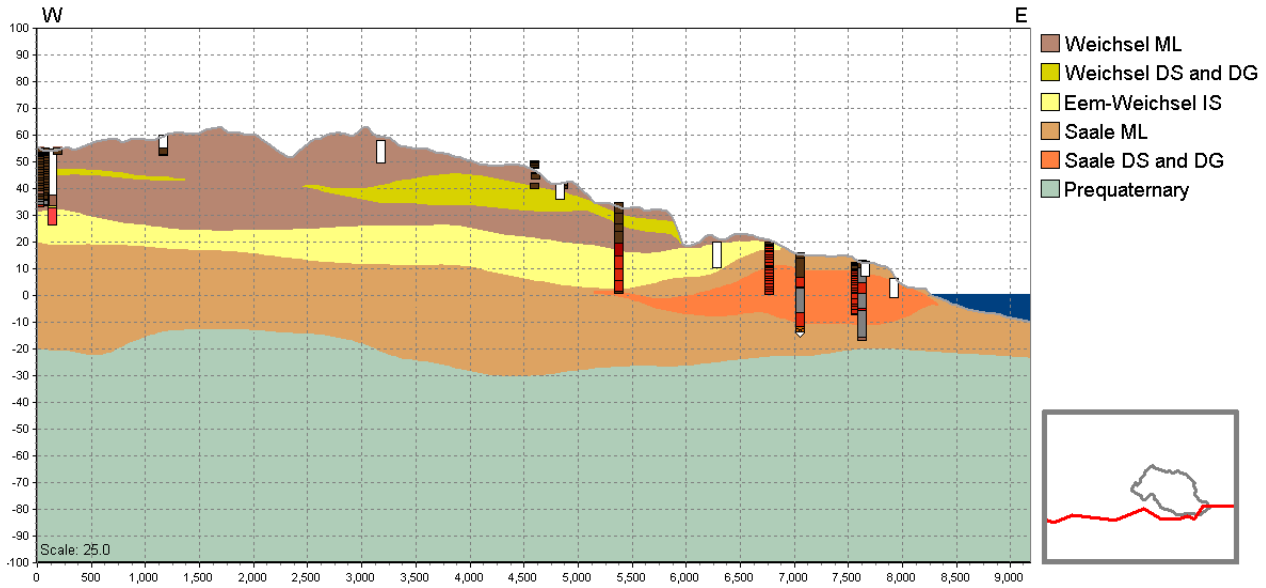
W
E
Weichsel ML
Weichsel DS and DG
Eem-Weichsel IS
Saale ML
Saale DS and DG
Prequaternary
Scale: 25.0

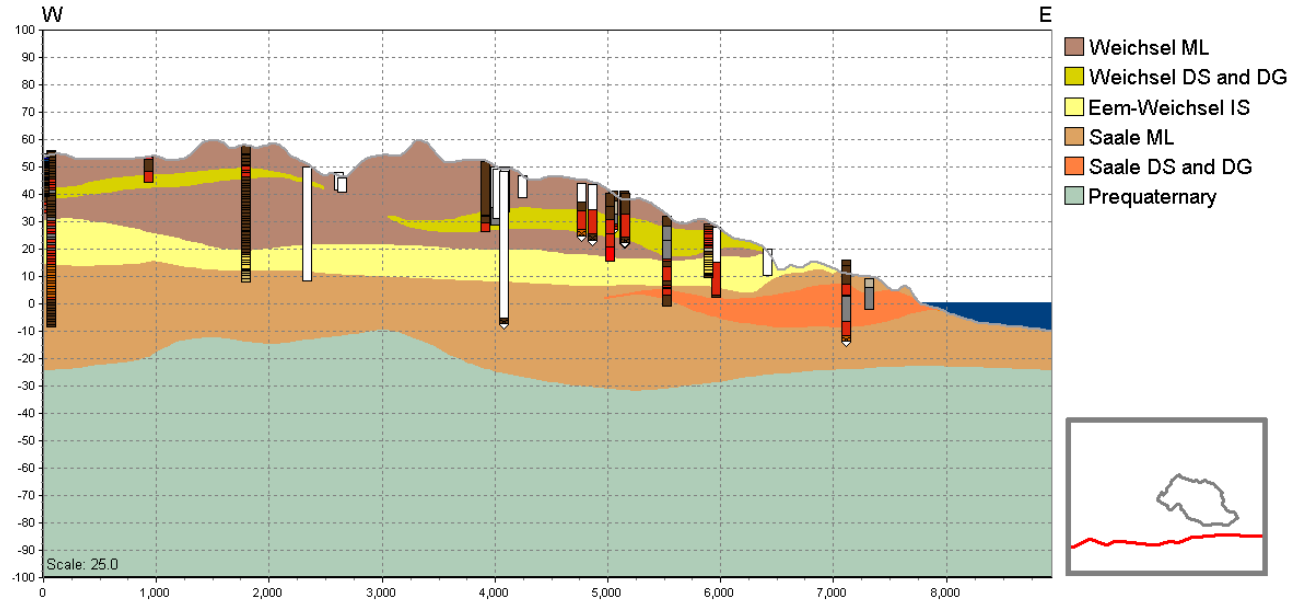
W
E
Weichsel ML
Weichsel DS and DG
Eem-Weichsel IS
Saale ML
Saale DS and DG
Prequaternary
Scale: 25.0

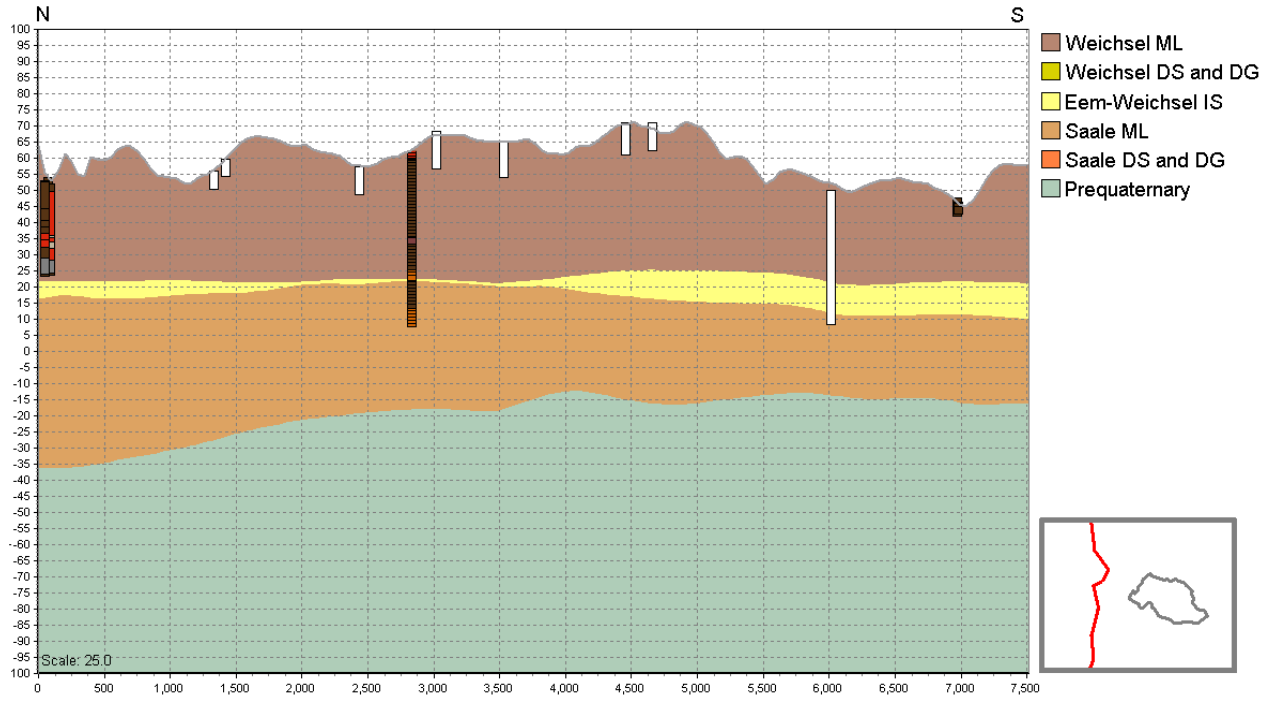
N
S
Weichsel ML
Weichsel DS and DG
Eem-Weichsel IS
Saale ML
Saale DS and DG
Prequaternary
Scale: 25.0

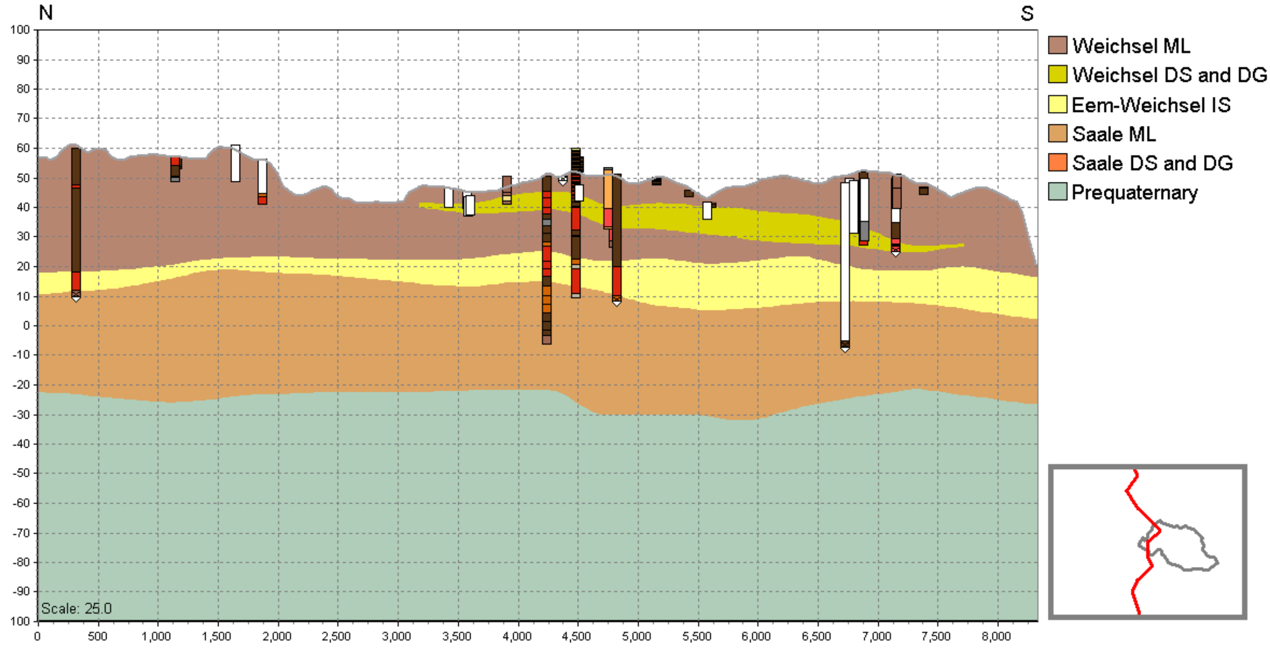
N
S
Weichsel ML
Weichsel DS and DG
Eem-Weichsel IS
Saale ML
Saale DS and DG
Prequaternary
Scale: 25.0

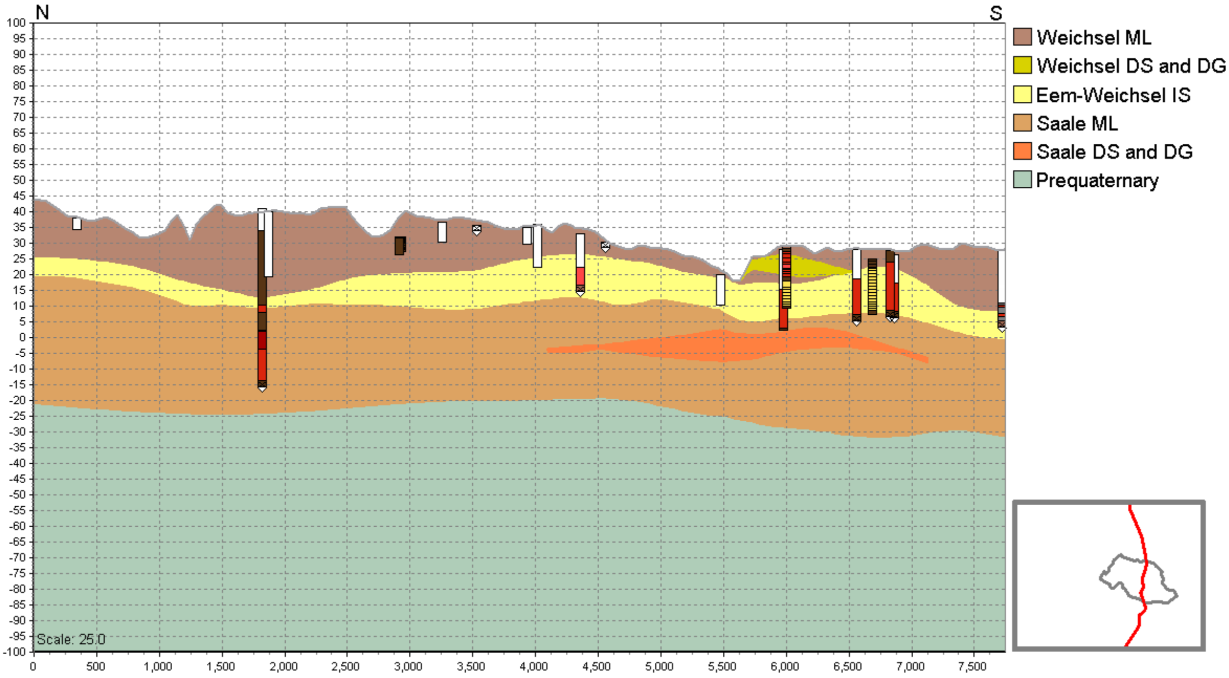
N
S
Weichsel ML
Weichsel DS and DG
Eem-Weichsel IS
Saale ML
Saale DS and DG
Prequaternary
Scale: 25.0

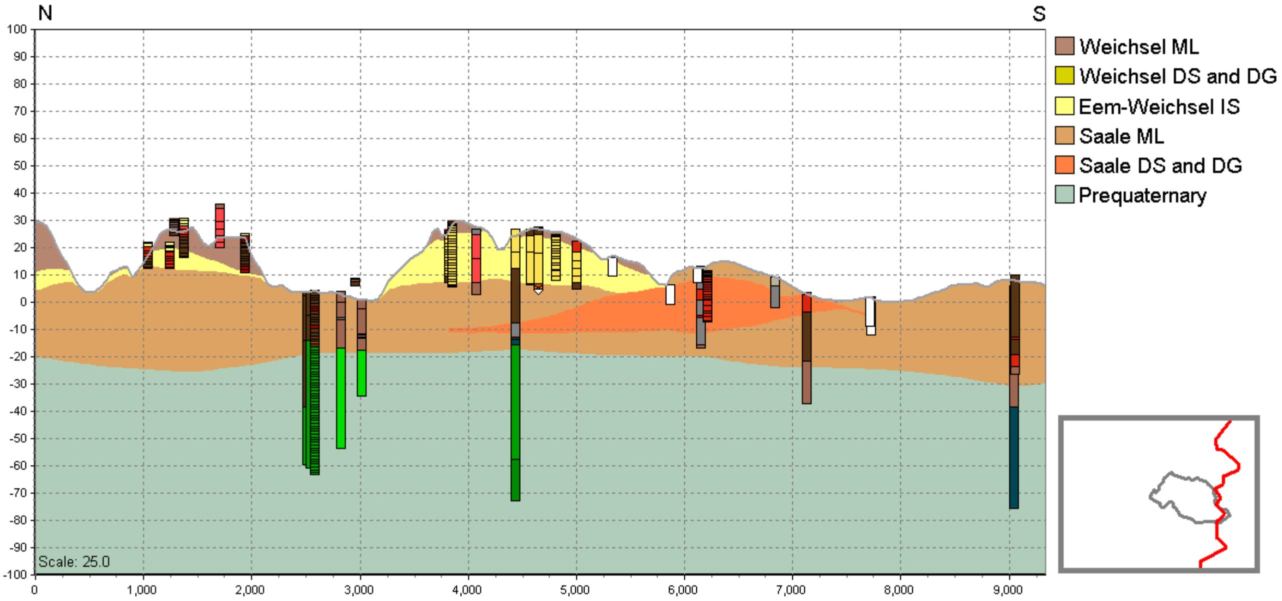
N
S
Weichsel ML
Weichsel DS and DG
Eem-Weichsel IS
Saale ML
Saale DS and DG
Prequaternary
Scale: 25.0

Appendix 4 Interpretation points in the geological model

Top of Eem-Weichsel interglacial sand layer

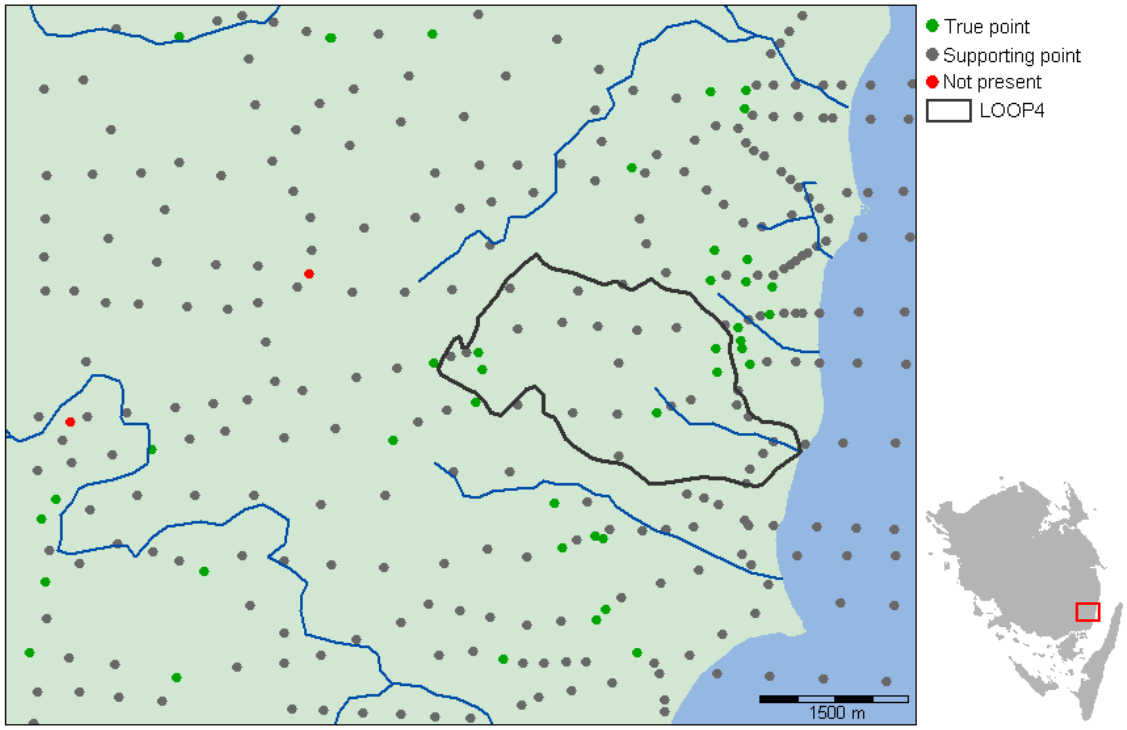

Bottom of Eem-Weichsel interglacial sand layer

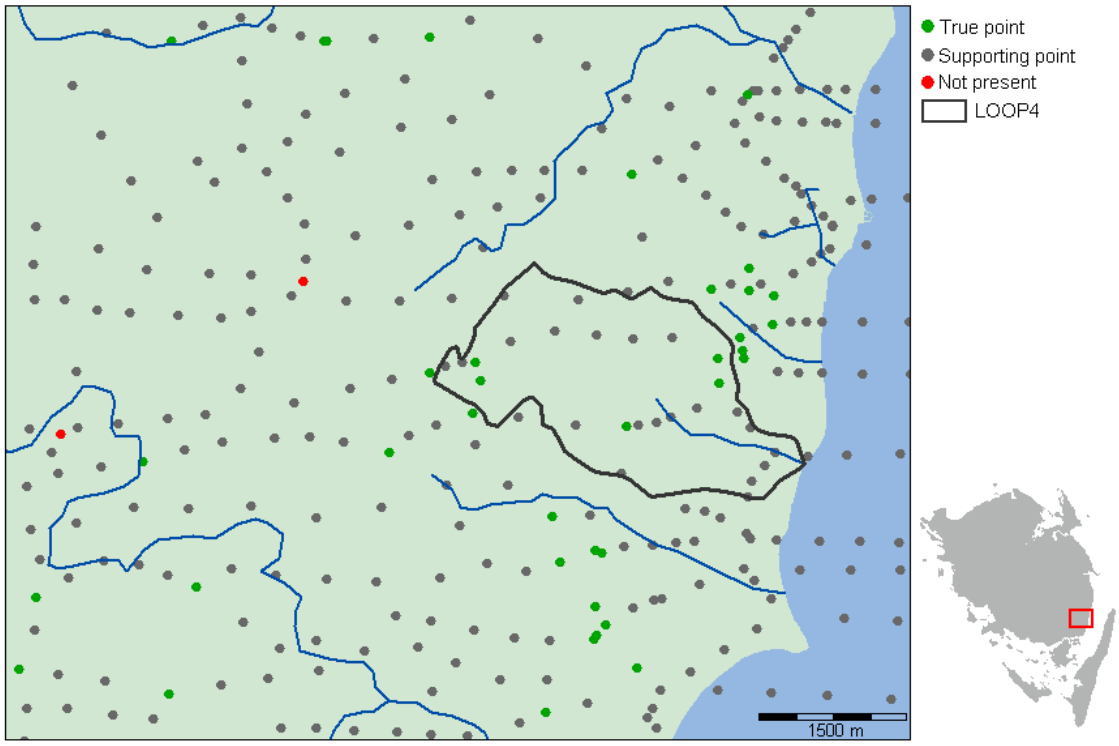

Top of Weichsel glacial sand and gravel

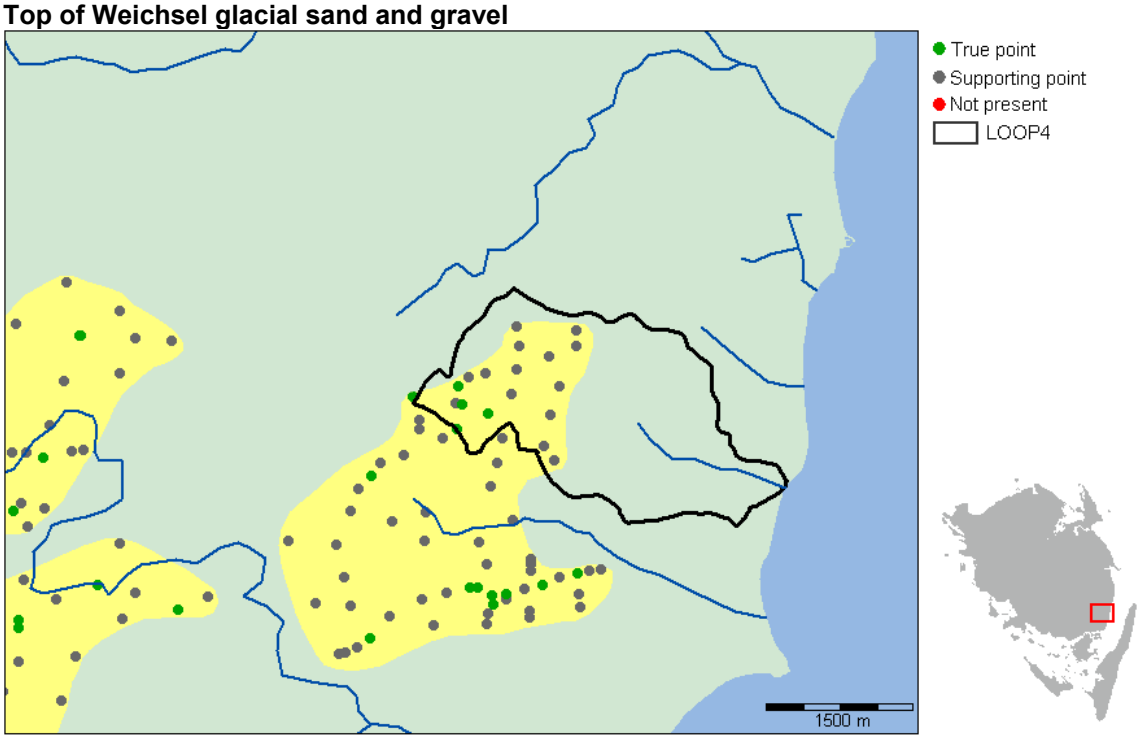

Bottom of Weichsel glacial sand and gravel

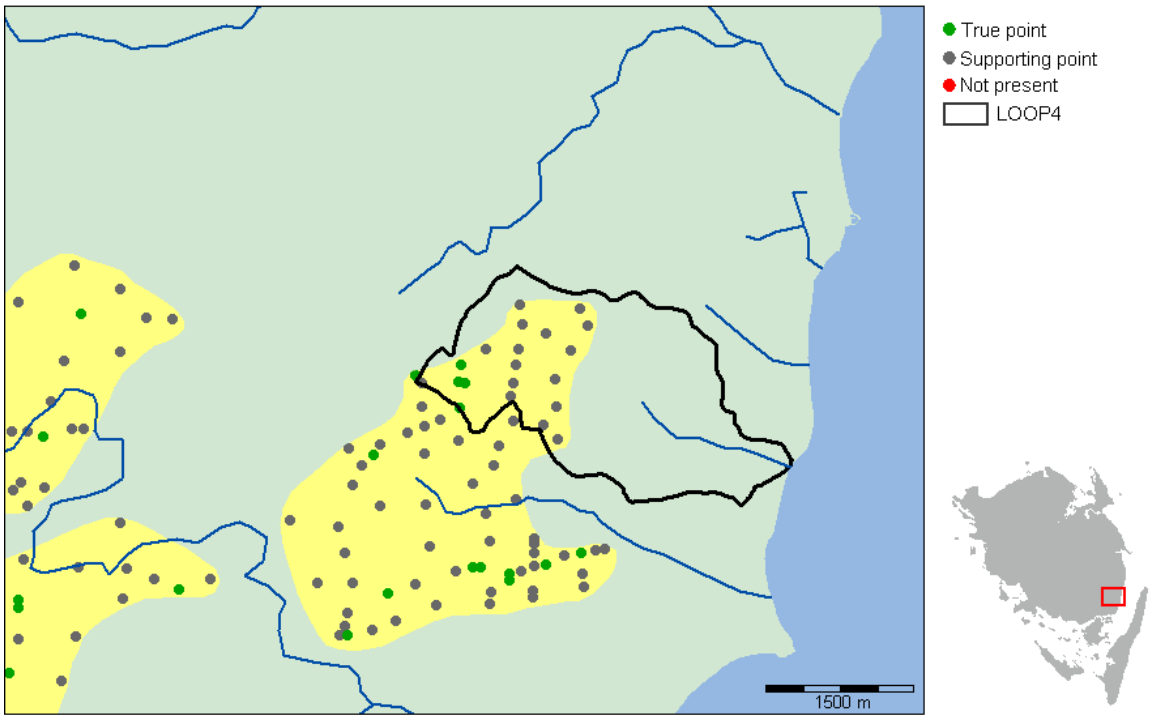

Top of Saale glacial sand and gravel

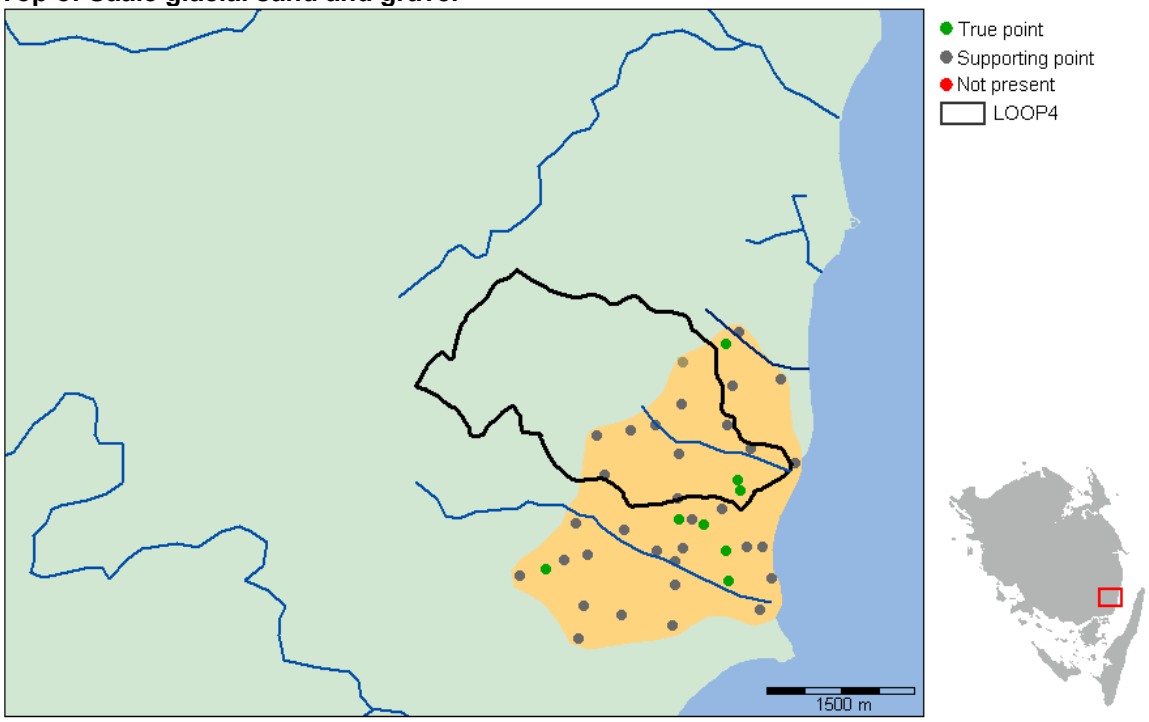

Bottom of Saale glacial sand and gravel

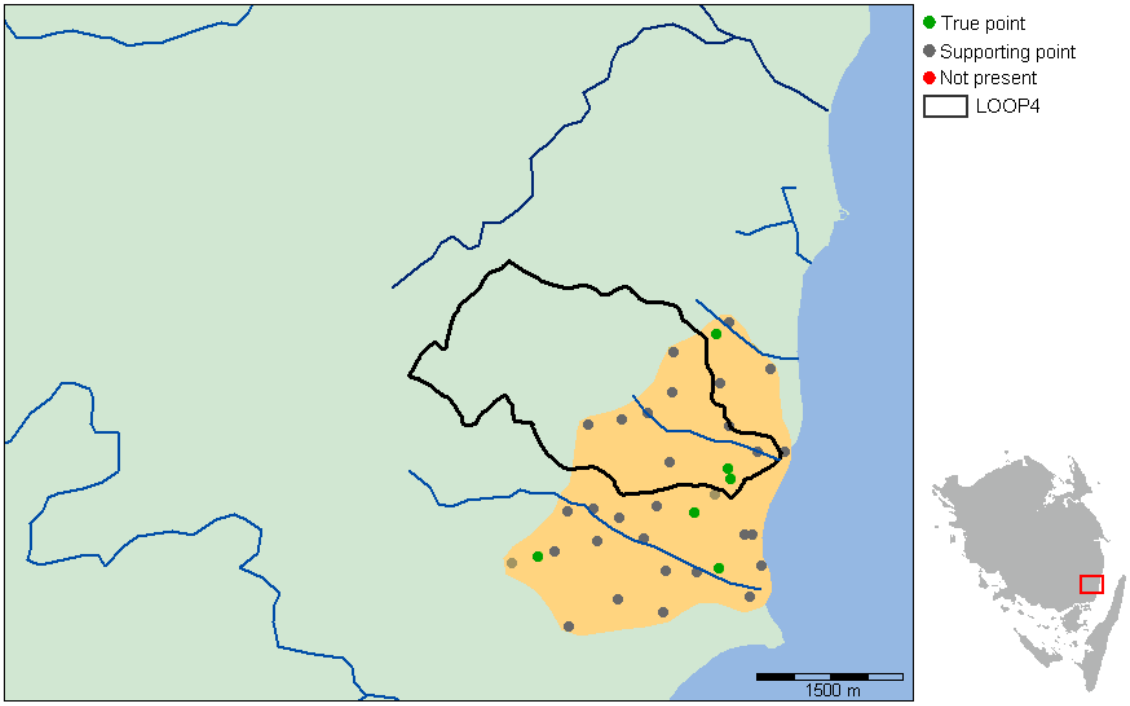

Appendix 5 Thickness of computational layers

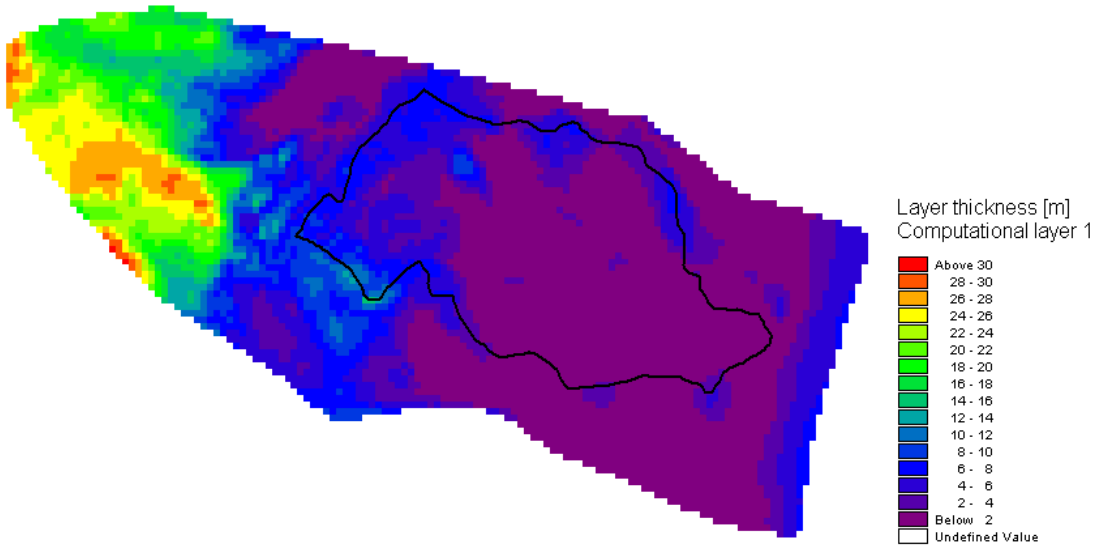

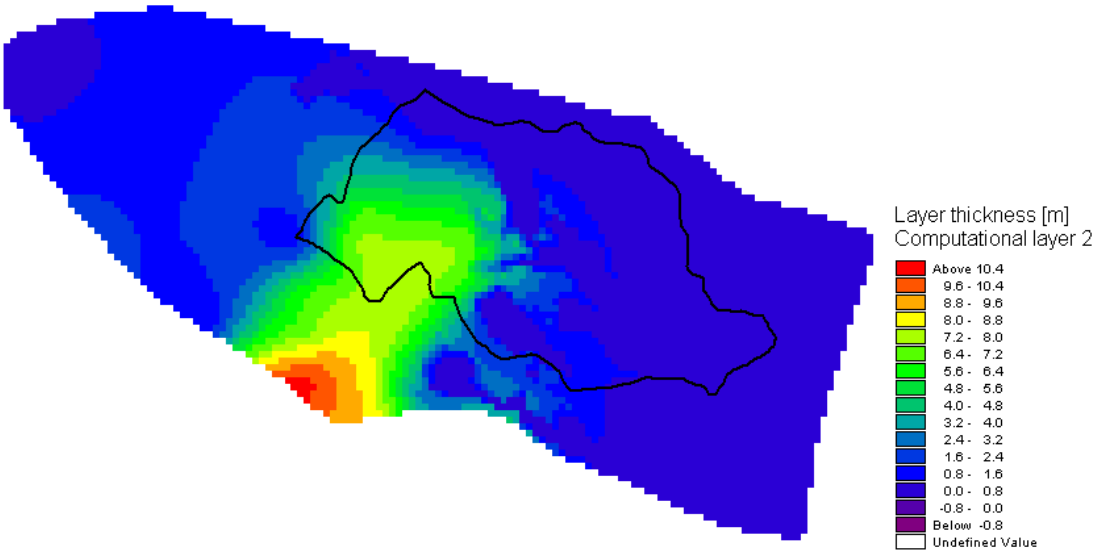

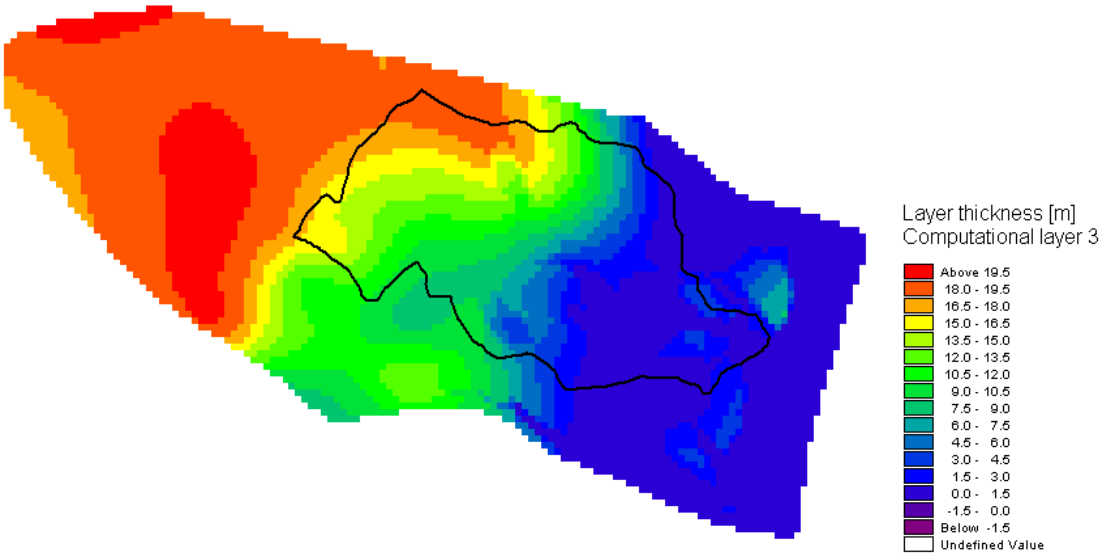
Layer thickness [m]
Computational layer 3
Above 19.5
18.0 - 19.5
16.5 - 18.0
15.0 - 16.5
13.5 - 15.0
12.0 - 13.5
10.5 - 12.0
9.0 - 10.5
7.5 - 9.0
6.0 - 7.5
4.5 - 6.0
3.0 - 4.5
1.5 - 3.0
0.0 - 1.5
-1.5 - 0.0
Below -1.5
Undefined Value

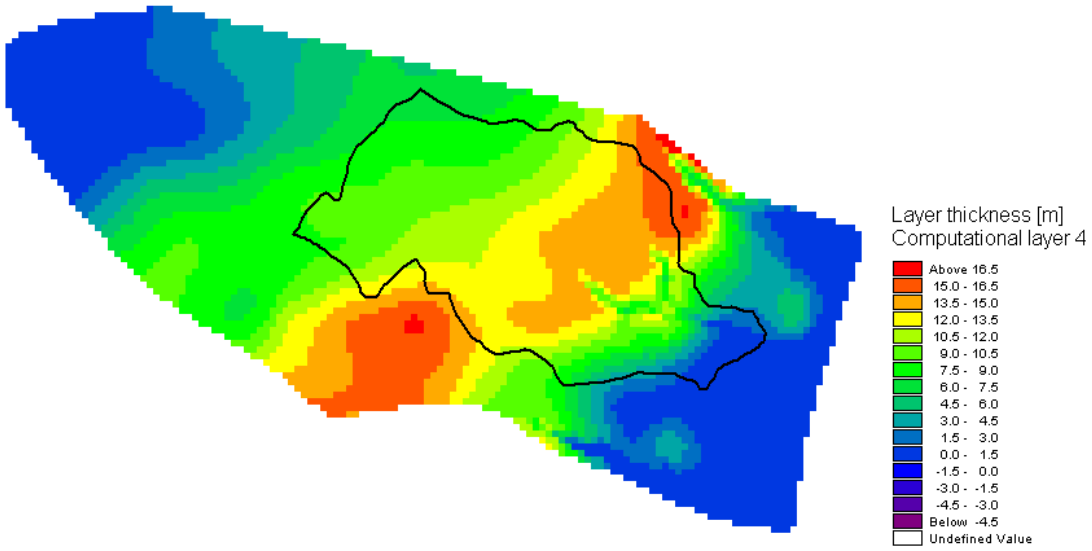
Layer thickness [m]
Computational layer 4
Above 16.5
15.0 - 16.5
13.5 - 15.0
12.0 - 13.5
10.5 - 12.0
9.0 - 10.5
7.5 - 9.0
6.0 - 7.5
4.5 - 6.0
3.0 - 4.5
1.5 - 3.0
0.0 - 1.5
-1.5 - 0.0
-3.0 - -1.5
-4.5 - -3.0
Below -4.5
Undefined Value

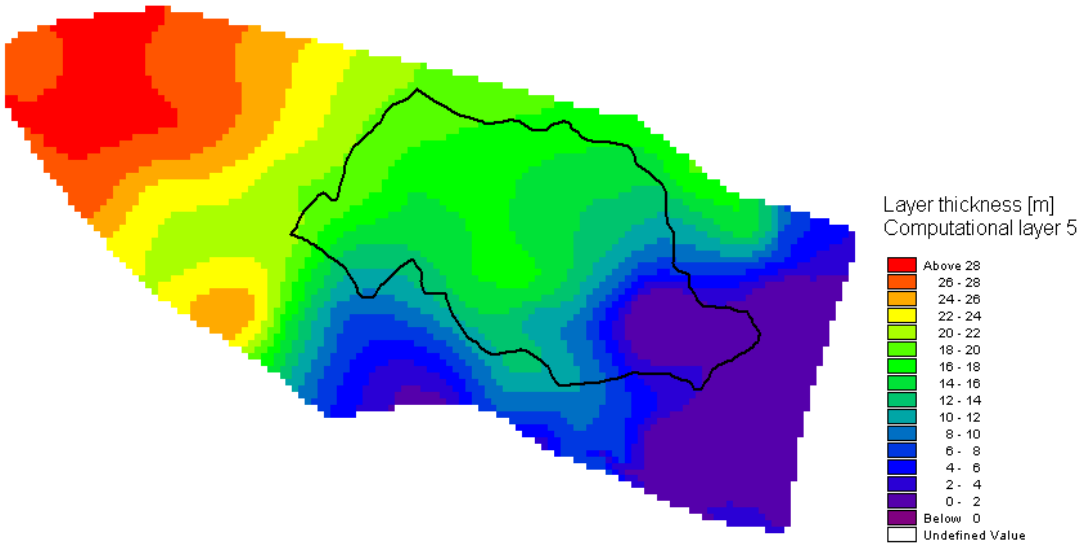
Layer thickness [m]
Computational layer 5
Above 28
26 - 28
24 - 26
22 - 24
20 - 22
18 - 20
16 - 18
14 - 16
12 - 14
10 - 12
8 - 10
6 - 8
4 - 6
2 - 4
0 - 2
Below 0
Undefined Value

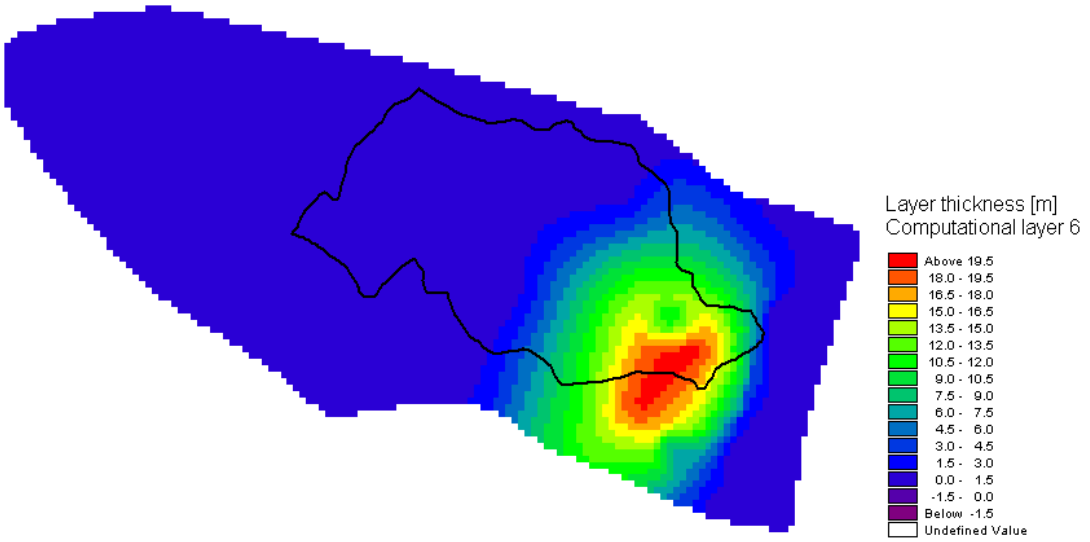
Layer thickness [m]
Computational layer 6
Above 19.5
18.0 - 19.5
16.5 - 18.0
15.0 - 16.5
13.5 - 15.0
12.0 - 13.5
10.5 - 12.0
9.0 - 10.5
7.5 - 9.0
6.0 - 7.5
4.5 - 6.0
3.0 - 4.5
1.5 - 3.0
0.0 - 1.5
-1.5 - 0.0
Below -1.5
Undefined Value

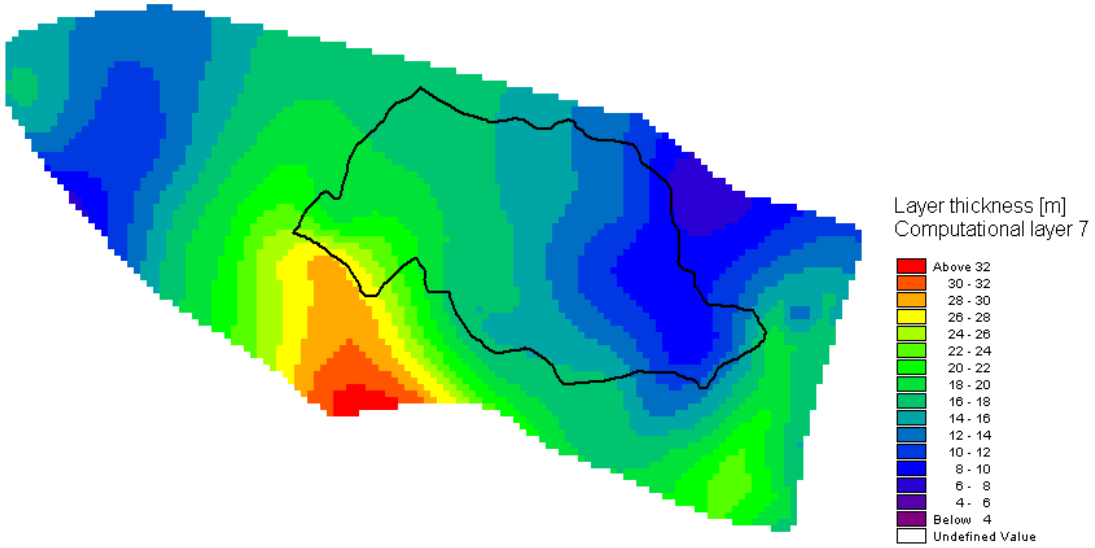
Layer thickness [m]
Computational layer 7
Above 32
30 - 32
28 - 30
26 - 28
24 - 26
22 - 24
20 - 22
18 - 20
16 - 18
14 - 16
12 - 14
10 - 12
8 - 10
6 - 8
4 - 6
Below 4
Undefined Value

Appendix 6 Simulated hydraulic head and flow vectors for 31/12 2004

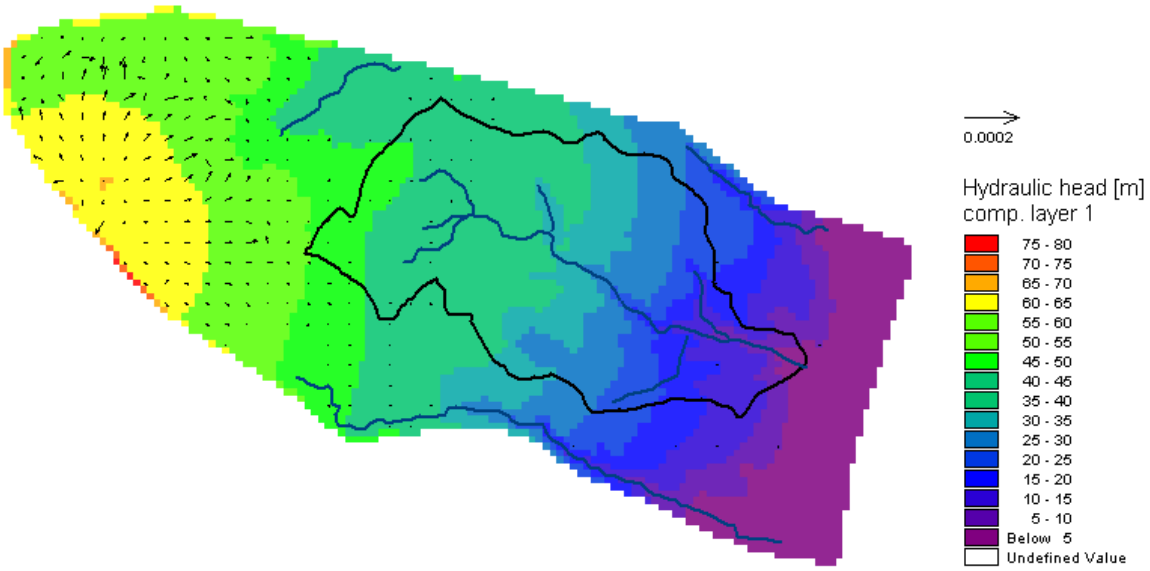

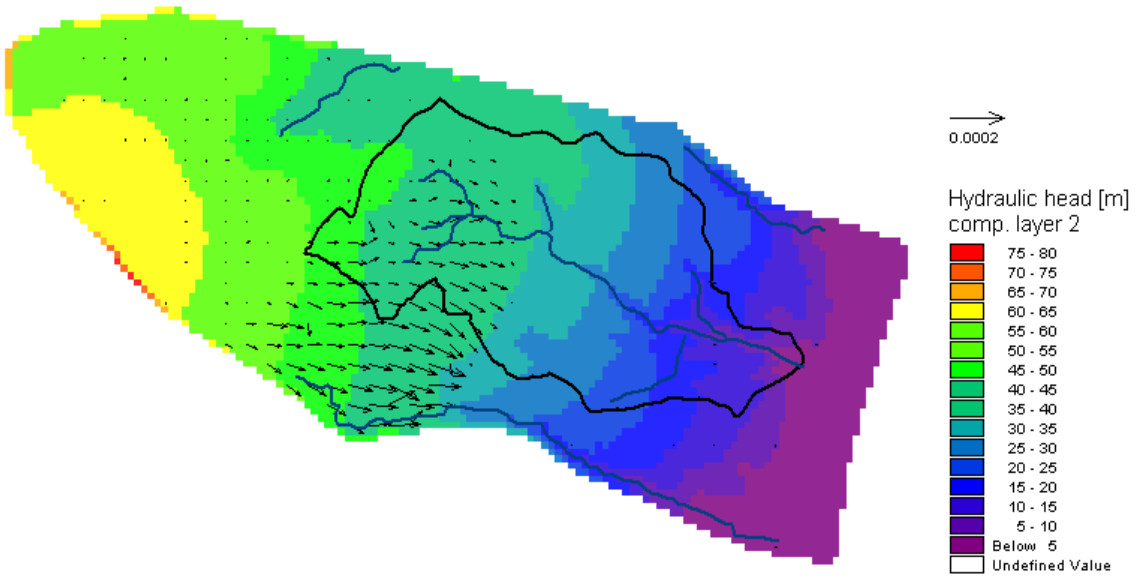

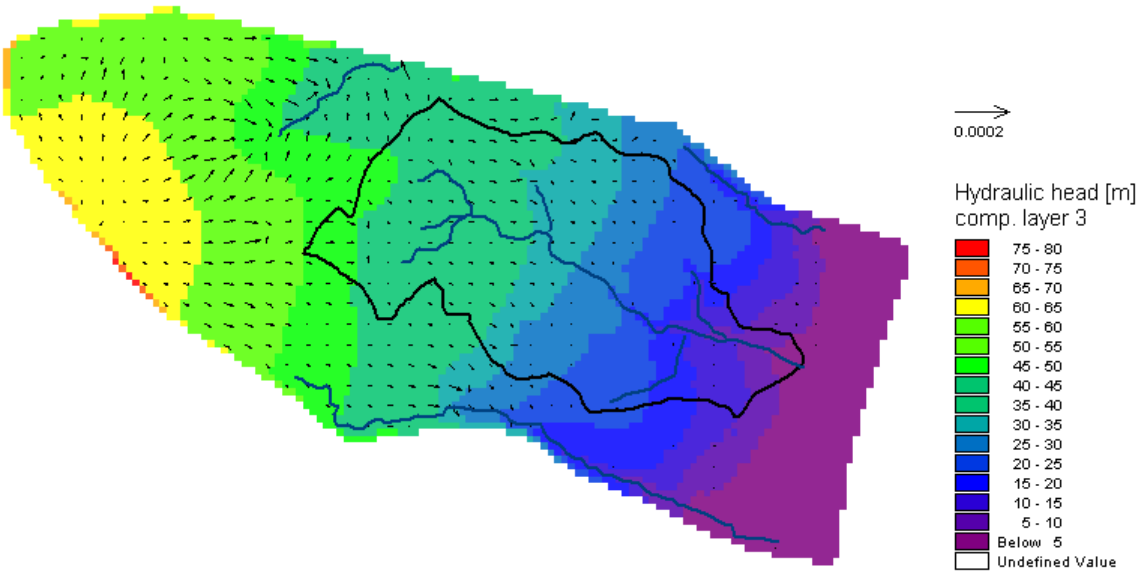
0.0002
Hydraulic head [m]
comp. layer 3
75 - 80
70 - 75
65 - 70
60 - 65
55 - 60
50 - 55
45 - 50
40 - 45
35 - 40
30 - 35
25 - 30
20 - 25
15 - 20
10 - 15
5 - 10
Below 5
Undefined Value

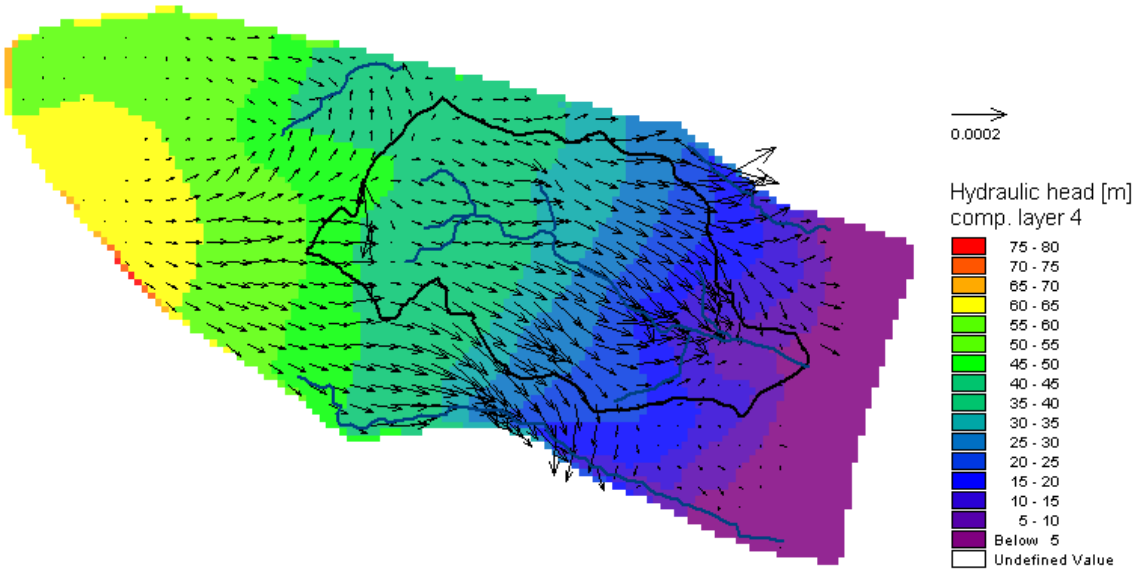
0.0002
Hydraulic head [m]
comp. layer 4
75 - 80
70 - 75
65 - 70
60 - 65
55 - 60
50 - 55
45 - 50
40 - 45
35 - 40
30 - 35
25 - 30
20 - 25
15 - 20
10 - 15
5 - 10
Below 5
Undefined Value

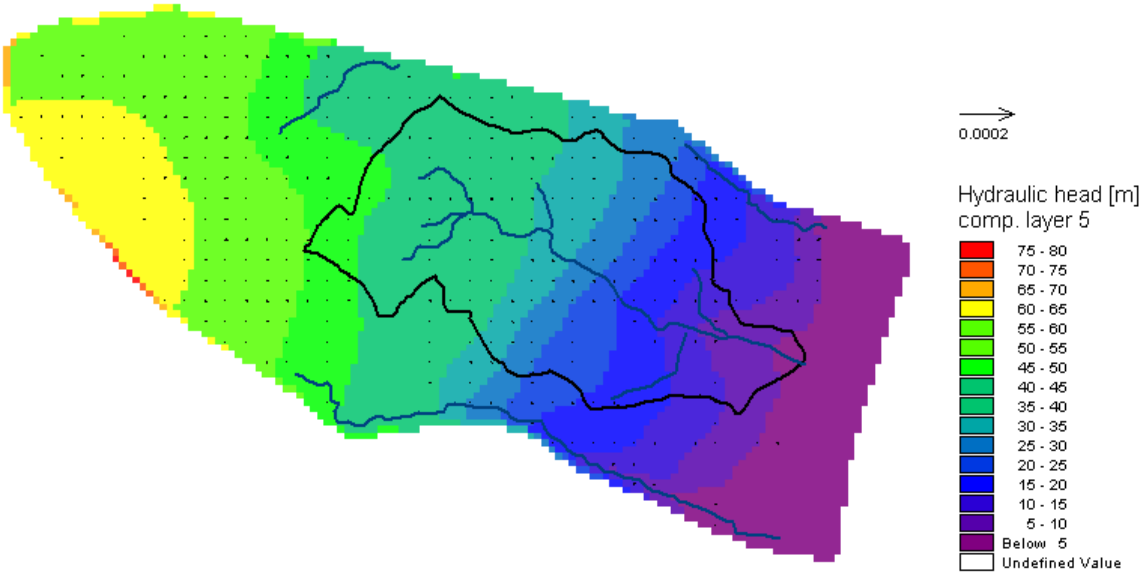
0.0002
Hydraulic head [m]
comp. layer 5
75 - 80
70 - 75
65 - 70
60 - 65
55 - 60
50 - 55
45 - 50
40 - 45
35 - 40
30 - 35
25 - 30
20 - 25
15 - 20
10 - 15
5 - 10
Below 5
Undefined Value

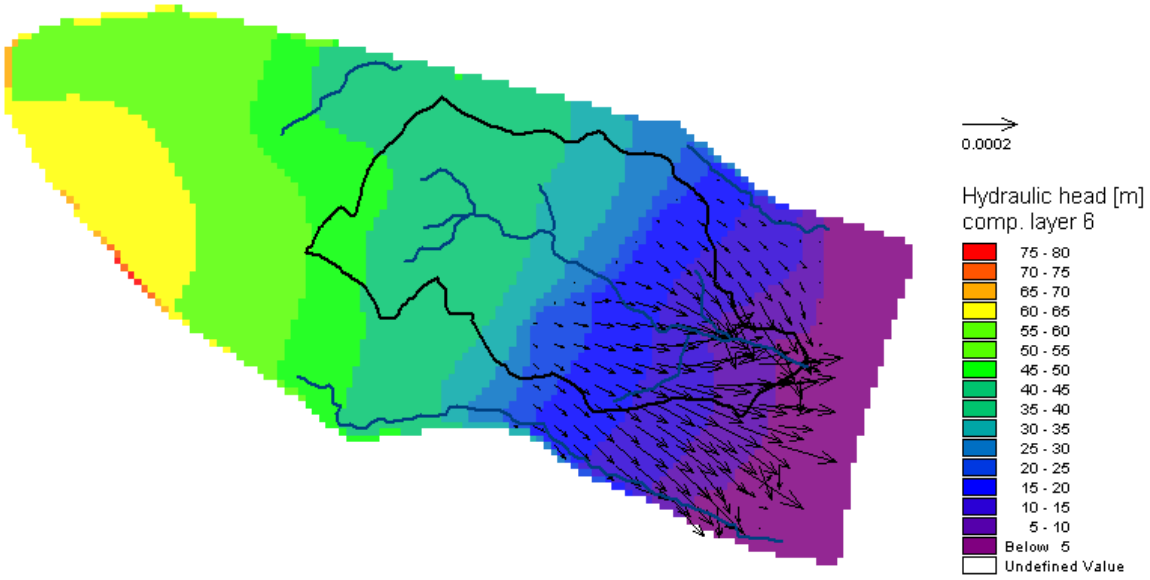
0.0002
Hydraulic head [m]
comp. layer 6
75 - 80
70 - 75
65 - 70
60 - 65
55 - 60
50 - 55
45 - 50
40 - 45
35 - 40
30 - 35
25 - 30
20 - 25
15 - 20
10 - 15
5 - 10
Below 5
Undefined Value

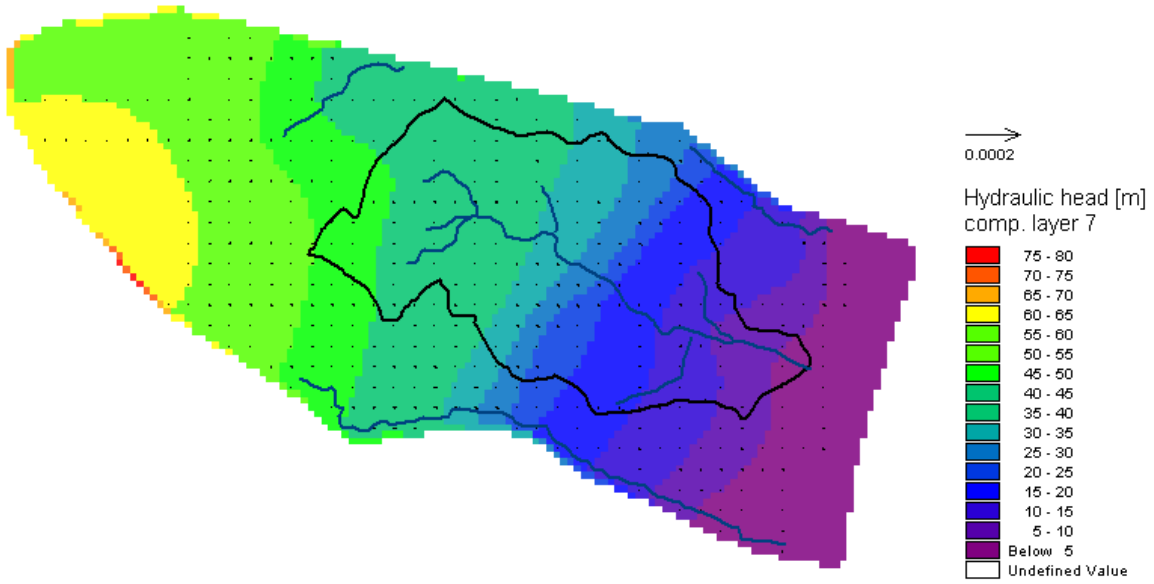
0.0002
Hydraulic head [m]
comp. layer 7
75 - 80
70 - 75
65 - 70
60 - 65
55 - 60
50 - 55
45 - 50
40 - 45
35 - 40
30 - 35
25 - 30
20 - 25
15 - 20
10 - 15
5 - 10
Below 5
Undefined Value